UNIVERSIDADE D
COIMBRA

Tiago Alexandre da Silva Marçal

A SINGLE CHANNEL HIGH-RESOLUTION SNORING SIGNAL AS A MEDICAL TOOL FOR OBSTRUCTIVE SLEEP APNOEA ASSESSMENT

Tese no âmbito do doutoramento em Engenharia Física, Instrumentação, orientada pelo Professor Doutor João Manuel Rendeiro Cardoso e pelo Professor Doutor Agostinho Rosa e apresentada ao Departamento de Física da Faculdade de Ciências e Tecnologia da Universidade de Coimbra

Junho de 2022

Faculdade de Ciências e Tecnologia da Universidade de Coimbra

A Single Channel High-Resolution Snoring Signal as a Medical Tool For Obstructive Sleep Apnoea Assessment

Tiago Alexandre da Silva Marçal

Supervisor
Professor Doutor João Manuel Rendeiro Cardoso

Co-Supervisor
Professor Doutor Agostinho Cláudio da Rosa

PhD in Physics Engineering | Doutoramento em Engenharia Física

PhD Thesis | Tese de Doutoramento

Tese no âmbito do doutoramento em Engenharia Física, Instrumentação, orientada pelo Professor Doutor João Manuel Rendeiro Cardoso e pelo Professor Doutor Agostinho Rosa e apresentada ao Departamento de Física da Faculdade de Ciências e Tecnologia da Universidade de Coimbra

Julho de 2022

1 2 9 0

UNIVERSIDADE D
COIMBRA

Para a minha esposa, Lúcia, e para o meu filho, Miguel.

Para os meus pais, Maria e Manuel.

Funding Support

The development of this work was financially supported by the Portuguese Foundation *Fundação para a Ciência e a Tecnologia* through the scholarship reference SFRH/BD/66442/2009 and by the research centre LIBPhys-UC through the scholarship references UID/FIS/04559/2013, and UIDB/04559/2020.

Agradecimentos

O percurso efetuado ao longo destes últimos anos no desenvolvimento deste trabalho só foi possível porque existiram pessoas e instituições que o tornaram possível. Gostava de começar por agradecer ao meu primeiro orientador, o Doutor José Basílio Simões por ter acreditado em mim e por me ter incentivado a iniciar o doutoramento, ao meu segundo orientador, o Doutor João Manuel Rendeiro Cardoso, pela sua disponibilidade e análise crítica, e ao meu co-orientador, Doutor Agostinho Rosa, pela sua preocupação com o desenvolvimento do trabalho e pelas dicas dadas. Ao saudoso Doutor Carlos Correia pela transmissão de conhecimentos e ao Doutor Requicha Ferreira pelo seu apoio e incentivo. O meu agradecimento ao Doutor José Moutinho dos Santos por autorizar a entrada no Centro de Medicina do Sono para recolha de dados e pelos conselhos clínicos prestados. Só foi possível usar todos os dados recolhidos graças à generosa colaboração dada pela técnicas de sono, Clara Santos, Conceição Travassos, Liliana Sousa, Lúcia Batata, Mafalda Ferreira e Marília Rodrigues.

A nível institucional, este trabalho só foi possível concretizar porque obtive o suporte financeiro da Fundação para a Ciência e a Tecnologia e do LIBPhys-UC, e porque o Centro Hospitalar e Universitário de Coimbra acedeu à criação de um protocolo com a Universidade de Coimbra para o desenvolvimento do trabalho de investigação sobre o ronco e a síndrome da apneia obstrutiva do sono, conduzido pelo LIBPhys-UC e pelo Centro de Medicino do Sono, este último liderado pelo Doutor José Moutinho dos Santos.

Queria também agradecer o companheirismo dos meus colegas, especialmente o Pedro e o Miguel, que com o seu espírito alegre e contagiante ajudaram a superar algumas das fases mais difíceis deste percurso, e a todos os amigos que se preocuparam comigo e com o desenvolvimento do trabalho e manisfestaram o seu apoio.

Por fim, a família. Aos meus pais, que tanto me deram para poder chegar aqui e ser o que sou hoje. À minha irmã, ao meu cunhado e aos meus sobrinhos pelos bons momentos e aos meus avós que foram sempre bondosos comigo e que procuraram transmitir a sua sabedoria. À minha esposa Lúcia pela sua paciência durante todos estes anos, pelo suporte dado, desde as contribuições feitas para este trabalho ao sacrifício feito sobrecarregando-se com tarefas, e por me ter dado um lindo filho. Miguel, estes agradecimentos também são para ti.

Para todos vocês, o meu obrigado!

Abstract

Obstructive sleep apnoea-hypopnea syndrome is a sleep-related breathing disorder, with a significant worldwide prevalence. Sleep is a human natural recurrent state, which is of critical importance to several processes in human physiology. A decrease in sleep quality, in the long term, may dangerously unbalance those processes, leading to the development of diseases. Among the diseases linked with this syndrome are some of the deadliest ones, as in the case of cardiovascular diseases, and some of the diseases with higher rate values. An example of this group of diseases is diabetes.

Snoring is one of the earliest and most common symptoms associated with obstructive sleep apnoea-hypopnea syndrome, and snoring generation is the result of loss of stiffness by the structures of the upper respiratory airway. Several factors may lead to the loss of tissue stiffness and snoring, but the most common one is fat deposits. Snoring follows the evolution of a subject from a healthy to the most severe obstructive condition, and its evolution can deliver interesting results to evaluate obstructive sleep apnoea-hypopnea syndrome.

Polysomnography is the gold standard, in sleep medicine, to evaluate sleep and diagnosis obstructive sleep apnoea-hypopnea syndrome in-laboratory sleep studies. Home studies use modified versions of the gold standard polysomnography or other simpler methods. In-laboratory sleep studies are expensive and the first night effect may change results, while at-home sleep studies may lack important data, giving the motivation to study and to develop a reliable solution based on the snoring signal.

The purpose of this work was the study of snoring, beginning with data acquisition at the *Centro de Medicina do Sono*, together with the acquisition of temperature, relative humidity, and gauge pressure. Snoring signal processing included snore detection, data synchronization between the high-quality sound signal file and the polysomnography study from the same subject, and feature extraction using different methods. An extensive set of features was calculated from the snores and analysed. Among the most relevant features are time duration, Kurtosis, band power ratio, in-out band power ratio, and Shannon entropy. Empirical Mode Decomposition and Synchrosqueezed Wavelet Transform are methods also implemented in the study of snores. The obtained results were compared against the subjects' medical classification group, their medical classification group in terms of obstructive sleep apnoea-hypopnea syndrome severity.

The relationship between snoring and the medical classification group returned promising results. Snore's time duration feature shows a consistent increase as obstructive sleep apnoea-hypopnea syndrome worsens. It starts with the lowest

value, $\mu = 1.106$ s, for the Control group, and it increases always, to $\mu = 1.178$ s, $\mu = 1.227$ s, $\mu = 1.368$ s, and $\mu = 1.493$ s. A statistical analysis concludes that all data organized according to the medical classification groups, for this feature, come from different distributions. Shannon entropy feature delivers a linear relation, it increases with the syndrome worsening when analysing data distribution and its quartiles. This linear relationship is an important remark using parameters wp_{25c} and wp_{50c}. The first parameter, wp_{25c}, has values of 2.539, 4.254, 4.599, 7.967, and 19.938 bits, while wp_{50c} has values of 6.198, 8.233, 10.101, 14.043, and 39.374 bits. Both parameters' values are for an increased level of the syndrome's severity. Frequency-domain features also revealed interesting relationships with medical classification groups. Band 8 of both band power ratio and in and out band power ratio features has consistently increased mean values as the syndrome worsens. Band power ratio has median values of 0.006, 0.007, 0.009, 0.013, and 0.019 for band 8, while in and out band power ratio has median values of 0.006, 0.008, 0.009, 0.013, and 0.019. Finally, a new method and almost unused in sleep studies, the Synchrosqueezed Wavelet Transform, decomposed the signal in its most important components, up to 10, and a statistic analysis identified frequencies characteristic of a single medical classification group. Examples of medical classification groups' characteristic frequencies are 2996, 1300, 1545, 2320, and 1146 Hz, for Control, Snorer, Mild, Moderate, and Severe groups, respectively.

Keywords: Snoring; High-Quality Sound Signal; Obstructive Sleep Apnoea and Hypopnea Syndrome; Signal Analysis and Processing; Feature Extraction; Single-Channel Audio Acquisition and Analysis; Synchronization

Resumo

A síndrome da apneia-hipopneia obstrutiva do sono é um distúrbio respiratório do sono, com uma significativa prevalência no mundo. O sono é um estado natural e periódico do ser humano, de elevada importância na fisiologia humana e na homeostasia de diversos órgãos e processos. Perturbações no sono levam a uma diminuição da sua qualidade e a distúrbios no equilíbrio desses processos, que levam ao aparecimento de doenças. Entre as possíveis doenças estão algumas das mais mortais a nível mundial, como por exemplo as doenças cardiovasculares, e as doenças com as mais altas taxas de crescimento, como é o caso da diabetes.

O ronco é um dos primeiros e mais comuns sintomas associados com a apneia-hipopneia obstrutiva do sono, e a origem do ronco está relacionada com a perda da firmeza por parte das estruturas da via área superior. Existem vários factores que podem contribuir para a perda da firmeza, e que conduzem ao ronco, mas a mais comum está relacionada com o aumento de peso e os depósitos de gordura. O ronco está, normalmente, presente em todas as fases de desenvolvimento apneia-hipopneia obstrutiva do sono, desde que o indivíduo é saudável até à forma mais severa da síndrome. A própria evolução do ronco pode ser uma fonte de informação útil para a avaliação da apneia-hipopneia obstrutiva do sono.

A polissonografia é o estudo de excelência, na medicina do sono, para avaliar o sono e diagnosticar a apneia-hipopneia obstrutiva do sono em ambiente hospitalar. Existem versões modificadas do estudo de polissonagrafia que são realizadas em casa, assim como métodos mais simples de aquisição de apenas 2 ou 3 sinais. Os estudos realizados em laboratório são dispendiosos e existe o efeito de dormir fora do lar na primeira noite que pode contribuir para ter resultados diferentes, enquanto que os estudos realizados em casa podem ficar privados de informação relevante. Estas observações dão a motivação para o estudo e desenvolvimento de uma solução fiável baseada no sinal do ronco.

O objectivo deste trabalho consistiu no estudo do ronco, começando pela aquisição de dados no Centro de Medicina do Sono em conjunto com a aquisição da temperatura, humidade relativa e pressão. O processamento do ronco incluiu a sua detecção, a sincronização do ficheiro áudio do ronco com o estudo de polissonografia do mesmo indivíduo, a extração de características do ronco usando diversos métodos. Um conjunto extensivo de características foi calculado a partir dos roncos e, posteriormente, analisado. Entre as características mais relevantes estão a duração, *Kurtosis*, *band power ratio*, *in out band power ratio*, e a entropia de *Shannon*. Os métodos *Empirical Mode Decomposition* e *Synchrosqueezed Wavelet Transform*

também foram usados no estudo do ronco. As características do ronco foram comparadas com a classificação médica, de acordo com a severidade da apneia-hipopneia obstrutiva do sono, dada aos indivíduos.

As relações entre o ronco e as classificações médicas deram origem a resultados interessantes. A duração do ronco revela uma evolução consistente à medida que a síndrome da apneia-hipopneia obstrutiva do sono piora. Começa por apresentar um valor médio, $\mu = 1,106$ s, mais baixo para o grupo Controlo, e aumenta sempre de um grupo para o seguinte, $\mu = 1,178$ s, $\mu = 1,227$ s, $\mu = 1,368$ s, e $\mu = 1,493$ s. A análise estatística conduzida a esta característica, e organizada de acordo com a classificação médica, revela que todos os grupos vêm de distribuições diferentes. A entropia de *Shannon* apresenta uma evolução linear, um aumento na entropia corresponde a um agravamento da condição clínica, quando se analisa a distribuição dos dados e dos seus quartis. Esta observação constitui um marco importante, alcançado a partir do uso dos parâmetros wp_{25c} e wp_{50c}. O primeiro parâmetro, wp_{25c}, apresenta valores de 2,539, 4,254, 4,599, 7,967, e 19,938 bits, enquanto que o parâmetro wp_{50c} apresenta valores de 6,198, 8,233, 10,101, 14,043, e 39,374 bits. Os valores apresentados para os dois parâmetros estão ordenados por ordem crescente de severidade da síndrome. As características extraídas no domínio das frequências também deram relações interessantes com os grupos das classificações médicas. A banda 8 das características *band power ratio* e *in and out band power ratio* tem uma evolução consistente com o agravamento da severidade. A característica *band power ratio* apresenta valores de mediana de 0,006, 0,007, 0,009, 0,013, e 0,019, enquanto que a característica *in and out band power ratio* apresenta valores de mediana de 0,006, 0,008, 0,009, 0,013, e 0.019. Por fim, um método novo e ainda pouco explorado na medicina do sono, a *Synchrosqueezed Wavelet Transform*, decompões o sinal nas suas componentes mais importantes, até um máximo de 10, e uma análise estatística identificou frequências características para cada classificação médica. Um exemplo de uma frequência característica para cada classificação médica é a frequência de 2996, 1300, 1545, 2320, e 1146 Hz, para o grupo Controlo, Ressonador, Ligeiro, Moderado, e Grave, respectivamente.

Palavras-Chave: Ronco; Sinal Áudio de Alta Qualidade; Apneia e Hipopneia Obstrutiva do Sono; Análise e Processamento de Sinal; Extração de Características; Aquisição e Análise de Canal Único de Áudio; Sincronização

Contents

List of Tables

List of Figures

Chapter 1

Introduction

The first chapter focus on the problem addressed by this thesis, giving a deep overview of the problem and enlightening the motivation to study new methods and develop new tools to help medical staff in the diagnosis of Sleep-Related Breathing Disorders (SRBD), specifically Obstructive Sleep Apnoea-Hypopnea Syndrome (OSAHS).

The chapter ends with the presentation of the thesis's objectives and an overview over each chapter.

1.1 Topic

Sleep is a natural state in human biology, and can be characterized as a state of reduced responsiveness to external stimuli and reduced activity. This state is characterized by being easy to reverse, usually returning to the state of wakefulness, and it is absolutely fundamental in human biology, but without clear evidence of death by sleep deprivation. Its importance can be assessed by the amount of time each human spent in it, roughly a third of his lifetime [1].

Historically, and during several centuries, sleep was considered a passive state, without any type of activity, a state between wakefulness and death. No significant breakthroughs happened in the comprehension of sleep until the 19^{th} century [2, 3]. During the 19^{th} century, some sleep observations were made, with important discoveries, such as the case of the Cheyne-Stokes respiration and the description of the clinical symptoms associated with narcolepsy [2,4]. However, it was not until the 20^{th} century that major breakthroughs occurred in the sleep medicine field, with the discovery, for example, of different patterns in the brain electrical activity during wakefulness and during sleep, and the discovery of Rapid Eye Movement (REM) sleep (duality of sleep) [2].

Sleep medicine physicians learned to identify normal sleep profiles, among the human population, and, more important, to identify deviations from normal sleep, in which sleep shifts from a normal/healthy to a pathological profile. OSAHS is

a type of sleep disorder, in which the upper respiratory airway collapses, partial or completely, and the airflow, respectively, decreases or is inexistent due to the obstruction. Untreated, this sleep disorder may worsen over time, decreasing the patient's life quality in the long term. Although there is no clear link between sleep deprivation and death, OSAHS, and other SRBD, decreases sleep quality and it has a strong impact on the human being function during the wakefulness state. If OSAHS persists over time, the impact of this disorder increases, with direct consequences in several human functions, as the case of the brain, the immune system, the cardiovascular system, and the endocrine system. Patients with OSAHS have to deal with serious problems during the day, damaging both personal life and work performance. Sleep modulates human function, but, it is also modulated by a great number of factors, both internal and external, as on the case of alcohol, tobacco, caffeine, and drugs. In the end, OSAHS has a huge impact in the patient's quality of life, with the patient having less lifetime of full health, and in the economy [3, 5, 6].

Sleep medicine physicians use the gold standard multichannel Polysomnography (PSG), but also other types of sleep studies, to diagnosis OSAHS. PSG is a time-consuming and expensive study and requires the presence of a sleep technician for an all-night patient monitoring in a clinical/hospital facility, which means sleeping in a strange environment.

1.2 Focus and Scope

World prevalence of OSAHS was estimated 6% in women and 13% in men. This estimation was performed in an adult population between 30 and 70 years old, from the Wisconsin Sleep Cohort study project [7]. More recently, a review of literature focused on 17 studies from 16 countries and estimates a prevalence of around 1 thousand million people, men, and women aged between 30 and 69 years old, with OSAHS. The social burden of OSAHS is huge, as well as the economic burden, with a 2015 report estimating a cost of 12.400 million US dollars spent in the diagnosis and treatment of this condition, only in the USA [8]. Accordingly to this estimation, sleep impairment by OSAHS hits around 13.0% of the world population, patients only, not considering the patients' families. Solutions are required to fight these numbers, performing early diagnosis and introducing policies to prevent the emergence of new cases, as in the case of fighting the pandemic of obesity, an associated OSAHS risk factor. New diagnosis methods must be considered to help physicians in the early diagnosis, by increasing sleep studies at a reduced cost.

The present research work focus on the study of snoring in subjects who underwent in-laboratory PSG study, without the application of treatments for SRBD. A particular SRBD was under analysis, OSAHS, and the interest related to the study of snoring is on its onset. Snoring is one of the first symptoms associated with OS-

AHS, and it can start even before a subject meet the criterion for OSAHS diagnosis. For this reason, snoring is of high interest to follow the evolution of OSAHS, from a healthy subject with sporadic snoring to a OSAHS patient. Characteristics associated with snore sound changes with the evolution of the subjects condition [9, 10].

1.3 Relevance

As previously stated, OSAHS is a serious condition, worsening the life of millions of individuals. OSAHS patients may develop other diseases, decreasing, even more, their quality of life, and among the diseases associated with OSAHS are the cardiovascular diseases and diabetes. The first one is the leading cause of death worldwide, while the second is increasing steadily over the past decades [11–13]. These data give the right perspective about OSAHS and the importance of managing this problem.

Research addressing OSAHS problematic is extensive, and it has different purposes. From the study of how OSAHS influences and changes a specific human function, the development of sleep questionnaires, diagnosis and the application of treatments, reviews in the topic, to the development of classification algorithms to predict and help in the diagnosis of the patient's severity, the search for "obstructive sleep apnoea" returned a total of 35.478 results at the PubMed website, from 1953 to the present day (March 2021). Alternatives to the current medical tools have been developed and tested using data from the PSG, or from an independent source, performing multichannel or a single-channel analysis with the implementation of a wide number of methods [14–17]. Although OSAHS is widely investigated, this project used, the overall, methods in a unique configuration, relating snores' features, in the time-domain, frequency-domain, time-frequency domain, and statistical features, with OSAHS severity. A new method was also proposed to assess the disorder.

1.4 Objectives

The project's original purpose was the study of human respiratory sounds. Normal respiratory sounds exist and they are produced by the structures, tissues and organs, of the respiratory system, their characteristics are not homogeneous and they are, strongly, dependent of the anatomic origin [18, 19]. Abnormal, or adventitious, respiratory sounds exist when changes, or interferences, occur in the respiratory system, and they are classified in either of one of these 2 classes: continuous or discontinuous [20, 21]. Wheezes are an example of continuous abnormal respiratory sound class, while crackles are an example of discontinuous abnormal respiratory sound class. Abnormal respiratory sounds may appear due to several factors: diseases, human behaviour, accidents, or foreign objects, partially, blocking the normal airflow [22, 23].

The study of human respiratory sounds was proposed to M.D. José Moutinho dos Santos, head of the Centro de Medicina do Sono (CMS) at the Centro Hospitalar e Universitário de Coimbra (CHUC). The goal was the definition of the procedure to acquire normal and adventitious respiratory sounds in the laboratory, under his supervision. Although M.D. José Moutinho dos Santos acknowledged the problem associated with abnormal respiratory sounds, he suggested to change the study to a scientific area with a greater interest. The head of the CMS suggested to study snoring and OSAHS, since it is, typically, one of the first symptoms to appear in this syndrome. The development of methods to study snoring and OSAHS would be helpful to physicians in the clinical diagnosis of this syndrome. Following the advice of M.D. José Moutinho dos Santos, the meeting final result was a shift in the thesis's main purpose to study snoring, and how it relates with OSAHS. OSAHS is a sleep-disrupting condition, and it may worsen as time goes by to a severe clinical assessment where it is most likely for the patient to lose quality of life, develop other health issues, and, ultimately, die.

The gold standard evaluation tool in sleep medicine to study SRBD is PSG, a multi-parameter study, in which several sensors are used to acquire signals from different anatomical regions. This study is performed in a clinical facility, under the supervision of a sleep technician the entire night, with each patient sleeping in a different room. The complete procedure may last for up to 11 hours, starting with patient reception, preparation, monitoring, and finishing by awakening the patient and detaching the sensors from the patient. The need for physical space and the continuous presence of a sleep technician allocate precious and expensive resources to perform the study. PSG requirements include wire connections between the sensors, either analogue or digital, and a local data concentrator unit. Those wires may interfere with the patient's sleep, thus interfering with the PSG results. An unfamiliar sleep environment may also unsettle the patient psychological state, resulting in modifications in the sleep patterns, with consequences in the results of the PSG study.

The development of a tool to help physicians in OSAHS diagnosis, based on single signal analysis, is of major importance and the ultimate objective. Snoring is one of the earliest symptoms in OSAHS development, being this symptom's signal a natural target to analyse and to find correlations between the signal's features and the clinical data. The project's objective was not to replace PSG study as the gold standard in sleep medicine, but instead to develop a tool able to perform a snore evaluation and deliver data to help physicians in the clinical decision. The project kick-off milestone was the establishment of a protocol between the research group Lab. de Instr., Eng. Biomédica e Física da Radiação (LIBPhys) from the University of Coimbra, at the time known as Grupo de Electrónica e Instrumentação, and the

CMS of the CHUC. At the development stage, getting a high-quality snore signal was the fundamental concern, and, for that reason, the sound signal acquire, important to the development of the work, by the PSG study was not considered for feature extraction. This also means there are no strings attached between the project and the PSG study in the future, if the project achieved the desired results. The snoring study was performed using a high-resolution audio signal device, independent of the PSG equipment, to acquire sound for the entire night. Together with the audio device, an *ad-hoc* electronic device was developed to acquire Slow Variation Parameters (SVP), temperature, relative humidity, and pressure. Data acquisition from the audio device, together with data from the SVP, questionnaires, and clinical data, PSG and its reports, represented the entire data set, with the patients' set selected by M.D. José Moutinho dos Santos based on clinical reports. Pre-processing step included data synchronization between the high-resolution audio signal and the PSG data, while the most important final milestone was the implementation of a new method, only applied in a few published scientific journals in the sleep field, the Synchrosqueezed Wavelet Transform, and the correlation, with clinical benefits, between snores' features and clinical data.

This work aims to answer the following questions:

- **Research question 1:** Is it possible to use a single signal to assess OSAHS?
- **Research question 2:** Which snore's features are the most valuable to assess OSAHS?
- **Research question 3:** Is snore signal a reliable source of information to assess OSAHS?

1.5 Contribution to Science

This section briefly summarizes the major contributions of this thesis to science in sleep medicine sleep, in particular, to improve knowledge over OSAHS and its assessment using data from a single channel, the snore signal. Major contributions are organized in 2 areas, in terms of feature analysis and terms of method.

- **Feature analysis:** The application of feature analysis in OSAHS and in snore signal isn't state-of-the-art work. However, data were analysed and processed in unique ways, delivering more knowledge to science. In this case, Shannon entropy highlights from the remaining features, clearing showing promising results for future development of new devices to assess OSAHS. The statistical results showed significant differences among all medical classification groups, which come from different data distributions. Parameter selection revealed,

from the Shannon entropy feature, a consistent trend in all medical classification groups, Control (Co), Snorer (Sn), Mild (Mi), Moderate (Mo), and Severe (Se) (figure 5.43). Parameters wp_{25c} and wp_{50c} have linear relationship with medical classification groups. As the syndrome worsens, the parameters' values increase. The first parameter starts with a value of 2.539 and increases to 4.254, 4.599, 7.967, and 19.938 bits. The second parameter has values of 6.198, 8.233, 10.101, 14.043, and 39.374 bits.

- **Method:** The Synchrosqueezed Wavelet Transform (SWT) is a recent method to analyse data in the time-frequency plane. Current state-of-the-art shows it has been barely exploited in the sleep medicine field, in particular, in the study of OSAHS and in the study of snoring. Snores' decomposition shows a clear separation between the different frequency components, especially, for the higher components. The histograms, for each medical classification group, highlight the most common frequencies. The selection of those frequencies revealed which ones are characteristic of a single medical classification group and, even more, are more interesting to select (present in the highest number of patients). A possible frequency to characterize Co medical classification group is the 2996 Hz component, present in 4 of the patients, with the highest single patient contribution to the histogram of 42.9%, and 31 Hz away from the closest frequency (from the frequency list of the other medical classification groups). The application of the same procedure, led to the selection of the 1300, 1545, 2320, and 1146 Hz frequency component for the remaining medical classification groups, respectively, Sn, Mi, Mo, and Se (for mode details see Table 5.31 and Table 5.32). SWT method is also a candidate for the development of commercials devices to assess OSAHS through snoring.

1.6 Thesis Structure

This thesis presents the developed methodology to study the high-resolution snoring signal as an alternative to the gold standard PSG for OSAHS. The single channel snoring signal records data from one of the earliest symptoms related to OSAHS, which allows tracking the syndrome from the beginning. The structure of this thesis can be systematized as follows: The Introduction presents the subject discussed in this thesis, the OSAHS and one of its earliest symptoms, snoring, enhancing the relevance and the contribution of the developed work to the knowledge in science. Sleep and Sleep Disorders develops the thematic further, introducing physiologic sleep, discussing its architecture, how sleep modulates other systems of the human body, and how it is modulated by multiple agents. Finally, this chapter presents the gold standard in the sleep medicine field to study sleep, PSG.

The State of the Art chapter reviews the literature in the sleep medicine field, presenting state-of-the-art methods to study sleep and its disorders, from playful/informative mobile applications, covering current medical tools, and scientific research on, mostly, algorithms.

Materials and Methods presents the followed methodology to answer the questions raised in Introduction. It starts with the presentation of the layout, protocol, and the equipment of the sleep medical centre, CMS, the population sample, and it continues with a detailed description of the types of equipment used to acquire SVP and high-resolution audio signals. At the end of the chapter, different methods for signal processing and analysis were implemented to synchronize data and extract features from snoring and relate it with medical data, from PSG and its reports.

The Results chapter presents information for the different steps in the high-resolution snoring signal processing. From the synchronization between this signal and the PSG data, following feature extraction, and the relationship between medical data and research data, several tables and figures are available to ease the interpretation of the achieved results. Finally, the results from the statistical analysis are presented.

Chapter Discussion analyses the main findings and the main contributions to science, while chapter Conclusion presents the final conclusions, and future directions to make automatic sleep assessment faster, cheaper and reliable. Finally, the scientific contribution to the knowledge in this field is available.

Chapter 2

Sleep and Sleep Disorders

This chapter introduces the concept of sleep, its structure, and the role of sleep in homeostasis. Sleep quality, sleep fragmentation, and sleep deprivation are related and they are modulated by a great number of factors, like stress, alcohol, and drugs.

The sleep medicine field deals with sleep-related problems and the most important tool to diagnose and track those health issues is the PSG study. It is a multi-parameter study with a special focus on neural activity of the head and in the respiratory muscles.

One of its parameters, the snoring, is very interesting because it is one of the earliest symptoms of OSAHS and it is present in the entire evolutionary process.

2.1 Introduction

Natural selection promoted the human species evolution towards a cyclic behaviour on a daily basis, known as circadian rhythm. Throughout a full day, a subject, of the human species, goes through different levels of activity. Sleep is one of the natural and reversible daily states in the human species. Besides the sleep state, wakefulness is an important state corresponding to the period of time with the highest activity. A state transition from wakefulness to sleep may be linked by a third state, drowsiness [24].

Sleep is recognized as a state of behavioural quietness, with eyes, usually, closed and there are ongoing complex physiologic and behavioural processes. Other less frequent behaviours may occur during sleep as is the case of sleepwalking and teeth grinding [3]. While asleep, a subject decreases its consciousness and its response to both internal and external stimuli to a point of little or even no response at all. The reduction of response to external stimuli is, however, selective. It depends on the origin of the stimulus, for example, the probability to awake due to a crying baby is higher than another sound of the same intensity [1]. This state has the lowest level of activity present in the circadian rhythm [3].

Sleep hygiene is essential to promote the quantity and quality of sleep. Together

with other conditions, inadequate sleep hygiene may boost SRBD, like insomnia. The last hours of the day, before going to bed, play an important role in sleep hygiene. Specialists do recommendations to keep or improve sleep hygiene. The first one is to take a time to relax and, then, go to bed, a cool, dark, quiet, and comfortable space, at the same hour. Wake up at the same hour and having regular meals. Avoid the consumption of products containing nicotine, caffeine, and alcohol before going to bed. Nicotine and caffeine are stimulants, and alcohol is responsible for sleep fragmentation [1, p. 7; 3, p. 869; 25, p. 98].

Sleep and wakefulness regulation is controlled by 3 components. The first 2 components, circadian rhythm and sleep homeostasis, work together to regulate timing and consolidation. Sleep homeostasis regulates sleep pressure by increasing it while a subject is awake and decreasing it when a subject is asleep [4, 26]. The process behind the circadian rhythm helps to keep a subject awake during the day. There are 2 peaks in which is less likely to fall asleep. The first one occurs late in the morning while the second one occurs early in the evening [4, 27, 28]. Sleep and wakefulness pattern follows the day and night cycle, but an internal circadian clock keeps the mechanism working even without external time evidence. The last component in sleep and wakefulness regulation is sleep inertia. Sleep inertia may last from 30 minutes to 4 hours, depending on the sources. It may also occur after oversleeping, and naps exceeding 30 minutes [1, 4].

2.2 Sleep Characterization

2.2.1 Sleep Architecture

Normal human sleep pattern is heterogeneous throughout the night and it is organized in 2 distinct types of sleep: the Non-Rapid Eye Movement (NREM) sleep stage and the REM sleep stage. The NREM sleep stage is further organized in NREM1 or N1, NREM2 or N2, and NREM3 or N3. Figure 2.1 is a representation of the sleep architecture.

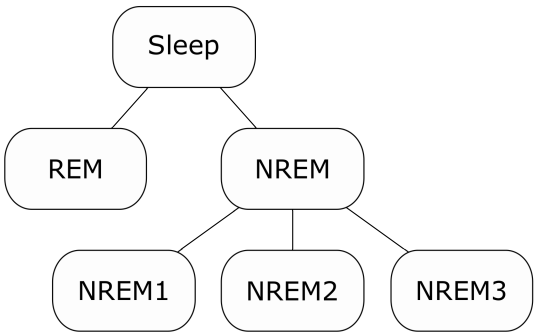

Figure 2.1: The sleep architecture organized in its different sleep stages for a healthy human, accordingly with the American Academy of Sleep Medicine (AASM) scoring manual.

The sleep onset starts with N1 sleep in a typical and healthy adult human, evolving, chronologically, to N2, then to N3, and, finally, to REM. The completion of a sleep cycle occurs when sleep enters in REM sleep, and it starts a new one when sleep returns to N1 or N2 sleep. Figure 2.2 is a representation of a hypnogram, a two-dimension graphic of the sleep architecture over time. Sleep profile is clear, with the predominant sleep stage and the respective transition.

A whole night of sleep may have 3 to 5 sleep cycles, each of which lasts between 90 and 120 minutes, and the contribution of each sleep stage to a sleep cycle changes overnight [4, 24, 25]. Sleep stage contributions to overall sleep are dramatically different with a subject spending, approximately, 5% to 10% of the Total Sleep Time (TST) in the N1 sleep stage, while sleep is in the N2 sleep stage between 45% and 55% of the time. The last REM sleep stage, N3, represents between 15% to 20% of the TST, and it is higher in the first sleep cycles than in the last sleep cycles. REM sleep stage contributes to overall sleep with values between 20% and 25% of the TST, lasting more time at the sleep's end [3, 4, 24, 25].

2.2.1.1 Non Rapid Eye Movement 1 Sleep

Healthy adult subjects fall asleep, usually, in the N1 sleep stage. Low Amplitude and Mixed-Frequency (LAMF) signals are characteristic of this sleep stage, and they encompass frequencies, mostly, between 4 to 7 Hz. During the N1 sleep stage there is lack of sleep spindles and K-complexes not associated with arousals. There is the possibility of slow eye movements occurring [24]. N1 is light sleep, from which the subject can wake up easily.

2.2.1.2 N2 Sleep

N2 sleep stage has sleep spindles or K-complexes not associated with arousals. Sleep spindles have a frequency range from 11 to 16 Hz, being the frequency range between 12 and 14 Hz more common, and duration between 0.5 and 2 seconds. The first sleep spindles start, gradually, to increase in amplitude, and the last ones lose, gradually, their amplitude [24, 25, 29]. K-complexes start with a hard negative wave

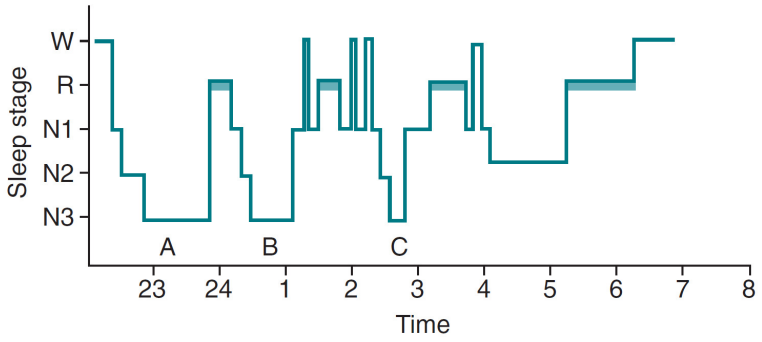

Figure 2.2: A hypnogram of a healthy and adult subject [24].

and progresses with a slower positive wave. They last for, at least, 0.5 seconds [24, 25]. Eye movements, typically, stop and the electrical signal has a lower amplitude than when a subject is awake, although those signals oscillate [3, 24].

2.2.1.3 N3 Sleep

N3 sleep stage is considered to be deep sleep, the hardest phase of NREM sleep to awake from. The transition from N2 to N3 sleep stage depends on the existence of slow-wave activity, a brain activity between 0.5 and 2 Hz with peak-to-peak amplitude higher than 75μV. When more than 20% of the time of an epoch has slow-wave activity, the sleep is at the N3 sleep stage [3, 24]. For this reason, N3 is, also, known as Slow-Wave Sleep (SWS). An epoch is defined as a period of time of 30 seconds, the basic unit of time for PSG scoring. Further discussion about PSG will be presented ahead.

2.2.1.4 Rapid Eye Movement Sleep

As the name suggests, the REM sleep receives its name because an exclusive characteristic of this type of sleep, the fast movement of the eyes. Skeletal muscle atonia is responsible for this behaviour. The skeletal muscle atonia is the result of the decrease in the activity of the electrical control signals by the neurons. The electrical signal, in the muscles, has, usually, the lowest amplitude of the entire sleep period.

Brain electrical activity, in REM sleep, resembles its activity when a subject is awake. REM sleep is known as paradoxical sleep because of this brain electrical behaviour. In REM, brain electrical activity have LAMF activity, theta and beta rhythms. Alpha waves are slower, 1 to 2 Hz, than the same type of waves present in the wakefulness and in the N1 stage. Sawtooth waves, with frequencies in the theta range, may, also, be present [4,24,30,31]. REM sleep is recognized as an active stage of sleep, with an increase in energy consumption, when compared with NREM [25]. People dream more and dreams are more elaborated at this sleep stage [4].

REM sleep is classified in two subclasses depending on the brain muscular and eyes electrical activity. Tonic REM sleep is characterized by desynchronization of the brain electrical activity, skeletal muscle atonia and absences of both reflexes, monosynaptic and polysynaptic [30, 31]. Phasic REM sleep has rapid eye movements in all directions, oscillations in the blood pressure and in heart rate, irregular respiration, tongue movements, and myoclonic twitching of the facial and limb muscles, and spontaneous middle ear muscle activity [30,31]. The classification of REM sleep in tonic and phasic is not, currently, recognized by the AASM in its scoring manual.

2.2.2 Sleep and Ageing

Sleep pattern is dynamic, it changes with age, and its duration decreases over time. Newborns sleep, around, two-thirds of the day, with an, roughly, even distribution between REM sleep and NREM sleep, while young adults have a sleep duration between 7.5 and 8.5 hours [3]. The elderly just need a few hours of sleep per day and its major component is NREM sleep. Figure 2.3 presents the relationship between the number of hours asleep and a subject's age. The number of hours in both NREM and REM sleep is, also, represented.

After reaching adulthood, subjects have a percentage of REM sleep, almost, steady throughout life, with values around 19% and 22%, depending on the sources. It starts to decrease later in life, with values between 11% and 19% for subjects above 60 years old [32, 33]. REM sleep density, also, stay steady [34, 35]. Young adults have a sleep efficiency of 95%, but it starts to decrease immediately, achieving values around 70% for subjects with more than 80 years old [1, 36, 37]. The percentage of N3, deep sleep, also decreases with age, and evidence has been found of a decrease in both the slow-wave activity and slow-wave density [38]. The percentage of N1 and N2 sleep, and the wakefulness periods, during the night, also increase with ageing. Sleep spindles decrease in number, amplitude and frequency [1, 3, 38].

Sleep architecture is also a function of age, with both genders having their sleep structure modified [3]. In men, N1 and N2 sleep stage percentage increases while stage N3 and REM percentage decrease over time. Men spend 5.8%, 61.4%, 11.2% and 19.5% of their time sleeping in, respectively, N1, N2, N3, and REM when aged between 37 and 54 years old, while older men, above 70 years old, the percentage value asleep is of 7.6%, 66.5%, 5.5%, and 17.8%. Women have a slight difference, with N1 and N3 sleep stage percentage increasing, while N2 and REM sleep stage percentage decreases over time. For the same age groups, the evolution of N1 goes from 4.6% to 4.9%, N2 goes from 58.5% to 57.1%, N3 goes from 14.2% to 17.2% and REM goes from 20.9% to 18.8% [3].

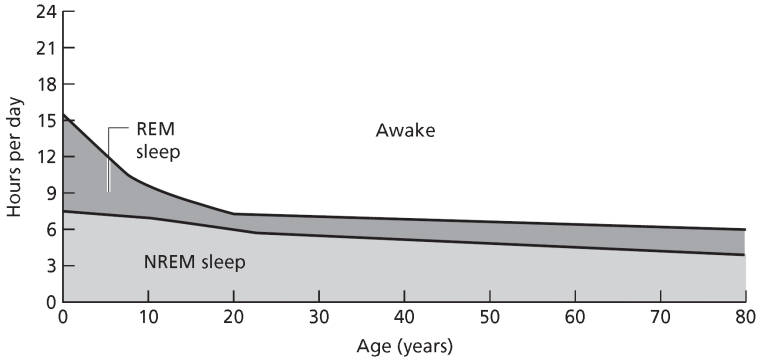

Figure 2.3: A representation of the relationship between the number of hours sleeping and ageing. The time spent in both REM and NREM sleep is, also, represented [1].

2.2.3 Gender and Sleep

Sleep pattern has slight differences between men and women, with men presenting more sleep impairment and disruption than women in advanced ages [38]. Men have, always, higher percentage values of N1 sleep stage than women, of all ages, and N1 sleep stage increases with ageing for men, while women don't correlate changes in N1 sleep stage with ageing.

Men and women also have significant differences in N2 and N3 sleep stages. Men have higher percentage values of N2 sleep stage, and its weight in the overall sleep increases with age, while women age with stable values of N2 sleep stage percentage. N3 sleep state decreases with age in men, while it increases with age for women. REM sleep is significantly affected by age in both sexes, with a decrease over the years, and men have lower REM sleep than women [33].

A study with the participation of 512 subjects with 25.3 ± 0.65 years old, 227 men and 285 women, analysed sleep duration and it found that women tend to sleep, 7.2 ± 0.82 hours, more than men, 6.8 ± 0.91 hours [39]. A study on circadian rhythm analysed sleep patterns of 52 women and 105 men, aged between 18 and 74 years old, with 33.1 ± 17.4 years old and it found that the women's circadian rhythm is significantly shorter, 24.09 ± 0.2 hours, than the circadian rhythm of men, 24.19 ± 0.2 hours [40]. Other factors, like the menstrual cycle, pregnancy, labour, lactation, and menopause, may play an important role in sleep modifications in women [1, 41].

2.2.4 The Function of Sleep

Sleep plays a critical role in the development of a healthy subject. Both the mind and the body benefit from good sleep hygiene, as well as the maintenance of homeostasis, and multiple functions are sleep-dependent. Sleep is recognized to be fundamental in survival, thermoregulation, promoting several brain tasks, the elimination of toxins, the immune system, energy conservation, and in anabolic processes. Sleep has, also, influence in performance, vigilance, attention, and concentration [4, 31]. Hereafter, some of the functions of sleep are described.

2.2.4.1 Brain Function

The brain is one of the structures of the human body taking more benefit from sleep. Sleep promotes an active consolidation of memory by reactivating the newly formed representations [42]. Memory function is the result of the implementation of 3 sequential processes. The first process is learning, in which a subject acquires and encodes the information to create the memory. The consolidation process helps to reinforce the newly formed memory, prone to disappear, while the recall process accesses memories stored, which helps to strengthen memory [43]. Sleep links to the second process, the consolidation process, although this process may, also, exist

during wakefulness [43, 44]. Researchers agree on the link between memory function and sleep, however, the mechanisms behind the different types of memories, their consolidation, and which sleep phase is, still, a subject of analysis and discussion [45]. Some authors claim the existence of a clear separation between functions [5,43]. Each sleep stage is associated with the consolidation of different types of memory. For example, N3 sleep is responsible for strengthening the consolidation of declarative memory, while REM sleep is important in the consolidation of procedural memory. Some authors defends a more complex structure for memory consolidation, with NREM sleep and REM sleep playing a complementary role [46]. There are evidence of N2 sleep to be linked with memory consolidation [46, 47].

2.2.4.2 Immune Function

The immune system is a defensive mechanism to protect the host against diseases and it has the ability to create memories. It remembers previous actions against suspicious elements inside the body [6]. There is a theory that mimics the brain memory formation to the immune system, with N3 sleep playing an important role [48]. Tests in animals are in line with this theory [49]. An experiment in vaccination against hepatitis A studied the effect of sleep deprivation the night following the vaccination. The results suggest that sleep improves the immunologic response, by increasing the formation of antibodies. Subjects who slept on the first night had 2 times more antibodies than those who does not, after 4 weeks [50]. Sleep deprivation may, also, promotes inflammatory response in healthy young subjects [51]. In other words, sleep is healing.

2.2.4.3 Endocrine Function

Sleep impairment and disruption have a real impact on the regulation of glucose [52, 53]. Studies had confirmed the relationship between the presence of SRBD and the development of type 2 diabetes. Hypoxia is a common condition in SRBD, and it is recognized to trigger the release of insulin antagonists, thus increasing insulin resistance [54]. The prevalence of Sleep Apnoea-Hypopnea Syndrome (SAHS), 1.9% of the total male diabetic population, was found to be significantly higher ($P < 0.001$) than among male subjects without diabetes, 0.4%. Even lean young subjects, without cardiometabolic diseases, may have an increased risk of developing type 2 diabetes when in the presence of OSAHS. Results of the experiment show OSAHS patients with a lower insulin sensitivity of 27% and an increase of 37% in insulin secretion when compared with control subjects [55]. SRBD prevention is fundamental to avoiding the development of metabolic diseases, but insulin resistance due to intermittent hypoxia could be improved by performing high-intensity exercises [56]. The relationship between sleep and the endocrine system is far more complex, with sleep quality and quantity being important to maintaining hormonal

balance. Growth hormone, prolactin, and sex hormones are examples of sleep-dependent hormone production [57]. This relationship, between sleep and the endocrine system, is bidirectional, and melatonin is an example of the influence of a hormone in sleep regulation [58]. The hormone promotes sleep and its production occurs in low light and night periods. Impairment in the endocrine system balance can affect sleep, significantly [57].

2.2.4.4 Energy Function

Energy conservation has been linked with sleep as a function of it [59]. Energy conservation during sleep is between 100 and 200 calories per day and, on average, a man spends 2500 kcal, while a woman spends 2000 kcal [1, 31]. In NREM sleep, the metabolic rate drops between 5% and 10%, when compared with wakefulness, while it is similar in REM [1]. Some researchers claim these values are insufficient to consider energy conservation a function of sleep, considering that one-third of the day is spent sleeping [31]. In an experiment with 7 healthy participants, 22 ± 5 years old, perform an energy consumption evaluation for 3 days. The first 24 hours were normal, 16 hours of wakefulness and 8 hours of sleeping, followed by 40 hours of wakefulness and 8 hours sleep. When compared with the first day, the second day, sleep deprivation, had a significant increase of 7% and on the third day, sleep recovering, had a significant decrease of 5% in energy consumption. A night period comparison revealed a significant increase of 32%, on sleep deprivation night, and a significant decrease of 4%, on sleep recovery night, in energy consumption when compared with the first night. Low energy savings may be justified as a balance between metabolic savings and an increase in processes sleep-related [60]. Energy consumption generates sub-products and they are accumulated by the body during wakefulness. Sleep allows the removal of those waste sub-products from the brain, avoiding an imbalance between oxidants and antioxidants. Some of those waste products, from brain activity, are linked with neurodegenerative diseases [61].

2.2.4.5 Cardiovascular Function

The cardiovascular system links with sleep and its functioning are sleep stage dependent. When compared with the wakefulness state, some of the cardiovascular system parameters have the following behaviours. During NREM sleep, the heart rate, the cardiac output, the blood pressure, and the cerebral circulation decrease, the peripheral vascular resistance keeps steady or with a slight decrease, and the cutaneous circulation increases. REM sleep separation in tonic and phasic allows to understand the cardiovascular system better. The tonic sleep is similar to the NREM sleep, with a difference in the cerebral circulation, it increases, in the peripheral vascular resistance, it decreases, and in the cutaneous circulation, it is variable. In the phasic sleep, all but one of the previous parameters increase, and the cuta-

neous circulation is variable [1, 4]. Sleep deprivation may trigger a brain response to increase the production of white cells, with an experiment in mice showing the increase in white cells production and the existence of more severe atherosclerosis [62] The response to sleep deprivation, also, triggers an inflammatory response, and [51]. A study on females, aged between 45 and 65 years old, and without coronary heart diseases in the beginning, was performed to assess sleep duration and coronary diseases. Of the 71617 females, there were 934 coronary issues reported. After adjusting for diabetes and hypertension, females sleeping less than 5 hours per day had an increase of 39%, when compared with females sleeping 8 hours. Oversleeping can be, also, harmful, with an increase of 37% for females sleeping more than 9 hours [63]. Other studies confirm these observations [64, 65]. Shift workers are, also, prone to developing cardiovascular diseases, with a significant risk of ischaemic heart disease higher than in day workers. The relative risk for shift workers was 2.2, $p < 0.04$, when working for 11 to 15 years and 2.8, $p < 0.03$, when working for 16 to 20 years under these conditions [66]. A study in a male population shows a significantly higher prevalence of SAHS in subjects with hypertension, 0.96%, than in subjects without hypertension, 0.34% ($p < 0.05$) [67].

2.2.4.6 Respiratory Function

The respiratory system decreases its activity during sleep. The respiratory drive, the upper respiratory airway dimension, and the chest wall muscles activity decrease during sleep, more during the REM sleep than during the NREM sleep. The respiratory pattern is regular in each of the NREM sleep, but it changes in the transition from one sleep stage to the next one. In REM sleep, it is widely accepted the existence of chest muscle atony in all muscles but one, the diaphragm muscle keeps its function, but more recently, new evidence point to a second muscle keeping its function, the parasternal intercostal [1, 68].

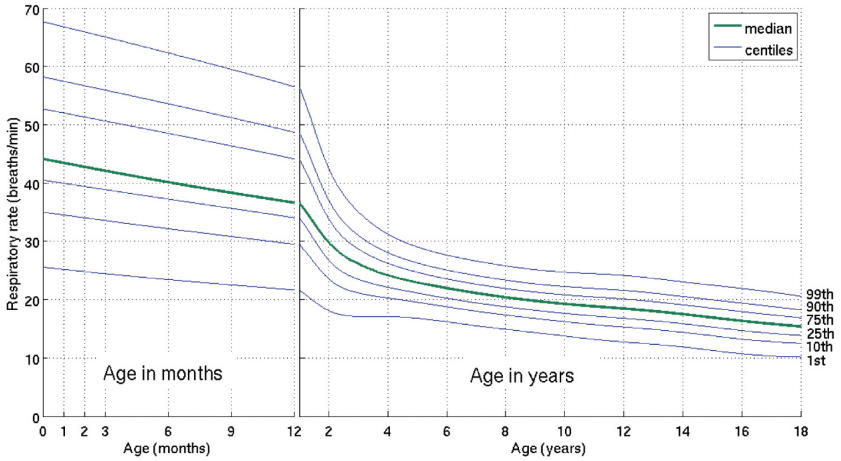

Figure 2.4: The relationship between respiratory rate and ageing from birth to the age of 18 years old. At the age of 18 years old, respiratory rate is similar to young adults [69].

The upper airway resistance is higher in sleep than in wakefulness, with the highest values of resistance being measured in NREM sleep [1,70]. Oxygen demands are correlated with body activity, the higher the activity. the higher is the demand for O_2. The respiratory system response is to change the volume of air inhaled, in each breath, and the respiratory frequency. During sleep, body activity decreases, the demand for O_2 decreases, and the respiratory rate, also, decreases. In healthy adults, the respiratory rate, at rest, is between 10 and 18 breaths per minute, with an average of 12 breaths per minute [3, 69]. Figure 2.4 has the evolution of the respiratory rate at paediatric age. Subjects who are 18 years old, already have a respiratory rate of an adult.

2.2.4.7 Social Behaviour and Mood

How we sleep and how long we sleep influence our social behaviour. A recent experiment by [71] found that the lack of sleep induces subjects to loneliness and to avoid social interactions. Those behaviours are known to increase the mortality risk [72]. Sleep affects the mood during the wakefulness state [73].

2.2.4.8 Thermoregulation

Another function of sleep is in temperature regulation [42]. There is a temperature drop immediately after the transition from the wakefulness state to NREM sleep [74]. The drop in temperature is, probably, due to the drop in metabolic rate and due to vasodilatation [1]. The body temperature drops between 1 and 2^{o}C [59]. The transition from NREM sleep to REM sleep is followed by an increase in temperature [74, 75].

2.2.5 Sleep Modulation Factors

A great number of factors may have a decisive factor in sleep modulation, and they are related to physiological function, but also to how we live.

2.2.5.1 Physical Exercise

The link between exercise and sleep is not fully acknowledged since most of the studies were performed on good and/or young sleepers [76]. Intense physical training in the hours before bed can disrupt sleep [24]. A subject performing regular exercise has less REM sleep, which acts as an anti-depressant over time [77]. Regular exercise increases SWS and TST, and it decreases Sleep Onset Latency (SOL) in good sleepers [78]. Subjects with SRBD may improve their sleep quality by executing moderate physical exercises [76]. Acute exercise have the same effect in REM sleep, SWS, TST, SOL. REM sleep latency also increases [78]. Children and young adults, with sleep quality, improve SOL by performing exercises 2 to 3 hours before bedtime [77]. Older adults may, also, improve their sleep by performing exercises [79].

Exercises may help in sleep duration, especially, if associated with depressive symptoms [80]. Nevertheless, exercise and sleep may compete for time, but exercise must not be performed at the expense of the duration of sleep [81].

2.2.5.2 Tobacco

Smoking is associated with a longer SOL and REM latency, and a decrease in TST (higher periods of awake time during the night), in SWS and in sleep efficiency [82, 83]. Active smokers are not the only ones that have their sleep changed by tobacco smoke, and passive smokers also have a modification in their sleep. Approximately 40% of the Japanese adolescents that never smoke are passive smokers, and a survey used several parameters to evaluate the quality of their sleep and identifies that passive smokers have, generally, worst scores when compared with subjects that never have been neither active smokers nor passive smokers [84]. A study, involving the nicotine effect on the brain, had discovered sleep spindles modulation by this molecule. Nicotine is known to enhance cognitive function, and the study reported that nicotine changes sleep spindles amplitude, density, and duration [29].

2.2.5.3 Alcohol

Alcohol abuse is acknowledged to be sleep disruptive [24]. A paper review analysed the alcohol impact on sleep for 3 levels of consumption, low ($0.15 \geq x \geq 0.49 mg/kg$), moderate ($0.5 \geq x \geq 0.74 mg/kg$), and high ($\geq 0.75 mg/kg$), and for sleep data from the first half of the night and from full night studies. Most of the studies analysed sleep quality after the subjects drank a single dose of alcohol, right after going to bed. Data analysis for the first half of the night reported, for most of the studies, an increase in SWS and a decrease for both SOL and Wake After Sleep Onset (WASO) for all the levels of alcohol consumption. REM sleep changed with the different levels of consumption. There is a balance, for low levels of consumption, between studies reporting an increase and the studies reporting a decrease in REM. Moderate and high levels of consumption had, respectively, a prevalence of studies reporting an increase and a decrease in REM. Most of the studies focusing in full night sleep analysis reported an increase in WASO and in the latency of REM onset. REM sleep increased for low levels of consumption but decreases for the remaining levels. SWS decreased for low levels of consumption, increased for high levels of consumption and it there is a balance between studies reporting a decrease and those reporting an increase for moderate levels of consumption [85]. Alcohol changes brain function at the neurotransmitter level. Drinking alcohol improves sleep in the first half of the night for non-alcoholic subjects but it induces sleep disruption, especially, in the second half of the night [86–88].

2.2.5.4 Caffeine

The consumption of caffeine before bed may change sleep, even in low doses [24, 89]. Caffeine is well known to interfere in sleep homeostasis, by slowing down sleep build-up during wakefulness [90]. In fact, drinking coffee in the afternoon, up to 6 hours before going to bed, may disrupt sleep. A study analysed the effects of drinking coffee, by ingesting a 400 mg caffeine pill, in a population of 12 healthy subjects without SRBD. Pill intake occurred 0, 3, or 6 hours before the subjects went to bed [91]. The results showed, for example, a reduction of sleep by 1 hour, SWS by 22 minutes and sleep efficiency by 9%, and an increase in WASO by 8 minutes and in SOL by 24 minutes, for subjects taking the pill 6 hours before bedtime. Other studies reported caffeine intake, $200mg$, 16 h prior to bedtime may disrupt sleep [92]. Sleep duration and non-restorative sleep are inversely proportional, and the higher the intake of caffeine, the higher the risk of non-restorative sleep for the same amount of sleep duration, especially for low values [93]. Caffeine may have a stronger sleep disruption effect in older adults than in younger adults [94]. High consumption of caffeine, $\geq 300mg/day$, by women during pregnancy and nursing did not increase awakening frequency in their 3-month-old babies [95]. A caffeine abstinence study reported sleep quality did not improve, significantly, for caffeine doses up to $120mg$ [96].

2.2.5.5 Medication

Medications are an important tool in Medicine to fight or prevent diseases, or to perform a diagnosis. Sleep disruption can be mitigated by using the appropriate medication. Sleeping pills target neurotransmitter brain cells to regulate their activity and promote sleep. Pharmaceutical industries have a wide offer of sleeping pills and they change sleep architecture. There are sleeping pills, benzodiazepines, effective in the treatment of insomnia and awakenings in short periods of time [97, 98]. Those pills have relatively long periods of elimination half-life (>5 hours) and can be a hazardous condition during the day, causing sleepiness or drowsiness. While effective in the short term, the long-term use of these medications is not proven to be effective. Addiction may occur with these and other medications, for example, barbiturates, chloral hydrate, and clomethiazole [99, 100]. Z-medication sleeping pills, zolpidem, zopiclone, and zaleplon, also improve insomnia and they belong to a group of sleeping pills with a short half-life. Elimination of half-life is fast as 1h, which means an individual can have a normal daytime lifestyle, without somnolence and drowsiness, due to the medication effect. On the other hand, high rates of half-life may be too fast to sustain sleep throughout the night [99]. Factors like the dose or group age may have an influence in the existence of sleep architecture changes [97, 101].

2.2.5.6 Substance abuse

Substance abuse is a world problem, with addiction-associated problems. Drug consumption, and its influence on sleep, are strongly related to the used substance [102]. A report from 2017 estimated that 5% of the world population used drugs, at least once in 2015, and 0.6% had drug use disorders and they require treatment [103]. Data from 2015 and compiled from the World Health Organization, the United Nations Office on Drugs and Crime and the Institute for Health Metrics and Evaluation pointed to a prevalence, among the adult population, of 3.8%, 0.77%, 0.37%, and 0.35% for, respectively, cannabis, amphetamine, opioid and cocaine in the last year [104]. In the same year, a report analysed the consumption habits in 24 European countries. A total of 18% of the teenagers, between 15 and 16 years old, had already consumed cannabis, and less than 5% consumed other drugs (MDMA/ecstasy, amphetamine, cocaine, methamphetamine, and hallucinogens). Estimation of drug consumption, at least once, among older individuals, between 15 and 64-years-old, was estimated to be around 25%. The prevalence was higher among male individuals, 56%, with cannabis being the most consumed drug [105]. In the United States of America, during the year 2016, 18% of the population used illicit drugs (including the misuse of prescribed medication) [106].

The influence of substance abuse on sleep is well known to induce disruptive effects and to increase the difficulty to fall and stay asleep [107]. Generally, the consumption of illicit drugs, both acute and chronic, is associated with the deterioration of sleep. Acute consumption of both cocaine and ecstasy leads to an almost suppression of REM sleep. SOL increases with cocaine and high doses of cannabis, TST decreases with cocaine and ecstasy long-term consumption. An increase in WASO and N1 and a reduction in N2 is associated with ecstasy long-term consumption. REM sleep decreases with cannabis. Low doses of cannabis may improve SOL, but it is followed by arousals [108]. Withdrawal also has implications in sleep architecture [102]. In the case of cocaine, SOL, TST and sleep efficiency deteriorates, but with an improve in REM. REM sleep time increases significantly in the first nights, but it decreases in the following nights [109]. SWS patterns follow an inverse pattern. Cannabis withdrawal increases SOL, WASO and REM, and it decreases SWS. There are benefits from the consumption of cannabis, specially cannabis-based pills, with improvements when the patients have chronic pain [108].

2.2.5.7 Behaviours

Healthy sleep habits include going to sleep when sleepy, but keeping, always, a schedule for bedtime and to awake, with a proper number of sleeping hours. Napping is a potential factor to disrupt sleep quality. The best practices for a good night of sleep require a routine to relax before going to bed. It is also recommended to ease

the mind, by avoiding worrying and brainstorming, and to neither eat large meals nor drink lots of liquids. The natural night is a good regulator of the circadian rhythm, by controlling the release of melatonin. The bedroom must be quiet, relaxing, at a comfortable temperature, with no or little light, and be used in tasks. Pet animals may be responsible for awakenings during the night, and they must be locked away from the bedroom. When there is an incapacity to fall asleep, the individual must get up after 20 to 30 m in bed [1, 1, 4, 24].

2.2.6 Sleep Deprivation

Sleep deprivation is a common and relevant condition in our society and it is linked to a vast number of factors. The most visible and immediate effect of this condition is Excessive Daytime Sleepiness (EDS). It may be reversed by some variables, like activity, temperature, drugs, and motivation among others, in the early phase. A study in sleep deprivation found that an individual is capable of delivering a subjective analysis of the degree of EDS up to some point. Beyond that point, the individual is unable to recognize that the condition is getting worse [110].

Work shift forces workers to, continuously, disrupt the sleep-wake cycle. In the United States, the most common alternate shift, the afternoon to midnight schedule, represents 6.8% of the total workforce [111]. Health problems, being capable of disrupting sleep, social or work pressures, and volunteer acts are other factors leading to sleep deprivation. As a consequence, health issues arise from this condition, like mood and performance impairments, in positive feedback, which leads to the deterioration of quality of life [112]. Insulin resistance, response time and accidents (they increase), and memory, performance, concentration, cognition, vigilance and attention (they decrease) may be unbalanced by sleep deprivation [24, 31, 113].

EDS may arise from sleep deprivation and their related factors lead to the increase in mortality and the number of years lived with disability. In its most severe form, on the edge of falling asleep, is present in 13.1% of the population of Iceland and Sweden [114]. Professional drivers are more sensitive, and EDS can significantly predict truck accidents (Odd Ratio = 1.73, CI95%=1.15–2.61) [115]. Young drivers are also more susceptible to accidents because even when they are aware of their sleepiness they keep driving [116].

Structural changes, in sleep, occurred in the nights of sleep recovery, after sleep deprivation, with an increase in SWS rebound in the first night at expense of the other sleep stages. In the second night there is, usually, REM rebound [25].

All age groups suffer from sleep deprivation, and students reported to their teachers they are sleepy, with some data pointing to a range between 40% and 80%, country-based data [117, 118]. A Swedish study focuses its analysis on the adult population, aged between 30 and 65 years old, and their sleep deprivation problems.

From the population under analysis, 28% of the women and 21% of the men had too little sleep [119]. The effects of sleep deprivation in the different group ages have a different impact. The younger the individuals are the more susceptible to the effects of sleep deprivation they seem to be [3, 4, 31].

2.2.7 Sleep Medicine

Sleep medicine is the field dedicated to the study and comprehension of normal sleep and the application of treatments for SRBD. Until the 19$^{\text{th}}$century, the sleep study focused on a subjective analysis of information provided by the sleeper and the observation of the sleeper's behaviour during sleep. The study of sleep evolved significantly in the 20$^{\text{th}}$, especially, in the second half, and, at this point, systematic methods, to study sleep, started to be implemented. Acoustic external stimuli, with different levels of sound intensity, were used to study the depth of sleep and the effects of sleep deprivation. The use of questionnaires and scales to assess sleep were some of the methods implemented [120, 121].

Until the 20$^{\text{th}}$century, most scientists and physicians believed that sleep was a passive and homogeneous state, without scientific interest. At the time, they understood sleep as a chain of events, with subjects entering this state as a result of a decrease in sensor input and, as a consequence, a decrease in brain activity. Nevertheless, some remarkable observations have been made. Jean-Jacques de Mairan observed the existence of an endogenous circadian rhythm, by keeping plants all day in the dark. John Cheyne and William Stokes were the first to describe the Cheyne-Stokes respiration, and Jean Géllineau was the first to describe narcolepsy [4, 122]. Hitherto, there was not any distinction between sleep and other states, like comma or hibernation, in the minds of scientists and physicians. This was the main line of thought until the discovery of REM, in the 20$^{\text{th}}$ [3].

The 20$^{\text{th}}$century was a time when major discoveries were made in this field, leading to a huge leap forward in the understanding of the importance of sleep. In the 1920s, Hans Berger recorded brain electrical activity in subjects and, then, he was able to observe electrical differences between the sleep state and awake state. Nathaniel Kleitman observed that subjects awake all night were, typically, less sleepy and impaired in the morning than in the middle of the night [3, 122]. The brain's electrical activity, and the different patterns associated with sleep, were described by Loomis, among others [123].

The discovery of REM sleep was a definitive turning point in the general acceptance of the importance of sleep. In the 1950s, Eugene Aserinsky and Nathaniel Kleitman started to register the electrical activity around the eyes and they observed bursts of electrical activity, REM sleep. The increase in heart rate and the existence of irregular respiration led them to associate, REM sleep with dreaming.

To confirm this assumption, they performed awakenings in the subjects when REM was occurring and when it was not. The sleep cycle, and its duration, were later found by William Dement and Nathaniel Kleitman when they decided to do full-night recordings. They, also, calculated the average amount of REM percentage, between 20% and 25%, and they observed that the amount of REM sleep was less common at the beginning of the sleep than later in the night [3, 31, 122].

2.2.8 Sleep Study - Polysomnography

The term PSG was coined to describe a study performing data recording of synchronized multiple physiologic parameters during sleep. Nowadays, it is considered the gold standard in the sleep medicine field and it allows the study of sleep, to enhance the knowledge about normal sleep and its disorders, the diagnosis of SRBD, and the assessment of the treatment.

The first known compilation of rules, with global acceptance, to score data from PSG was suggested by Allan Rechtschaffen and Anthony Kales and it was published in 1968, the R&K Manual. The R&K manual was the first world reference, for decades, for sleep laboratories until 2007 [121, p. 96]. In that year, AASM published the *The AASM Manual for the Scoring of Sleep and Associated Events*, a new manual to gather and add state-of-the-art information in the scoring process. Since that year, AASM is the responsible to keep updated the most important manual in the world in sleep assessment.

Those subjects with medical prescriptions to undergo a PSG study, in the sleep laboratory, should prepare to sleep away from home. At the CMS, the overall process starts at 21h30m, with the sleep technicians following the protocol to prepare the subject to perform the PSG study. Sleep technician asks for details about the subjects, sleep habits, anthropometric data, medication, and consumption habits are among the typical questions. The sleep technician starts the patient's session, on the computer, and, then, the subject's preparation starts with the measurement of the head, which is followed by the placement of the sensors on the skin's surface. The multi-parametric PSG records are detail in the following sections.

A local concentrator receives all the signals and provides the first data processing techniques, implementing signals' amplification, filtering and digitization. Data collected from the subject was transmitted, via cable, to a computer room, in a dedicated room. This room has computers with the appropriated software to manage data storage and data visualization. Both physicians and sleep technicians can visualize, and perform offline scoring to assess the subjects' sleep quality. An infrared webcam, with video and audio capability, also streams data to the dedicated room, providing more information about the patient's sleep quality [4].

Sleep technicians must ensure the skin-sensor interface has low impedance values

and proceed to correction if necessary. At the onset of sleep time, subjects lay on the bed and the PSG data acquisition, for sleep evaluation, starts, by pressing the software lights out button. Sleep technicians are an all-night vigilance to help subjects and solve acquisition problems.

The full-night PSG has a flexible time duration and, at the CMS, the study must have, at least, 6 hours of data acquisition and, in normal situations, it does not need to exceed 8 hours. Around 7 a.m., sleep technicians end the data acquisition procedure, formally by pressing the software lights on button, and woke up the patients. Sleep technicians detach sensors, in most cases, from the subjects, and they finish the reports of each subject.

2.2.8.1 Channels

The study of sleep, based on PSG, is versatile, and the number of channels as well as the type of data collected is adjusted to the requirements of each patient [4]. Data collected for the PSG study may be categorized into 3 different types. The bioelectrical potentials are electrical signals produced by the body, and the brain, the eyes, the heart, and specific skeletal muscles activity are important to understand sleep and they are collected to have, respectively, the Electroencephalogram (EEG), the Electrooculogram (EOG), the Electrocardiogram (ECG) and the Electromyogram (EMG). Non-electrical physiological signals are collected by sensors known as transducers, and they work by converting non-electrical physiological signals into electrical signals. The snore, the oronasal respiration, the thoracic and abdominal respiratory movements, and the body position are collected using transducers. Auxiliary devices are the third category and the pulse oximetry sensor is the most common example.

2.2.8.1.1 Electroencephalography Most of the PSG studies use 6 derivations from the complete EEG, according to the International 10–20 System of Electrode Placement, to monitor the brain electrical activity. A complete EEG may be required to rule out epilepsy. At the CMS, the PSG derivations are the O1, C3, F3, O2, C4 and F4. The first 3 are a reference to M2 while the remaining 3 are a reference to M1.

The O1/M2 and the O2/M1 derivations are important to assess occipital electrical activity, the C3/M2 and the C4/M1 to assess central electrical activity, and the F3/M2 and the F4/M1 for the frontal electrical activity. The occipital derivations are suitable for alpha rhythms detection, while the central derivations are suitable for the detection of spindles and the frontal derivations allow to identify of K complexes and slow-wave activity. The CMS team uses reusable electrodes of gold cup or silver-silver chloride type [25,31].

2.2.8.1.2 Electrooculography The movements of the eyes are recorded by the E1/M2 and E2/M1 derivations. An electrode, E2, is located near the outer canthus, with an offset of 1 cm above the horizontal line of the right eye. The second electrode, E1, has the same location in the left eye, but 1 cm below the horizontal line of that eye [31]. Data from EOG are necessary to assess REM sleep. The same type of electrodes used in EEG are used in EOG [25].

2.2.8.1.3 Electrocardiography ECG signal records data from a single derivation and it allows to monitor heart electrical activity. The first electrode position is 2 to 3 cm below the midpoint of the right clavicle. The second electrode position must be in the midpoint of the left clavicle and below the breast crease. ECG uses a type of electrode equal to the ones used in EEG [31].

2.2.8.1.4 Electromyography The EMG monitors skeletal muscle electrical activity from 3 different areas of the body, chin, left, and right leg. A single derivation monitors the electrical activity of each area. The chin electrodes placement is 2 cm apart to detect bruxism, while each leg has also two electrodes 2 cm apart to evaluate leg movements. EMG uses also the same electrodes used in EEG [25].

2.2.8.1.5 Respiratory Sensors The monitor of the respiratory function uses 4 different sensors, 2 sensors monitor the oronasal airflow, and 2 sensors monitor chest and abdominal movements. The nasal cannula is a pressure sensor to, exclusively, monitor nasal airflow, and it is placed under the nasal area, and above the upper lip. It has 2 tubular prongs directed to the nostrils. The thermistor is sensitive to temperature and monitors airflow from both the mouth and the nose. It has 2 temperature-sensitive wires and it must be placed between the nose and the upper lip, atop the cannula. Monitoring the thoracic and abdominal movements requires the use of the chest and the abdominal respiratory inductance plethysmography, respectively [31].

2.2.8.1.6 Oxygen Saturation Pulse oximetry is a method to measure Oxygen Saturation (Pulse Oximetry) (SpO_2) in the blood, it is non-invasive and it performs measurements, usually, in the index finger.

2.2.8.1.7 Body Position The body position sensor is a piezoelectric sensor, and, at the CMS, is attached to the chest respiratory inductance plethysmography, located between this respiratory sensor and the subject's body.

2.2.8.1.8 Snoring A piezoelectric sensor monitors the upper respiratory airways to detect snoring, and its placement is in the neck.

2.2.8.2 PSG Score

PSG score requires, at least, an additional 2h to analyse data, search for abnormal events, and to deliver reports. The fundamental time for sleep evaluation is 30

seconds, one epoch. The AASM rules for sleep scoring split sleep evaluation in 5 stages. Each epoch can be scored with one, and only one, of the following stages. The first one is stage W, which represents epochs of wakefulness. The remaining 4 stages are related to sleep architecture, REM sleep and NREM sleep, divided into N1, N2, and N3.

2.2.8.2.1 Stage W Wakefulness does not belong to the architecture of sleep but it plays an important role in sleep evaluation. The human state wakefulness is characterized by parameters from EEG, EMG and eye movements. Immediately before sleep onset, EEG is characterized by low amplitude signals, with the predominance of alpha and beta activity. Muscle activity is higher during wakefulness which may increase artefacts in the EEG. Eyes may present movements in multiple directions, vertical, horizontal, or oblique, and in slow or fast movements [31]. EMG activity is often higher, at the chin, in this stage than in each one of the sleep stages.

Individuals with the capacity to generate alpha activity, with their eyes closed, should have an epoch scored as awake when they are more than 50% of the time with alpha activity over the occipital region. In the absence of alpha activity, the score rules state that one of the following criteria, if verified, is enough to score the epoch as W. Eye blinking at a frequency between 0.5 and 2 Hz, the existence of eye movements in reading behaviour, or the presence of irregular conjugate REM, together with normal or high EMG activity at the chin.

2.2.8.2.2 Stage N1 An epoch is classified as an N1 sleep stage when alpha rhythm attenuates, it represents less than 50% of the epoch, and it is replaced by LAMF, theta activity, present in more than 50% of the epoch. Entering in N1 is often followed by a decrease in chin activity.

Some individuals can't generate alpha rhythm with their eyes closed, and for these cases, stage N1 starts when the first of the following criteria appears. There is theta activity and background frequencies with a decrease of, at least, 1 Hz when compared with stage W, vertex sharp waves in the EEG, or slow eye movements in the EOG.

2.2.8.2.3 Stage N2 The rules to define the beginning of stage N2 demand to look to the epoch under evaluation, but, also, to the previous epoch. The epoch under evaluation must not exceed 6 seconds of slow-wave activity, a feature of N3. It is N2 if the first half of the epoch under evaluation or the second half of the previous epoch has K-complexes not associated with arousals and/or a sequence of sleep spindles.

The subject continues in sleep stage N2 in the presence of LAMF, and even in the absence of K-complexes not associated with arousals or sleep spindles when they exist, at least one, in the previous epoch. Sleep is no longer in stage N2 when there

is a transition to stage W, N3, or R, an EEG arousal, resulting in a transition to N1 or W, or the existence of a major body movement followed by slow eye movements and LAMF, but without neither sleep spindles nor K-complexes not associated with arousals. In the case of existing slow eye movements, the epoch following the major body movement is scored as N1. In the case of the absence of slow eye movements, after the major body movement, the epoch is scored as N2.

2.2.8.2.4 Stage N3 To score an epoch as N3, the epoch must have, at least, 6 seconds of slow-wave activity. Sleep spindles may be present, and eye movements are, usually, absent. The EMG signal, at the chin, is variable, but typically lower than at stage N2, and can be as low as in stage R.

2.2.8.2.5 Stage R Stage R, REM sleep, exists in the presence of LAMF, low amplitude EMG signal at the chin, which is, typically, the lowest amplitude values of the entire sleep, and REM. Sleep stays in stage R even in the absence of REM when, following a score of stage R epochs, EEG continues to show LAMF, but without K-complexes and sleep spindles, and chin activity stays at the typical REM level. The end of stage R occurs when there is a transition to stage W or N3, EMG chin signal increases above the typical REM level and with criteria to score the epoch as N1 are met, or arousal followed by LAMF and slow eyes movements. If the last criterion is met, the epoch must be scored as N1. Stage R also ends if a major body movement occurs and it is followed by slow eye movements and LAMF but without sleep K-complexes associated with arousal and sleep spindles. The epoch after the major body movement must be scored as N1. The last rule to end score sleep as R is the existence of K-complexes not associated with arousal or sleep spindles in the first half of the epoch, without REM and even if the EMG chin signal is at the typical stage R level. Those epochs in these circumstances should be scored as N2. The transition between stage N2 and stage R may occur in other cases. The first rule states to score R in the absence of REM when the EMG shin signal drops to the typical REM levels or there are neither K-complexes not associated with arousals nor sleep spindles. A second rule states to score N2 when the EMG shin signal clearly drops to the typical REM levels in the first half of the epoch, there are K-complexes not associated with arousals and sleep spindles, and there are not REM. The third, and final rule, states to score stage R in the absence of REM when the EMG shin signal is at the typical REM levels the entire epoch, or there are neither K-complexes not associated with arousals not sleep spindles.

2.3 Sleep Disorders

2.3.1 Physiology of Respiration

Air flows from a space of higher pressure to a space of lower pressure. In the inspiration phase, the respiratory muscles lower the pressure, below the atmospheric pressure, inside the lungs. The chain of events leads to lower pressures along the entire respiratory airway and to an air movement inward. In the expiration phase, the process inverts with the respiratory muscles increasing the pressure inside the lungs. In the respiratory airway, the air pressure, also, increases to expel air from the lungs into the atmosphere. A decrease in the air pressure, inside the respiratory airways, promotes the collapsibility of those structures, but several muscles are responsible to keep the airway open.

Tonic activity stimulates upper airway patency, while the phasic activity, during inspiration, responds to the negative pressure reflex and acts in the muscles responsible for the upper airway patency. The upper respiratory muscles are activated first and they reach the maximum response to inspiration before the respiratory muscles [3]. The control, both phasic and tonic activity, of the muscles responsible for the upper airway patency, differs from the state of wakefulness to the state of sleep. During wakefulness, the activity is higher than while asleep, but the decrease is different from muscle to muscle. The tensor palatini muscle, with tonic activity, has a higher decrease than the genioglossus, the palatoglossus, and the levator palatini, all with phasic activity [3]. The behaviour of the tensor palatini muscle, in activity, is compensated by the genioglossus muscle. Both muscles are under the control of the same central nerve drive. Muscles responsible for respiratory movements may also change their work pattern in sleep. This results in an increase in upper airway resistance and a decrease in its aperture [3]. The necessary muscle activity to keep upper airway patency changes with orientation [124]. A higher level of activity is necessary when an individual changes the upper respiratory airway axis from a transversal orientation to an anteroposterior orientation [3, 125].

2.3.2 Adult Obstructive Sleep Apnoea Hypopnea Syndrome

Sleep disorders are responsible for the increase of difficulty in breathing, during sleep, are acknowledged as SRBD, and the most common disorder is the SAHS. SAHS is classified as OSAHS or Central Sleep Apnoea-Hypopnea Syndrome (CSAHS), depending on the source of the disorder, but can also be classified as Mixed Sleep Apnoea-Hypopnea Syndrome (CSAHS), if it is a combination of both OSAHS and CSAHS [126]. The beginning of the respiratory event CSAHS is characterized by the absence of respiratory effort and the complete cessation of the respiration without both thoracic and abdominal movements. At the end of the CSAHS event and,

gradually, movements resume [127, 128]. A fourth type of SAHS, complex sleep apnoea-hypopnea syndrome, was identified in patients undergoing OSAHS treatment. Those patients may have persistence or an increase in central apnoeas or hypopnoeas [126]. Episodes of CSAHS are the result of the reduction, or absence, of a central nerve drive over the respiratory muscles and the absence of respiratory effort [129, 130].

OSAHS, more common than CSAHS, is related with the obstruction of the upper respiratory airway albeit respiratory muscles continue to work [129]. The blockage decreases airflow when it is partial, but, when there is a total blockage, airflow is inexistent throughout the respiratory structures. The limitations in airflow have direct consequences on the availability of O_2, on which the cells of the body relay to work normally. The human body needs a minimum amount of O_2 to function properly, and when the airflow goes below the necessary minimum, arousals or awakenings occurred [131]. These events interrupt sleep, leading to sleep disruption, and are responsible for the decrease in sleep quality.

Patients with OSAHS, and their families, are not fully aware of the implications of this condition and, often, they underestimate the effects and consequences of living with it undiagnosed and untreated. Lack of attention to this condition may be linked with the disorder itself, once there is not an immediate and associated disability that raises a red flag, a life threatening, or a significant life disability event. Instead, the first symptom associated with OSAHS is, often, snoring, a sleep abnormal sound, capable of disrupting the sleep partner, but with a slow, progressive implementation over the years, both in frequency (number of events) and loudness. All neglect the initial symptoms, and other symptoms may also emerge in the meantime, and the diurnal consequences, like EDS, may be misleading with other causes.

To measure OSAHS and understand its severity, a method was developed, which relies on the Apnoea-Hypopnea Index (AHI) parameter. The AHI is the result of the calculation of the number of apnoeas (A) and hypopnoeas (H) per hour (t) of TST:

$$AHI = \frac{A + H}{t} \tag{2.1}$$

Results interpretation for the AHI splits data in 4 categories. Those subjects with an AHI$\leq$5 are considered healthy, belonging to the Sn group if they snore, otherwise, they belong to the Co group. An AHI$\geq$5 suggests an OSAHS patient, using the AHI parameter to organize OSAHS patients, by their severity, in 3 medical classification groups. The medical classification groups, by increasing order of OSAHS severity, are identified as Mi, Mo, and Se, and a patient is classified, in the respective class, when its AHI obeys the following criteria: 5>AHI$\geq$15, 15>AHI$\geq$30 and 30>AHI, respectively [132].

Further research revealed the existence of hypersomnolence among subjects with a normal AHI but in the presence of SRBD similar to apnoeas. They discovered the existence of different respiratory events with implications for the normal function of sleep. Those events are responsible for flow limitations during inspiration, abnormal respiratory efforts, and cortical arousals, and they were named Respiratory Effort-Related Arousal (RERA) [133]. To respond to these new findings, which have a substantial impact on sleep quality, a second parameter was defined to replace AHI, and it is known as the Respiratory Disturbance Index (RDI) parameter. The classification of OSAHS patients remains the same, but the definition of RDI is different. This parameter also takes into account RERA events, that do not fulfill the criteria to be scored either as apnoeas or as hypopnoeas [134]:

$$RDI = \frac{A + H + RERA}{t} \tag{2.2}$$

2.3.2.1 Epidemiology

OSAHS epidemiology has been studied for decades, and one of the first studies about OSAHS pointed to a prevalence of 9% in women and 24% in men [135]. This estimation is outdated, since it was performed a long time ago and, nowadays, the population, in the most affected countries, is older and fatter. Current values for OSAHS vary, depending on the criteria, but it was estimated a SRBD prevalence, in the United States and in 2012, of 6% in women and 13% in men, for an AHI$\geq$15. The population set was constituted by an adult population between 30 and 70 years old, from the Wisconsin Sleep Cohort Study, but pregnant women were excluded from this study [7]. A major conclusion of this study is the evolution of SRBD, with an increase in prevalence between 14% and 55%, depending on the subgroups, and an evolution from the baseline, years from 1988 to 1994, to the years 2007 to 2010. A study subsampled data from a questionnaire from the Municipally of Uppsala in Sweden, and the questionnaire's goal was to study "Sleep and Health in Females". They found that 50% of the women, between 20 and 70 years old, had an AHI$\geq$5 [136]. In Iceland, a study found that 43.1% of the population had an AHI$\geq$5 [137]. In Asia, OSAHS prevalence was 16% in women and 27% in men, in a study performed over 457 Korean subjects [138]. There is, also, evidence of sleep problems in Africa, with a survey, in 4 different countries and in subjects with more than 50 years old, reporting sleep problems in 15% of the population.

Estimation of the world prevalence of OSAHS is not easy but some authors predict values between 4% to 10% for the adult population [139]. OSAHS prevalence over the world is not homogeneous and there are several factors responsible for this distribution. Studies about the global prevalence of OSAHS are uncommon. Efforts have been made and a paper review focused on 17 papers from 16 countries to do

data extrapolation for the remaining countries was made by [8]. Estimated values are overwhelming, since, almost, 1 billion, one-eighth, of the world population has OSAHS, with an AHI≥5, for men and women between 30 and 69 years old. The population with an AHI≥15 was estimated to be more than 400 million. The biggest countries, by population, have the highest numbers of OSAHS in terms of absolute values. However, and somehow surprisingly, the extrapolation raises bigger concerns about OSAHS in countries, like Brunei, Malaysia, and the Maldives, where three-quarters of the population, in that group age, had an AHI≥5. A second review paper reviewed data for 24 studies and it found, for an AHI≥5, a prevalence between 9% and 38%, peaking as high as 90% in men and 78% in women, for advanced age groups [140]. Mo and Se AHI have a global prevalence between 6% and 7%, and the highest incident is among middle-aged men [7].

2.3.2.2 Anatomy of the Upper Respiratory Airway

The upper respiratory airway must perform several actions: swallowing, phonation, olfaction, and respiration, which includes warming and the humidification of the air [141]. The anatomy of the upper respiratory airway encompasses the larynx, the pharynx, and the nose, although mouth breathing may occur in some situations, such as the case of intensive exercise or during sleep. Some references include the extrathoracic trachea [3], albeit the book definition for upper airway is not consistent [3]. A detailed diagram of the respiratory tract is in Figure 2.5.

The trachea and the larynx have cartilaginous structures, which give support, and the collapse of those structures is very unlikely. Some diseases change the anatomy of those structures, and they may contribute to their collapse and the worsening of OSAHS [142, 143]. Structures without rigid support are more likely to develop obstructions to airflow, which is the case of the pharynx.

2.3.2.2.1 Pathophysiology and Risk Factors of OSAHS The pathophysiology of OSAHS is influenced by multiple factors [145]. Anatomical modifications, like neuromuscular drive and weight gain, are among the decisive factors in the development of OSAHS. The low neuromuscular drive is associated with low activity in the respiratory dilator muscles, which increases the probability of airway collapse [146].

The most important anatomic factor, believed to occur in OSAHS, is a higher value of the total body fat, although is not an essential condition. More important than the total body fat is the upper body fat in the risk of developing OSAHS [141]. Fat deposits, around the upper respiratory airway, are heterogeneously distributed across the neck, which increases neck circumference, becoming a OSAHS predictor [124, 146]. Those deposits may narrow the calibre of the airway passage, but also increases the force of gravity, which may lead to the collapsibility of the same

passage. The decrease in the calibre will increase airflow resistance. Narrowing the upper respiratory airway results in a decrease in its diameter and in an increase in airspeed, and according to the Bernoulli equation, an increase in airspeed leads to a decrease in air pressure. Intraluminal pressure drops even more than in normal conditions, which promotes a higher degree of collapsibility of the respiratory structures. Lung volume at the end of the expiration phase may play a role in the development of OSAHS [141]. The cross-sectional area and the lung volume are directly related, which means that when the lung volume lowers, the cross-sectional area decreases and there is an increase in the probability of collapse [146].

One of the muscles responsible for the upper airway patency, the genioglossus, has higher EMG activity in OSAHS patients than in the control group when wakefulness [147]. The muscle could increase its EMG activity to compensate for the higher degree of collapsibility of those structures. Even muscle cells adapt to the development of OSAHS, with an increase in the representation of type II muscle cells and a decrease in the representation of type I muscle cells [141]. Healthy middle-aged men, without snoring or upper airway obstruction, have a muscular activity, in the upper respiratory airway, in values midway between those of healthy young adults and patients with OSAHS. This suggests an evolution towards the OSAHS, with the emerge of this condition, and the speed to reach it, depending on several factors. During sleep onset, upper airway muscle activity decreases, with similar values in young and middle-aged adults, but with a higher fall in OSAHS. The underlying cause may be linked with the loss of the wakefulness stimulus rather than the loss of responsiveness to the negative pressure [147].

Excessive fluids in the body have an impact on airway mechanics. Fluids migrate from lower regions, considering the standing position, of the body, as the case of the legs, to higher regions, as the case of the neck and head, at night [146]. A subject can still develop OSAHS even in the absence of anatomical or neuromuscular factors [148]. Being men increases the probability of developing the syndrome when compared with women because men tend to have fat more deposits in central regions and longer airways than women. Menopause has been described as another factor to OSAHS [146]. The increase of fat deposits in the upper respiratory airways appears to have a greater impact on men than on women. Anatomical measurements of the tongue, total soft tissue volume, and lateral pharyngeal wall linked genetic factors with OSAHS, while Afro-Americans have an increased risk of developing OSAHS at an earlier age than Caucasian [141].

2.3.3 Snoring

The study and comprehension of OSAHS as a health problem was a major step in the treatment of this syndrome. Snoring comprehension as a symptom of OSAHS,

besides the previous thinking of just an acoustic inconvenient, helped find solutions to solve or mitigate the syndrome [3].

Snoring is one of the first and one of the most common symptoms of OSAHS and can be induced by a great number of causes [129, 149, 150]. Snoring generation comes from the vibration of the structures of the upper respiratory airway when a subject breaths, while asleep.

2.3.3.1 Epidemiology

OSAHS patients have snoring symptoms in 70% to 95% of the cases, making this symptom common in this disorder [151]. Snoring prevalence was estimated to be 27.8% in men and 15.3% in women, in the 1990s, with the study achieving its results in a questionnaire made to a population of 1222 Hispanic-American adults [152]. Nowadays, the snoring prevalence in the global adult population is around 32% [3]. Other sources found a prevalence of snoring in 19% to 29% of women and in 32% to 52% of men of middle-age or older [153]. Different sources of data point to different ranges with some defending higher prevalence values [154]. Another source reports snoring prevalence as low as 7.9% in women and 19.1% in men for the same age groups [31].

Subjects often don't are aware of their condition as snorers, or even, as OSAHS patients. They rely on bed partners, or close relatives, to acknowledge the problem and report it. Although snoring is not a homogeneous problem across the world and the existence of ethnic differences in the snoring prevalence is well accepted, the study of snoring shows the existence of diverging results. The comparison between objective and subjective methodologies showed how divergent the results may be [3].

2.3.3.2 Pathophysiology

The genesis of snoring is complex, but it is often located in the soft tissues of the upper respiratory tract. Such tissues are the soft palate, the pharyngeal walls, the uvula, the epiglottis, and the tongue [25, 150]. Snoring may be the result of the vibration of a single or multiple anatomical sites and research has been done to perform the identification of those sites using automatic algorithms. Sound characteristics are depending on the site of obstruction [25]. A review paper identifies the soft palate as the source of the lower frequencies of snoring, while the higher frequencies are generated by the tongue [150]. In [155], both single and multi sites of obstruction were analysed, and a multi-variable approach allowed to predict obstruction, in both single and multiple sites. In [156], an analysis of different features, and classifiers were implemented to evaluate their performance to identify the sites of obstruction. A multi-feature analysis with a random forest classifier reported the best results, 78%, against 86% performance by human specialists.

In order to keep the upper airway patency, the central nervous system is con-

tinuously sending commands to the muscles [3]. This process can be voluntary, but it is, mainly, an autonomous process that occurs permanently while in either wakefulness or asleep. While asleep, the central nervous system decreases its activity over the respiratory system muscles, and the decrease in the triggering mechanism increases the odds of airway closure [1]. Upper airway patency is state-dependent, sleep vs wakefulness, but also stage-dependent. In healthy young adults and during SWS those muscles have more activity than in the other stages, N1, N2, and REM. Data from OSAHS patients show a decrease in the number of obstructions while in slow-wave activity [157, 158].

The heterogeneous behaviour of the muscles responsible for the upper airway patency changes the intrinsic characteristics of snoring. Snoring loudness and snoring frequency is higher in SWS than in N2 or in REM sleep [159]. An automatic algorithm was able to identify, with an accuracy of 81%, if they belong to NREM sleep or to REM sleep [160]. The algorithm used artificial neural networks after selecting a total of 43 features.

Snoring onset occurs when the soft tissues lost their stiffness and the respiratory airway patency decrease. The loss of tissue stiffness leads to the generation of turbulent airflow through those structures and sound, snoring, is created. Although it can happen in any phase of respiration, it is more common during inspiration. A paper for automatic snoring detection found that 97.5% $\pm$2.2% of the breathing cycles have an inspiration phase much louder than the expiration phase [161].

2.3.3.3 Risk Factors

Smoking, alcohol consumption, drugs, medications, nasal congestion, sleep deprivation, and being overweight are some of the risk factors for the development of snoring. Sleep position plays, also, an important role in snoring, with the supine position the most critical to snoring.

Subjects without OSAHS but with snoring are described as primary snorers, and they have an increased risk of developing cardiovascular diseases [162,163]. There are evidence of the importance of snoring in sudden death [3], and in the modification of the voice, hoarseness development, with statistically significant differences [164].

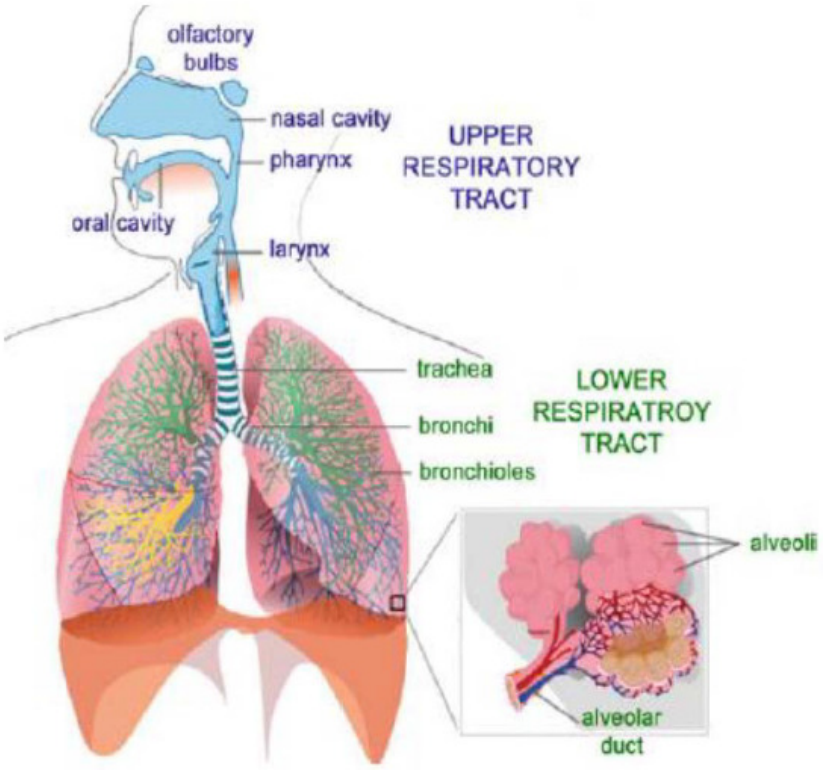

Figure 2.5: Diagram of the respiratory system's respiratory tract [144].

Chapter 3

State of the Art

The State of the Art chapter gathers the most important information about the latest developments in sleep medicine. Instead of solely focusing on scientific research, this chapter presents how, currently, the study of sleep is performed by the sleep medicine field. New technologies bring new tools to explore and analyse sleep disorders from a new perspective. The forthcoming of smartphones increased, drastically, the hardware capabilities and software complexity when compared with the previous mobile phones. They allowed the development of mobile applications, and for this purpose, the development of applications to track sleep.

The State of the Art chapter starts by presenting mobile applications capable of performing some degree of sleep analysis. Then, there is a review of medical devices used in a hospital environment, followed by the most important research performed in the latest years in this area.

3.1 Mobile Applications

Smartphone applications present an advantage over other devices because the smartphone is a multi-purpose device and it is extremely portable, accompanying the owner all the time and everywhere. Smartphones' popularity has been increasing over time, reaching 3500 million users in the year 2020, around 44.9% of the world population, and with an estimate of 3800 million users in the following year [165]. Smartphone usage is higher in countries with the highest population, like China, India, and the USA, with, respectively, 851, 346, and 260 million smartphone users. Adjusting smartphone users to the country population, the highest percentage values of smartphone users are in several European countries, with the United Kingdom at the top (82.9%). United Arab Emirates (82.1%), EUA (79.1%), Canada (73.8%), Taiwan (72.0%), South Korea (70.4%) and Australia (69.3%) also have high percentage values [166].

Among the most important examples, in smartphone applications, are access to communications. With a phone call, an SMS, an e-mail, or other types of communi-

cations, like Whatsapp, a person is, constantly, connected to the world. Sleep-related smartphone applications have been developed to perform sleep analysis. Such tools are not medical devices and they can't be used as a substitute to perform medical diagnoses.

The primary target of these applications is recording and analysing snore, using the microphone embedded in the smartphone. From the collected data, a statistical profile is generated and examples of snoring are available to listen [167]. Raw data storage as well as building up statistic information across several nights deliver a more trustful analysis and, potentially, an evolution profile. Apnoea evaluation is a feature available in some sleep-related applications. The implemented algorithm searches for absences in breathing sounds, followed by the appearance of sudden and loud sounds, to identify an apnoea.

Actigraphy is a tool widespread to evaluate sleep at home, but, also, daily activity [168, 169]. Smartphones have embedded 3D accelerometer sensor capable of deliver information to perform actigraphy [170, 171]. Smartphones should be worn close to the human body, without any relative movement between them, to detect human activity and work properly. At sleep, the use of objects in touch with the body may disrupt sleep and a less invasive approach may be preferred. For that, the logical decision is to place the smartphone next to the sleeper, in the bed. In situations like this, an alternative to actigraphy exists and is known as the sonar method. This method needs access to both speaker and microphone to work properly [170].

The learning mechanism considers an initial period dedicated, only, to learning sleep patterns. Sleep study encompasses tracking and splitting sleep in, solely, 2 phases to trigger the alarm: a deep and a shallow sleep phase. After the learning period, the user sets the clock alarm to an hour and the smartphone application adds flexibility by adjusting the hour to a more appropriate moment when the subject is in a shallow sleep [170–172]. Among the features included in the application is the capability to activate anti-snoring measures. The application's algorithm performs snore detection in real time and, in the presence of snores, the smartphone emits sounds intending to stop snoring. Statistics are available, and it includes sleep duration, noise, snoring, sleep cycles, and the amount of deep sleep, in percentage. Data storage enables to study of data trending from the previous nights and it gives advice, to improve sleep quality patterns [170–173].

Business models associated with smartphone applications are broad. The implemented business models use one of the following strategies: a free-to-use, a pay-to-use, free-to-use with in-app products purchasing, and a free trial. The free-to-use version has fewer features available than the pay-to-use version [170]. In-app product purchasing allows users to add new features, by purchasing features, to the application's basic edition [167, 173, 174]. The free trial version may have all the

features available but, only, during a limited time [173, 175].

Few sleep-dedicated applications have been tested and compared with the gold standard for sleep evaluation, the PSG study. One study tested smartphone applications Sleep Time, MotionX 24/7, and Sleep Cycle against the gold standard, and all of them had poor results [176]. High variability in the results can, also, be expected due to hardware differences implemented in the different models and brands of smartphones [177].

All the applications presented had more than 50000 downloads and they were classified, at least, with 4 stars, as of July 2019.

3.2 Wearables

The method to acquire electric brain activity is of harder implementation than the methods required to acquire the remaining signals of the PSG study. EEG monitoring requires more electrodes, precise relative positioning between them, and, often, placed among hair, guaranteeing a good contact between the sensor and the skin surface. Muse S is a wearable headband, placed around the forehead, and it acquires electrical brain activity, but also, breath, heart, and body movements. The wearable connects to the smartphone's app to send data to it, which is then analysed to decide which bird songs should be played by the earbuds. The equipment tries to help people relax to fall asleep easier, but it also tracks sleep overnight, identifying sleep stages, sleep position and body movements, and heart rate by using EEG, accelerometer, gyroscope, and photoplethysmography. The smartphone's app uses Bluetooth 4.2 to connect to wearables, and it integrates features like bird song selection, pre-sleep, and sleep history, showing the progress of the signals measured and sleep stages [178].

Wristbands were developed primarily to track physical activity. Fitbit is a well-known brand, one of many companies, of consumer electronics to monitor biomedical signals. They develop wristbands to track physical activity but it also has sleep monitoring applications. Their wristbands record data and deduce a person is asleep when the body is at rest and after the body is quiet for 1 hour. For a better sleep visualization, an app is available to install on the smartphone, and it comes with information regarding snoring and time spent awake, restless, and asleep. Evaluation of sleep stages is, generally, possible in wristbands with heart rate measurement capability. SpO_2 is also a feature available to track sleep. Sleep results are available to see in either the wristband or the app [179, 180].

Smartwatches are also multi-purpose devices, with the latest models developed to mimic smartphones, capable of supporting apps, an operating system, and wireless connectivity. They also track biomedical signals at the wrist, applying a similar work principle, to study sleep. Acquired data allow calculating SpO_2, heart rate,

breathing, and to do sleep staging. Besides the previous parameters, sleep results, score, time asleep in each one of the sleep stages, graphics, and historic, are available for consultation either in the smartwatch or the smartphone's app. Garmin is one of the brands supporting sleep tracking in their smartwatches [181, 182].

Tracking sleep is also available in ring-type wearables, although they aren't so acquainted and common as the previously presented wearables types. The Oura ring tracks movements using a 3D accelerometer or by importing data from a third-party app, like Apple Health or Google Fit. The decision-making process classifies data into one of the following 3 groups: active, at rest, and asleep (naps included). It acquires more data, to calculate heart rate, heart rate variability, and respiration, using infrared photoplethysmography, with a sampling rate of 250 Hz. Finally, it acquires temperature data using a negative temperature coefficient sensor with a sensitivity of 0.1^{o}C. The available app for smartphones allows to have a visual representation of all acquired data, and their processing, like sleep stage, but also audio and videos to help, for example, in sleeping. Future upgrades include SpO_2 sensing [183].

Withings is a non-wearable sleep tracker but is worth mentioning in this section. It is a sleep tracking pad, placed under the mattress, plugged in, and capable of detecting sleep stages and their duration, awakenings, and heart rate, and it has a built-in microphone to help track snoring. There are sleep sensors to control and adjust the lights and the thermostat to set the best sleep conditions. An app receives all data and it displays them to be observed by a person [184].

3.3 Medical Evaluation Tools

3.3.1 Questionnaires

Sleep-related questionnaires are used as both a research and a medical tool to perform sleep evaluation, but questionnaires are subjective tools, sometimes filled by non-professional agents, like the patient himself or his bed partner. Questionnaires may be used to study sleep in either the paediatric or adult population. The adult population, the population under study in this project, has different types of questionnaires available. Figure 3.1 organizes some of the existent questionnaires by the subject in analysis, accordingly to the Thoracic website [185]. However, there are more questionnaires to assess sleep, and in 2 different articles, [186, 187], more of them are listed.

3.3.1.1 Sleep Apnoea

3.3.1.1.1 Sleep Disorder Questionnaire Sleep Disorder Questionnaire was originally suggested in 1994 by M.D. A. Douglass and its development was based on other 2 questionnaires, the Sleep questionnaire and the Assessment of Wakeful-

ness [188]. It encompasses a total of 175 questions, with the first 152 questions using a grading scale from 1 (Never) to 5 (Always). The patient selects the answer which fits better his case. The remaining questions, 23, are multiple choice, also 5, to evaluate some quantitative variables, like the number of hours asleep and weight. Different sources suggest different periods to consider when answering the questionnaire, with the previous month and the previous 6 months the common suggestions to be considered. The questionnaire focuses their questions on sleep apnoea, narcolepsy, Periodic Limb Movement (PLM) and psychiatric sleep disorders [185, 186].

M.D. A. Douglass tested the questionnaire on 519 people, of whom 435 were patients with sleep disorders. People were grouped into 5 groups, control, sleep apnoea, narcolepsy, psychiatric and nocturnal myoclonus, achieving a sensitivity between 65% and 88%, and specificity between 46% and 81% [188].

3.3.1.1.2 Berlin Questionnaire Berlin questionnaire was firstly published in Annals Of Internal Medicine by a group of researchers, led by M.D. Nikolaus C. Netzer, in 1999. It is used to find patients with Sleep Apnoea, and it asks about risk factors, snoring, wake time, sleepiness, fatigue, obesity, and hypertension. The questionnaire has 14 questions divided into 3 categories. The first one evaluates snore severity, the second one evaluates EDS and the final category evaluates hypertension. It asks also for height, weight, age, and gender to know about obesity. The application of this questionnaire resulted in a sensitivity of 86%, a specificity of 77%, a Positive Predictive Value (PPV) of 89%, and a likelihood ratio of 3.8% for RDI$\geq$5. The patient set was 744, of whom 100 underwent sleep studies [189].

3.3.1.1.3 STOP BANG STOP BANG questionnaire was proposed by Frances Chung and his colleagues in 1998 to evaluate OSAHS in surgical patients. It analysis

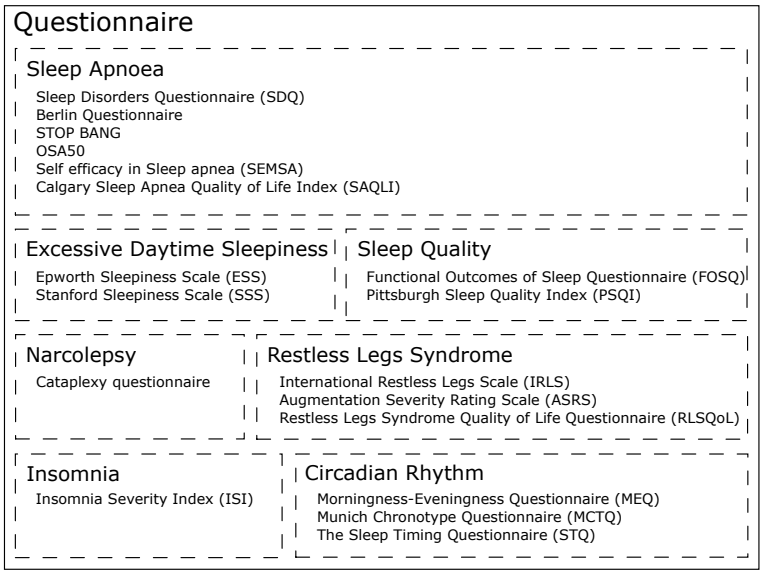

Figure 3.1: Sleep-related questionnaires grouped according with the purpose of their evaluation. Questionnaires are organized in 7 subgroups and their target is the adult population [185].

the risk for sleep apnoea and it addresses postoperative complications, due to an increased risk associated with OSAHS, trying to predict them. The questionnaire has been validated in primary care patients and it has 8 questions, and its name addresses each one of those questions, snoring, tiredness, observed (anyone watches the patient stop breathing), pressure (blood pressure), body mass index, age, neck circumference, and gender. The original article tested the questionnaire on 2467 patients, 27.5% of them at high risk of developing OSAHS. The questionnaire sensitive for Mi, Mo and Se OSAHS groups was 83.6, 92.9 and 100%, respectively. Predictive values vary depending on the population, with a sensitivity of 86% in primary care patients, 62.5% in patients in the process of pulmonary rehabilitation, and ranging from 57% to 68% in sleep laboratory patients [190].

3.3.1.1.4 OSA50 OSA50 is a questionnaire with 4 questions to address sleep apnoea and was proposed by M.D. C. Chai-Coetzer and his colleagues in 2011. The questionnaire's goal is OSAHS evaluation, by asking for obesity, snoring, apnoea, and age (under or above 50 years old), with a scale from 0 to 3 to the first 2 items and a scale from 0 to 2 for the other 2. The validation of this questionnaire encompasses the study of 157 patients with ages between 25 and 70 years old. Two subgroups were created and they have a similar number of patients, with the first group, composed of 79 patients, for development, and the second group, composed of 78 patients, for the validation purposes. The validation group had a sensitivity of 88%, a specificity of 82%, a PPV of 56% and a Negative Predictive Value (NPV) of 96% [191].

3.3.1.1.5 Self efficacy in Sleep Apnoea Self efficacy in Sleep Apnoea measures the expectancy for OSAHS and Continuous Positive Airway Pressure (CPAP) before treatment in adults, and it also evaluates adherence-related cognitions. It has 26 questions, grouped in 3 different categories, to evaluate risk perception, outcome experiences and treatment self-efficacy [185]. The first category has 8 questions, while the second and third categories have 9 questions each. The patient answers each question grading them on a scale from 1 to 4, depending on his statement's agreement. Weaver and his colleagues are the authors of this questionnaire and to test its performance, a study was developed with 213 patients, recently diagnosed with OSAHS. Most of them were men, 60%, 55% were Caucasian and 39% were Afro-American, with 47.72±12.25 years old, and a Body Mass Index (BMI) of 38.08±9.66 kg/m^2. Patients came from 3 different clinics, clinics 1, 2, and 3 with, respectively, 38, 22, and 153 patients. Statistical analysis was implemented to evaluate the test-retest reliability, using a set of 20 patients, from clinic number 2, to do the Self-efficacy in Sleep Apnoea a second time. The reliability coefficients, the ratio of true score variance to the sum of true score variance plus error variance, were

estimated by calculating the test-retest Pearson correlation coefficient. It returns a result of 68% (P=0.001), 77% (P≪0.0001), and 71% (P=0.0005) for perceived risk, outcome expectancies, and treatment self-efficacy, respectively [192].

3.3.1.1.6 Calgary Sleep Apnoea Quality of Life Index Calgary Sleep Apnoea Quality of Life Index was designed to evaluate the quality of life in the previous 4 weeks in adults by M.D. W. W. Flemons and his co-worker Marlene Reimer. The questionnaire addresses topics in 4 distinct domains, daily functioning (11 questions), social interactions (13 questions), emotional functioning (11 questions), and symptoms (5 questions). In cases where the patient undergoes a clinical treatment, a fifth domain, treatment-related symptoms (5 questions), can be also added to study the negative impact on the quality of life of the treatment. Domain symptoms have 21 questions and the option to include even more symptoms, but the 5 most important symptoms should be selected to include in the questionnaire analysis. The fifth domain also has more questions, 26 fix questions, and it allows to include more symptoms not contemplated in the previous questions, with the 5 most important symptoms selected and used in the questionnaire evaluation. The response to each question uses a scale from 1 to 7. The development of this questionnaire started with 133 questions and the need for determining which ones were most commonly experienced and were most important to patients with sleep apnoea. Three hundred patients were selected to participate in the development of this questionnaire, and those with disorders, other than sleep apnoea, or who lived outside the Calgary city were discarded, remaining, in the end, 163 patients [193].

3.3.1.2 Sleep Quality

3.3.1.2.1 Functional Outcomes of Sleep Questionnaire Functional Outcomes of Sleep Questionnaire is a questionnaire to assess sleepiness effects on the daily ability of a person to function and it has 2 versions, a short version with 10 questions and a longer version with 30 questions. The original version, the longer, was developed by a team of researchers led by Ph.D. Terri Weaver in 1997. Questions are organized into 5 domains, activity level (9 questions), vigilance (7 questions), intimacy and sexual relations (4 questions), general productivity (8 questions), and social outcome (2 questions), and each question uses a scale from 0 to 5. The questionnaire was originally analysed to verify its validity and reliability using 3 samples, with 153, 24, and 51 individuals. Sample 1 consisted of 133 individuals for the first time in a SRBD appointment and an additional 20 healthy individuals, while individuals in samples 2 and 3 all had OSAHS. Individuals, the 133 individuals in sample 1 and all individuals in samples 2 and 3, are 49.11±13.04, 41.75±9.14, and 49±9.76 years old, and an RDI of 35.96±32.15, 50.67±32.71 and 28.44±24.54, respectively. The 20 healthy individuals from sample 1 are 43.17±8.20 years old.

Sample 1 was used to assess both the validity and reliability of the questionnaire. The analysis of the results from the validity test shows significant differences between the 2 subgroups in sample 1, patients (n=133) and healthy subjects (n = 20), with overall results of 68.05±21.24 and 89.59±8.64 (p=0.0004), respectively. Reliability determination was performed using the Pearson correlation in a set 0f 32 patients (sample 1). The retest was performed 1 week after the first appointment, and the results go from 81% to 90% for all the domains [194].

More recently, a short version was developed by Chasens to decrease the time necessary to respond to all questions and to be more practical in clinical and research implementation. The shortened version has 10 questions, representing all 5 domains. To test this new version, 3 samples were created, one with 155 patients (AHI of 63±31 and 46.3±9.18 years old) was used to develop the questionnaire. The second sample, with 51 subjects (AHI of 51±28 and 48±10 years old) was used to test the design of the questionnaire. A third sample, with 57 subjects (AHI≤5 and 43.17±7.54 years old) was used as the control group, without SRBD. The short version performs similarly to the longer version in terms of internal consistency (Cronbach α of 0.87 vs 0.95, above the minimum criterion of 0.70), and the Total score, pretreatment, was robustly associated with (r=0.96, P≤0.0001). After post-treatment, both questionnaires detected a large change in the Total score (r=0.97, P≤0.0001), with clinical relevance [195].

3.3.1.2.2 Pittsburgh Sleep Quality Index Pittsburgh Sleep Quality Index was developed to measure sleep disturbance and typical sleep routines in the past month. Created by M.D. Daniel Buysse and his colleagues, it has 19 questions, organized into 7 domains, subjective sleep quality, sleep latency, sleep duration, habitual sleep efficiency, sleep disturbances, use of sleeping medications, and daytime dysfunction, and rated on a scale from 0 to 3. The validation of this questionnaire was performed using 3 groups of subjects, group 1 with 52 healthy subjects, working as the control group, group 2 and are consisted of, respectively, 34 and 62 poor sleepers. Poor sleepers in group 2 had depressive disorder, while patients in group 3 had a disorder of initiating and maintaining sleep (subgroup 1) or disorders of excessive somnolence (subgroup 2). Groups 1, 2, and subgroups 1 and 2 had an average of 59.9, 50.9, 44.8, and 42.2 years old, respectively. The internal homogeneity had a global reliability coefficient of 0.83 (Cronbach's α), which is an indicator of a good degree of internal consistency, meaning that the domains measure different features to evaluate sleep. The questionnaire was completed twice by 99 patients to verify the performance consistency. The test-retest reliability was implemented together with paired t test and the Pearson product-moment correlations. The paired t test reveals no significant differences between both answers and the Pearson correlations results showed the existence of stability (0.85 and p≤0.001) [196].

3.3.1.3 Restless Legs Syndrome

3.3.1.3.1 International Restless Legs Scale International Restless Legs Scale questionnaire was designed to study, on a subjective scale, the severity of Restless Legs Syndrome (RLS) in the previous week. It has 10 questions organized into 2 domains, the subjective assessment of primary features of RLS and the intensity and frequency, associated with sleep problems. The questionnaire uses a 5-scale grading system, with 0 meaning no RLS and 4 meaning severe RLS. The International RLS Study Group created a task force to develop this questionnaire with the participation of 20 centres, from which 17 centres contributed with RLS patients and 14 with control patients. In the end, 407 subjects participated in this study to validate the questionnaire, from which 196 had RLS and 209 were control subjects. Results for the internal consistency, using the Cronbach α parameter, were 0.93 and 0.95, ($p \leq 0.001$) for the first (n=196) and second (n=187) questionnaire, respectively, and separated by 2 weeks. From the total of 196 patients with RLS, 9 lost the follow-up between the first and the second questionnaire. Patients were asked to fill the first questionnaire twice, each time with a different examiner and in the absence of the other examiner, which helped the patient clarify any doubts. Two weeks later, in the second questionnaire, the presence of a second examiner was optional, but, when present, the blind mechanism remains. The inter-examiner reliability was assessed using the intra-class coefficient and achieved a score of 0.93 and 0.97 ($p \leq 0.01$) for the first and second questionnaires. The test-retest reliability was conducted on 145 patients and the difference was not significant [197].

3.3.1.3.2 Augmentation Severity Rating Scale Augmentation Severity Rating Scale questionnaire was the effort promoted by the European RLS Study Group, which created a task force led by Diego García-Borreguero. The questionnaire goal was to provide a quantitative measure of the severity of worsening of RLS symptoms during treatment. It starts with a baseline evaluation and continues its evaluation throughout the treatment phase. Each question, in a total of 3, has a grading scale from 0 (no changes) to 8 (severe augmentation). The evaluation of the questionnaire was performed with the participation of 60 subjects, 36 of which are augmentors (worsening of RLS symptoms) and 24 are non-augmentors, with 53 ± 13 years old. Global test-retest reliability was 0.72 and the inter-examiner reliability was 0.94. Correlation between items were high for item 2 and 3 (0.662), moderate between item 1 and 2 (0.3419) and poor between item 1 and 3 (0.144). Cronbach α was 0.62 [198].

3.3.1.3.3 Restless Legs Syndrome Quality of Life Questionnaire Restless Legs Syndrome Quality of Life Questionnaire assesses the impact of RLS on daily life, emotional well-being, social life, and work life in the previous 4 weeks. The

questionnaire addresses topics in the overall life impact (10 questions), employment (1 question), sexual interest (2 questions), and work (5 questions). Thirteen of the questions used a 5 grading scale, while the remaining 5 questions have either a numerical or dichotomous response, with low scores meaning a low quality of life. The validity and reliability of this questionnaire were tested in a study with a population of 85 subjects. The population age was 62.4±14 years old, of which 63.5% were women, 36% were in paid employment, and, of those, 86.7% worked day shifts. The internal consistency calculation results in a Cronbach's α of 0.92, and the test-retest reliability has a mean difference between baseline and week 2 of -0.1±15.7 for the total sample. The different is very low and not statistically significant (t=-0.05, p=0.96) [199, 200].

3.3.1.4 Circadian Rhythm

3.3.1.4.1 Morningness-Eveningness Questionnaire Morningness-Eveningness Questionnaire was developed to assess morningness and eveningness by Horne and Ostberg, focusing the questions on the subject's desire, such as the preference to awake and go to sleep hours. The questionnaire has 19 questions with multiple scale gradings. There is a scale grading from 0 to 5 (2 questions), from 1 to 5 (3 questions), from 1 to 4 (13 questions), and from 0 to 6, but in steps of 2 (1 question). Subjects scoring 41 or below are considered of evening type, while a score of 59 or higher suggests subjects are of morning type. In between those values, subjects are considered of intermediate type. Almost half of the population, 49.8%, was classified as morning type, while only 5.6% of the population was classified as evening type. Studies about the internal consistency were conducted, achieving a Cronback's α of 0.83 [185].

3.3.1.4.2 Munich Chronotype Questionnaire Munich Chronotype Questionnaire was developed to assess subjects' sleep times, self-reported light exposure, and self-assessed chronotype, splitting data analysis by work and free days by Till Roenneberg and his colleagues for the previous 4 weeks. The questionnaire has a total of 19 questions, which are organized into 4 domains, work schedule, work day sleep schedule, free day sleep schedule, and self-assessment of chronotype. Some questions must be rated from 0 to 6, but the majority require answers without the scale, as the example of the time at which the subject must get up. The final score ranges from 16 to 86, with the lowest values indicating a subject of extreme-late chronotype [201].

3.3.1.4.3 The Sleep Timing Questionnaire The Sleep Timing Questionnaire's goal was to assess habitual bed and wake times, and it was suggested by Ph.D. Timothy Monk and Daniel Buysse and their colleagues. The questionnaire is 18 questions long, focusing on 2 domains, good night time and good morning time, in a single administration. The test-retest reliability was performed on 40 subjects,

although a single administration goal, with a period of less than a year, with the response from the first administration not available to bias the second administration results. Those were healthy subjects with 46.3±20.5 years old, and the results point to a positive correlation in both periods, 0.705 in bedtime, and 0.826 in waketime ($p \leq 0.001$). It also estimates SOL and WASO, with reliable correlation of -0.707 in bedtime and -0.739 in waketime ($p \leq 0.001$) between the questionnaire and a 2-week sleep diary. The 2 measurement instruments were less than a minute apart [202].

3.3.1.5 Insomnia

3.3.1.5.1 Insomnia Severity Index Insomnia Severity Index is a questionnaire to assess the subjective symptoms, nature, severity, and impact of insomnia. It was developed by Ph.D. Charles Morin and it is a brief self-report tool to measure the patient's perception of his insomnia and it has 7 questions. The domains evaluated by this questionnaire include the severity of sleep-onset and sleep maintenance difficulties, the satisfaction with current sleep pattern, the interference with daily functioning, the notice-ability of impairment attributed to the sleep problem, and the degree of distress or concern caused by the sleep problem. Each question rates from 0 (no problem) to 4 (very severe problem), with higher scores suggesting more severe insomnia. The internal consistency was calculated in a study with the participation of 145 patients. Eighty-four women and 61 men with 41.4±13.1 years old responded to the questionnaire in their first appointment. The internal consistency was evaluated using Cronbach's α coefficient, with a result of 0.74, and the concurrent validity was assessed using sleep diaries and achieving an average of 0.54. The correlation coefficients were significant for $p=0.01$ [203].

3.3.1.6 Excessive Daytime Sleepiness

3.3.1.6.1 Epworth Sleepiness Scale Epworth Sleepiness Scale goal is the assessment of daytime sleepiness with 8 self-administrated questions, using a 4-scale grading system (0-3). The questionnaire asks subjects to rate their predisposition to dozing off or falling asleep in a range of situations or activities, common to most people in, almost a daily routine. All questions were grouped in a single domain, the propensity of falling asleep. M.D. Murray Johns developed this questionnaire in 1991, introducing modifications in 1997. A total of 180 subjects completed the questionnaire, of which 30 subjects were controls, and 150 patients with various sleep disorders, snoring, OSAHS, narcolepsy, idiopathic hypersomnia, insomnia, and PLM disorder. Patients answer the questionnaire during their first appointment. Statistical tests using the one-way ANOVA revealed significant differences between all groups, control, and the patient groups, with different disorders ($F=50.00$; $df=6,173$; $p \leq 0.0001$). One-way ANOVA for the Epworth Sleepiness Scale of primary snores and the 3 levels of OSAHS severity showed significant differences between these

groups (F=23.11; df=3,82; p≤0.001). All 55 OSAHS patients presented a significant correlation between the questionnaire and the RDI (0.550, p≤0.001), and between the questionnaire and the minimum SpO_2 (-0.457, p≤0.001). The questionnaire also presented a significant correlation with sleep latency (-0.379, p≤0.001) for the patients (n=138) who underwent PSG [204].

3.3.1.6.2 Stanford Sleepiness Scale Stanford Sleepiness Scale is a questionnaire to quantify progressive steps in sleepiness at a specific time, and it was proposed by E. Hoddes and his colleagues. The questionnaire has a single question and it uses a 7-scale grading system, with the lowest score, 1, meaning feeling active, vital alert, or wide awake, and the highest score, 7, meaning almost in reverie, sleep onset soon, lost struggle to remain awake. Five healthy college students participate in the study to evaluate the relationship between this questionnaire and decrements in mental task performance. It also evaluates if sleepiness, measured by the questionnaire, increases following sleep deprivation. The researchers found that the questionnaire's scores were, on average, significantly elevated in the following 24 h of sleep deprivation. The questionnaire is good to predict the performance in the execution of tasks related to alertness [205].

3.3.1.7 Narcolepsy

3.3.1.7.1 Cataplexy questionnaire Cataplexy questionnaire has 51 questions, organized into 3 domains, muscle weakness trigger, type of attack, and other concerning injury or witnessed by others, and developed by Emmanuel Mignot and his colleagues. Nine hundred and eighty-three subjects filled the questionnaire (639 men, 344 women) with an average of 48.32 years old, and data was analysed in a study to develop and validate the questionnaire. Two groups were created based on the evidence of clear-cut cataplexy (defined as "brief episodes of weakness in the knees, jaw, face, or neck triggered by laughter, joking, anger, elation, happiness, or excitement with game playing" [206]), 63 patients had, while the remaining 920 did not have. Non-narcoleptic subjects were found to experience muscle weakness when there are various intense emotions (1.8% to 18.0%), or athletic activities (26.2% to 28.8%) [207].

3.3.2 Sleep Prediction Algorithms

3.3.2.1 Morphometric Models

Morphometric models uses craniofacial parameters to do OSAHS prediction. Several measurements of the oral cavity, BMI, and neck circumference were the parameters originally used to develop this model. The 6-month prospective study with the participation of 300 patients, in their first appointment, collected the parameter values to build the model. A sensitivity of 97.6%, a specificity of 100%,

PPV of 100%, and NPV of 88.5% was achieved. Two people, one experienced physician and one non-experienced physician measured morphometric parameters in 20 patients and their results were compared to assess how similar data were. The correlation coefficient was 0.992, representing a high degree of reliability. Test retest reliability was executed by an experienced physician in 10 patients, measured in the first and follow-up appointment, and the correlation coefficient was 0.994 [208].

3.3.3 Sleep Assessment

The diagnosis of OSAHS, and other SRBD, follows rules, guidelines, and it uses equipment to record data. The PSG is the gold standard in the evaluation of SRBD, but it is not the only tool for sleep assessment. In fact, sleep diagnosing tools can be organized into 2 major groups depending on the place of assessment, home sleep assessment, and in-laboratory sleep assessment, and in 4 different types, Type I, II, III, and IV. The ones without a sleep technician following the data acquisition procedure are classified as Type II, III, or IV [209].

3.3.3.1 Monitoring At Home

At-home sleep assessment usually uses less equipment, is less costly, but allows the patient to sleep in a well-known environment, which may recreate the normal patient's sleep more easily. This type of sleep evaluation has potential disadvantages because it uses fewer sensors and there is not a sleep technician available to do real-time monitoring and to do sensor placement correction. It is also impossible to initiate sleep treatment during at-home sleep monitoring. AASM calls this type of evaluation, home sleep apnoea testing. [209].

Type III and Type IV PSG do not use sensors to monitor electrical activity in the brain, EEG, and in the muscles, EOG and EMG. It is not possible to know sleep time which represents a problem with both AHI and RDI definitions. For these levels of sleep studies, a new definition exists, the respiratory event index, which uses the recording time parameter to calculate the index value.

3.3.3.1.1 PSG Level II Type II PSG sleep study uses the same sensors as the PSG in-laboratory gold standard study, but the difference is in the absence of a sleep technician to monitor data acquisition [209].

3.3.3.1.2 PSG Level III Type III PSG sleep study measures limited cardiopulmonary activity, by measuring respiratory effort, using either the chest or the abdominal respiratory inductance plethysmography, or both. It also acquires data from airflow (cannula), sleeping position, and oximetry (oxygen saturation and heart rate) [209].

3.3.3.1.3 PSG Level IV Type IV PSG sleep study measures very few parameters, and it is used to track patients to perform a more complete sleep study.

Oxygen saturation and heart rate or just the cannula are the measured parameters. Sometimes, those 3 parameters are acquired together [209].

3.3.3.1.4 Actigraphy Actigraphy is a method to monitor rest and activity cycles by measuring the subject's movements, and, normally, used on the wrist, with the ankle and the trunk as alternative locations. It can continuously record data for long periods of time, weeks, or even more time. This method has been used in the sleep medicine field for, at least, 40 years to monitor SRBD and disturbances in the circadian wake rest cycle [168]. Several studies had compared actigraphy results against PSG results and they suggested that actigraphy can estimate TST, sleep percentage, and WASO [169]. The use of actigraphy is recommended, in adults, to estimate sleep parameters in patients with insomnia disorders, TST (when there isn't an alternative) in at-home sleep monitoring in patients with SRBD, and total sleep time in patients with suspected insufficient sleep syndrome, to assess patients with circadian rhythm sleep-wake disorders, and to monitor TST before Multiple Sleep Latency Test in patients with suspected central disorders of hypersomnolence [210].

3.3.3.2 In-Laboratory Monitoring

3.3.3.2.1 PSG Level I Type I PSG level is the most complete medical tool, and the gold standard in the sleep medicine field, to assess sleep and its disorders. The study can track for OSAHS and other sleep disorders diagnosis, but also assess their severity. It quantifies respiratory events, and their physiologic consequences, such as the case of hypoxia, arousals, and awakenings, responsible for the daytime symptoms [211].

It is recommend in the diagnose of SRBD and as a preoperative procedure, to repeat in cases of a previous negative result in PSG for strong evidence of OSAHS and after weight loss of, at least, 10% to assess the necessity of continuation for CPAP treatment, to follow-up after surgery for Mo or Se OSAHS, if OSAHS symptoms return after surgery and after oral appliance adjustment for OSAHS. Type I PSG level is also recommended to assess the application of the correct positive airway pressure treatment and to repeat sleep assessment when a weight gain of, at least, 10% exists and when symptoms return.

Performed in a health facility, with sleep technicians undertaking the task, it requires a wide range of equipment and software, besides being time-consuming. PSG equipment requirement is versatile, without a rigid protocol when concerned with the type and number of sensors used. Most of them are always present, but there are a few used only when required. PSG studies have 6 inputs to monitor electrical brain activity, EEG, 1 input to monitor each eye activity, EOG, 1 input to monitor muscle activity at the chin, 1 input to monitor the electrical activity of the heart, ECG, 1 cannula, 1 thermistor, 1 piezoelectric sensor for snoring, 1

abdominal respiratory inductance plethysmography, 1 chest respiratory inductance plethysmography, 1 body position attached to the previous sensor, 1 pulse oximetry, and 1 input to monitor each leg muscle activity. This is the usual setup used at the CMS, but more sensors may be required, like the sensor to do capnography.

3.3.3.2.2 Multiple Sleep Latency Test Multiple Sleep Latency Test was designed to evaluate the clinical significance of excessive daytime sleepiness. The subject undergoes the test during the daytime, following a methodology of naps, of 20 minutes duration each, including an interval of 2 hours between naps. The first nap, from a total of 4 to 6 naps, starts, also, 2 hours after the initial awakening in the morning. At the CMS, Multiple Sleep Latency Test is implemented after a PSG study [3, p. 1625]. The CMS uses the EEG, EOG, EMG at the chin, and the ECG to perform the multiple sleep latency test.

Subjects are instructed not to try to stay awake and let themself fall asleep, to leave the bedroom during the intervals, and not to engage in intense activities. Finally, the room should be quiet and dark.

3.3.3.2.3 Maintenance of Wakefulness Test The objective of the maintenance of the wakefulness test is to check the capability of the subject to stay awake, by giving him instructions to stay awake. The test assesses the alertness capacity, when the order/asked to, during the day in a quiet, and non-stimulating environment, in a very low light environment. The subject sits and he is not allowed to have any activity, like watching TV or reading. The protocol is similar to the multiple sleep latency test, with the laboratory monitoring his activity by acquiring from the same parameters. It starts 2 hours after the initial morning awakening, and there is a 2 hours interval between test sessions. The test duration does not have a standardized time duration, and it may vary between 20 and 60 minutes. A test session finishes when there are 3 consecutive epochs of N1 sleep, or a single epoch of N2, N3, or REM sleep [3, p. 1627].

3.4 Medical Tools for Treatment

OSAHS is a treatable/manageable condition with a great variety of many available treatments, considering the specificities of each clinical case.

3.4.1 Weight

Weight is one of the anthropometric parameters which increases the risk of developing OSAHS. By losing weight, a patient with OSAHS decreases, especially in obese patients, significantly assessment parameters, as is the example of AHI. Evidence of this statement was found in seven randomized controlled trials, 519 subjects, which concluded a mean decrease in AHI of 6 events per hour [212]. Weight loss may

be achieved by changing the patient's diet or, in extreme cases of overweight, the patient may undergo bariatric surgery [213, 214]. Weight loss proved to be more efficient for men than for women [215].

3.4.2 Lifestyle Therapy

Subjects with SRBD may improve their sleep quality with the implementation of some lifestyle changes. Consumption habits, smoking, coffee, and alcohol, are recognized as decreasing sleep quality and increasing sleep fragmentation. Quitting smoking, stopping drinking alcohol, and stopping ingesting coffee, at least a few hours before bedtime, may improve sleep [1, p. 7; 3, p. 869; 25, p. 98]. Subjects with allergies may also improve sleep by taking medicine to relieve nasal congestion [216]. Avoiding the consumption of illicit drugs, besides its consumption being a world scourge, help sleep stability and normal functioning [108, 109]. Nevertheless, some illicit drugs may help in the improvement of sleep quality in some particular conditions [108]. Some medical drugs can also change sleep patterns, and in situations like this, the patient and the physician should discuss the possibility of a medication change (dose or a different medication) [25, p. 58].

3.4.3 Positional Therapy

Positional therapy is a strategy to treat positional OSAHS since some patients have a predominance of OSAHS when sleeping in the supine position. By using objects on the back, the patient is discouraged from sleeping in the supine position, and there is a decrease in the AHI [213] [214]. This method appears to work in patients with SRBD due to heart failure [211]. An alternative to the use of objects in the back is a device with vibrotactile feedback. Set in the neck, it vibrates when the patient is in the supine position [216].

3.4.4 Oxygen Therapy

The application of oxygen therapy during sleep decreases the severity of CSAHS and Cheyne-Stokes Respiration by approximately 50%. The therapy also improves hypoxaemia levels related to apnoea in a period ranging from 1 night and 3 months, the quality of life, and the cardiac function. The evolution of the AHI is remarkable with values of 20.0 ± 11.5 at baseline to 8.6 ± 10.5 12 weeks later for the population under oxygen therapy, and values of 19.5 ± 11.3 at baseline to $18.7.6 \pm 12.2$ 12 weeks later for the control population [217]. The impact associated with an oxygen-based therapy is not well established, and the consequences are still unknown [211].

3.4.5 Oral Appliance Therapy

Oral appliances therapy prevents the collapse of the respiratory airway, and they are useful to improve sleep quality and prevent snore [213]. Mandibular advancement

devices may significantly decrease AHI in subjects with retrognathism [211]. These devices are custom-made and they use both upper and lower jaws, and their teeth, to force the mandible in a forward position or by holding the tongue in position [218, 219]. Mo to Se OSAHS patients may use an oral appliance device if they can't tolerate CPAP [216].

3.4.6 Nasal Dilators

Nasal dilators prevent nostrils collapse by opening the nasal passage, increasing airflow, and decreasing nasal resistance (different types of nasal dilators at Figure 3.2). There are 2 types of nasal dilators, the first one, internal dilators, are inserted inside the nostrils to keep airway passage open, while the second type, external dilators, is a nasal strip placed outside the nose, and it works by pulling out the nostrils [214]. The use of internal nasal dilators helped to significantly decrease the CPAP operating pressure from 11.4±1.5 to 10.8±1.5 (p=0.012) in 21 patients [220]. The number of studies on nasal dilators and their effectiveness as a OSAHS treatment is reduced and, so far, there are few pieces of evidence of nasal dilators as a good treatment for OSAHS [214, 221]. The nose has minor implications on the pathogenesis of the OSAHS, but it plays a role in snoring [222].

3.4.7 Medication-Based Therapy

Several family groups of medication have been tested in the treatment of SRBD. A class of medication, acetazolamide, had resulted in the decreasing of the number of AHI and in increasing oxygen saturation in patients with heart failure and CSAHS [211]. Medication-based treatments for OSAHS are available but lack to be effective in clinical results [213, 214].

(a) (b)

Figure 3.2: Types of nasal dilators. In (a), an example of an internal nasal dilator and in (b) an example of an external nasal dilator. Both figures are from [167].

3.4.8 Electrical Stimulation

Respiratory muscles are responsible to keep the upper respiratory airway open to allow people to have normal breathing, but in OSAHS patients this function is impaired. A possible therapy to solve OSAHS is the implementation of electrical stimulation to the hypoglossal nerve, which controls the genioglossus muscle, a respiratory muscle. A trial with 8 Mo or Se patients analysed this therapy during 6 months. A statistically significant decrease in AHI was achieved from a range of 48 to 52, at baseline, to a range of 17 to 23 ($p<0.001$) just with a month of nerve stimulation. Sleep results also show a decrease in N1 and an increase in SWS [214]. A 5-year cohort study reported statistically significant improvements in the assessment of PSG parameters. Throughout the 5 years period, the AHI evolved from 32.0±11.8 at baseline (n=126), to 15.3±16.1 after 12 months (n=124), and to 12.4±16.3 at the end of the study (n=71) [223].

Phrenic nerve stimulation is the stimulation of the phrenic nerves using a device developed for such a task. They control breathing by sending commands to and receiving information from the diaphragm. Used to improve health, it is used to treat CSAHS or Cheyne-Stokes Respiration. Results showed a substantial improvement in central respiration events by 50%. A study points to a reduction in 55% of the AHI in 3 months and for a population of 57 patients [211].

3.4.9 Surgery

Surgery is an invasive method and it is applied as a last resort to help improve the patient's quality of life. A type of surgery is bariatric surgery, which has the objective of decreasing the patient's weight. Patients may underwent bariatric surgery if they have, at least, a BMI of 35 kg/m^2.

OSAHS is high among overweighted patients, with a direct relationship with an increasing in BMI. Those patients may undergo bariatric surgery, but there are no guarantees in solving by itself SRBD [213, 214]. A cohort study on bariatric surgery was performed with 24 overweight patients. At baseline, before surgery, the patients were 47.9±9.3 years old, and they were assessed again 1 year later. The patients evolved from a BMI of 51.0±10.4kg/m^2 to 32.0±5.5kg/m^2 ($p\leq0.001$), and from a AHI of 47.9±33.8 events per hour to 24.5±18.1 events per hour ($p\leq0.0001$). All but 1 patient did not have resolution of OSAHS [224].

Bariatric surgery has different procedures available, and laparoscopic sleeve gastrectomy, biliopancreatic diversion, or Roux-en-Y gastric bypass are some examples available. A review of 69 studies, a total of 13900 patients, reports a great impact of the surgery in OSAHS, with 75% of the patients improving their OSAHS scores. The biliopancreatic diversion procedure was the most successful procedure achieving 99%, at least, in improving the patients' OSAHS (82.3% had OSAHS resolution).

The laparoscopic sleeve gastrectomy was the least successful with 86%, at least, in improving the patients' OSAHS (72% had OSAHS resolution) [225]. An increase in the patients' weight is possible and should be closely followed up to control that weight evolution. Review studies reported the lack of a clear definition of weight to regain, and the scarce research and report about this thematic [226].

Other anatomical sites can be targeted by different surgical procedures. Nose treatments include septoplasty (septum correction), polypectomy (polyps removal) and turbinectomy (partial or total turbinate bones removal) [218]. Uvulopalatopharyngoplasty is a procedure targetting the soft palate, at the back of the top of the mouth. Its objective is to remove or reposition tissues, soft palate, uvula, tonsils, and muscles in excess, in that area, to have the airway wider. Laser-assisted uvulopalatoplasty targets the soft palate and the procedure uses a laser to scar and stiffen the tissue. Although less painful than the uvulopalatopharyngoplasty, is also less effective [213, 218]. Radiofrequency volumetric tissue reduction is a treatment solution for patients with Mi to Mo OSAHS. The target tissues are the soft palate, tonsils, and tongue and it cauterizes the tissues to shrike them. The genioglossus advancement and the hyoid suspension procedure target the advancement of the major tongue and a piece of bone of the jaw, and the hyoid bone, respectively, to open space behind the tongue. The midline glossectomy and lingualplasty is a procedure to perform a partial removal of the back of the tongue to make it smaller and the airway wider. Maxillomandibular osteotomy and advancement is for Se OSAHS cases, where the upper and/or lower jaw are move forward [219]. Palatal implants may be used in snoring or Mi patients, and the procedure inserts fiber rods in the soft palate to stiffen it, decreasing fluttering. Surgical procedures to treat snoring, outside the nose, include radiofrequency surgery of the soft palate, Laser-assisted uvulopalatoplasty, and palatal implants to improve flutter [227].

A surgical procedure to treat SRBD, changes local anatomy and, as a consequence, the resonance chamber of the upper respiratory also changes. An analysis of the fundamental frequency and the first and second formant frequencies of the 5 Italian vowels was performed before and after surgery. The fundamental frequency was unchanged, but the formant frequencies were significantly different. These patients underwent surgeries in different anatomic locations [228].

3.4.10 Positive Airway Pressure Therapy

Positive airway pressure refers to all treatments based on a stream of compressed air into the respiratory airway. The machine connects to the patient through a tube with a mask at one end, either nasal or facial, and it is the interface machine-patient, to equalize air pressure between them, and higher than the atmospheric pressure. The higher pressure prevents the collapse of the upper respiratory airway structures,

allowing normal breathing, and improving the patient's quality of life and the sleep assessment parameters.

Therapy prescription requires an in-laboratory sleep evaluation to optimize machine configurations. The mask should be selected, facial or nasal, and different brands, accordingly to patients' face morphology and the capacity to eliminate air leaks between the mask and the face. Air pressure configuration, in cmH_2O, should be balanced between low pressure, to avoid air leaks, and high pressure, to be effective (to avoid the collapse of the respiratory airway structures) in the treatment of the sleep disorder. Usually, air pressure is configured between 4 and 20 cmH_2O. It is necessary for some time to adapt to the new environment, during which the patient may have headaches or stomach bloating, just to name a few, which should be temporary [216, 229].

3.4.10.1 Continuous Positive Airway Pressure

CPAP-based treatment uses a single pressure, in-laboratory pre-determined, during the entire night, and in both inspiratory and expiratory phases. It was developed by Colin Sullivan in 1981, Australia [229]. Besides improving sleep assessment parameters, studies reported a reduction in hypertension [230], daytime sleepiness [231], an improve in blood oxygenation [232], and in mortality [233, 234]. CPAP is to OSAHS treatment, as the PSG is to OSAHS assessment [214, 219].

3.4.10.2 Bilevel Continuous Positive Airway Pressure

Bilevel Continuous Positive Airway Pressure (BiPAP) is an evolution of the CPAP treatment because it uses 2 pressures, one to the inspiratory phase, and a second, lower than the first, to the expiratory phase. By using 2 different levels of pressure, the lungs may work more efficiently. Spontaneous BiPAP machines work by switching air pressure as a response to a shift in the respiratory phase. In more severe pulmonary disorders, such as the case of chronic obstructive pulmonary disease and emphysema, it may be necessary for the BiPAP machine sets the respiratory rate. The treatment of CSAHS using BiPAP is also effective. These machines may use pressures up to 30 cmH_2O [229].

3.4.10.3 Auto Continuous Positive Airway Pressure

An auto titration positive airway pressure machine has some intelligence incorporated because it has the capability of adjusting air pressure as a response to changes in the respiratory patterns. The incorporated algorithm allows pressure variations across the night, which means the machine can decide to not interfere when the patient has normal respiratory patterns, and it helps when the respiration is abnormal, with snoring or abnormal sleep events [229].

3.4.10.4 Servo

The Adaptive Servo-Ventilation is a type of ventilatory therapy to treat SRBD, especially, central sleep apnoea by using 2 different pressures. Ventilation pressure during the expiratory phase may be adjusted to control obstructive events, but it differs from the other therapies, BiPAP and CPAP, by featuring a dynamic pressure adjusting capability, from a respiratory cycle to the following one, in the inspiratory phase and by normalizing the respiratory rate to a predefined value [235].

3.5 Highlights of PSG Research

3.5.1 PSG Automatic Scoring

The diagnosis of OSAHS is PSG-dependent, and its scoring is critical to achieving accurate and precise results. Manual scoring of PSG studies is the current gold standard, but an automatic scoring, with equivalent results to the manual scoring, would increase speed, and dramatically decrease scoring time, since a sleep technician spends a couple of hours to complete the task. Notwithstanding, there are differences in scoring among sleep technicians. AASM has an inter-scorer reliability program to estimate the epoch by epoch agreement between sleep technicians. The latest results of this program show overall inter-scorer reliability for scoring respiratory events of 93.9% (κ=0.92). Epochs without respiratory events had an agreement of 97.4%, while epochs had an overall agreement of 88.4% (κ=0.77) for the existence of some type of respiratory event. Obstructive sleep apnoea, central sleep apnoea, and hypopneas had an agreement of 77.1% (κ=0.71), 52.4% (κ=0.41), and of 65.4% (κ=0.57), respectively [236]. A second, prospective, study on inter-scorer agreement achieved strong evidence of an agreement among experienced sleep technicians among the 9 Sleep Apnea Genetics International Consortium centers. The study included a total of 15 PSG to score, and each epoch was evaluated to sleep stage, arousals, apnoeas, and hypopneas, using AASM guidelines. Nine sleep technicians, 1 from each site, score all the PSG studies, and the intraclass correlation coefficient was used to do agreement analysis. The results for the inter-scorer agreement returned intraclass correlation coefficient of 0.95 for AHI, 0.77 for total apnoeas, 0.80 for total hypopneas, and 0.68 for arousals index [237].

Important research efforts have been made to implement an automatic solution by exploring the computational resources. The most important milestone, in the development of an automated solution, is to achieve, at least, the same manual scoring performance. One of the first projects to use computational resources to score PSG studies was developed in the SAMOA project, using an integrated software program, in which the algorithm uses the information gathered during the entire medical process of the SAHS diagnosis. The software integrates conventional programming with

"artificial intelligence techniques" while dealing with different time references [238].

The development of automatic algorithms is a state-of-the-art concern in the research community, intending to put machines performing repetitive tasks as well as complex tasks. In sleep, they have been developed to do automatic sleep stage classification [239–244], OSAHS events detection [245, 246], EDS detection [247], OSAHS severity [248], and sound classification [249, 250].

A study with 70 PSG studies conducted a research to assess automatic scoring of those PSG files, and inter-scorer agreement was also tested, using 10 sleep technicians. Automatic scores were compared with the manual scoring and using intraclass correlation coefficient, the results showed a great amplitude, depending on the parameter analysed. Some parameters had very good results, like global AHI, AHI in REM sleep, and obstructive apnoea with values above 0.9. Other parameters had poor results, all below 0.6, as is the case of arousals in REM, sleep stage N1 and N3, and latency to REM. Details about the methods used in software development for automatic scoring were not detailed [251, 252].

More recently, new approaches have been implemented to improve automatic scoring results and to improve reliability in those results among medical staff. A so-called "human-computer sleep scoring" (HCSS) system was proposed, and it is a middle term between fully automatic and fully manual scoring. Implement in 30 PSG already manually scored, they were again manually scored by 2 sleep technicians. Scoring a sleep stage for a long period reveals a low level of disagreement, but when there are constant stage changes the disagreement increases. The concept performs automatic scoring in regions of high reliability, and low disagreement, using stage change distance, stage change frequency, and slow wave-related features, as their metric to define those regions as high or low. High disagreement regions were manually scored by a sleep technician. The overall agreement between the HCSS system and the manual scoring was 89.74% and 91.10% for sleep technicians 1 and 2, respectively (κ=0.84 and κ=0.86). A comparison was made between a fully automatic and the HCSS system, splitting PSG in terms of sleep efficiency, a threshold of 85% (good vs poor sleep quality). For subjects with good sleep efficiency, the agreement was 84.74% between the fully automatic system and the initial manual score, 88.88% between HCSS system and sleep technician 1, and 89.53% between HCSS system and sleep technician 2. For subjects with poor sleep quality, the agreement felt for 79.02% between the fully automatic system and the initial manual score, 88.44% between HCSS system and sleep technician 1, and 87.27% between HCSS system and sleep technician 2 [253]. The HCSS system performed better than its fully automatic version, although the latter should have been compared against manual scoring of sleep technicians 1 and 2.

3.5.2 Data Acquisition

3.5.2.1 Channels

The configuration of the PSG study allows using a great number of sensors, besides the use of other equipment, only for research purposes, for data acquisition. Data from PSG offer different combinations in channel analysis with 2 degrees of freedom: the number of channels and the type of channels selected. Some studies were conducted using more channels than the typical PSG study, increasing the number of EEG channels to 21 (following the International 10–20 system) [241]. An example of parallel data acquisition to PSG is the use of non-contact microphones to acquire and analyse snoring in patients [239, 254].

Data from EEG, EOG, and chin EMG channels were used in [15, 16], while data from abdominal and thoracic movements and pulse oximetry were used in [255]. Single channel-based research was performed using the EEG [17, 240, 256], but also EOG [257], ECG [258, 259], EMG [260, 261], pulse oximetry [247, 262–264], cannula and thermistor [265, 266], abdominal and thoracic belt sensors [127], and the snoring piezoelectric sensor [137, 267].

3.5.2.2 Hardware

Multiple studies used only data collected from the equipment of the sleep medical centres, and from the questionnaires performed by the sleep technicians. This methodology does not require more equipment for data acquisition, speeding up the acquisition phase [15, 241, 255, 258, 262]. A methodology following data acquisition from both the sleep medical centres data and from research equipment is also very common. Research equipment may improve data quality by using better filters, increasing sampling frequency, using a different type of sensor (e.g. non-contact vs contact microphone), by increasing the number of channels in one particular type of signal (increasing the EEG channels to 21, following the International 10–20 system)), or by increasing the the number of channels in one particular signal of signal, but in different anatomical areas [239, 241, 260].

Snoring analysis follows different methodologies, varying in the number of microphones and their type (non-contact vs contact microphones). Researchers may use more microphones, but the most common methodology uses either 1 or 2. Contact microphones, of piezoelectric type, are placed in the neck, close to the upper respiratory airway (trachea). Non-contact microphones are placed at a distance between 30 to 100 cm to the head (due to subject movements in bed), above the head, and it usually uses directional configurations, like hypercardioid patterns [137, 239, 268]. Analogue sound acquisition is digitized at a sampling frequency between 8 kHz and 44.1 kHz and 16 bits of resolution [137, 239, 268, 269]. The microphone may also be

used in a contact profile and during the day, with the subjects awake [248].

3.5.3 Feature Extraction

3.5.3.1 Anthropometric Features

Anthropometric data are collected in the questionnaires, together with the diseases and medication, and consumption habits, and are useful to evaluate OSAHS. Some of the anthropometric features used in this field includes the neck circumference [248, 270], height [248, 271], weight [248, 271], craniofacial shape [272], age [248,271], gender [248,270,271], Mallampati score [248], race [272], position [263], and genetic factors [272].

3.5.3.2 Time-Domain

Time-domain features are calculated directly from the time series. The sleep medicine field, regardless of the type of signal under analysis, had already implemented a long set of feature extraction methods, and the hereby list is a compilation of those features. The features' list used in this research field includes time duration [246, 264], area [246], amplitude [264], maximum and minimum [243], zero-crossings [254, 273], *Hjorth* parameters (activity, mobility and complexity) [240], Empirical Mode Decomposition (EMD) [258, 264], detrended fluctuation analysis [274, 275], mutual information measure [276], matched filtering [277], period-amplitude analysis [273,278], energy [15,16,254], likeness method [279], canonical detection method [279], and Fujimori's method [280, 281].

3.5.3.3 Frequency-Domain

Frequency-domain features can not be directly calculated from the time series, but rather from the signal transformation into its representation in the frequency domain. The Fourier Transform (FT) is the most widely used mathematical operation to transform the time series signal in its equivalent in the frequency domain, with its frequency components [268].

Due to the stochastic nature of the PSG data, the analysis of the distribution of power over the frequency range may help to characterize better those signals. The Power Spectral Density (PSD) estimates the spectral density of the signals, and several methods are available to calculate the signal's PSD, which are grouped in one of these 2 classes: parametric or non-parametric methods [262]. The parametric methods are known as model-based methods, assuming the model for data, and they work based on the estimation of the model's parameters. Then, the estimation of the PSD is achieved by replacing the model's parameters in the expression of the PSD. Non-parametric methods rely on the calculation of the FT of the signal's estimate autocorrelation, and they have limitations associated with spectral leakage and resolution. Weak signals are masked and hard to detect in the PSD and to

overcome resolution issues and improve PSD estimation, data has to have long data records. Non-parametric methods used windowing which adds distortion due to window effects, but they are more robust than parametric models, which may contain spurious frequency peaks if the assumed model is wrong.

The parametric class encompasses the moving average, the autoregressive, and their junction in the autoregressive moving average [282, pp. 987]. From these methods, other approaches were developed to calculate PSD, including time-varying autoregressive, time-varying autoregressive moving average, autocorrelation, Burg, covariance, modified covariance, Yule-Walker, Burg, and Kalman filtering [240, 245, 249,269,283–286]. The non-parametric methods include the periodogram, the correlogram, and modified versions of the first 2 [282, pp. 974]. Among the modified versions are the Welch [246,248,262,263,287], Bartlett [288,289], Blackman-Tukey [290], Capon (Minimum Variance Spectral Estimator) [288, 291], multi- window spectral estimator [268], Daniell [292, 293], and Lomb-Scargle [247] have being used in OSAHS research. Figure 3.3 presents the organization of the PSD methods and it gives examples of methods in each subgroup.

From the different available mathematical tools to get the signal in the frequency domain, several features can be calculated, including the total spectral power [15, 240, 246, 262, 263], symmetry coefficient [239], spectral power [239, 240, 243, 294], power ratio [15, 239, 240, 246, 262, 263], spectral centroid [15, 239, 240, 242, 250], spectral spread [242, 250], spectral decrease [242], spectral roll-off [242, 250], spectral slope [242], spectral density [241], maximum and minimum [243], power at central frequency [240], respiratory frequency [246], spectral edge frequency [295], spectral flux [250], spectral flatness [242], and spectral correlation [294].

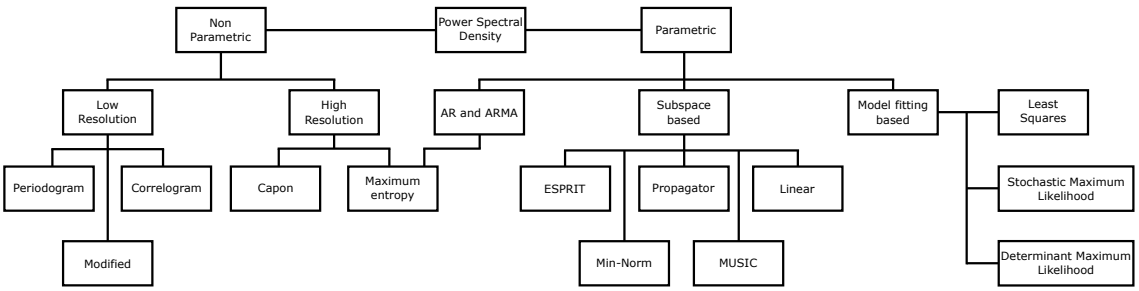

Figure 3.3: How PSD methods organize in different categories. The main division is between the parametric and non-parametric groups. Examples of modified low-resolution non-parametric methods are the Welch, the Bartlett, and the Blackman-Tukey. Among the parametric methods, there are the autoregressive (AR), the autoregressive moving average (ARMV), the multiple signal characterization (MUSIC), and the estimation of signal parameters via rotational invariance techniques (ESPRIT). These methods have been used in the sleep medicine field, to a better comprehension of the OSAHS.

3.5.3.4 Time-Frequency Analysis

Real-world data, in particular biomedical signals, are non-stationary signals, in which the frequency composition of the signal changes over time, and where new frequencies emerge, others disappear, and some change their overall importance in the signal structure. Time-frequency analyse focus on the study of the signal, simultaneous, both in the time and in the frequency domain, and it is quite popular in OSAHS studies. Methods like short-time fourier transform [240, 268], wavelets [16, 240, 257, 258, 296], constant Q transform [268], mel-frequency cepstral coefficients [250, 268], synchrosqueezed wavelet [127], matching pursuits [297], joint time and time-frequency analysis [298], Hilbert–Huang Transform [296], Wigner-Ville distribution [299], and Choi-Williams distribution [296] were already used to deliver signal's features.

3.5.3.5 Non-Linear Methods

Non-linearity is of interest in many areas, including mathematics, engineering, and biology, and they are, also, implemented in OSAHS field study. The following non-linear methods have been used in the study of sleep and SRBD. It is the case of the correlation dimension [240, 246, 300], Lyapunov exponents [240, 246, 300], fractal dimension [240, 300], Hurst exponent [240, 243, 300], Higuchi Fractal Dimension [246, 297], dimensional complexity [240], central tendency measure [262, 264, 287], Lampel-Ziv complexity [246, 262–264, 287], synchronization likelihood [301], recurrence plot [300, 302], phase space plot [300], delay vector variance [303], Green-Savit measure [304], fuzzy sets [305], petrosian fractal dimension [243], mean curve length [243], mean energy [243], mean Teager energy [243, 295], temporal energy [243], energy [243], and correlation exponent [306] methods.

3.5.3.6 Statistical Methods

Getting features from statistical methods is domain-independent, and features as the case of mean [239, 240, 259, 262, 263, 287], mode [239], median [240, 262], variance [239, 259, 262, 263, 287], standard deviation [239, 240, 259, 307], root mean square [240, 259], percentiles [246], skewness [239, 240, 262, 263, 287], kurtosis [239, 240, 262, 263, 287], correlation coefficient [16], and entropy (Boltzmann-Gibbs, Tsallis, Shannon, Spectral, Sample, Maximum, Approximate, Kolmogorov-Sinai) [241, 243, 246, 257, 262–264, 276, 287, 300, 308–312] have been used in sleep, and particularly, in OSAHS research.

3.5.3.7 Other Methods

Other methods may be implemented to get features as the case of independent component analysis [244, 313], principle component analysis, tomography [128, 313], EEG generation model [277], coupled oscillators model [314], and random walk

theory [315].

3.5.4 Feature Selection

Feature extraction may generate a set of features unsuitable for classification, and a pre-classification step should be designed to select the appropriate features. Feature selection eases downstream processing and analysis by reducing the number of features, redundant or insignificant features, used by the classifier, and choosing the best features to have discriminant capability among the different medical classification groups. Methods for feature selection can be classified accordingly with the existence of label information or search strategy. Label information-based classification organizes methods in supervised, semi-supervised, and unsupervised, while search strategy-based classification organizes them in a filter, wrapper, embedded, and hybrid methods [316–320]. Wrapper methods have a high computational requirement and perform feature selection based on the classifier performance over different feature subsets. Analysing the results for the different subsets, it predicts the benefits of adding or removing a feature [245]. Methods like genetic algorithm [271, 287, 297], particle swarm optimization [271], artificial neural networks (back propagation) [271], logistic regression [271], F-score [246], recursive feature elimination [246], k-nearest neighbourhood [245], support vector machine [271], decision tree (C4.5) [271], random forest and stepwise [250], unpaired t-test [248], Wilcoxon test [245], and non-parametric Kruskal-Wallis one-way analysis of variance [242] were already used in this field.

3.5.5 Classifiers

All methods implemented in data processing and analysis return a matrix of data to perform classification by finding a model capable of discriminating the existing classes or concepts [321–324]. Several classifiers have been tested in the sleep medicine field research. Artificial neural networks [240, 243, 245, 247, 270], bootstrap aggregation [242], fuzzy classification [244], logistic regression [239, 248, 287, 307], maximum likelihood [249], linear discriminant analysis [258], quadratic discriminant analysis [258], support vector machine [127, 243, 246, 250, 325], hidden Markov model [250, 267], decision tree [15, 250], k-nearest neighbours algorithm [243, 245, 250, 276], theory of evidence [326], Bayesian classifier [327], and conditional random field [328] are some of the classification methods used. A common practice in classifiers is the creation of hybrid classifiers to improve performance, as the case of the rule-based case-based hybrid classifier [329], or the neuro-fuzzy classifier, which works well with no *a priori* information [276].

3.5.6 Statistical Analysis

Statistics is the science related to collecting and analysing data, and it works in 2 directions. Sampling a population to do descriptive statistics of the sample, mean, and standard deviation, among other methods, and to do inferential statistics, to infer a characteristic of the population based on a sample from the same population. Data from the sample can be classified as categorical, ranked (ordinal), discrete, or continuous, and hypothesis testing consists of the formulation of a question to test the population's sample. Hypothesis test methods are classified as parametric and non-parametric. Parametric methods are selected when it is possible to assume that the sample data comes from a specific data distribution, and non-parametric methods are used when the knowledge about the population's sample distribution is reduced, and they typically need more data to achieve statistical significance for the same degree of confidence. These methods test the veracity of the null hypothesis, against the alternative hypothesis, and there 2 types of errors associated with the test. Type I error happens when the hypothesis test finds a significant difference, with the rejection of the null hypothesis, but there is no difference. Type II error happens when the hypothesis test does not find a significant difference, no rejection of the null hypothesis, but there is a difference.

Choosing the correct statistical tool to evaluate the sample is of high importance, and several methods are available to evaluate statistical significance. Table 3.1 presents a possible method to apply depending on the variables' conditions, type and number.

The statistical analysis of data does not follow a straight rule to implement the methods available, but rather guidelines and each case should be carefully analysed. As in any research field, sleep and OSAHS study use statistical tools to know if there is statistical significance among the groups, and some examples are presented below. The non-parametric Mann-Whitney U test and the Kolmogorov–Smirnov test were used in [262, 286, 287], the non-parametric Kruskal-Wallis test and the χ^2 test were used in [263], the ANOVA test was used in [137, 257, 260, 278, 300], the Fisher'spartial least-squares difference was used in [260], the Student's t-test was used in [137], MANOVA test and the Bonferroni test were used in [274], one-way ANOVA and Kolmogorov–Smirnov test were used in [286], the Student's t-test and the paired Student's t-test were used in [283], and the two-tailed z-test was used in [330].

Table 3.1: Statistical methods for hypothesis testing in 1 of 2 scenarios, without or with 1 independent variable (predictor). The dependent variable (predicted) under evaluation may be of type interval, ordinal, or categorical. Hypothesis testing depends on the sample (nature of the independent variables) and the nature of the dependent variable. This table is based in [331]. *Assumption of normal distribution for hypothesis testing.

Independent Variables (IV)	**Nature of Dependent Variables**	**Test**
0 IV (1 sample)	Interval*	One-sample t-test
0 IV (1 sample)	Ordinal or Interval	One-sample median
0 IV (1 sample)	Categorical (2 categories)	Binomial test
0 IV (1 sample)	Categorical	χ^2 goodness-of-fit
1 IV (2 independent samples)	Interval*	Unpaired sample t-test
1 IV (2 independent samples)	Ordinal or Interval	Wilcoxon-Mann Whitney test
1 IV (2 independent samples)	Categorical	χ^2 test
1 IV ($\geq$2 independent samples)	Interval*	One-way ANOVA
1 IV ($\geq$2 independent samples)	Ordinal or Interval	Kruskal Wallis
1 IV ($\geq$2 independent samples)	Categorical	χ^2 test
1 IV (2 dependent samples)	Interval*	Paired sample t-test
1 IV (2 dependent samples)	Ordinal or Interval	Wilcoxon signed ranks test
1 IV (2 dependent samples)	Categorical	McNemar
1 IV ($\geq$2 dependent samples)	Interval*	One-way repeated measures ANOVA
1 IV ($\geq$2 dependent samples)	Ordinal or Interval	Friedman test
1 IV ($\geq$2 dependent samples)	Categorical (2 categories)	Repeated measures logistic regression

Chapter 4

Materials and Methods

This chapter focuses on the methods for data acquisition in this thesis. Due to the nature of the data, and prior to starting data acquisition, a formal request was submitted to the Ethics Committee of the CHUC to gather data. The main sources of data were a commercial, high-quality, audio device, the PSG study and its reports, and the questionnaire to the patient.

This project was developed, mainly, on a laptop with an Intel i7-3610QM @ 2.3GHz CPU, with 6 GB of RAM (later upgraded to 10 GB) in the MS Windows environment. Tasks related to data storage, data management, and data processing were performed in MATLAB software, a licensed product from Mathworks. Most of the tasks were executed using the 32-bit MATLAB R2012a software version. Later, the implementation of a specific method required the use of a more recent version, the 64-bit MATLAB R2017b.

The implementation of the project followed two independent paths, as summarized in the diagram of Figure 4.1. In one direction, the steps followed from data acquisition to data processing and analysis, and in the second direction which work was developed by the medical centre and which was developed by the research team. These topics are described below.

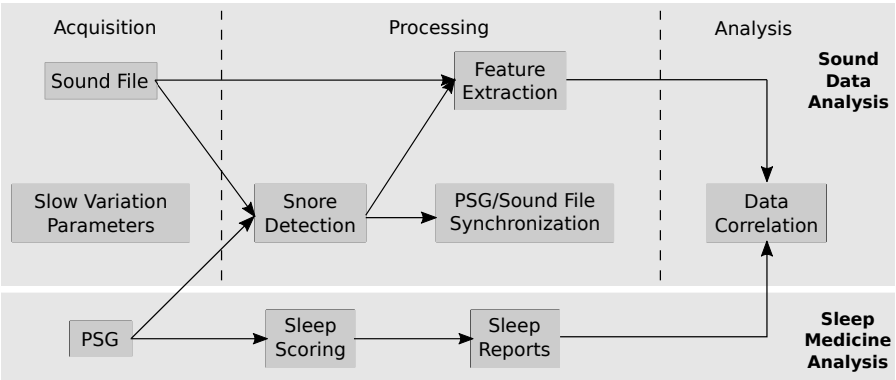

Figure 4.1: A diagram representing the entire process. From the different steps to data interpretation, data acquisition, processing and analysis, to the different purposes, clinical and research [332].

4.1 The Protocol between LIBPhys-UC and CHUC

Prior to data acquisition, a formal request to access the installations of the CMS was submitted to the ethical committee and to the board of directors of the CHUC. The request should answer important questions. A description of the work, its goals, and the scientific framework supporting it was presented, with reference to the physical healthcare facility requiring clearance. The strategy for the project setup, the informative conversion with the patients and their agreement (with signed formal documents), and the template of the questionnaire was also clarified. A declaration should also guarantee the existence of no financial costs, associated with this project, to the CHUC.

4.2 CMS Healthcare Facility

The CMS functions on a shift work basis, with different tasks assigned to the day shift and the night shift. During the day, there are several tasks assigned to sleep technicians and M.D.s. Sleep technicians, among other tasks, review sleep studies and teach patients to use sleep screening devices. M.D.s have medical appointments to attend with their patients in the facility division M1 or M2 (see Figure 4.2). They decide the patients' treatment and which patients perform portable sleep studies, at home, and which ones must be assessed at the clinical facility.

4.2.1 Night Shift

The night shift is dedicated to performing PSG studies and it begins at 21h30m, with 2 sleep technicians welcoming a maximum of 4 patients. The CMS has 4 beds, R1 to R4 in Figure 4.2, and the sleep technicians must manage the assignment of patients, to the rooms, following criteria, like the patient's weight. The preparation starts with a questionnaire to the patient, which includes anthropometric questions and the gathering of diverse information, on the impact in sleep.

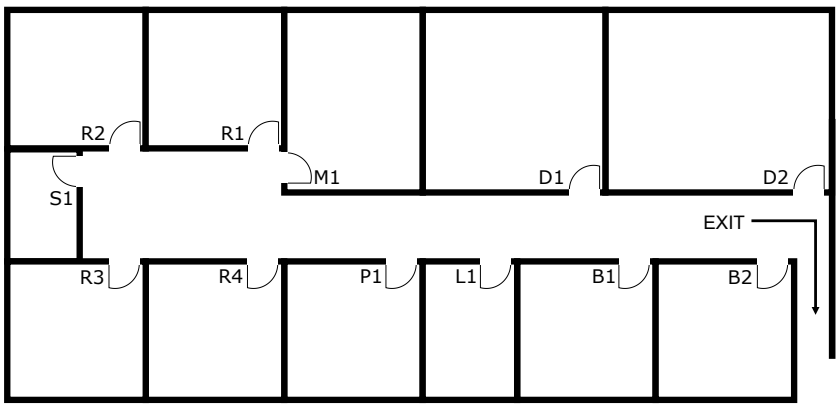

Figure 4.2: A partial layout of the CMS, including only the floor where the PSG study took place. PSG studies were perform in rooms R1 to R4, while sleep technicians monitored data acquisition in M1, and medical appointments are at D1 and D2. S1 is for sleep equipment storage.

The sleep technician starts sensor placement in the head, with its measurement to a correct EEG placement. Following the EEG placement, the EOG and the EMG are the next ones. The area under the electrode should be properly clean, with an abrasive material, to remove dead tissues and to decrease the impedance of the skin surface to acceptable ohmic values. The signal conductivity also improves using a conductive paste, placed between the skin surface and electrode, they use cup gold electrodes. To hold the sensors in position the entire night, the technicians use a combination of gaze with either plaster or colloid. The upper limit for EEG and EOG ohmic values are 5kΩ, and 10kΩ for EMG and ECG. Between the same type of electrodes, the ohmic values should be as closely matched as possible. ECG, snore, and EMG leg movements sensors placement require the use of an abrasive product to clean the skin surface and to reduce impedance.

The remaining sensors are transducers and do not require the application of abrasive materials to improve conductivity. The nasal cannula is a pressure sensor and the thermistor is a temperature sensor. They do not need skin contact and they only require a proper placement in the front of the nose and the mouth. The thoracic and the abdominal belt sensors rely upon the movements of expansion and contraction of the thorax and the abdomen. The body position sensor does not measure any intrinsic body signal, but rather, the relative position of the body to the external environment. The pulse oximetry sensor measures O_2 saturation in the index finger, which obliges the nail to be in its natural state, which means, without any type of painting or polishing. Adhesive tape should be used to help to secure the different sensors in place.

Electrodes are connected to a local device and each room has its acquisition system, with the CMS using 2 different hardware models of acquisition systems. One hardware model is in rooms R1 and R2 and the second is in rooms R3 and R4. All data go to computers, one computer for each room, in division M1 (see Figure 4.2), where sleep technicians monitor the PSG study. There are different acquisition systems in the market and they may have different amplification, filtering, and calibration settings, but they must follow AASM guidelines as close as possible.

Patients' preparation ends before midnight with all of them going to sleep around midnight and data, for sleep assessment, starts to count after marking this moment in the acquisition software. During the night, sleep technicians keep a close look at the data to assess their quality and patients' sleep quality. Poor data quality requires sleep technician intervention, for example, of a sensor detachment, and poor sleep quality may require the application of sleep treatment to the patient. The end of data acquisition is scheduled to be around 7 a.m. The final procedure included the removal of sensors, their cleaning, and the writing of reports to describe the patients' sleep.

4.2.1.1 PSG Equipment

PSG data acquisition was performed in 4 bedrooms (layout in Figure 4.2), with rooms R1 and R2 using the SomnoStar z4 (Viasys), and rooms R3 and R4 using the Jaeger to receive, to amplify and to send data to M1 room, through an Ethernet cable. Sleep technicians monitor the PSG study in room M1, using 4 computers, each computer receiving data from one of those devices, with the SomnoStar 9.1f software.

4.3 Population Characterization and Subject Sampling

The selection of patients to participate in this study was the result of a discussion between the sleep technicians, under the advice of M.D. José Moutinho dos Santos, and the researcher responsible for gathering data. The selection method to participate in this study was not probabilistic, in the sense that each individual does not have the same probability of being sampled. The method followed a non-probabilistic sampling known as convenience sampling and was based on the presence of the subject in a well-defined geographic location, the CMS [333].

Patient selection criteria included a full basal PSG study, which means that patients scheduled to perform a PSG study with the application of a nasal or an oro-nasal mask for sleep treatment were, immediately, excluded. Sleep technicians performed real-time sleep evaluation and there were patients meeting the criteria for the immediate application of treatments (mask). The PSG sleep study was no longer a basal type study, but rather a split-night study, which met the exclusion criteria. The decision to include only PSG basal studies is related to a modification in the snore signals properties by using masks and the corresponding increased air pressure inside the upper airway structures. Another exclusion criterion was related to the sound acquisition device performance, which often failed to complete a sound acquisition. Overall, 165 patients were invited to participate in this project and, due to multiple causes, the exclusion criteria process resulted in 67 patients validated, an acceptance rate early 41%. The entire sequence of patient selection is in Figure 4.3, with all the criteria leading to the final selection.

At the beginning of data acquisition, the normal functioning of the CMS included a 4-night schedule per week to perform PSG studies, but it changed to 5 nights per week, later. From the date of the first acquisition to the date of the last acquisition, the period of acquisition lasts for 373 days, which is equivalent to nearly 53 weeks. This means a mean of nearly 3 data acquisitions per week. The main reasons to get a mean below of 4 data acquisitions per week were related to holidays, vacations, and the missing of patients suitable to participate in the study.

All patients selected to participate in this study received a brief description of the project, with an emphasis on aspects directly involving the patients, like data acquisition and questionnaires. Patients willing to participate in the study should give formal consent and answer a questionnaire. The questionnaire focused on 3 main areas, anthropometric information, medical history, and consumption habits. The anthropometric information included questions about age, gender, weight, height, and cervical perimeter. The medical history focused on diseases related to OSAHS, the beginning of OSAHS and related complaints, medication, and nocturia. The questionnaire also had questions regarding the intake of coffee and alcohol and smoking, including consumption frequency. The questionnaire should be more complete with questions regarding the consumption of drugs, bedding time, and the number of hours of sleep.

The final set of 67 patients, 41 males, and 26 females was classified by the M.D. José Moutinho dos Santos in 1 of the 5 possible medical classification groups. Results from PSG scoring helped to classify as non-OSAHS patients, either a Co or a Sn subject, or as OSAHS patients, with increasing severity from Mi, to Mo and to Se. A detailed statistical characterization of the population is in Table 4.1, with separation by gender and with the inclusion of some of the collected anthropometric data. To know the complete and detailed data of the questionnaire see Appendix B.

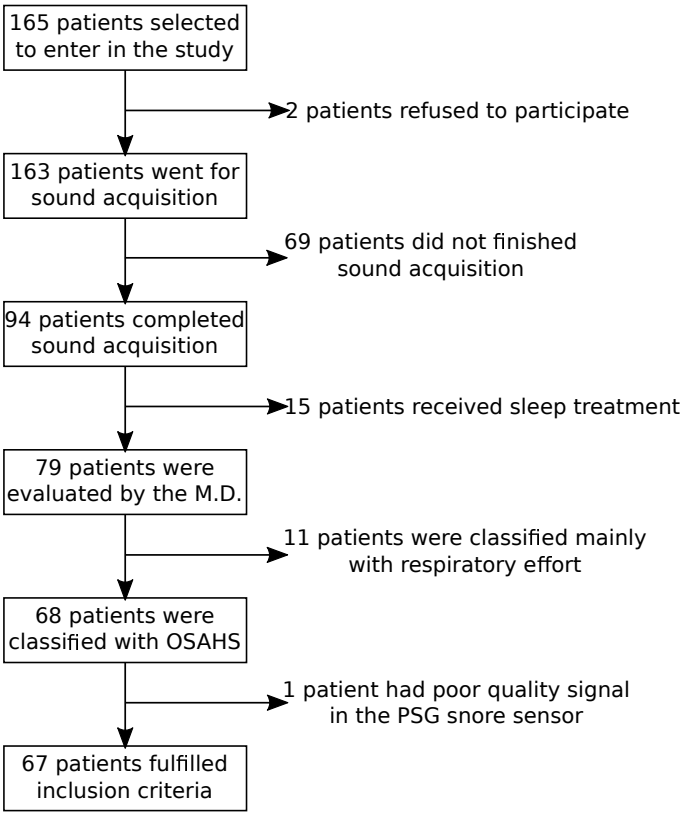

Figure 4.3: The implementation of exclusion criteria to the patients from the moment they were selected to participate in the study.

Table 4.1: Patients' anthropometric, age and gender data organized according to their medical classification group. There are 5 medical classification groups: Co, Sn, Mi, Mo, and Se. The mean, μ, and the standard deviation, σ, of the patients' height, weight, cervical perimeter (Cervical P.) and age are the statistical information available in the table. The number of males and females in each medical classification group is also available [332].

Parameter		**Non-OSAHS**		**OSAHS**		
$[\mu \pm \sigma]$		*Co*	*Sn*	*Mi*	*Mo*	*Se*
Height	(cm)	167±11	167±10	166±11	167±9	170±8
Weight	(kg)	76±20	77±23	77±11	91±20	88±17
Cervical P.	(mm)	386±45	393±46	390±35	418±40	436±50
Age	(years)	43±15	49±15	49±10	55±12	56±12
Gender	M	4	14	7	8	8
	F	5	10	6	5	0

4.4 Data Acquisition "Channels"

4.4.1 Sound Acquisition

The first important decision to make was related to the sound acquisition device. The development from scratch of an *ad-hoc* device for sound recording was discussed against the option of using a commercial device. During the decision-making process, pre-emptive actions were taken, in the case of a decision favouring the development of an *ad-hoc* device, and exhaustive research on commercial microphones and a short list of microphones was created along with some of their most important characteristics. Both options, the commercial sound acquisition device and *ad-hoc* device, have strengths and weaknesses. Table 4.2 presents all the weighting factors considered for each case.

Prior snoring studies have been performed between the LIBPhys and the CMS [334]. A dedicated solution was developed to perform data acquisition, but considerable levels of noise were always present due to the electrical grid. Filters were unable to suppress the majority of the noise, resulting in poor values of signal-to-noise ratio. Another decisive factor was the developing time necessary to get ready an *ad-hoc* device. Hardware design and assembly, and the implementation of tests require several months to ensure that all hardware and software function as expected. Investing the required amount of time in the development of a dedicated solution knowing the problems associated with noise filtering was considered a hazard, and, in the end, a commercial solution was preferred. A brief search for commercial sound acquisition devices led to the selection of the H4n, from the Zoom Corporation (Figure 4.4 (a)) [335]. From an economic point of view, the investment in the high-quality sound acquisition H4n device pays off, because the cost associated with this device was less than 200€. *Ad-hoc* device development would surpass significantly that cost if the developing time and the price of the components to assemble were take

Table 4.2: Advantages and disadvantages associated with a commercial device to perform sound acquisition against the hypothesis of developing an *ad-hoc* device with the same purpose.

Commercial Device		***Ad-hoc* Device**	
Advantages	*Disadvantages*	*Advantages*	*Disadvantages*
Data acquisition may start faster	Less control of both the acquisition and storage phase	Broad control over the data acquisition configuration	Development and test phases delay acquisition phase
Reliability		Allows to choose the microphone	Electrical grid 50Hz noise is hard to filter
Economically cheaper		Increase available information	

in account.

The H4n device has 2 built-in non-contact stereo condenser microphones, in an XY pattern and positioned at an angle of 90^{o} or 120^{o}. The orthogonal configuration minimizes phase error while each microphone is unidirectional and presents a cardioid polar pattern (Figure 4.4 (b)). Each microphone has a gain range between +7dB and +47dB. H4n records sound either in stereo or in mono sound and stores data in an SD card. All data recording sessions were performed in mono mode and uncompressed, with a sampling frequency of 44.1 kHz and 16 bits of resolution. Data was saved in a .wav file type extension. Other H4n specifications are in Table 4.3. The device creates a single file at the beginning of a new acquisition session and has the capability of addressing 2^{32} bytes (2GB). Settings for the sampling frequency and the number of bits of resolution create a constrain in the total acquisition time of 6h45m. The constrain is within the time interval, establish by the PSG protocol, of 6 to 8 hours.

4.4.2 Slow Variation Parameters

SVP were recorded using a combination of both commercial and *ad-hoc* hardware (Figure (4.5)). The Arduino company develops open-source hardware and software products for multi-purpose objectives and is capable of accepting expansion boards. An Arduino Uno board was selected to work as an interface between a computer and the custom-made expansion board.

4.4.2.1 Arduino Uno

Arduino Uno board functions based on a microcontroller ATMEGA328-PU and it offers multiple options to be powered. The microcontroller works with a 5V

Table 4.3: Main specifications of the sound acquisition device H4n.

Characteristics	Description
Inputs	Built-in stereo mic, 2 XLR inputs, 1 external stereo mic
Sampling frequency	44.1/48/96 kHz
Resolution	16/24 bits
Storage	Up to 32GB
Data Type	MP3, WAV
USB	USB 2.0
Outputs	Monaural speaker/jack for headphones
Display	128 x 64 dots LCD with backlight
Phantom Power	24/48V, Off
Power Supply	DC 5V 1A, 2 AA Batteries
Dimensions	73(W) × 156.3(D) × 35(H) mm
Weight	280 g

power supply and can be powered via a USB connection, an AC to DC converter, or a battery. Its characteristics include a 10-bit Analog-to-Digital Converter, digital and analogue ports, a serial communication protocol (I^2C) and interrupts.

4.4.2.2 *Ad-hoc* Hardware

Ad-hoc hardware was developed to acquire temperature, relativity humidity, and gauge pressure in the room. A single silicon chip, SHT25, was capable of delivering both temperature and relativity humidity. Developed by the Sensirion AG company, the sensor measures the temperature with a resolution of 14 bits, $\pm 0.1^{o}C$ repeata-

(a)

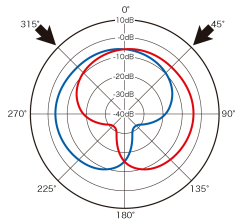

(b)

Figure 4.4: The H4n high-quality, sound acquisition device. Built-in microphones in XY pattern (a). Microphone sensitivity, in dB, for a frequency of 1 kHz (b). Left microphone sensitivity is represented in blue, while right microphone sensitivity is represented in red. Microphone direction are represented by black arrows [335].

bility and a low drift ($\leq$0.02^{o}C/year), and the relativity humidity with a resolution of 12 bits, $\pm$0.1% RH repeatability and a low drift ($\leq$0.5% RH/year). SHT25 is a digital sensor with an I^{2}C communication interface for user configuration and data reading. The MPXV7007GP analogue pressure sensor (from NXP Semiconductors) measured small variations in the atmospheric pressure using a reference value (gauge pressure). Capable of measuring in a pressure range between -7kPa and +7kPa, the sensor has a maximum error of 5% and a sensitivity of 286 mV/kPa.

The design of the hardware included an Real-Time Clock (RTC), an EEPROM memory (both from STMicroelectronics), and an amplification circuit for the analogue sensor. The RTC keeps track of the current time, with the aid of a 32768 Hz crystal, to timestamp data acquisition. The M41T81S RTC has 8 bytes available for the clock/calendar function, and it tracks time from the tenths of milliseconds to the switch of the century. For the purpose of the work, seconds, minutes, hours, days, months, and years were used to timestamp data acquisition. The M24512 EEPROM memory is a type of non-volatile memory capable of data retention for decades. The memory organizes storage in a page configuration of 128 bytes each, with a maximum storage capacity of 64 KB. Both memory and RTC share the same communication protocol with SHT25. Photography of the hardware is at Table 4.5, connected to Arduino Uno.

External interrupts, triggered by the RTC, keep the pace for data acquisition. The acquisition of a new set of data generates a block of 12 bytes distributed as follows. Half of the bytes are for SVP measurements, 2 bytes per parameter, and the remaining 6 bytes for the timestamp. Time and date were stored in the format hh:mm:ss and dd/mm/yy, respectively. The data acquisition period was of 3 minutes, which allows writing data for almost 11.4 days to the memory before it runs out of space. Measurements of data, using lower periods, were considered not suitable due to the possibility of memory storage roll-over and data loss. For example, for a period of acquisition of 1 minute, the memory would be full after 3.8 days, which can be achieved in a weekend followed by a holiday the next Monday. Due to the nature of the parameters, their variation is very slow and the period of acquisition

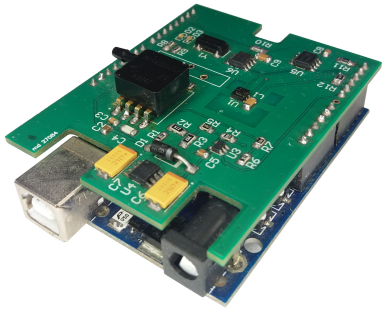

Figure 4.5: Hardware dedicated to the acquisition of SVP, temperature, relativity humidity and gauge pressure, (green board) using an Arduino Uno (blue board) to manage data acquisition and to communicate with a computer.

selected was convenient.

4.4.2.3 *Ad-hoc* Software

The data acquisition process needed 2 types of software, one to run in the Arduino and to manage the data stream between the Arduino and the *ad-hoc* hardware. A second software, running on a computer and to communicate with the first software, to configure and read data from the first software.

The second software was developed in Microsoft Visual Studio C#, 2010 version, with a Graphical User Interface (GUI). Its operation consisted of a serial communication, via USB port, to update RTC parameters, and to read both data and memory and RTC status (Figure 4.6). Data from timestamped slow variation parameters were saved in a Microsoft Excel file.

The description of the first software is not presented in this section since its functioning can not be dissociated from the hardware, previously discussed. The Arduino Software Integrated Development Environment is an application to develop software for the Arduino board and it was used to develop the data acquisition software, using the 1.0 version.

Gauge pressure sensor is an analogue sensor, and Equation 4.1 and Equation 4.2 are in its datasheet to convert from volts to Pa.

$$V_{out} = V_S \cdot (0.057 \cdot P + 0.5) \pm (PressureError \cdot Temp.Factor \cdot 0.057 \cdot V_S) \quad (4.1)$$

$$V_S = 5.0V \pm 0.25V_{dc} \quad (4.2)$$

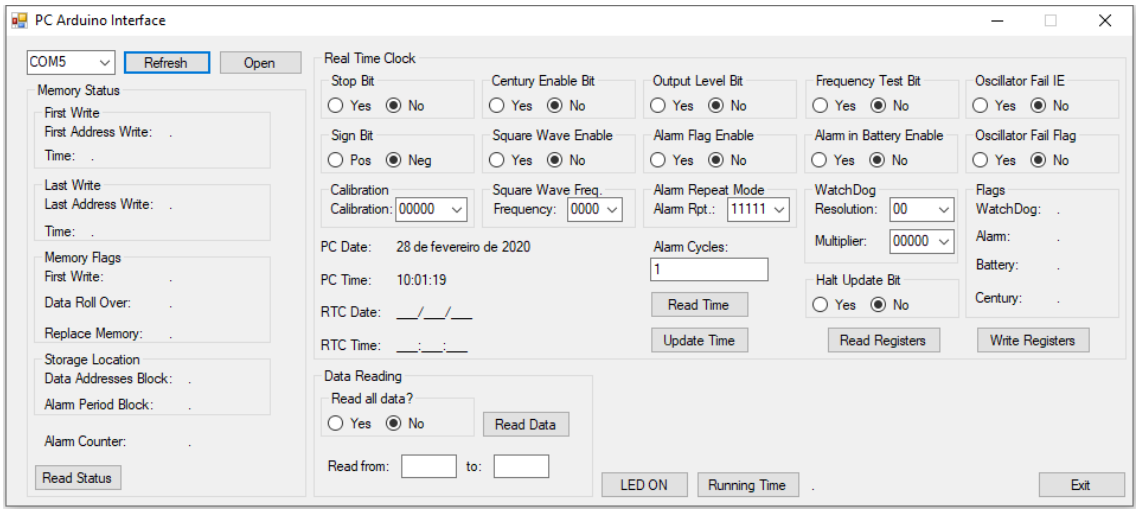

Figure 4.6: Software interface for Arduino computer communication. The interface reads and updates RTC registers, reads memory status and data storage in the memory.

4.4.3 Data Acquisition Apparatus

Both the H4n and the acquisition device for SVP were installed in a general-purpose framework and placed behind the bed (Figure 4.7). The *ad-hoc* hardware position was not critical and it was installed in local 1 of the figure (Figure 4.7 (a)). The framework had 2 degrees of freedom to adjust the H4n microphone's direction and point it, with the help of a LASER pointer, to the cushion and the midline of the bed. The microphones were positioned around 70 cm above the patient's head. Although there isn't a protocol to define how sound acquisition should be done in sleep studies, some researchers had chosen to acquire data from the perspective above the patient's head. They selected a distance from the source to the acquisition device of 30 cm [336] and 50 cm [337]. We used a higher distance to prevent incidents with the patient.

The CMS had a maximum capacity of 4 beds, which means it could run 4 PSG studies per night, with 2 sleep technicians monitoring the biomedical parameters. Patients were assigned to bed following CMS criteria and, depending on where the selected patient was placed, the setup might be moved to a different room.

(a) (b)

Figure 4.7: Setup of the sound acquisition system. In (a), H4n is positioned at the upper right corner and the *ad-hoc* hardware, although missing in this figure, was placed in 1. A LASER pointer helps, in 2, to redirect H4n's microphones to the midpoint of the bed's head. In (b), the final positioning for data acquisition during the night.

4.5 PSG Analysis

4.5.1 PSG Scoring

The commercial software developed to acquire and store PSG data also allowed to score the study and to identify sleep stage and abnormal medical conditions. Among its features is the capability for automatic scoring, as an alternative to the manual scoring performed by the sleep technicians. Nowadays, sleep technicians do not completely rely on software algorithms and they choose to perform either a 100% manual scoring or an automatic scoring followed by a manual rectification. The software at the CMS was one of the few to allow to split the arousals into two categories based on their duration: arousals and awake. The PSG scoring at the CMS followed the rules established at the AASM guidebook, *AASM Manual for the Scoring of Sleep and Associated Events*, from 2007.

4.5.2 PSG Reports Conversion

The PDF file type was the standard implemented to generate medical reports and it is a formatted file type. A formatted file type, in opposition to plain text, can not be directly readable by a generic text editor or a computer program. The PDF files have information regarding heart rate, sleep events, sleep position, sleep stage, and the beginning and the end of the PSG study, for sleep evaluation. The appropriate software can convert PDF files into a readable file type, and some of such tools are available online and with a free license. After testing some tools and assessing the achieved results, the Xpdf software package was the selected tool. The conversion from PDF to text used a particular tool, pdftotext.exe, part of a more comprehensive package, version xpdfbin-win-3.03 [338].

4.5.3 PSG Study Visualization and Processing

4.5.3.1 Read European Data Format Data

Acquisition software stored PSG studies in 2 files. The video signal from the patient's room webcam was stored in a file while the remaining data were gathered in a single European Data Format (EDF) file type. This work doesn't use and there wasn't access to the video signal, but the second file was of critical importance. In order to ensure patients' confidentiality, EDF files don't have personal information. The purpose of the development of the file extension EDF was the creation of a file capable of storing medical signals. The header storages information like the beginning and the end of data acquisition and the number of channels recorded. It has multi-channel storage capability, allowing the configuration of different acquisition frequencies, filters, signal units, and other calibrations for each channel. The EDF specifications were adopted by the sleep medicine field and they are, currently, the

standard for PSG recordings [339].

The specifications for the EDF data format are available for free, which allowed the development of software capable of reading the file and of extract the desired data. Several solutions were already available as EDF file viewer, the EDFbrowser, and the Polyman are some of the available solutions [339, 340]. It is possible to find online viewers [341] as well as applications for smartphones (OS Android) [342].

In this project, the purpose was to have not just an EDF viewer but a tool far more powerful, to deal with a second entry, the H4n file, and to allow access to data in both files. Although some scripts were available to run in MATLAB, the final decision was the development of a tool adapted to the need of the project. A GUI was developed, in MATLAB, to read, plot, and process the data from both the EDF and the H4n files.

4.5.3.2 PSG Graphical User Interface Development

The visualization of both the PSG study and the H4n high-quality sound data was fundamental to understanding faster and better how data behaves. Throughout the time dedicated to building our set of 163 patients, the sleep technicians had to adjust the typical PSG configuration to acquire more signals. From the final set of 67 patients all but 4 PSG studies had 20 sensors. Of the 4 remaining PSG studies, 1 of them had 19 sensors and the other 3 had 23 sensors.

At the CMS, the PSG study visualization follows a set of rules and they were taken in account in the development of the PSG's GUI. Figure 4.8 is a screenshot from the developed GUI to plot PSG data. Data were grouped according to their type and the use of a map colour increases the easiness of data type identification. From top to bottom, 2 signals (in blue) from the EOG, 6 signals (in black) from the EEG, 1 signal (in orange) from the EMG chin, 1 signal (in red) from the ECG, 2 signals (in green) from the EMG legs, 1 signal (in blue) from the snore, 1 signal (in grey) from the cannula, 1 signal (in pink) from the thermistor, 1 signal (in magenta) from the chest belt, 1 signal (in brown) from the abdominal belt, 1 signal (in red) from the oximetry, and 1 signal (in black) from the sleep position. The remaining channels were, usually, unused, and data stored for those channels has no physiological meaning. An example of uncommon data acquisition is the plethysmography.

The GUI is, essentially, a data viewer which justified the large area dedicated to plotting data, mainly to plot PSG data, but, also, a data processing tool. The left side was reserved for the plot area, with the PSG data plotted at the top while the H4n sound file was plotted at the bottom. The viewer features include, for each signal, its identification is at its left, and a +/- button to adjust its vertical scale is at its right. Time adjustments, for detail vs general data view, are controlled by the

Set button and by the adjacent time value and units selection box. More features available in this GUI include the PSG panel, which allows the control of which signals should be plotted, and the listen capability of the snoring signal, from both files. At the right lower corner, the $<$, $>$ and the Go To buttons are to navigate the data. The last button allows for faster navigation, while the other 2 are for decremental and incremental time jumps, respectively. The Sync Graph button synchronizes the visualization of both files, the Load button is to upload a new patient's data, and, finally, an PSG epoch identifier

The processing tools, present in the PSG, include the calculation, manual and automatic, of the time delay between both files to synchronise them. The acquisition of data unsynchronized created a problem related to the visualization. When files are synchronized, at the beginning and at the end of data acquisition, dummy data should fill time intervals when one of the acquisition files has no data. The PSG pauses also create useless sound chunks in the H4n file (it hasn't corresponding data in the PSG study). The PSG panel is for PSG processing and searching for pauses in the study and calculating the respiratory frequency. The panel also calculates the energy of the snoring signal, for a time interval of 0.1 s and without overlap, and searches for energy peaks (snore candidates) and their peak boundaries.

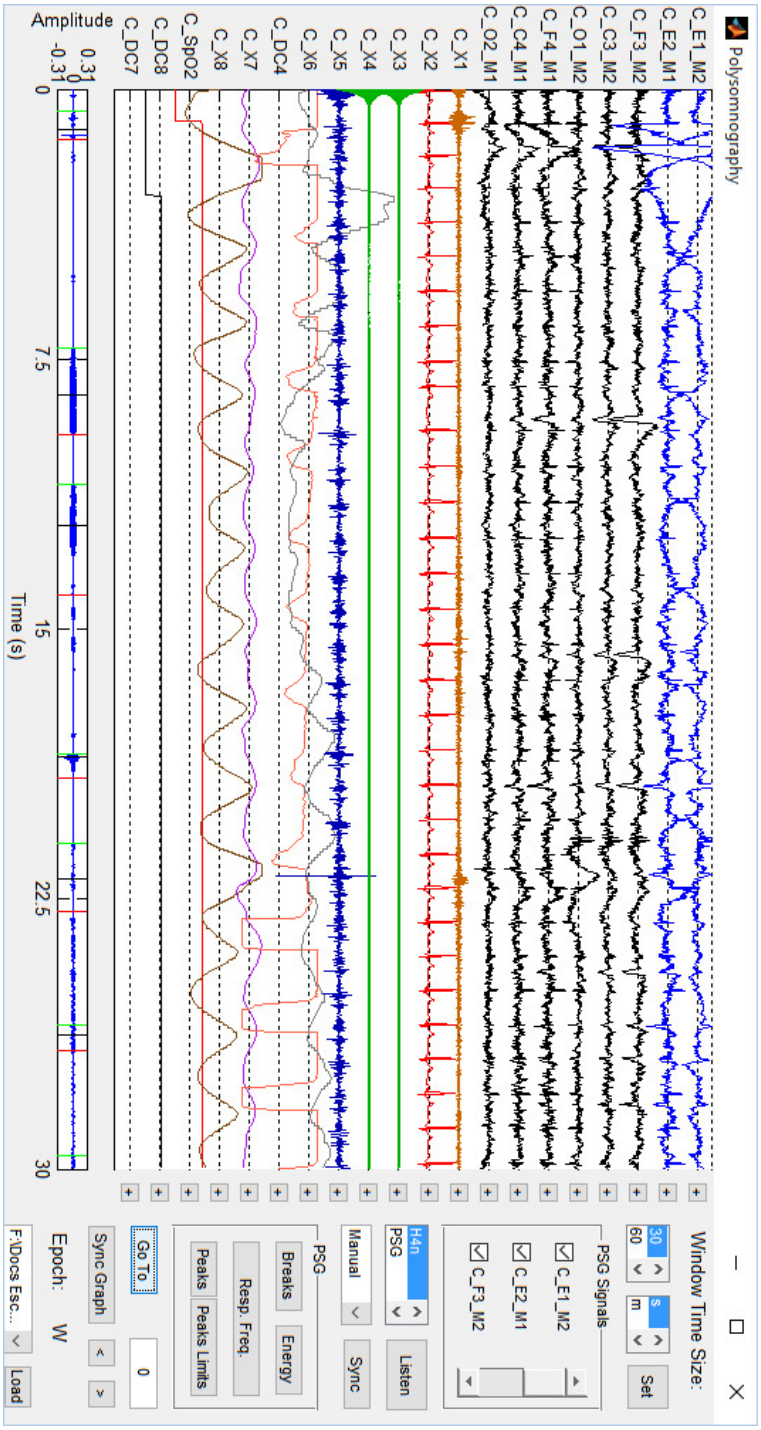

Figure 4.8: The developed GUI dedicates the majority of the area to plot data. The PSG data use the top plot area while the bottom plot area was dedicated to the H4n sound file. To the left are the labels associated with each signal, in the case of the PSG study and the signal amplitude, in the case of the H4n file. To the right are the commands to manage all the GUI functioning. The buttons next to the PSG plot area, one for each signal, are responsible for the regulation of the scale. In the upper right corner, the command allows to set the plot time, duration either seconds or minutes, while the panel *PSG Signals* below controls which signals should be plotted. The Listen command gives the user the capability to listen sound recording, either from the H4n file or the PSG. Processing tools are available in Sync Button and in PSG panel, with the first one dedicated to the synchronization between the files, manual and automatic. The PSG panel was design to work with PSG studies, to find pauses (Break button) in the PSG, the respiratory frequency, calculate the snore signal energy, its energy peaks and their boundaries (snores). The other commands allow to navigate in normal pace ($<$ and $>$ button) and in a faster way (Go To button), to observe both files either synchronized or unsynchronized (Synch Graph button), to identify PSG epoch and to load a new patient's data.

4.6 PSG and Sound Analysis Framework

The entire process of data acquisition and data processing results in the generation of multiple files, with all of them ensuring the patient's confidentiality. Data related to the PSG and data resulting from the analysis and processing performed by the implemented algorithms demand a high level of organization. The systematic organization of the patients' files is in Figure 4.9.

4.6.1 Data Management

Data collected from all the patients' questionnaires were gathered in a single file. To systematize the task, a proper software tool was developed (Figure 4.10). It has the option to create, delete and edit the profile of the patient, as well as its session questionnaire. It searches patients by their ID, order, either ascending or descending and calculates both age and BMI. The file to store the results, from data processing, is selected here.

4.6.2 Feature Extraction Environment

Most of the data processing was concentrated in a single, user-friendly, GUI. It also has the function to do pre-processing, visualization, and hearing tasks (see Figure 4.11 for more details).

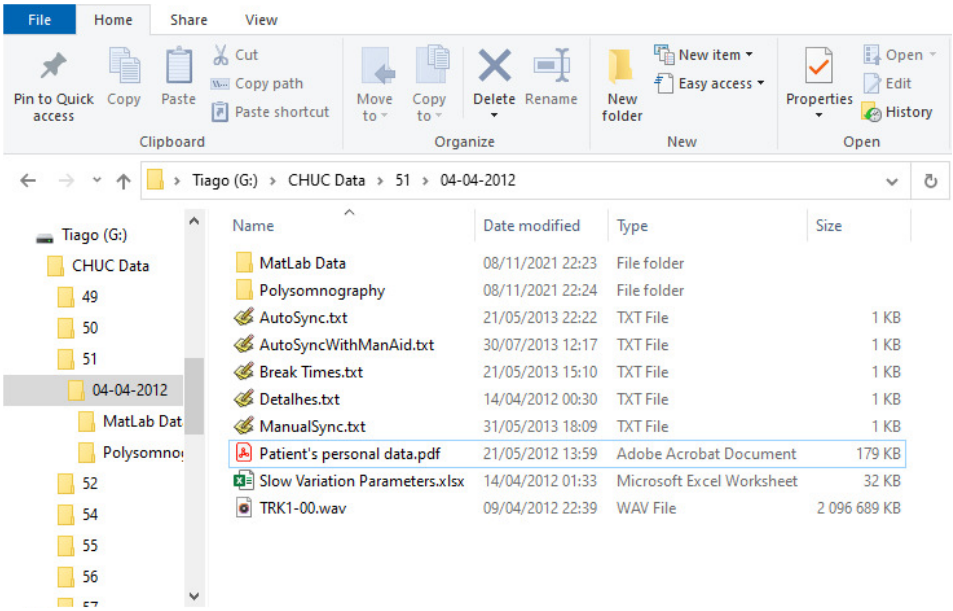

Figure 4.9: The implemented methodology for both files and folders organization. The first level of organization creates a folder for each patient, with the patient's ID as the folder identifier. All these folders belong to a single main folder, CHUC Data. The second level has a folder for each PSG performed by the patient. The folder's name is the PSG date. All content from a single PSG is stored inside the second level. The questionnaire, the sound file, SVP data, PSG pauses and the different synchronization methods are in here. Sub-folders Matlab Data and Polysomnography are to store data from MATLAB processing and from PSG acquisition, respectively.

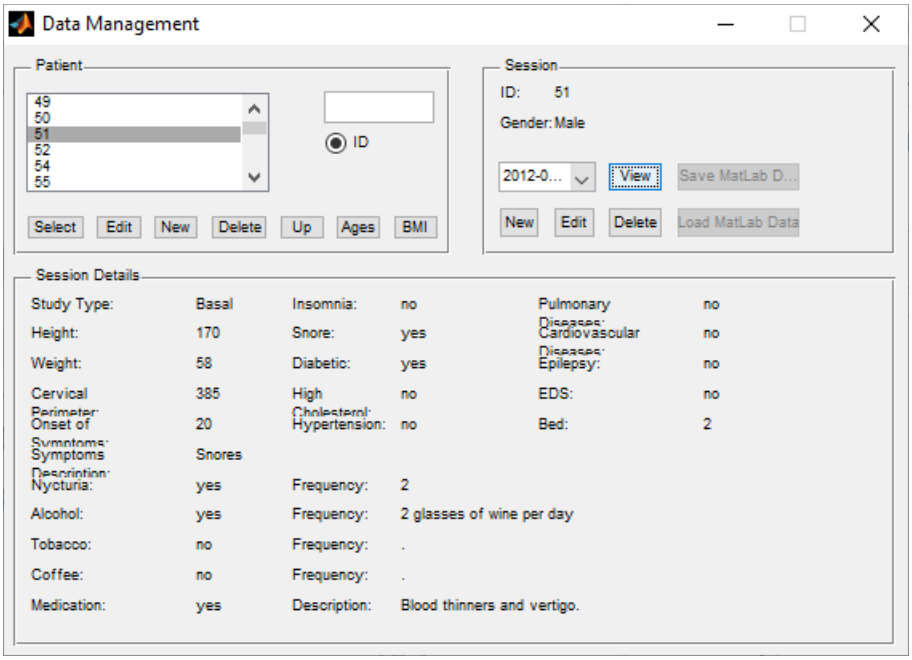

Figure 4.10: Three panels help to manage the patients' questionnaire. The Patient panel adds, edits, deletes and selects a patient. It also calculates patient's age and BMI, searches by the patients' ID and order either ascending or descenting the patient by their ID. The Session panel manages the session of the selected patient. Sessions can be created, or edited and selected. The View option load the complete information of that particular session to the bottom panel. The last option, Load Matlab Data, pop-ups a new window to create a new, or select an existing, file to load and save data resulting from data processing.

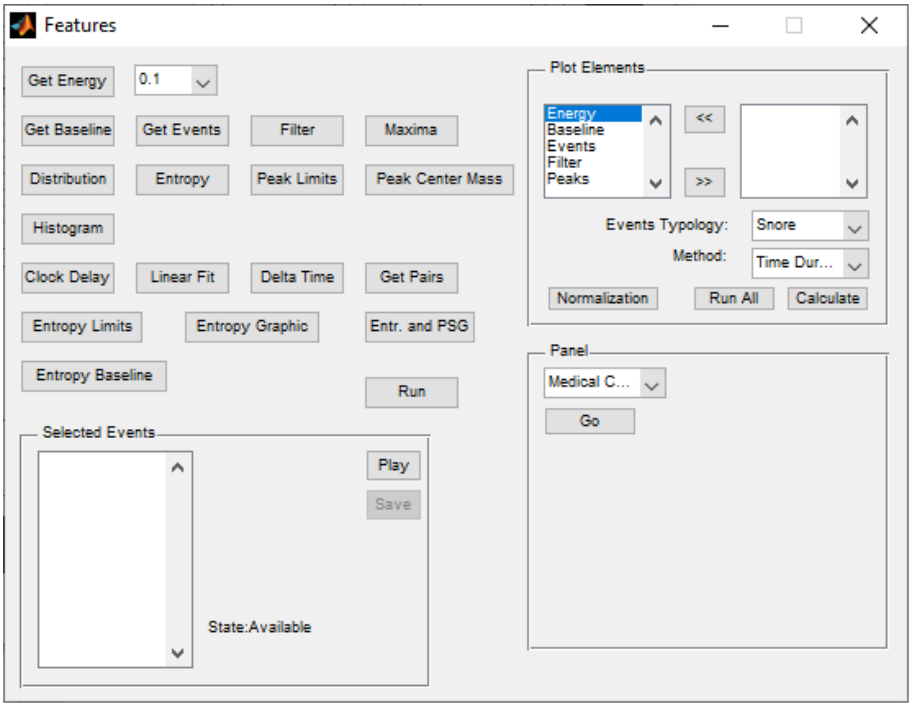

Figure 4.11: A tool to perform features' extraction. The upper right panel implemented multiple methods to do features' extraction. It also draws several results of the pre-processing phase and, by selecting a time span in the image, a list of detected sound peaks is listed in the lower left panel to listen and to, manually, classify. The lower right panel is dedicated to the study of snores around a medical event. The commands, in the upper left corner, are dedicated to the multiple tasks, related with the pre-processing phase.

4.7 High-Quality Audio Time-Series Analysis

4.7.1 Data Pre-Processing

The following topics are dedicated to explaining the methods implemented to extract, from data, useful features to characterize the patients accordingly to their pathology severity.

4.7.1.1 Snore Definition

In this thesis, the definition of snore must obey the following premises:

- A sound acquired in both the piezoelectric sensor of the PSG study and in the high-quality sound acquisition device;
- A short-duration increase in the sounds' energy obeying the rules identified in section 4.7.1.4, 4.7.1.5 and 4.7.1.7.

4.7.1.2 High-Quality Sound Energy

Several of the hereby described algorithms, make use of pre-processed time-series variables determined from the original sound data streams. One of such data series is the here called Energy. The energy data series should not be considered a particular property of a snore or of any other type of event. In fact, the purpose is to make use of such a data series in order to help in the identification of events in the raw data (like snores, glitches, etc.). In this scope, the energy data series results in a time-series of local sums from the sequential application of the expression

$$E^* = \sum_{i=1}^{N_p} x^2[i] \tag{4.3}$$

where N_p represents the width in the raw data that produces a value E_j of energy corresponding to segment j. The generic expression for the energy array is then given by

$$E[j] = \sum_{i=(j-1)\times N_p+1}^{j\times N_p} x^2[i] \tag{4.4}$$

The resulting array is a good approximation to the raw signal energy distribution over the whole time-series and gives an important hint of where to look while searching for interesting information in the raw data. An important remark that should be made here is that this energy array is calculated without introducing overlapping segments. The introduction of overlapping would greatly increase the processing effort with a limited improvement, at this level of pre-processing.

Concerning the dimensioning of this expression, it was considered that a reasonable interval to look for energy changes would be something in the order of 100 ms. No great variations are expected within this time range, and this is a good compromise with the amount of data to pre-process (around 2 GB for each patient record). This basically means that each segment is summed over 4410 samples, considering the original signal was sampled at 44.1 kHz and with 16 bits of resolution. Finally, it should be mentioned that like most other processing algorithms, a direct application of this expression is not possible mainly due to memory limitations. For this reason, the original file was sequentially processed in intervals of 300 seconds. The overall process to calculate energy data series takes less than 120 s for each sound file.

4.7.1.3 Energy Filtering

Raw real signals composition are most likely to have noise. Unwanted noise was recorded together with the signal. This means that the original sound file has both signal and noise, and it was not removed by the calculation of the sound's energy array.

In digital signal processing, convolution is a mathematical operation commonly used to get a third signal, the output, from two signals. It reveals how a signal modifies the shape of the second signal. The linear time invariant system with an impulse response, $h[n]$, convolves with the input signal, $x[n]$, and the result is an output signal, $y[n]$. When the impulse response is a filter, the name changes to filter kernel.

$$y[n] = x[n] * h[n] \tag{4.5}$$

Two filters were implemented to reduce noise in the energy time series and before using algorithms to identify snore events. From the definition of the frequency response of a Linear Time-Invariant system, in Equation 4.6, both frequency responses were inferred.

$$H^*[\omega] = \sum_{m=-\inf}^{+\inf} h[m] \cdot e^{-i \cdot \omega \cdot m} \tag{4.6}$$

The frequency response is the discrete time FT of the impulse response, $h[m]$. The used filters are of Finite Impulse Response type, which reduces the frequency response to a finite sum.

The first one was an one-dimensional high-pass filter with the impulse response

$$h[n] = \begin{bmatrix} 1 & 0 & -1 \end{bmatrix} \tag{4.7}$$

with 3 entries. The convolution between the input signal, energy time series, and the filter kernel produces a filtered signal with $p + q - 1$ entries, where p represents the length of the input signal and q the length of the kernel filter. Frequency response of

this high-pass filter is $H[\omega]$ in Equation 4.8. The magnitude, in dB, and the phase for the respective frequency response are available in Figure 4.12.

$$H[\omega] = 1 - e^{-2 \cdot i \cdot \omega} \tag{4.8}$$

To remove low amplitude peaks and adjacent peaks, a second filter, low-pass type, was used in the filtered energy array time series. The low-pass filter was a moving average filter with 11 samples, L, and impulse response $h[n] = \frac{1}{L}$, $0 \leq n \leq L-1$. The final result was an array with the same number of elements as the original energy data series. The low-pass filter has the following frequency response.

$$H[\omega] = \frac{1 - e^{-i \cdot \omega \cdot L}}{L \cdot (1 - e^{-i \cdot \omega})} \tag{4.9}$$

The magnitude, in dB, and the phase of the frequency response, Equation 4.9, is at Figure 4.13.

4.7.1.4 Gaussian Fit

The filtered energy data series, E_f, had less noise and an excel in sound events because of the nature of the mathematical expression to calculate the energy, x^2. Mathematical models were considered to search for energy peaks in the E_f array, including polynomial, logarithmic, power, and trigonometric functions. Local data analysis (data windowing) and the use of empirical methods identified a bell-like shape among the energy peaks, which led to the consideration of the Gaussian function as the most promising tool for data modelling. The definition of the Gaussian function is at Equation 4.10

$$G(x)^* = \frac{1}{\sigma \cdot \sqrt{2\pi}} \cdot e^{-\frac{(x-\mu)^2}{2 \cdot \sigma^2}} \tag{4.10}$$

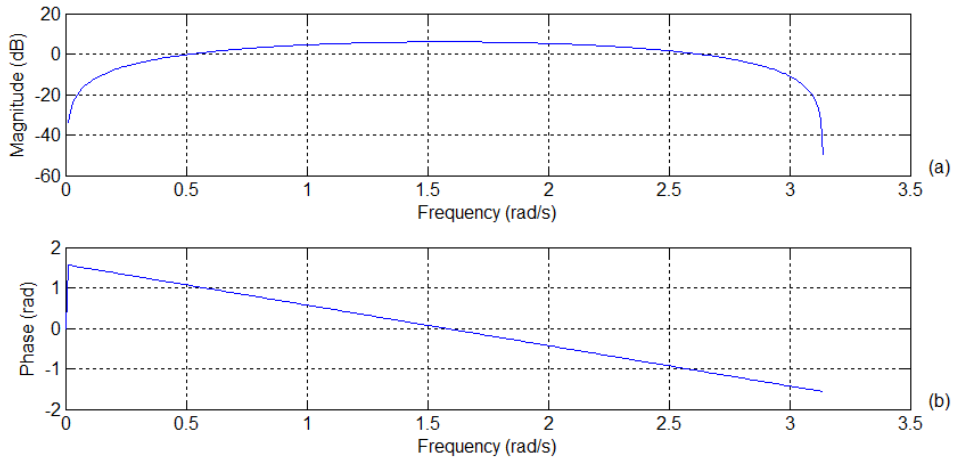

Figure 4.12: The magnitude, (a), and phase, (b), of the high-pass filter's frequency response used in the energy data series.

Equation 4.11 is a model of Gaussian type, with parameters a, b, and c, the coefficients to be modelled and to fit the data. To work properly, the Gaussian model should not be implemented in the entire E_f array, but rather only after slicing the filtered energy time series with a sequential sliding rectangular window and with overlapping.

$$G(x, a, b, c) = a.e^{-\frac{(x-b)^2}{c^2}} \tag{4.11}$$

At rest, a healthy adult human being has a respiratory rate between 10 and 18 breaths per minute, with an average of 12, meaning a single breath every 5 seconds [343, p. 175-176]. To get the same single sound event in more than one window, the time chosen for the rectangular window length was 4 s with overlapping of 3.5 s, i. e., 87.5%, meaning a 40-point window, w_l, and stepping 5 points, s_l, from one window to the next one. This relationship between time and the number of points comes from the energy calculation where a single energy value is calculated using 4410 samples of a signal with a sampling frequency of 44.1 kHz.

If the first window is $S[1]$ set, the second window is $S[2]$ set, then the $S[j]$ set represents j^{th} window. The first element of window $S[j]$ is the value at E_f in the position given by the element j of U set at the Equation 4.12. Following the same thought, the last element of window $S[j]$ is the value at E_f in the position given by the element j of T set at the Equation 4.13. The number of elements of E_f is d_l.

$$U = \{i : i = 1 + s_l \cdot n \wedge i \leq 1 + d_l - w_l\} \tag{4.12}$$

$$T = \{i : i = w_l + s_l \cdot n \wedge i \leq d_l\} \tag{4.13}$$

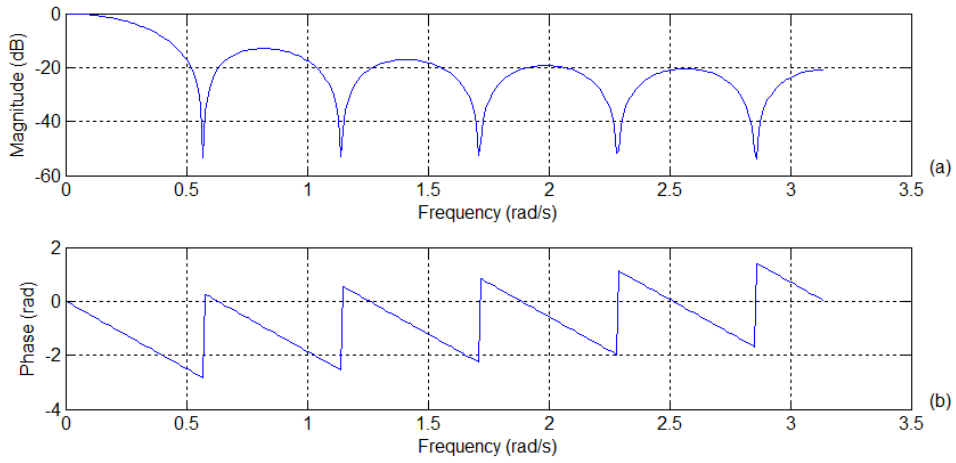

Figure 4.13: The magnitude, (a), and phase, (b), of the low-pass filter's frequency response used in the energy data series.

$$n \in \mathbb{N}_0 \tag{4.14}$$

The elements of the j^{th} V set, Equation 4.15, has all the positions to read from E_f to build the $S[j]$ set, Equation 4.16.

$$V[j] = \{k : k \leq T[j] \wedge k \geq U[j] \wedge k \in \mathbb{N}\} \tag{4.15}$$

$$S[j] = \{x : x = E_f[V[j]]\} \tag{4.16}$$

The implementation of this model in each window S must take into account a set of criteria, some of them are constant and others are dynamically calculated. These criteria define boundaries, coefficient starting values, and algorithm settings.

The chosen method to fit data was the non-linear least squares because it allows controlling more parameters during the Gaussian model implementation, the extensive number of functions that can be fit, the efficient use of data, and due to its capability to give good estimates over relatively small amounts of data [344]. The algorithms available in the MATLAB software to use in the fitting procedure were the Levenberg-Marquardt and the Trust-Region. Accordingly, with [345], the best choice is the Trust-Region, an evolution of the Levenberg-Marquardt and a faster algorithm. Although one disadvantage of the non-linear least squares is its sensitivity to outliers, the robust option wasn't used since the filtering process implemented minimized this problem. The maximum number of interactions was 400 and the maximum number of evaluations was 600.

The algorithm required coordinates in order to search for a proper fit. The parameter c was defined as a constant, and with the value of 0.01, after some trial and error iterations. The remaining 2 parameters, a and b were both calculated dynamically using the centroid of each window S. The definition of a centroid, C, is

$$C^* = \frac{\sum_{i=1}^{N_p} m_i.r_i}{\sum_{i=1}^{N_p} m_i} \tag{4.17}$$

where N_p represents the width of each window S, m_i represents $S[j]$ values and r_i represents the time of which one of this samples. The result for each centroid gives the initial value to parameter b and the maximum value of $S[j]$, around the centroid, and considering a neighbourhood of 2 elements, gives the value of parameter a.

The fitting algorithm returned an array with 3 values, to parameters a, b, and c, which represent the best fit to the submitted data. The interpretation of these values deserved some caution since the Gaussian function might lie outside the $S[j]$ window, especially, the mean value. This might happen when there is not a peak of energy, a peak of energy is starting to appear or to disappear, or when there are 2

peaks of energy in the $S[j]$ window. To accept the values of the fitting process, the mean value of the Gaussian fit should be inside the $S[j]$ window. When inside the $S[j]$ window, the mean value represents a sound event and it was considered a snore event candidate.

4.7.1.5 Sound Events Filtering

The Gaussian fit identified sound events but this step did not distinguish between the snoring sound and other sounds (noise). The fitting process only calculated the parameters' values to get the best data fit and returned a set of points candidates to be identified as a sound event. Smart algorithms were necessary to analyse all the detected sound events and discard non-snoring events. They are presented below as well as the implemented algorithm sequence:

- The first criterion for the separation between a snore sound event and a noise sound event was a selection based on the highest value peaks. A sequential search was performed in the sound event data series and for each sound event, e_i, the position of the maximum value inside the boundaries $[t_i - \frac{r_p}{2}, t_i + \frac{r_p}{2}]$ replaces the old position. The t_i parameter is the time where the sound event e_i was detected. The r_p parameter is defined as the patient's mean respiratory period and it was calculated based on the PSG study signals, more specifically, the respiratory sensors. More details about the calculation of the patient's mean respiratory period were discussed in section 4.5.3.2.

- The second criterion was the removal of electronic noise, a low amplitude, short duration, and low frequency noise, and the strategy was to define 2 threshold values:

  - The first one is the sound event energy peak;
  - The second one is the cumulative energy around the sound event.

    To analyse electronic noise without the interference of snoring, a period of time was selected where it was most likely to have the absence of snoring in the recording of the H4n device. Data acquisition, by the H4n device, started immediately after the patient lies down on the bed, which means he was awake and did not snore. The first 10 m of data recording were chosen to study the electronic noise and to maximize the probability of the absence of snoring. The cumulative energy of each sound event inside the period of time of 10 m was calculated for 1 s around each sound event, $[t_i - 1, t_i + 1]$. A 1 s time period was chosen because:

    * Electronic noise is a single burst noise with a duration of a few ms;
    * A single snoring sound lasts substantially more than the electronic noise. Even if 2 s can not include all the snoring's energy, it fulfills

the purpose because the snore energy value will be much higher than the electronic noise energy value.

The normal respiratory rate range at sleep of a healthy adult human being is already known, which means the minimum respiratory period at sleep of a healthy adult human being is 3.3 s. Using a value of 1 s to calculate the cumulative energy, it was guaranteed the use only of the energy values of the sound event e_i and not the energy values of the neighbour sound events, in the case of neighbour snores.

For both thresholds, the 10^{th} percentile was calculated and then it was multiplied by a factor of 4 to give the final threshold values. The 10^{th} percentile was used to guarantee that the threshold value represents an electronic noise and then it was multiplied by a factor of 4 to try to include the majority of electronic noise events. Factor 4 was empirically chosen.

- After the calculation of the cumulative energy of each sound event only sounds events with an energy peak above the peak threshold or, if not true, cumulative energy above the cumulative threshold are not discarded.

- A third criterion discarded close sound events around the sound event e_i, in the time interval $[t_i - \frac{r_p}{2}, t_i + \frac{r_p}{2}]$. Just the sound event with the highest energy peak was not discarded.

The quality of the algorithm to detect snore events and discard noisy events was evaluated and compared against a second algorithm, well known, developed to run on MATLAB and known as the peakdet algorithm [346]. The comparison between the algorithm implemented in this project and the peakdet algorithm, henceforward identified as Bellauer's algorithm, was performed in a consecutive 5 min window for each patient. Bellauer's algorithm, version 3.4.05, accounts for a local maximum if there is a point, between such local maximum and the previous one, with a value lower by a predefined hard threshold. The 5 min window, which represents around 1.23% of the entire dataset, was randomly selected from a manually selected region containing snores.

All the True Positive (TP), False Positive (FP), False Negative (FN), and True Negative (TN) cases were grouped by patient, and a comparison was made at 2 different levels. At the first level, the sensitivity (Equation 4.18), the specificity (Equation 4.19), the PPV (Equation 4.20), and the NPV (Equation 4.21) were calculated for each medical classification group and globally and, finally, compared.

$$Sen = \frac{TP}{TP + FN} \tag{4.18}$$

$$Spe = \frac{TN}{TN + FP} \tag{4.19}$$

$$Ppv = \frac{TP}{TP + FP} \tag{4.20}$$

$$Npv = \frac{TN}{TN + FN} \tag{4.21}$$

4.7.1.6 High-Quality Sound Data Distribution

The H4n recorded a signed signal with 16 bits of resolution, corresponding to 2^{16} possible numbers, meaning that each analogue sample would be converted to a digital number between -32768 and 32767. The 2 GB file has 1,073,504,256 samples to analyse the profile of the data distribution. A typical sound acquisition system is engineered and calibrated to have a DC component of 0.

4.7.1.7 Snore Events Boundaries

Locating sound events represent the beginning of sound events detection, with the definition of sound boundaries important to the following steps, the implementation of algorithms for feature extraction. The typical respiratory rate of a human being at sleep (see section 4.7.1.4) was used to delimit the search for snore boundaries to just 3 seconds around the snore event.

Sound behaves like a sin trigonometric function, with a 0 DC component and lower pressure regions (troughs) intercalated with higher pressure regions (crests). This behaviour does not help the boundaries search algorithm and, for that reason, a different approach was implemented, the study of the sound envelop.

$$m = \{n : n \geq 1 \wedge n \leq 2 \cdot Fs \cdot t_{env} + 1; n \in \mathbb{N}\} \tag{4.22}$$

$$U_k = \{j : j = m - 2 \cdot Fs \cdot t_{env} + k - 1; j \in \mathbb{N}\} \tag{4.23}$$

$$Env_i[k] = max\{Sdu_i[U_k]\} \tag{4.24}$$

$$k \in \{1, ..., 265042; k \in \mathbb{N}\} \tag{4.25}$$

The Snd_i data series is the segment of sound file representing the i^{th} sound event. The acquisition frequency of 44100 Hz, Fs, and the selection of a 3 s neighbourhood to calculate the upper envelope, lead to a Snd_i data series with 264601 elements. The upper envelope, Env_i, of Snd_i was calculated, Equation 4.24, by finding the

maximum value around each element of Snd_i using data from a neighbourhood of 10 ms, t_{env}, empirically set.

The calculation of the upper envelope, Env_i, encompasses the implementation of accessory techniques to improve the algorithm. Dummy data was incorporated in the Snd_i data series, with $Fs \cdot t_{env}$ elements added at the beginning and the same number of elements at the end, all with 0 value, creating a new time series named Sdu_i. A vector position, m, composed of $2 \cdot Fs \cdot t_{env} + 1$ natural elements, from 1 to 883, was used to define the length of time series data used in the calculation of each envelop element.

A new set for vector positions, U_k, stores the Sdu_i positions for the calculation of the k^{th} element of the envelop (Equation 4.23). The highest sound value of Sdu_i for the positions given by each set U_k was the k^{th} element of the envelope Env_i. Later, the first $Fs \cdot t_{env}$ elements of the envelop Env_i were discarded to have the same number of elements of Snd_i.

Snores have different profiles, depending, among other factors, on time duration, inspiration and/or expiration phase, and amplitude. High amplitude snores are easier to detect than low amplitude snores, and different definitions were implemented to find snores' boundaries. Snores with higher amplitudes, highest envelop value above 0.03, have a threshold of 5 times the 10^{th} percentile of the upper envelope positive values, and for snores with the highest envelop value below 0.03, the threshold definition was 3 times the 10^{th} percentile of the upper envelope positive values. Snore's boundaries were calculated by splitting the upper envelope Env_i into 2 subsets. The first and the second subset contain the data before and after the time instant of the snore detection, respectively. Each subset has a different purpose with the first subset assigned to search for the beginning of the snore while the second subset is assigned to search for the end of the snore.

Using the previous threshold, each subset was transformed into a binary data type subset, B, with a n_{el} number of elements. Equation 4.26 removes small variations in sound using a filter of 4410 elements, $n_p = Fs \cdot t_p$, with t_p equal to the time interval to calculate the energy time series (100 ms). The subset B may have different n_{el} elements, which justifies a correction factor in Equation 4.26, $\frac{100}{n_p}$.

$$B_{sum}[i] = \frac{100}{n_p} \cdot \sum_{j=i}^{i+n_p-1} B[j] \tag{4.26}$$

$$i \in \{1, ..., n_{el} - n_p + 1; i \in \mathbb{N}\} \tag{4.27}$$

Data in each element of set B_{sum} only has little variations when compared with its neighbourhood, since the overlapping of B is maximum, with only one element replaced in a universe of n_p elements for each segment. Thereafter, noise present in

the data has little impact, because one element represents only $\frac{1}{n_p} * 100\% = 0.02\%$ of the total number of elements. A steady increase in the number of elements above the threshold in B leads to the surpass of the second threshold of 5%, applied to B_{sum}, which defines the boundary between a snoring sound and just noise. Such limit is much higher, around 250 times than the minimal possible variation of 0.02% and noise interference in this calculation should be minimized. The closest point before and after the detected snore where the limit of 5% is crossed was considered as the boundaries of the respective snore.

Patients snore mainly during the inspiration phase but there are snores in the inspiration phase as well as in the expiration phase [10, 347]. Adjacent periods of snoring may exist and the algorithm discards them in the first approach, which led to a complementary search by the algorithm to, eventually, expand the snore boundaries. Not all the adjacent peaks of energy were considered, which means they should last, at least, a 200 ms time duration and not be more than 1 s apart from the main snore.

4.7.1.8 PSG and High-Quality Sound Synchronization

The synchronization of data between the PSG and the H4n files was a crucial milestone in the pre-processing data. Data synchronization enables the comparison of medical results with the experimental/scientific analysis results, which may validate the method, and use it in real-life applications. The synchronization of data was accomplished by correlating the energy data series of the PSG snore channel and the H4n sound file (coarse correlation), and, then, the study of the clock mechanism errors from both devices (fine synchronization). The following sections focus on the discussion of the coarse synchronization, with the implementation of 3 different approaches: manual, automatic, and automatic with manual adjustment.

4.7.1.9 PSG Study Pauses Detection

The first method was strongly based on the observation of both data, PSG and H4n. At the beginning of H4n data acquisition, the patient followed the instructions and generated a vocal sound to be registered in both recording devices, while during each PSG acquisition, a log was created to register all pauses in the PSG study. Manual synchronization did not make use of algorithms to search for pauses in data acquisition, relying on the handwritten notes log.

Detection based on an algorithm is free of human mistakes, especially, in the conditions the studies were performed, during the night-shift when the people are tired. A pause resume sequence in the PSG study created a distinct behaviour in data acquisition. The pause does not happen in the time instant selected by the sleep technician, but rather in the transition from the current epoch to the next one,

which narrows, significantly, the time instants possible to pause the study.

The first detection method, the manual, was discarded and an automatic method approach relied on the analysis of a single channel of the PSG study, the SpO_2, and in the transition from one epoch to the next one. The existence of a pause resume sequence creates a visible discontinuity in data acquisition, with the SpO_2 signal dropping to 0, or values close to it. The algorithm search criteria included a SpO_2 mean value above 50% in the epoch immediately before the transition under evaluation, and a drop to values below 40% in the transition between epochs.

4.7.1.10 Synchronization of Data

Manual synchronization consisted in the use of the developed GUI for PSG and H4n data visualization. The vocal sound wittingly generated by the patient was the reference signal to perform the initial synchronization. PSG studies with pauses required additional synchronizations, with the time reference for those cases, the handwritten notes log. The manual synchronization relied on marking each point of synchronization at the precise instant of time, first, in the PSG data visualization area, followed by the same procedure in the H4n data visualization area. This procedure should be implemented in the initial synchronization, and, when exists, in all pause resume sequences, following a chronological order.

The automatic synchronization algorithm used the detected pauses to split both energy arrays' data series into subsets, clusters. The formation of clusters from the PSG sound energy data series relied, solely, on the pause resume sequence information. A new cluster was created, and finished, at each one of those points. During the preparation for the PSG study, sleep technicians needed to test PSG data acquisition and, occasionally, pause resume sequences were introduced to the study. When present, the last of those sequences was used to define the beginning of the first cluster. H4n energy data series clustering was not so straightforward and it relied on information from the PSG data series clustering. Clustering the H4n energy data series began with the detection of the vocal sound. The cluster's time duration was set by the corresponding first PSG cluster. Building the following H4n energy data series clusters required the knowledge of the previous synchronization time delay, besides the time duration of the corresponding PSG cluster. For synchronization purposes, the first and last epoch of each cluster (from both energy data series) were removed due to the low probability of snores in those registers (patient awake). The final synchronization cluster made use of the remaining H4n data, and, from the corresponding PSG data, a smaller subset of data was selected, with the same time duration. If the corresponding PSG cluster was shorter, then the entire PSG cluster was used to perform the synchronization. A summary of the data synchronization process is available in Figure 4.14. In PSG studies without

pause resume sequences (after marking the start of sleep assessment point), there was a single cluster in both PSG and H4n data.

The synchronization between clusters was performed by the implementation of cross-correlation analysis. The cross-correlation analysis is a mathematical tool to evaluate two data series similarity and the time shift to the point of more similarity of one data series relative to the second one. The calculation of the time shift was essential to get snores synchronized, besides the remaining data. The cross-correlation definition, for continuous signals, is at Equation 4.28. Since data are of discrete signal type, the cross-correlation definition for this type of signal is at Equation 4.29.

$$w(t) = u(t) \star v(t) = \int_{-\infty}^{+\infty} u^*(\tau) \cdot v(\tau + t) d\tau \tag{4.28}$$

$$w(t) = u(t) \star v(t) = \sum_{n=-\infty}^{+\infty} u^*[n] \cdot v[n + t] \tag{4.29}$$

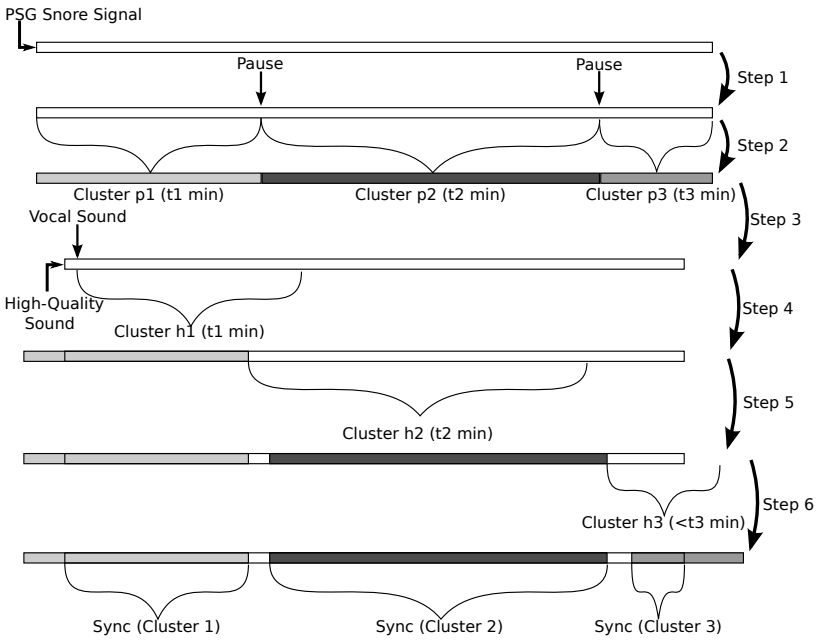

Figure 4.14: Synchronization between PSG and the high-quality sound signal. The process starts with the detection of pause-resume sequences (Step 1), in this case there are 2 Pauses, and the separation of data according with those pauses (Step 2). The second part of the process is the implementation of synchronization between 2 clusters, usually, of equal duration. Step 3 corresponds to the detection of Vocal Sound, while Step 4 starts synchronization, between p1 and h1 and with a duration of t1 min, for the first cluster. Step 5 and 6 correspond to the synchronization of the remaining clusters. The first and, usually, the last PSG epochs are discard due to lack of data in the high-quality sound signal (Step 6). At the middle of data acquisition and if there is pause-resume sequence, high-quality sound signal is discard due to lack of PSG data.

4.7.1.11 Linear Equation Compensation

The patient's snores were, ideally, acquired by both the PSG and the H4n sensors. The coarse synchronization calculated the time delays between the corresponding energy time series clusters and, therefore, between both registers. A matrix of n lines and m columns was built, for each cluster, and it represented, respectively, the number of snores detected in the H4n data and the PSG data. The $n \times m$ matrix has the time difference between the i^{th} H4n energy peak and all the PSG cluster peaks. The algorithm used the beginning of the energy peaks to calculate the synchronization loss profile. A temporary snore pair was defined between the i^{th} H4n energy peak and the closest PSG energy peak. Pairs of peaks with a time difference above 1 s were discarded and further analysis did not take them into account.

Crystal oscillators are electronic components that made use of the mechanical properties of the quartz crystal, which include an electrical signal with a precise frequency. This frequency allows to keep track of time, for example, to give the acquisition frequency, but they are not free of error. Several factors contribute to the introduction of errors in the nominal frequency. Temperature is one of those factors, introducing crystal errors on a daily and year cycle basis. Other sources of errors are related to ageing and manufacturer procedures like impurities in crystal growth, imprecision cut process of the device, and uneven thickness.

The PSG acquisition system and the H4n device run independently, which means each one has its crystal oscillator, and the influence of the resultant error should be different. This means that the crystal nominal frequency does not correspond, usually, to the, slightly shifted, crystal running frequency. This configuration has influenced the acquisition frequency, once it relies on the crystal mechanism. For short periods, the accumulation of crystal errors is not enough to visualize it, which is not the case in this project. To increase the quality of synchronization, a new implementation, complementary to the first synchronization, should be applied to decrease the delay between the detected snores representing the same sound.

All the CMS rooms, a total of 4, were used to record data, and each room had its PSG acquisition system. A new level of synchronization was necessary, but this time between the H4n device and each one of those PSG acquisition systems. The best patients to study synchronization loss were the ones with a continuous PSG data acquisition and the higher the number of detected energy peaks, the better. Four PSG studies were selected, each one accomplished in a different room.

A total number of 50 points were manually selected, for each patient, from the graphic with the synchronization loss profile (pairs of peaks plotted). Empirical observations revealed a constant rate in the synchronization loss profile, with a linear regression model function best suiting those data. Linear regression tries to

model the relationship between two variables X and Y and for a specific value x of X, it can be possible to predict the value of Y [348, p. 15-30].

$$E(Y|X = x) \tag{4.30}$$

This equation gives the expected value of variable Y when variable X has the specific value x. In this practical application, the variable Y represented the delay (synchronization loss) and the variable X represented the time since the last synchronization. To be linear regression, the relationship between these 2 variables must respect the equality

$$E^*(Y|X = x) = \beta_0 + \beta_1 \cdot x \tag{4.31}$$

with β_0 and β_1 representing, respectively, the interception of y axes and the slope of the equation. The statistical process for estimating relationships between variables is associated with an error. Including a new term in the previous equation

$$Y_i = E^*(Y|X = x) + e_i = \beta_0 + \beta_1 \cdot x + e_i \tag{4.32}$$

the error e_i of Y_i allows to have a regression $E(e|X) = 0$.

In order to decrease the error associated with the linear regression, the method of the least squares was used to find the parameter values that best fit the data. In a linear regression model, errors have a mean of zero, they are not correlated and they have equal variance. In this situation, the best linear and unbiased estimator is the least squares estimator. The goal of this method is to minimize the Sum of Squared Errors (SSE), i.e., the difference between an observed value, y_i, and the fitted value, $\hat{y}_i$, given by the model.

$$SSE = \sum_{i=1}^{n} \hat{e}_i^2 = \sum_{i=1}^{n} (y_i - b_0 - b_1 \cdot x_i)^2 = \sum_{i=1}^{n} (y_i - \hat{y}_i)^2 \tag{4.33}$$

$$\hat{y}_i = b_0 + b_1 \cdot x_i \tag{4.34}$$

The parameters b_0 and b_1 were chosen in order to get an equation of the line near to y_i, and $\hat{y}_i$ was the i^{th} fitted value of y_i.

The coefficient of determination is a tool used in statistical analysis to evaluate how well data fit a statistical model and it returns a single value between 0 and 1. If the regression model fits perfectly the data, all points lie exactly on the curve and the value returned by the coefficient of determination will be 1. When the chosen regression model does not represent the data, at all, then the coefficient of determination will be 0. Generally, and using the value in percentage, it means that

$p\%$ of the variation of variable y can be explained by the variation of variable x. The $(100-p)\%$ can not be explained by x.

The coefficient of determination, r^2,

$$SST = SSR + SSE \tag{4.35}$$

$$SSR = \sum_{i=1}^{n}(\hat{y}_i - \bar{y})^2 \tag{4.36}$$

$$SST = \sum_{i=1}^{n}(y_i - \bar{y})^2 \tag{4.37}$$

$$r^2 = \frac{SSR}{SST} = 1 - \frac{\sum_{i=1}^{n}(y_i - \hat{y}_i)^2}{\sum_{i=1}^{n}(y_i - \bar{y})^2} \tag{4.38}$$

is the quotient between the sum of squares due to regression and the total sum of squares [349, p. 268-270].

Linear regression returned the synchronization loss rate over time, which allows the application of time corrections, and a fine synchronization.

4.7.1.12 Snore Pairing

The accomplishment of fine synchronization led to pairing peaks of energy, from both records, and to the identification of snores. A histogram of the time difference distribution, between a peak energy from the H4n register and the closest energy peak from the PSG data, gives the time delay profile and a maximum value to consider both registers as the same snore. Data distribution resembles a Gaussian function and data modelling was implemented using Equation 4.10. Fitting results for the standard deviation, σ, and for the mean, μ, were used to define the maximum time delay of each bed. That upper limit was $\mu \pm 3 \cdot \sigma$.

A time threshold was calculated for each bed, and from the 4 calculated time thresholds, the longest time value was chosen and applied to all the data.

4.7.2 Features Extraction

The characterization of the medical condition, using sound, relied on the extraction of features from these sleep-related events. Henceforth, a list of methods is presented for the purpose of feature extraction. The following sections organize the description of the algorithm, for data processing, accordingly to the domain in which the signal's features were extracted.

4.7.2.1 Time-Domain Analysis

Algorithms applied, for signal processing, in the time domain are described in this section.

4.7.2.1.1 Time Duration Snores' boundaries were calculated during the preprocessing phase, which means that the calculation of the snores' time duration was just the difference between the end and start of each snore. Some academic researchers explored the feature Time Duration and its distribution to study snores [161].

4.7.2.1.2 Signal Amplitude The Signal Amplitude feature is calculated by searching inside the boundaries of the snoring sound for the maximum absolute value. The amplitude of the signal is related to the energy of the signal and further ahead this feature will be also presented.

4.7.2.1.3 Energy The energy was already used during the preprocessing phase and details about Energy calculation are available at section 4.7.1.2. The principle to calculate the snores' Energy here is the same and the calculation is delimited by the boundaries.

4.7.2.1.4 Skewness The coefficient of skewness is a statistical tool to evaluate data distribution. With the coefficient of skewness, it is possible to study data distribution absence of symmetry.

The general definition for the calculation of the skewness value is [349, p. 18]:

$$\gamma_1^* = \frac{\mu_3}{\mu_2^{3/2}} \tag{4.39}$$

The calculation of the coefficient of skewness is dependent on different central moments, and it is calculated by dividing the third central moment by the second central moment.

$$\gamma_1^* = \frac{E[(X - E[X])^3]}{(E[(X - E[X])^2])^{3/2}} \tag{4.40}$$

The second central moment, or variance, is related to the standard deviation. From this, the coefficient of skewness is related to the standard deviation as follows:

$$\gamma_1^* = \frac{E[(X - E[X])^3]}{(\sigma^2)^{3/2}} \tag{4.41}$$

The final equation identifies the coefficient of skewness depending of the third central moment normalized by the standard deviation raised to the third power:

$$\gamma_1^* = \frac{E[(X - E[X])^3]}{\sigma^3} \tag{4.42}$$

The third central moment is already a measure of asymmetry of data distribution of a random variable X and the presented coefficient of skewness, γ_1, is normalized to get a skewness value independent of the measuring unit [350, p. 89-107].

An example of symmetry is the Gaussian distribution with a mirror at the μ position. For data distributions with this behaviour, Skewness value is 0 [351, p. 110]. When the coefficient of skewness is rather positive this means that the bulk of the data is at the left with a long tail to the right. When negative, this means that the bulk of the data is at the right with a longer tail to the left [352, p. 75-83]. Data with this behaviour is, respectively, called skewed right and skewed left.

4.7.2.1.5 Kurtosis The third central moment is already a measure of the asymmetry of data distribution of a random variable X and the presented coefficient of skewness, γ_1, is normalized to get a skewness value independent of the measuring unit [350, p. 89-107].

An example of symmetry is the Gaussian distribution with a mirror at the μ position. For data distributions with this behaviour, the Skewness value is 0 [351, p. 110]. When the coefficient of skewness is rather positive this means that the bulk of the data is at the left with a long tail to the right. When negative, this means that the bulk of the data is at the right with a longer tail to the left [352, p. 75-83]. Data with this behaviour is, respectively, called skewed right and skewed left.

$$\gamma_2^* = \frac{\mu_4}{\mu_2^2} \tag{4.43}$$

The coefficient of kurtosis, γ_2, is the result of the division between the fourth central moment and the second central moment squared [351, p. 111].

The general definition of a moment of a continuous random variable X is:

$$E[X^n] = \int_{-\inf}^{+\inf} x^n \cdot f_X(x)dx \tag{4.44}$$

The first moment, $E[X]$, returns the expected value or mean of a random variable X [353, Ch. 2, p. 11-17].

The general definition for the central moment of a continuous random variable X is:

$$\mu_n = E[(X - E[X])^n] = \int_{-\inf}^{+\inf} (x - E[X])^n \cdot f_X(x)dx \tag{4.45}$$

The second central moment is the variance, $var(X)$, and its definition is [352, p. 75-83]:

$$var(X) = \mu_2 = E[(X - E[X])^2] \tag{4.46}$$

The standard deviation value, σ, and the variance value are related as follows, $\sigma = \sqrt{var(X)}$. The final definition to calculate the coefficient of kurtosis is:

$$\gamma_2^* = \frac{E[(X - E[X])^4]}{(E[(X - E[X])^2])^2} = \frac{E[(X - E[X])^4]}{\sigma^4} \tag{4.47}$$

In the presence of a Gaussian distribution, the kurtosis value will be 3, named mesokurtic. For kurtosis values lower than 3, data distribution is designated by platykurtic and for kurtosis values higher than 3 those distributions are acknowledged as leptokurtic [350, p. 99-104]. A platykurtic type means data are distributed more evenly between all the points of the set, a flatter distribution, while leptokurtic type means data is more concentrated near the mean value, data peak at the mean value is more sharply and with longer tails [354].

4.7.2.1.6 Empirical Mode Decomposition Signal analysis in time-frequency plane gave a powerful tool to a better understanding of the signal itself. New insights to the signals allowed interpretation from a different point of view, as an example, the FT allowed to known which single-frequency sinusoidal functions were in the signal and the importance of each one by calculating the associated energy. The basis behind the transformation of a signal in the time domain to a signal in the frequency domain is the purpose of the FT method. It uses a set of predefined templates to perform the calculation of the inner product with the signal. Signal decomposition in its constituents frequencies, using templates, has a negative impact as it can influence data interpretation in the time-frequency plane. Also, the Heisenberg uncertainty principle states that it is not possible to improve simultaneous both frequency resolution and time resolution, more precisely, if frequency resolution is improved then the time resolution worsens. The EMD appears has a solution to overcome, or at least mitigate, this drawbacks related with non-stationary signals and the appearance in the signal of local components, which may be of interest to understand as much as possible. An example of decomposition is at Figure 4.15.

The EMD is a method belonging to a more extended tool, the Hilbert-Huang Transform and it was presented by Huang in 1998 for time series analysis [355]. This new method of signal decomposition is very recent when compared with other older methods far more implemented as it is the case of the FT, from the first half of the 19^{th} century, and the Wavelet Transform, from the beginning of the 20^{th} century.

The development of solutions making use of the EMD shows confidence and use them in real-time devices is already addressed [356]. The method had already been used to evaluate snoring in OSAHS and extracting features from the resulting Intrinsic Mode Function (IMF). Mean and standard deviation were the retrieved from the IMF. The results for the EMD method to detect snores and breathing achieved an accuracy of $96,3\% \pm 5,5\%$, sensitivity of $97,8\% \pm 1,9\%$ and specificity of $92,8\% \pm 10,6\%$. They were recorded from 5 patients, 2 females and 3 males, with $32 \pm 16,5$ years old suspected of OSAHS. From the set, 2 were simple snores with AHI of $5,6 \pm 5,2$ and the remaining 3 were OSAHS patients with AHI of $22,4 \pm 20,7$. Data was recorded all night long with an ambient microphone, ME52, away from the patient's head between 20 and 30 cm [357].

Table 4.4: Advantages and disadvantages of the EMD method.

Advantages	Disadvantages
EMD keeps signal in its domain (Information preservation)	Does not always guarantee a perfect instantaneous frequency under all conditions
Non-linear and non-stationary time series analysis	Lack of theoretical analysis
Data driven basis(Adaptive)	-

The most interesting feature of the EMD is its capacity to break down the signal without leaving the time domain. Other features of the EMD method are the capacity to work well with non-linear and non-stationary data and it allows time information preservation. The EMD method allows to decompose the original signal, most likely a complex signal with multiple frequencies, in a finite number of IMF and the implementation of the Hilbert Transform over these IMF gives well-behaved transformations. The time series decomposition performed by the EMD method is based on the energy's extraction related with each time scale present in the original time series.

Data analysis with, for example, FT and Wavelet Transform are based on predefined functions. EMD has a different approach since it relies on the local characteristic time scale of the data [358]. This feature allows an adaptive decomposition and, thereby, the EMD method could be more efficient. The resulting IMF are approximately orthogonal. Table 4.4 has a brief list with the EMD method advantages and disadvantages.

In neural data analysis, a comparison between EMD and FT methods proved that the first method returned better both temporal and frequency resolution [358]. EMD method helped to determine the gamma-band activity to be mainly at the highest frequency component.

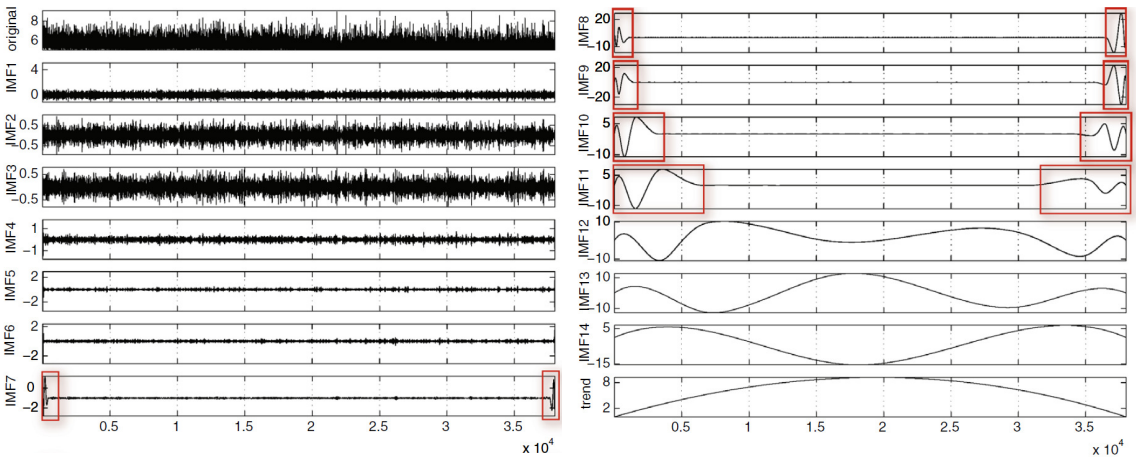

Figure 4.15: Example of the EMD for the first fourteen IMF [359].

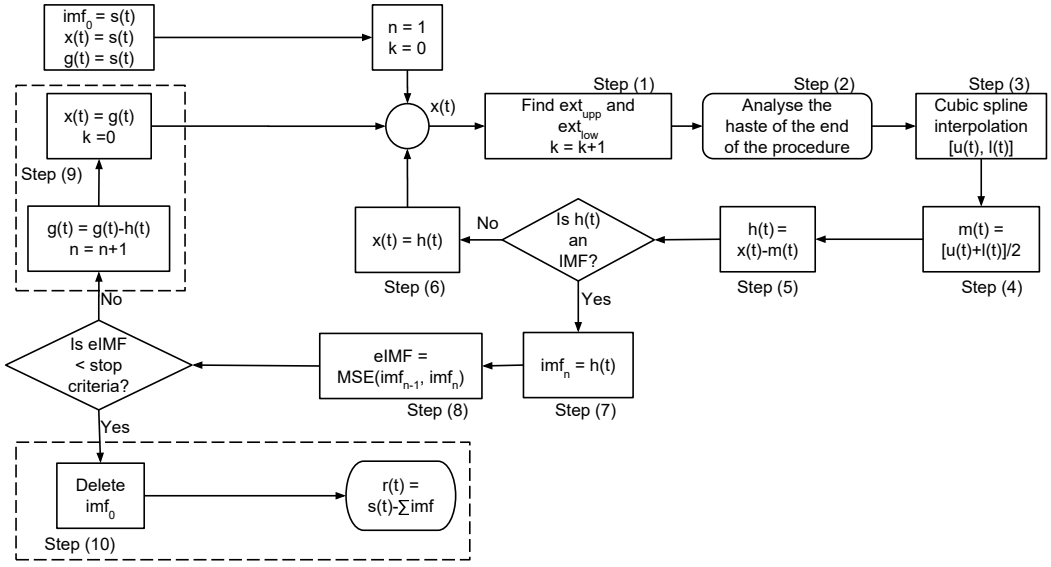

Figure 4.16: Fluxogram of the most important steps of the EMD method sifting process to calculate the IMF and the residue.

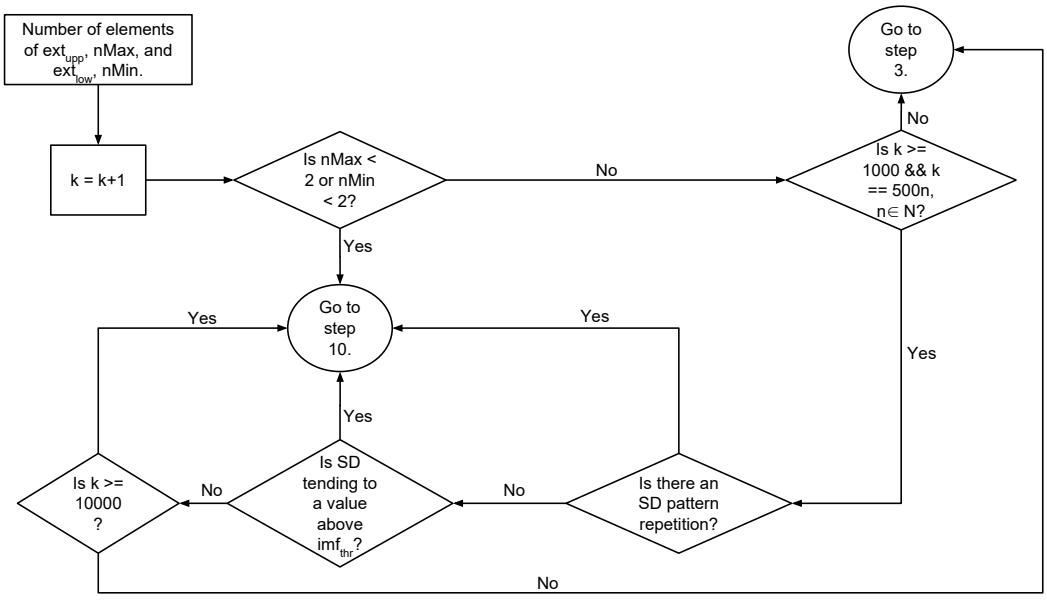

Figure 4.17: Fluxogram of the self-control mechanism to decide the sifting process continuity.

The decomposition of time series by the EMD method gives a finite number of IMF, but their calculation should meet 2 rules [355,358]. An IMF candidate should obey the following rules to be a *de facto* IMF:

1. The number of extrema and the number of zero crossings must not differ more than one unit in the entire data set;

2. At any point, the mean value of the envelope defined by the local maxima and the envelope defined by the local minima is zero.

The process behind the IMF calculation is designated as the sifting process. Figure 4.16 is a fluxogram and represents the sifting process with the key important steps and how the algorithm should be implemented. The key important steps are also enumerated in the following list [355, 360]:

1. It starts by calculating all local maxima, ext_{upp} set, and all local minima, ext_{low} set, of the original time series, $s(t)$;

2. Verify the current conditions of the procedure to infer if it can continue;

3. A fitting model, in this case a cubic spline interpolation, was used to connected all the ext_{upp} set points. The procedure was repeated to the ext_{low} set. The first and the second cubic spline interpolation give, respectively, the upper envelope, $u(t)$, and the lower envelope, $l(t)$, of the $s(t)$;

4. Calculate the mean envelope, $m(t) = \frac{u(t)+l(t)}{2}$;

5. Subtract the mean envelope to the original time series, $h(t) = s(t) - m(t)$;

6. If $h(t)$ does not match the criteria to be an IMF, then $s(t) = h(t)$ and the procedure returns to step 1;

7. If $h(t)$ matches the criteria to be an IMF, it is stored;

8. Calculate the mean squared error, $eIMF$, between the actual $s(t)$ and $h(t)$;

9. If $eIMF$ does not match the criteria, then $s(t) = s(t) - h(t)$ and the procedure returns to step 1;

10. If $eIMF$ matches the criteria, it calculates the residue, $r(t)$, of the original time series $s(t)$ and the procedure ends.

A cubic spline is a piecewise function of third-order polynomials and it does not need of high computational requirements. The interpolation of a cubic spline function relies on a set of p points, previously selected to create the cubic spline function. The function passes through all the given p points.

An IMF must retain what they call "enough physical sense of both amplitude and frequency modulations" [355]. A definition was established to encompass this term, to known when an IMF fulfils this requirement and to stop the sifting process. The current candidate to an IMF must be compared with the previous IMF candidate by calculating the standard deviation, σ:

$$\sigma = \sum_{i=1}^{N} \frac{|h_{k-1}[i] - h_k[i]|^2}{h_{k-1}^2} \tag{4.48}$$

The algorithm did not work in a satisfactory way, using Equation 4.48, since the denominator was 0 in some cases. To avoid this problem, a new factor, NZD, was incorporated in the denominator of the Equation 4.48.

$$\sigma = \sum_{i=1}^{N} \frac{|h_{k-1}[i] - h_k[i]|^2}{h_{k-1}^2 + NZD} \tag{4.49}$$

Equation 4.49 resolves the previous problem with a chosen value to the NZD factor of 10^{-4}. The implementation of a threshold value was suggested, to accept an IMF candidate as a *de facto* IMF [355]. Such threshold should have a standard deviation value inside the limits $\sigma \in [0.2, 0.3]$. To this thesis, the chosen σ threshold value was 0.3.

A self-control mechanism over the sifting process was implemented to avoid calculus perpetuation over time, and to end the process whenever justified. The workflow of this mechanism corresponds to step 2 in the sifting process and Figure 4.17 summarizes the process. The end of the sifting process does not follow a single rule, with the algorithm adjusted to the research objective. For example, at [356] the sifting process ends when 1 of these 2 conditions occurred:

- The set of IMF already discovered has 90% of the original signal power;
- A new discovered IMF has the dominant frequency in a predefined band.

Here, different types of mechanisms were implemented to end the sifting process, but there are 2 that can be considerer natural (all different mechanisms are at Figure 4.18). The first, and the most important one, is the comparison between the current IMF and the previous IMF. The calculation of the $eIMF$, Equation 4.50, between them, allows to infer if the process should stop. Decision making is based on the comparison between the calculated $eIMF$ and a threshold value. If $eIMF$ is lower than 10^{-9}, then the sifting process stops. The second natural process is the evaluation of the current $s(t)$. When $s(t)$ is a monotonic function, no more IMF can be extracted and the sifting process stops.

$$eIMF = \frac{1}{N}\sum_{i=1}^{N} |imf_{k-1}[i] - imf_k[i]|^2 \tag{4.50}$$

The other types of mechanisms, altogether 3, are not natural but forced and they take action when there is a huge number of attempts to find an IMF but always without success. From these mechanisms, the simplest one is the definition of an hard threshold to stop the sifting process when there are more than 10000 consecutive unsuccessful tries to find an IMF. The other 2 types of mechanisms analyse periodically how the σ evolves. One of them searches for repetition patterns in the σ and the second one searches for a σ evolution toward an asymptote, above the chosen threshold value to considerer the candidate time series to an IMF as an IMF. A diagram, with all the different mechanisms to stop the sifting process, is available in Figure 4.18, and the dynamic of the self-control mechanism is available in Figure 4.17. At the end of the sifting process, the decomposition of the original time series is represented by the following relationship:

$$s(t) = \sum_{i=1}^{n-1} imf_i + r(t) \tag{4.51}$$

Creating both upper and lower envelope of the signal, using cubic spline interpolation, can introduce overshoots, undershoots and swings at the beginning and at the end of the data [355,361]. This effect on the time series decomposition transmits for the next calculations and it will be clearly visible in the IMF. If left untreated, the swings, initially present at the data tail, propagates inward and worsen data corruption. A solution was implemented in the sifting process, and already previously performed by the literature, in order to eliminate the swing effect [361]. After ext_{upp} and ext_{low} calculation, the first point and the last point of the time series were both considered as an extrema and added to both sets.

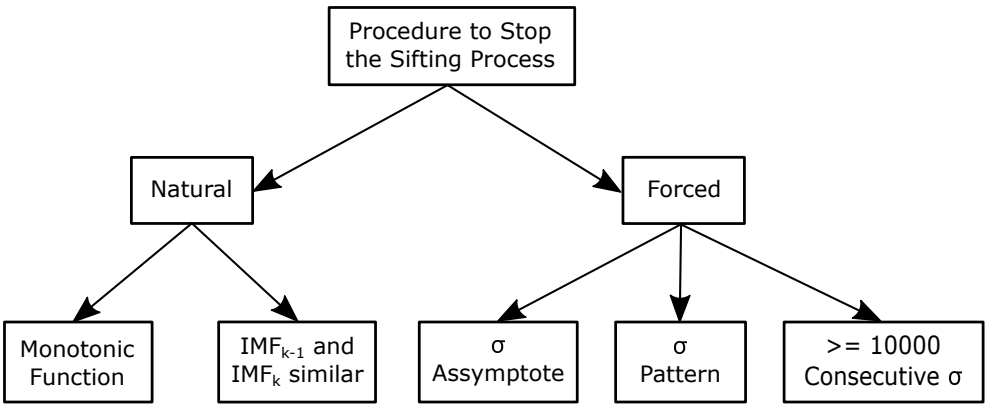

Figure 4.18: Diagram of the different mechanisms to stop the sifting procedure.

The introduction of large swing effects by the cubic spline interpolation creates a problem without an ideal resolution. When the algorithm only uses the maximum and minimum calculated values, the decomposition might introduce swing effects in some IMF. Adding the first and last point to ext_{upp} and ext_{low} leads to more IMF and to less similar of those IMF to single frequency pure sinusoidal waves. The second solution increases computational requirements, spending more time in the sifting process, and IMFs might lost, more easily, its single frequency sinusoidal wave characteristic. These side effects were decisive to discard the solution to solve the swing effect. After the EMD had been performed, 2 features, amplitude and period, were selected to our database.

4.7.2.1.7 Period The period of each IMF of the EMD method was calculated by finding the maximum value and defining a region around it to calculate the period using local maximum values.

4.7.2.1.8 Amplitude The amplitude of each IMF of the EMD method is the global maximum value.

4.7.2.1.9 Shannon Entropy The entropy may be interpreted as a measure of the disorder of a system. For this thesis, the formal definition of entropy in the classical thermodynamics, $dS = \frac{\delta Q}{T}$, isn't of interest, but, rather, the entropy definition in the information theory field. Entropy, more precisely the Shannon Entropy, in the information theory field is defined as

$$H^* = -\sum_{a \in A} p(a) \cdot ln[p(a)] \tag{4.52}$$

The Shannon Entropy depends on the probability mass function $p(a)$ of each element a and, by definition, when an element is not present in the set A, $p(a) = 0$ and $0 \cdot \log(0) = 0$. Each element a of the set A is unique.

Instead of the natural logarithm, it is possible to implement a logarithm of a different base, such as base 2. The Shannon Entropy unit for a natural logarithm is 'nats' and it is usually more suitable for mathematical purposes while the unit for the logarithm of base 2 is 'bits' and it gives "more intuitive descriptions". The logarithm of base 2 was selected to calculate the entropy [362, p. 17-18].

The probability mass function p of an element a of the set A is defined as the quotient between the number of times that element a exists in the entire sound data series s_i and the number of elements of the same data series, Equation 4.53.

$$p(a) = \frac{\#\text{ total of element } a}{\#\text{ total samples}} \tag{4.53}$$

The mathematical equation implemented to calculate the entropy of snore i^{th} is

at Equation 4.54.

$$H_i = -\sum_{a \in A} p(a).log_2[p(a)] \tag{4.54}$$

4.7.2.2 Frequency-Domain Analysis

Analysis of signals in the frequency domain gives important additional information to characterize them. Although the transformation does not add new features to the signal, its visualization and identification improve in the frequency domain, revealing previously hidden features. The FT is one of the oldest methods to perform signal analysis in a different domain, and it decomposes the signal in its constitute frequencies. It uses a set of predefined functions, function as templates, to perform the decomposition of the signal.

4.7.2.2.1 Power Spectrum Density using Welch Method Feature extraction in the frequency domain was accomplished by estimating the signal PSD. The PSD of a time series signal provides its power distribution over the frequency range. This type of analysis characterizes stationary random processes. PSD is defined as the discrete time FT of the autocorrelation of a function $x[n]$:

$$P(f) = \sum_{k=-\infty}^{+\infty} r[k]e^{-j \cdot 2 \cdot \pi f k} \tag{4.55}$$

Where $r[k]$ is the autocorrelation function of the random process $x[n]$. The estimation of the PSD is a function of the data acquisition length. The longer the data recording of the signal, the better the estimation of the PSD.

The study of non-stationary and stationary random processes is different, and a longer data acquisition does not guarantee an improvement in the estimation of the PSD [363]. The calculation of the PSD may be performed by either parametric or non-parametric methods. Parametric methods make use of a small number of parameters, and based on assumptions (criteria), to create a model to estimate the PSD [364, ch. 14]. These methods are capable of delivering estimations with better resolution, than the non-parametric methods, which do not use parameters and the respective parametric models for the PSD calculus. The calculation of the PSD, based on non-parametric methods, relies on their strategy in the estimation of the autocorrelation. Once they do not make use of models, they are robust and less sensitive to noise [365].

The Periodogram method strategy uses the autocorrelation $r[k]$, followed by the calculation of the discrete time FT. Zero padding a time series, before discrete time FT, might improve amplitude and frequency estimation, but not the frequency resolution. PSD estimation is usually performed after signal windowing, and 2 important windows' features should be balanced to choose a type of window. The

first feature is related to the width of the main window's lobe, with a lower width meaning a better resolution. The second feature is related to the window's side-lobes, and lower side-lobes improve the smoothing of the estimated spectrum [364, ch. 14] [282, ch. 14].

The Welch method is an evolution of the Periodogram method, with the introduction of overlapping, usually between 50% and 75%, in the time series signal segmentation. Data segmentation reduces the variance when compared with the Periodogram method, but there is a trade-off with the resolution since it worsens. PSD estimation is the result of the average value for each PSD segment estimation [364, ch. 14] [282, ch. 14].

PSD estimation was implemented using the Welch method, with overlapping of 50%, and several features were calculated based on that estimation. Time series segments were windowing by a Hamming window, with 42.5dB side lobe attenuation.

4.7.2.2.1.1 Frequency-Domain Features Using a binary search algorithm, the first features retrieved were the $f_{MaxPower}$, frequency with the highest PSD, and the f_n, frequencies for the quartile 25%, 50% and 75% of the PSD. PSD data was also used to calculate the spectral centroid, $f_{SpecCentroid}$ (see Equation 4.56), standard deviation frequency, $f_{FreqSTD}$, (see Equation 4.57) and the coefficient of symmetry, $f_{CoefSym}$ (see Equation 4.58) [239].

$$f_{SpecCentroid} = \frac{\sum_{i=1}^{N} f_i \cdot PSD_i}{\sum_{i=1}^{N} PSD_i} \tag{4.56}$$

$$f_{FreqSTD} = \sqrt{\frac{\sum_{i=1}^{N} f_i^2 \cdot PSD_i}{\sum_{i=1}^{N} PSD_i}} \tag{4.57}$$

$$f_{CoefSym} = \sqrt[3]{\left|\frac{\sum_{i=1}^{N} f_i^3 \cdot PSD_i}{\sum_{i=1}^{N} PSD_i}\right|} \tag{4.58}$$

The frequency bandwidth, calculated using the Welch method, was split into 10 bands in each snore to calculate the remaining features. adaptative The first band was always from 0 to 100 Hz, and the remaining ones were determined using adaptive calculation. Those 9 bands were calculated using a logarithm scale, base 10, from 100 Hz to the highest frequency in the PSD estimation of each snore. The Band Power Ratio, f_{BPR}, calculates the ratio between the sum of the PSD values of frequencies inside each one of frequency bands and the sum of all PSD values, while the In Out Band Power Ratio, f_{IOBPR}, calculates the ratio between the sum of the PSD values of frequencies inside each one of frequency bands and sum of all PSD values outside that band. The Spectral Flatness, $f_{SpecFlat}$, was also calculated (Equation 4.59).

$$f_{SpecFlat} = \frac{\sqrt[N]{\prod_{i=1}^{N} PSD_i}}{\frac{\sum_{i=1}^{N} PSD_i}{N}} \tag{4.59}$$

4.7.2.3 Synchrosqueezed Wavelet Transform

The SWT method was, firstly, proposed to study auditory nerve-based models, and to improve identification by sound [366]. Originally, it was the result of merging two methods, wavelets and reassignment. The synchrosqueezed starts with the construction of the time-frequency plane, by decomposing the time series, using wavelets. The idea behind the reassignment method is the analysis of the time-frequency plane, in small portions of the representation, and it searches for close energy concentrations and reallocates those small portions to a single concentration [367]. The energy reallocation occurs in the frequency axis, which allows keeping time resolution, and it sharpens the time-frequency plane representation. Allocation factors rely on the local behaviour of the plane [368, 369]. A continuous wavelet transform over the signal s, was implemented accordingly with the definition given in [366]:

$$W_s(a,b) = \int s(t) \cdot a^{-1/2} \cdot \psi(\frac{t-b}{a}) \cdot dt \tag{4.60}$$

The ψ function is the chosen wavelet, with $W_s(a,b)$ reallocated to concentrate the time-frequency profile.

More recently, researchers improved the method to incorporate the concept behind the EMD method [368]. Most of the time series are multicomponent, and the construction of the time-frequency plane highlights the most important components, at each instant of time, with the method returning components of IMF type. Considering signal $s(t)$ might be a sum of amplitude-modulated frequency-modulated intrinsic mode type components $s_i(t)$,

$$s(t) = \sum_{i=1}^{N} s_i(t) = \sum_{i=1}^{N} A_i(t) \cdot \cos(\phi_i(t)) \tag{4.61}$$

where the $A_i(t)$ is the amplitude with slow variations, and the $\phi_i(t)$ is the instantaneous phase. $\phi_i'(t)$ and $\phi_j'(t)$ are well separated in the time-frequency plane, for $i \neq j$, which means that each $s_i(t)$ might be considered an individual component. Accordingly with the EMD method, the Instantaneous Frequency (IF), at time instant t and for the i^{th} component, is then $\omega_i(t) = \phi_i'(t)$. Up to the first 10 IF of each snore were calculated for future data analysis.

SWT is a recent tool for data processing, and the current literature in the OSAHS field is scarce. Only 3 papers were found using SWT to study OSAHS. The first

paper studied the use of SWT to detect sleep spindles, getting a maximum sensitivity of 96.5% and specificity of 98.1% [370]. The second paper used the method to detect K-Complexes [371]. The third, and final, paper used the method to detect sleep apnoeas and hypopneas by using a single ECG channel [372].

A downsample factor of 4 was implemented to each snore signal to decrease computational costs associated with the SWT method. No significant information losses were expected and, before resampling, downsampling was performed using an anti-aliasing filter, using a Chebyshev Type I low-pass filter, with a cut-off frequency at 0.8*(Fs/2)/R. Fs parameter represents the signal's acquisition frequency, while R is the downsampling parameter, in this case, 4. SWT calculation was performed using an analytic family wavelet family function, called Morlet.

4.7.2.3.1 Patients' Set Synchrosqueezed Wavelet Transform changes the signal from the time-domain to the time-frequency domain, and the calculation of the first up to 10 IF generated a great amount of data, which required a dedicated physical storage unit and a 4 TB external hard drive was selected. The external hard drive had the capability to store SWT data processing results for the first 1000 snores of each patient, with the highest signal-to-noise ratio values, in the case they exist. The total number of snores analysed with this method was 33,383.

4.7.3 Hypothesis Testing

A hypothesis testing procedure was implemented to analyse an assumption regarding the behaviour, and if the differences have statistical significance, of features among medical classification groups. The first step was to test data with the Kolmogorov-Smirnov test, which analyses data to check if the samples come from a normal distribution. The significance level (α) was set to 5%. Depending on the result, if the null hypothesis is either rejected or not, a complementary test is implemented.

The rejection of the null hypothesis, data don't come from a normal distribution, led to the complimentary test, the Kruskal-Wallis H test. The test's null hypothesis states that data in all groups come from the same distribution, and it was performed to a 1% significance level. When the test rejects the null hypothesis, a final a *post-hoc* test is implemented to verify which groups come from a different distribution. The multiple comparison test identifies those groups.

A second hypothesis testing procedure was implemented solely to analyse sound event filtering (section 4.7.1.5). The McNemar's test, a method to compare matched-pairs data, was used to evaluate one sensitivity against the second sensitivity, and one specificity against the second specificity. The method has several definitions, including the classic (Equation 4.62) and the mid-p-value (Equation 4.63) definitions, and they were compared against other definitions of the McNemar's test [373]. These

2 definitions performed better than the other definitions, when compared to their type I error rates and power. The classical method is considered the most powerful definition and it should be implemented cautiously if it is used on small samples (the paper only builds scenarios up to N$\leq$100 samples), once it surpasses the nominal type I error value of 5% in some case scenarios, at a maximum of 5.37% [373, 374]. The mid-p-value definition never violates the nominal type I error rate in all the scenarios under analysis, and it has a power similar to the classical definition [373].

The test consists of the analysis of a 2x2 matrix, specifically the off-diagonal values, and the detection of snore/noisy sounds by one method but not by the second method. Equation 4.62 to Equation 4.65 use the off-diagonal values b, number of snores detected by method 1 but not by method 2, c, number of snores detected by method 2 but not by method 1, and n=b+c. The null hypothesis states that both methods are equally likely in snore detection (sensitivity) and in noise rejection (specificity). The result of the classical classification χ^2 has chi-squared distribution with 1 degree of freedom.

$$\chi^2 = \frac{(b-c)^2}{(b+c)} \tag{4.62}$$

$$\textit{mid-p-value} = 2 \cdot [\textit{one-sided p-value} - \frac{1}{2} \cdot f(b|n)] \tag{4.63}$$

$$\textit{one-sided p-value} = \sum_{b=0}^{\min(b,c)} f(b|n) \tag{4.64}$$

$$f(b|n) = \binom{n}{b} (\frac{1}{2})^n \tag{4.65}$$

Chapter 5

Results

This chapter presents the most important results and findings associated with this thesis. It starts with the presentation of results related to PSG scoring, and their medical reports, and continues with the pre-processing phase. The last results relate to data processing and analysis. Correlation of snore data with other sleep parameters was also implemented.

5.1 Slow Variation Parameters

The development of both hardware and software to manage SVP data was not ready when data acquisition began for the snoring signal. SVP data acquisition began weeks later, and a total of 65284 data acquisitions were performed, with one acquisition every 3 minutes. Unlike high-quality sound acquisition, the acquisition of SVP data did not stop in the morning, but continues throughout the day, until new commands were ordered to the device like a data read command.

All data in this section were the result of all SVP data acquisitions, including patients excluded from the final set and periods without any PSG study ongoing. There are 3 figures to represent data from each SVP. The first figure is a histogram to understand how data behaves, in general, while the second and the third figures are of box plot type. In the second figure, data are grouped accordingly with the time of day of the register. Humans divide the day into 24 hours, and data was placed in one of the 24 groups accordingly with the following rule. Datum belongs to group n when its record was inside the time interval $[n-1, n[$ h.

In the third figure, data belonging to the same week were grouped. It was defined as the beginning of a week on Mondays, with data recording starting on the 26 of March, in a total of 39 weeks. No data were acquired during week 26.

5.1.1 Pressure

SVP gauge pressure presented very stable values as it shows Figure 5.1. With low variability, a single value, 475 Pa, has almost two-thirds of all the records, presenting

a standard deviation of 0.602 Pa.

Gauge pressure distribution was analysed for both times of the day and weeks. Figure 5.2 has 24 box plots to describe gauge pressure distribution on an hourly basis, using data quartiles. The n box plot has all the data acquired during the time of the day comprehended between $[n-1, n[$ h. As previously stated, almost two-thirds of the data have a value of 475 Pa, and in Figure 5.2 the effect is clear. Most of the time of the day, the quartiles and whiskers, of the box plot, have the same value, the mode value.

Figure 5.3 shows gauge pressure distribution over the weeks, which were also represented in box plots. It confirms the trend in Figure 5.2. For the 39 weeks, most of the box plot parameters, both quartiles, and whiskers, are concentrated in a single value, the mode value. At week 17, there is a data distribution distinct from all others, where percentiles 25, 50, and 75 have different gauge pressure values.

5.1.2 Temperature

The temperature reading presented has more variability, than the readings from the gauge pressure sensor, with an indoor temperature range between 18.8 and 37.1°C. The profile of the temperature distribution is in Figure 5.4.

Figure 5.5 is a histogram-type figure, with temperature data organized on an hourly basis. The most significant modification is in the first hours of daylight, with a well visible decrease in temperature. Temperature tends to decrease slightly during the night, and increase, also slightly, during the day. Maximum values were achieved at the end of the day and the beginning of the next day. The lowest temperature values were recorded when the PSG studies ended and the CMS opens.

Although the device measured indoor temperatures, the outdoor temperature was capable of influencing indoor temperatures as seen in Figure 5.6. Season impact on indoor temperature is visible. The period of higher temperatures, from week 17 to 25, corresponds to the period from the middle of July to the middle of September. Lower temperatures are linked with the coldest months recorded, March and April, and November and December.

Two particular weeks had temperature records different from the others, with wider Interquartile Range (IQR). Week 17, mid-July, had 2 data acquisitions with significant temperature differences. The mean temperature was higher on the first day when compared with the second day. The mean temperature difference between the first and the second day was of the was of 9.9°C. The second week, week 25, also had remarkable differences in the temperatures and, again, only 2 data acquisitions were performed. The difference in the mean temperature was -5.4°C, meaning the second day was hotter.

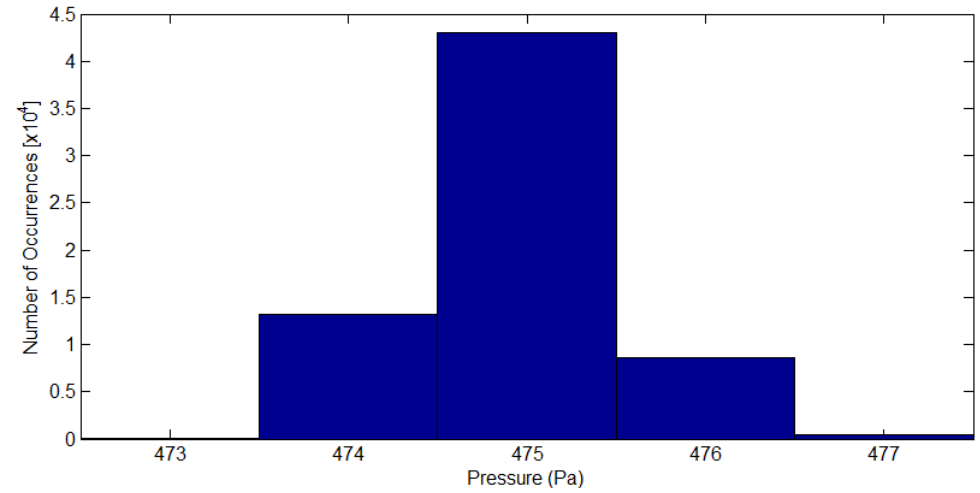

Figure 5.1: Histogram of all gauge pressure records. Gauge pressure has little oscillations, with only 5 different records. Mode value, 475 Pa, accounts for 65.8% of all pressure values, while minimizer and maximizer values of 473 and 477 Pa, respectively, and they accounts, together, to 0.8%.

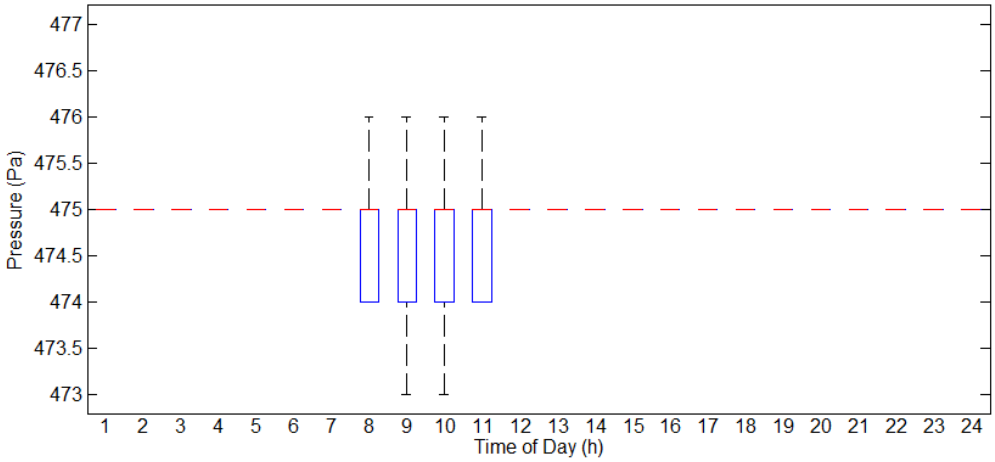

Figure 5.2: Gauge pressure data were grouped in a hourly basis. The first hour of the day, 1, includes data belonging to the range $[0, 1[$ h, while the second hour of the day, 2, includes data belonging to the range $[1, 2[$ h. The remaining 22 h of the day followed the same rule. Evidence of gauge pressure stability exists with most of the time of the day with the same value for all the box plot parameters. Outliers were removed from the figure.

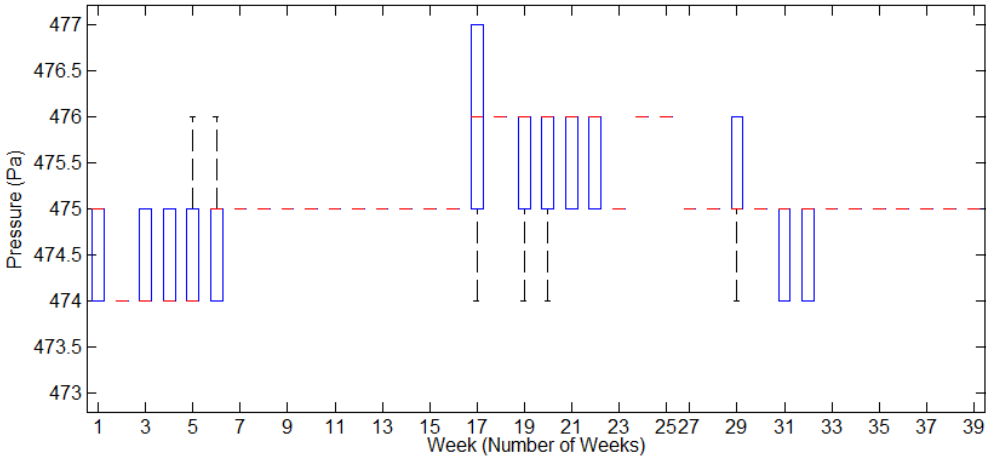

Figure 5.3: A box plot to evaluate gauge pressure over the weeks. Gauge pressure shows evidences of stability on a week basis, with the majority of the weeks with the same value for all the box plot parameters. The figure does not include outliers.

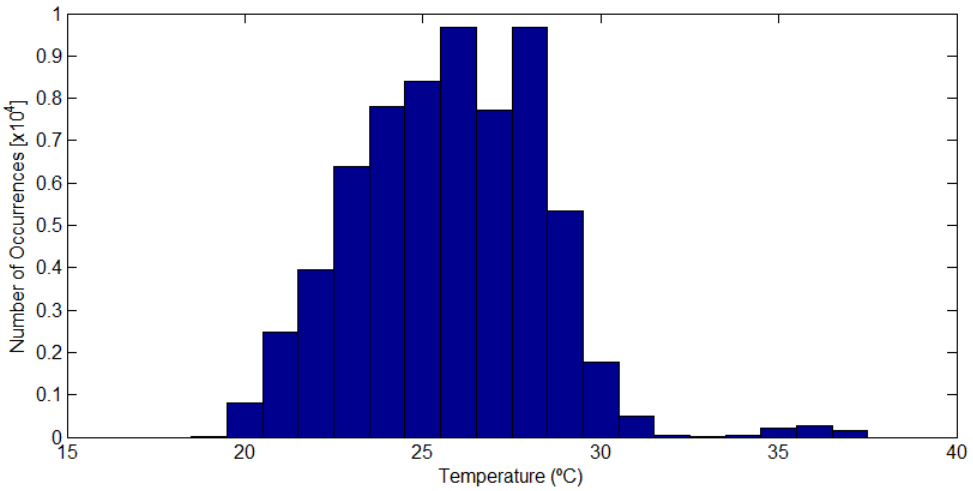

Figure 5.4: Histogram of the temperature distribution with a temperature span of 1°C. Two temperatures, 26 and 28°C, have the highest number or records. The first one has a total of 9681 records, while the second one has the maximum number of records, with a total of 9683 records.

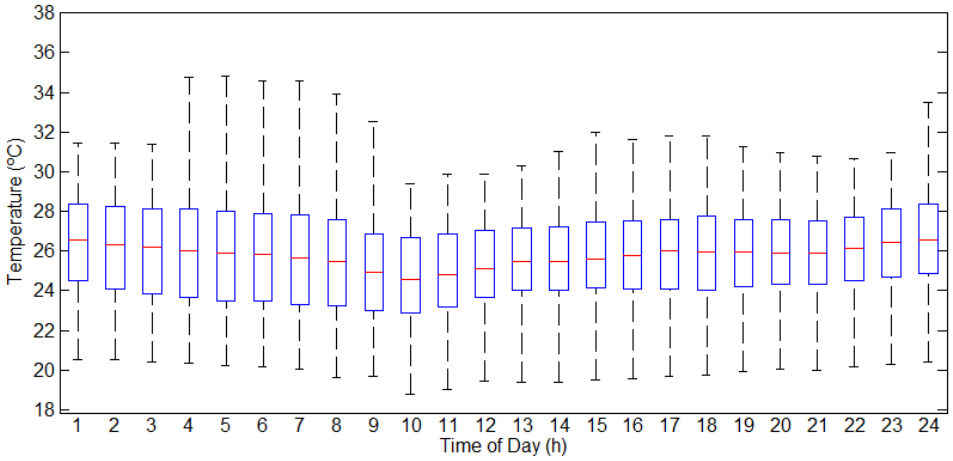

Figure 5.5: Evolution of the temperature during the day in an hourly basis. Temperatures recorded in the first hour of the day, $[0, 1[$, were grouped and their box plot is at position 1. Similar analysis was performed for the remaining 23 h of the day.

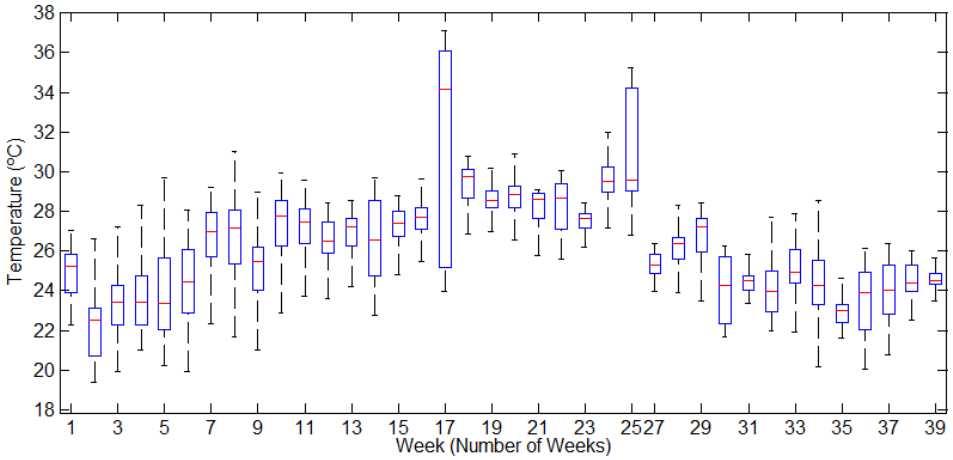

Figure 5.6: Evolution of the temperature over the weeks. Season impact in temperature is clearly visible, with higher temperature values between week 17 and 25, and lower temperature values in weeks 1 to 7 and 35 to 39.

5.1.3 Relative Humidity

Recommendations for relative humidity indoor point to values between 30% and 50% [375]. From the total number of records, 42107, or 64.5%, of them have their values between the recommended limits for relative humidity. Figure 5.7 presents an histogram for all relative humidity records. The remaining data are above the 30% to 50%, with 21928 records, 33.6%. Below the recommended range, there are only 1.9% records.

Relative humidity has a smooth evolution throughout the day, achieving its highest value at the end of data acquisition, and its lowest value at the end of the afternoon. The median amplitude, percentile 50, is 5.43%.

Unlike relative humidity behaviour in an hour analysis (Figure 5.8), the study of its distribution throughout the weeks shows a behaviour less predictable. Figure 5.9 presents the relative humidity distribution over the weeks. The highest relative humidity values happen in the last weeks, in the Autumn, while the minimum value occurred in the summer. Four weeks have distinct behaviours when compared with the remaining weeks. Two of those weeks are week 17 and week 25, and they have a common factor. In each of these weeks, only 2 acquisitions (patients) were performed. In week 17, data were acquired with significant differences in relative values. On the first day, the mean relative humidity value was 27.2%, while on the second day it increased to 40.9%. In week 25, the first day had a relative humidity mean value of 43.8%, while the second day had a relative humidity value of 28.4%.

The other two weeks, weeks 1 and 29, had data acquisition during more days. Data acquisition lasted for 6 and 4 days, respectively, for weeks 1 and 29. During the first week, daily mean relative humidity was 36.5%, 32.7%, 28.6%, 32.2%, 39.3% and 41.5%. Week 29 had a daily mean relative humidity of 61.1%, 59.9%, 48.4% and 47.2%.

5.1.4 Temperature vs Relative Humidity

The relationship between temperature and relative humidity was directly studied in scatter plots. The parameter percentile 50, from both variables, was used in Figure 5.10 and in Figure 5.11.

In Figure 5.10, a scatter plot was built on an hourly basis. The profile of a hysteresis-like curve exists and, considering the beginning of data at midnight, it stars with a decrease in temperature and an increase in relative humidity. At the 7^{th} hour of register, the trend changes to a decrease in both temperature and relative humidity. A few hours later, the temperature starts to increase while relative humidity continues to fall. Seventeen hours after the beginning of the day, data stabilizes without a clear trend during the next 4 hours. The observation of the last 4 hours reveals an increase in both variables. Figure 5.11 does not have the same

hysteresis behaviour. Even so, dark blue and dark red dots, representing the coldest months, have lower temperature registers.

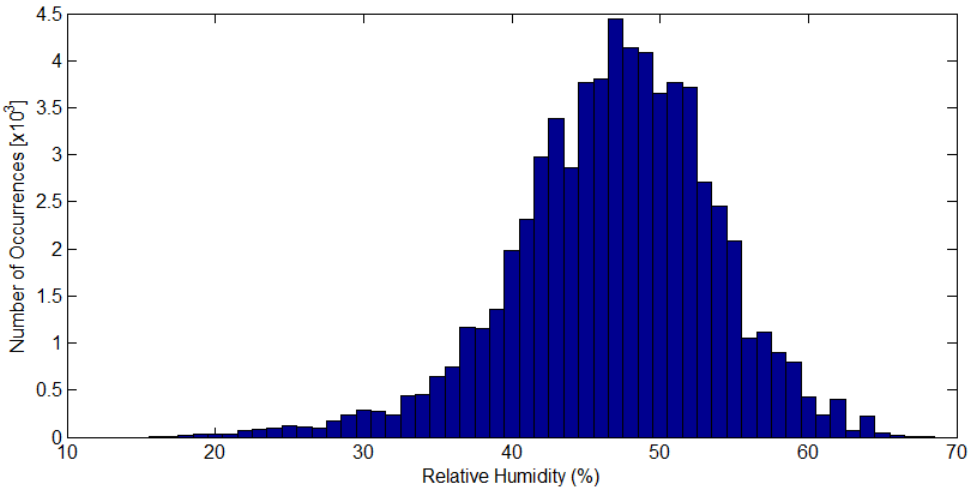

Figure 5.7: Distribution of relative humidity values. The histogram identifies the mode value at 47%, inside the recommended window, 30% to 50%, for comfort.

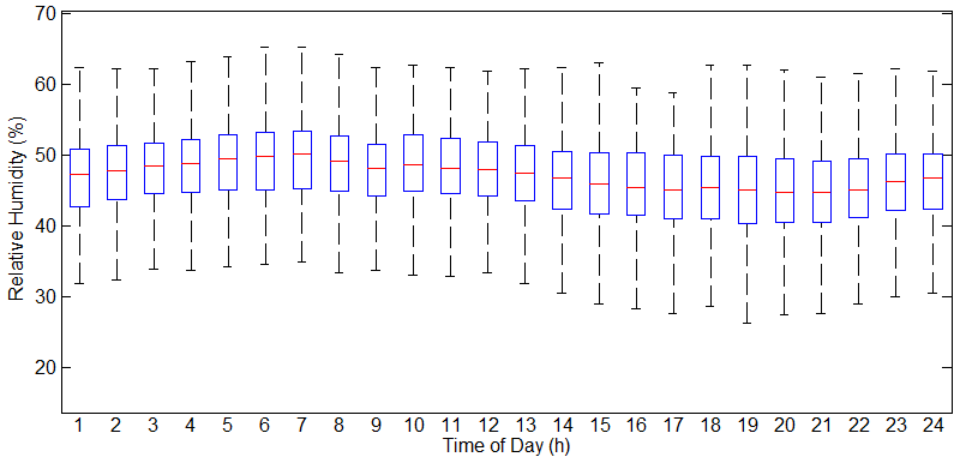

Figure 5.8: Relative humidity data distribution in an hourly basis. Higher values were achieved during the night, with a peak, 50.18%, just before PSG study ends. Daylight time decreases relative humidity values, achieving the lowest value, 44.75%, at the end of the afternoon.

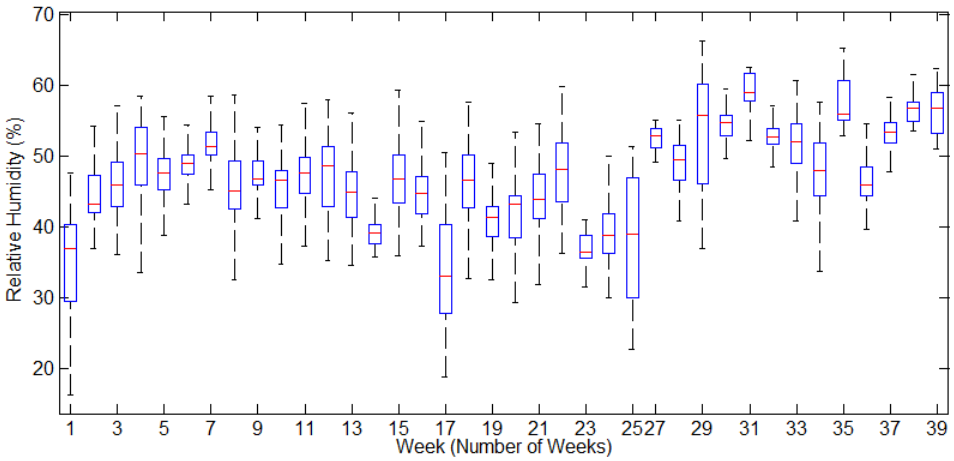

Figure 5.9: Box plot of relative humidity for each week. Relative humidity achieved higher values in the first weeks and in the end of data acquisition, the last 13 weeks. In the middle, summer time, relative humidity achieved its lowest values.

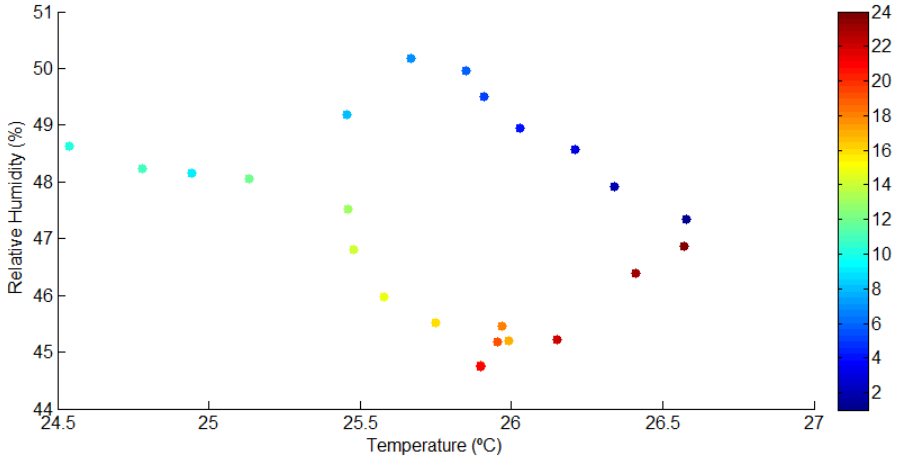

Figure 5.10: A 3 variables scatter plot. In this Cartesian coordinate system, the variables are temperature, X-axis, relative humidity, Y-axis, and the hours of the day, represented by a colour code. Both temperature and relative humidity values are the percentile 50 calculated for each hour.

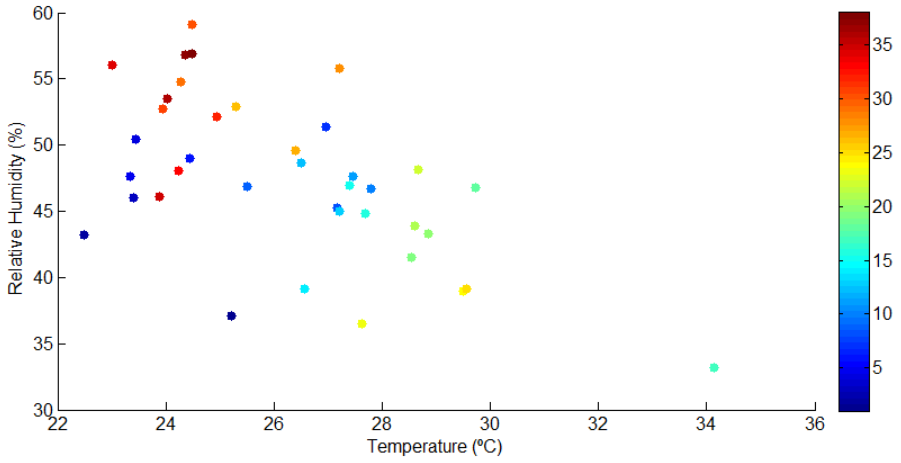

Figure 5.11: A 3 variables scatter plot. The temperature, X-axis, and the relative humidity, Y-axis, form the Cartesian coordinate system. The third variable, time in number of weeks, is represented by a colour code. Both temperature and relative humidity values are the percentile 50 calculated for each week.

5.2 PSG Scoring

PSG scoring was performed by the sleep technicians at the CMS, but their results were crucial to finding useful relationships between medical and research data. A resume of some of the most important results, coming from PSG scoring, is available at Table 5.1. It splits the results, presented in terms of mean and standard deviation, accordingly with the patients' medical classification group. For each group, the relative REM sleep and NREM, divided in N1, N2 and N3, sleep is presented along with the total amount of RERA. The table also has the indices AHI and RDI, important in sleep evaluation, and TST, in minutes.

The hypothesis testing was implemented to analyse the percentage of each sleep stage, with a p-value of 0, the highest p-value$\approx 10^{-7}$, for each sleep stage/medical classification group pair. With the null hypothesis rejected, the second test was performed and the p-value calculated was 0.022, 0.962, 0.063, and 0.802, for the different percentages of sleep stage, N1, N2, N3, and REM, respectively. These results don't allow to reject the null hypothesis, which means that data comes from the same distribution.

The final number of 67 PSG studies resulted in the acquisition of 60292 epochs, but not all the epochs count the same for sleep evaluation. Instead, the beginning of data acquisition does not mean the beginning of data recording for sleep evaluation, which starts later. Data for sleep evaluation start, and end, when the sleep technician gives an input to the computer software to mark the beginning and the end of data for sleep evaluation. Of the 60292 epochs, 1673 epochs were discarded, remaining only 58619 epochs, in which 8 of them remained unclassified, either as awake or in one of the sleep stages, representing 0.01%. Each unclassified epoch, epoch 35, 232, 707, 128, 58, 5, 679 and 9, belongs to a different patient, with ID 63, 64, 77, 106, 126, 133, 134 and 147, respectively.

The patients took, on average, 42.2 ± 44.5 epochs to fall asleep, from the moment data acquisition effectively start to count for sleep evaluation. Taking in account the medical classification group of the patient, they fall asleep after 48.9 ± 37.3, 41.8 ± 40.9, 37.7 ± 40.2, 44.2 ± 67.4, 40.3 ± 30.6 epochs for Co, Sn, Mi, Mo, and Se groups, respectively. Visual information regarding both Lights Out and First Sleep epochs is at figure 5.12. Table C.4, in Appendix C, has information about the first epoch for sleep evaluation and the following first epoch of sleep.

5.2.1 Sleep Stages

The patient's hypnogram is the graphical chronological representation of the patient's sleep, after scoring all PSG epochs, giving the sleep profile of the patient. The hypnogram allows the physician to understand the patient's sleep as either

Table 5.1: Patients' PSG results for important features in sleep evaluation, organized accordingly with their medical classification group. There are 5 medical classification groups: Co, Sn, Mi, Mo, and Se. The mean value, μ, and the standard deviation value, σ, for each medical classification group were calculated for the different sleep stages, for the RERA, AHI, RDI and the TST [332].

Parameter $[\mu \pm \sigma]$	**Co**	**Sn**	**Mi**	**Mo**	**Se**
N1 (%)	17.5±15.0	15.4±8.3	17.5±9.8	16.6±8.3	33.7±20.0
N2 (%)	42.5±5.8	41.7±8.9	43.1±10.3	42.9±9.6	38.4±13.1
N3 (%)	26.2±15.4	27.2±12.0	24.2±8.4	22.7±9.6	13.1±9.3
REM (%)	13.7±6.5	15.6±6.0	15.1±5.1	17.8±7.3	14.9±6.9
RERA (#)	1.7±1.8	13.8±12.8	26.7±20.9	36.6±26.1	33.5±39.7
AHI	0.4±0.4	2.4±2.2	6.4±4.2	16.2±6.8	55.2±26.7
RDI	0.8±0.5	4.7±2.4	11.2±3.2	22.8±3.9	62.0±21.2
TST (min)	309±84	364±68	331±75	352±64	292±124

normal or disrupted, and how disrupted it is. The relationships between sleep stages and other variables of the PSG study are presented below.

A total of 3523 epochs had their body position register identified in position N, from the 58611 epochs classified as one of the sleep stages. This sleep position is in fact a reference for a faulty acquisition, and there are different causes responsible for the problem. A bad sensor connection to the concentrator may justify the temporary data missing, solved after the intervention of the sleep technician. Patients with ID 100, 104, 105, 112, 113, 130, 145, and 147 had their sleep position temporarily halted in some epochs (max of 11), and all but patient ID 105 had the sleep position N in a row. Patients with ID 52, 90, 107 and 126 had their sleep position unidentified the entire PSG recording time. A full night without sleep position may be the result of a faulty sensor, depleted sensor batteries, or a bad connection. Table 5.2 presents the distribution of the sleep position, in percentage, for each sleep stage. With

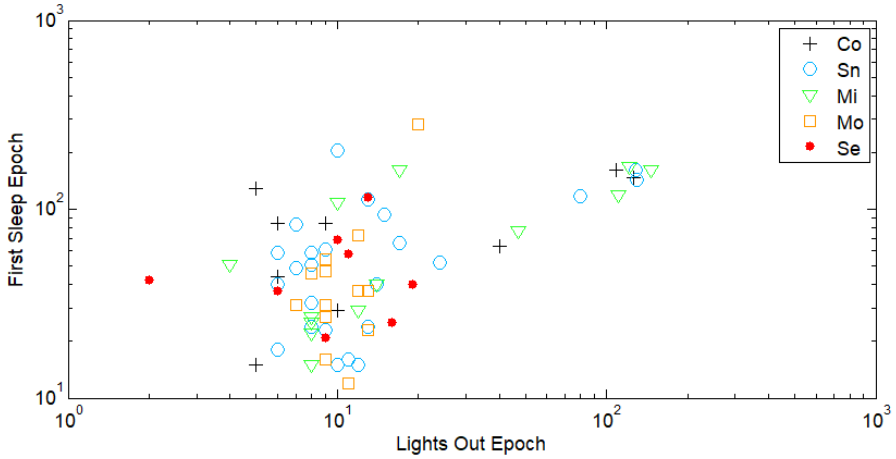

Figure 5.12: Lights Out and first sleep epoch for each one of the patients. Patients were coloured accordingly with their medical classification group. Sleep registers with a high number of epochs are likely associated to the performance of a SIT test.

Table 5.2: Distribution of the possible sleep positions, in percentage, accordingly with each sleep stage. The most common sleep position is the back (B) position, closely followed by the left (L) position. The right (R) position was still a common position, however half the B position, while the prone (P) sleep position was the preferred position in rare occasions.

Body Position	**W** (%)	**N1** (%)	**N2** (%)	**N3** (%)	**R** (%)
L	33.8	32.1	33.9	41.6	32.1
R	18.0	20.3	21.1	18.8	23.6
P	1.3	1.7	2.4	2.5	2.4
B	47.0	46.0	42.6	37.1	41.9

23627 epochs (42.9%) registered in sleep position back (B), it was the preferred sleep position, closely followed by the left (L) position (19204 epochs or 34.9%). Finally, the less common sleep positions are the right (R) position, with 11122 epochs (20.2%), and the prone (P) position, occurring only in 1135 epochs (2.1%).

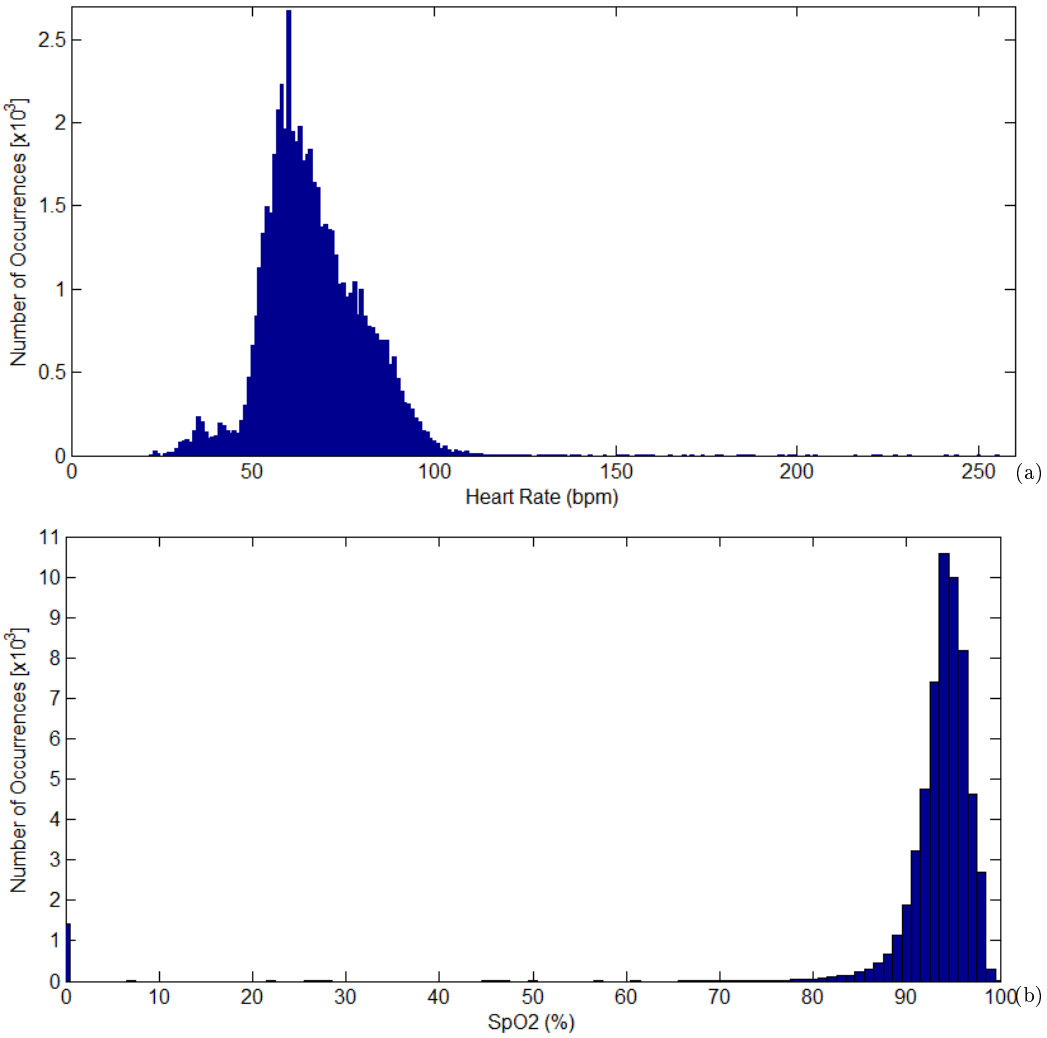

Figure 5.13: Histogram for all the PSG epoch registers for both heart rate and SpO_2. Each epoch has a single entry for heart rate and SpO_2. Heart rate distribution, (a), reveals a 60 bpm mode value with 22 and 255 bpm being the lowest and highest record values, respectively. O_2 saturation registers, (b), with a 94% mode value, and more than 91.4% of the pulse oximetry registers with 90% or more of saturation.

Histogram of the entire population under study (all epochs) for heart rate is available at Figure 5.13 (a). Heart rate variability points to minimum and maximum heart rate values of 22 and 255 bpm. A thumb rule for the maximum age-related heart rate states to subtract 220 to subject's age [376]. Following this thumb rule and the patients' profile for this project, all heart rate registers above 200 bpm were discarded, in a total of 20 registers, 0.03% of all registers. The distribution of the remaining heart rate registers was studied according with the respective classified sleep stage epoch or the patients' medical classification group.

Oxygen saturation, measured by a pulse oximetry device, is an important marker to evaluate gas exchange, and airflow, in the respiratory system. Figure 5.13 (b) is a histogram of the oxygen saturation distribution, with evidence that the vast majority of the pulse registers is above 90%. Common values for oxygen saturation are above 90%, while values between 70% and 90% are not so common. Extremely rare are the cases of pulse oximeter reading below 70%, which raises another concern related with the precise calculation of pulse oximetry at those levels [377,378]. A cut-off filter was implemented with a value equal to the highest pulse oximeter possible value, but without a single register. That value was 65%, and all pulse oximetry register values below this value were removed, in total number of 1461 registers.

Figure 5.14 presents 2 relationships, one between heart rate and sleep stage (Figure 5.14 (a)), and a second between O_2 saturation and sleep stage (Figure 5.14 (b)). Both heart rate and O_2 saturation present small to none variability in Q2 (median) values. Figure 5.14 (a) shows higher heart rates during sleep stage awake, REM and N1, decreasing for N2 and N3 sleet stage. Q1 values are 59, 58, 57, 56 and 60 bpm for awake, N1, N2, N3 and REM sleep stage, and the Q3 values are 80, 75, 73, 72 and 76 bpm (same sleep stage order).

Figure 5.14 (b) shows that all the sleep stages have the same median, 94%, and similar IQR, with the REM sleep stage presenting a slightly different distribution, more wide in both IQR and in the maximum-minimum difference. IQR value is 3 bpm for all but REM sleep stage, with a 4 bpm value. The mean and the standard deviation acknowledge the stability observed with Q2 ($93.9 \pm 2.7\%$, $93.4 \pm 3.4\%$, $94.0 \pm 2.8\%$, $94.1 \pm 2.2\%$ and $93.4 \pm 3.9\%$ for awake, N1, N2, N3 and REM sleep stages, respectively).

The hypothesis testing was implemented to evaluate the heart rate feature, with a p-value of 0, for each heart rate/sleep stages group pair. With the null hypothesis rejected, the second test was performed and the p-value calculated was 0, $\approx 10^{-299}$. The rejection of the Kruskal-Wallis H test led to the implementation of the *post-hoc* test. The result points to a significant difference between all sleep stages once the intervals are disjunct, as it is possible to see in Figure 5.15. Table 5.3 summarizes this process. The same hypothesis testing procedure was implemented to evaluate

SpO_2 among sleep stages, and the results of both tests are similar, with the p-value of 0, $\approx 10^{-37}$, to the last test. The multiple comparison *post-hoc* test points to significant differences only for N1 and N2 sleep stages, with the remaining sleep stages with intervals not disjunct.

Different types of sleep events are detected and registered in a epoch basis. They are an important tracker for sleep disorders, and they give useful information regarding sleep disruption, and which sleep events were responsible. Table 5.6 shows how the detected sleep events are related with the different sleep stages.

5.2.2 Medical Classification Groups

Table 5.4 presents the distribution of sleep positions for each medical classification group. Back (B) position is most common in the majority of the medical classification groups, changing number 1 position with left (L) sleep position in Co and Mo groups. Prone (P) position is very rare in any medical classification group.

Figure 5.16 presents 2 relationships, one is the relationship between heart rate

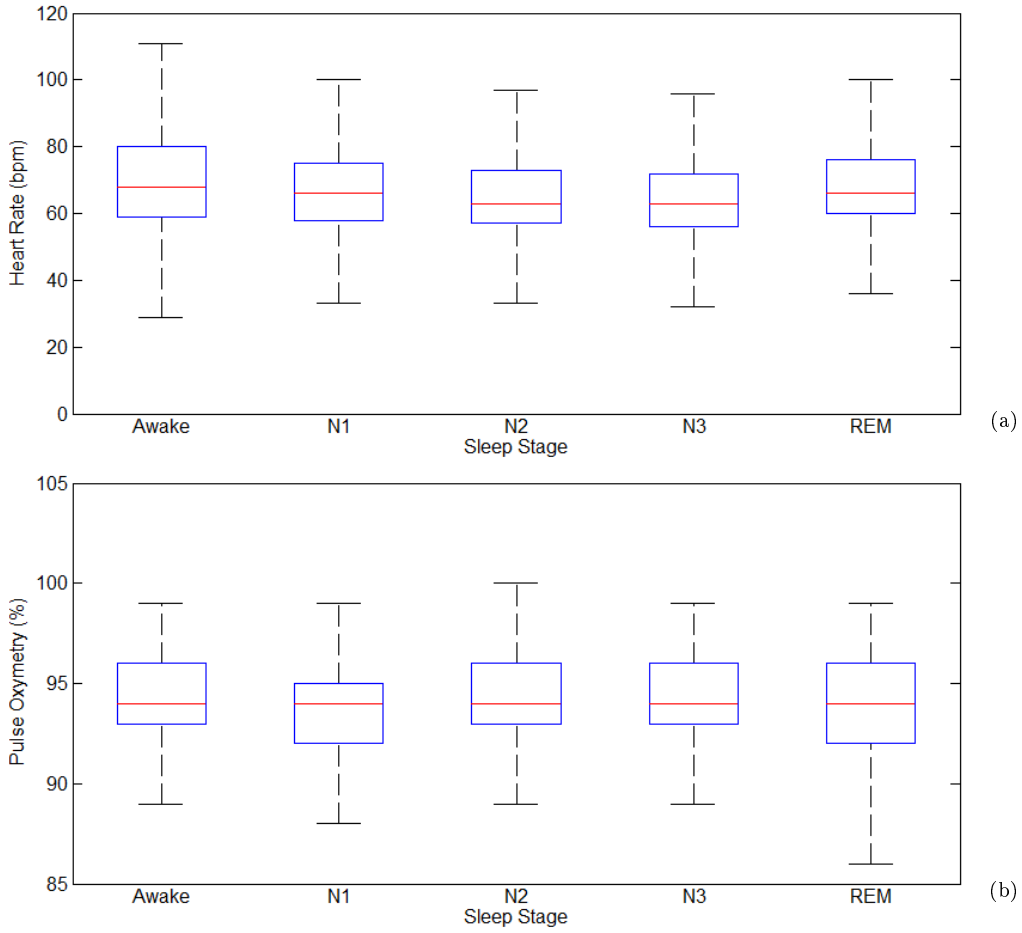

Figure 5.14: Two box plots to represent the relationship between the sleep heart rate and sleep stage (box plot a), and the oxygen saturation and the sleep stage (box plot b). Both box plots were build after removing unwanted data from the set (explained in the text). In graphic (a) and during awake stage, heart rate presents the highest values, 68 bpm in Q2 (median), decreasing in REM and N1 sleep stages, both with 66 bpm, and it achieves the lowest value, 63 bpm, in N2 and N3 sleep stage. Graphic (b) shows that pulse oximetry is not sleep stage dependent, presenting a Q2 value of 94% for all the sleep stages.

Table 5.3: The application of the Kruskal-Wallis H test (**p-value<0.01) and the post-hoc test. The mean ranks of each sleep stage and the minimum and the maximum give the intervals for analysis. All the intervals are disjunct and all the sleep stages are considered significantly different for the heart rate data.

Parameter	**Aw ****	**REM ****	**N1 ****	**N2 ****	**N3 ****
Mean Ranks	33167	31177	30014	27179	26554
Standard Error	147	196	191	123	161
Minimum	32883	30794	29643	26935	26245
Maximum	33451	31560	30385	27423	26862

Table 5.4: Distribution of the sleep positions, in percentage, accordingly with the patients' medical classification group.

Body Position	**Co (%)**	**Sn (%)**	**Mi (%)**	**Mo (%)**	**Se (%)**
L	21.2	42.7	21.8	34.7	43.4
R	26.0	17.6	31.4	14.4	17.6
P	4.2	2.1	1.3	0.2	3.6
B	48.6	37.6	45.5	50.7	35.4

and medical classification group, while the second is the relationship between pulse oximetry and medical classification groups. The influence of OSAHS in health is pretty clear in both parameters, with a consistent variation as the disorder worsens. Figure 5.16 (a) shows evidence of augmented health risks when OSAHS severity is higher, with higher Q2 heart rate values, a body response to arousals [379]. Percentile 25 (Q1) values tend to increase with the worsening of the OSAHS severity to 54, 56, 56, 63, and 62 bpm, while percentile 75 (Q3) values do not have a clear trend with values of 75, 75, 69, 76 and 82 bpm. Mean and standard deviation values for the Co, Sn, Mi, Mo and Se medical classification groups are 63.8 ± 14.8, 65.7 ± 13.1,

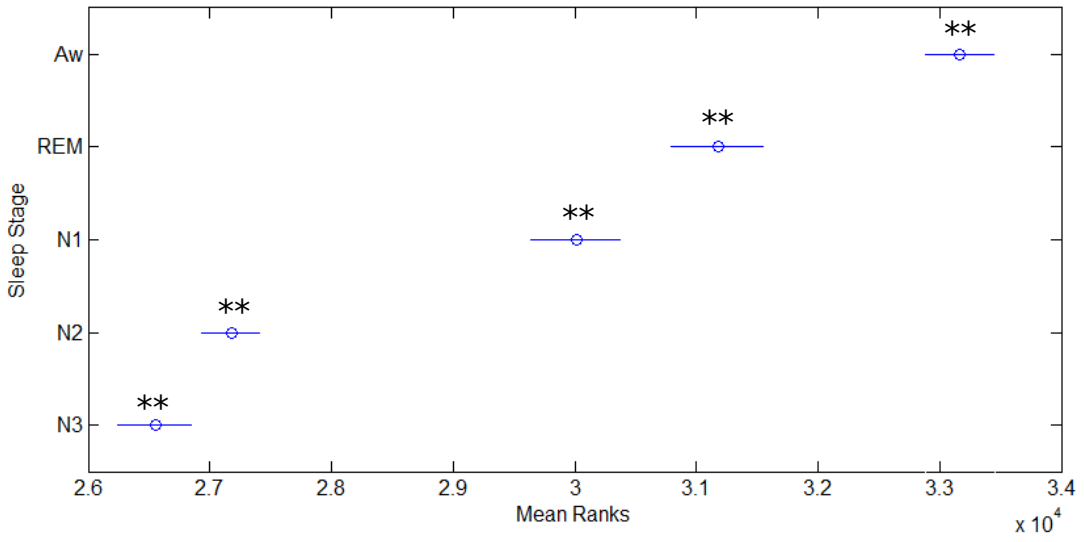

Figure 5.15: Results from the multiple comparison test to the heart rate dataset. All sleep stages have significant differences between them (**p-value<0.01), once the intervals are disjunct.

Table 5.5: The application of the Kruskal-Wallis H test (**p-value$<$0.01) and the post-hoc test. The mean ranks of each medical classification group test and the minimum and the maximum give the intervals for analysis. All the intervals are disjunct and all the medical classification groups are considered significantly different for the pulse oximetry data.

Parameter	**Co ****	**Sn ****	**Mi ****	**Mo ****	**Se ****
Mean Ranks	39220	35543	24261	20724	14861
Standard Error	187	113	163	151	199
Minimum	38857	35313	23948	20433	14472
Maximum	39583	35773	24574	21016	15250

62.4 ± 12.5, 70.5 ± 13.5 and 73.4 ± 14.3 bpm, respectively.

The behaviour of pulse oximetry registers with the worsening of the medical classification group is also interesting. Figure 5.16 (b) shows a consistently decrease in the pulse oximetry from a healthy subject, Co group, to the most severe group, Se. The mean and the standard deviation have the same pattern, with values of $95.4 \pm 2.0\%$, $95.0 \pm 1.9\%$, $93.5 \pm 2.1\%$, $92.7 \pm 2.7\%$ and $90.7 \pm 4.4\%$. Percentile 25 values are 94, 94, 93, 91 and 89 for an increase in OSAHS severity, and the percentile 75 values are 97, 96, 95, 94 and 94 (for the same order of OSAHS severity).

SpO_2 and heart rate data distribution among the medical classification groups were analysed using hypothesis testing. Both tests returned p-value=0, to both features. *Post-hoc* test results to the SpO_2 feature, available in Figure 5.17, point to significant differences among all medical classification groups once the intervals are disjunct. Table 5.5 summarizes this process. On the other hand, *post-hoc* test results to the heart rate feature point to significant differences among the Mi, Mo, and Se medical classification groups.

Patients with a higher OSAHS severity have a poor sleep quality, associated with sleep disruption caused by different types of sleep events. The interference of sleep events in the patients' sleep quality and how they relate with the patient's medical classification group is in detail in Table 5.7.

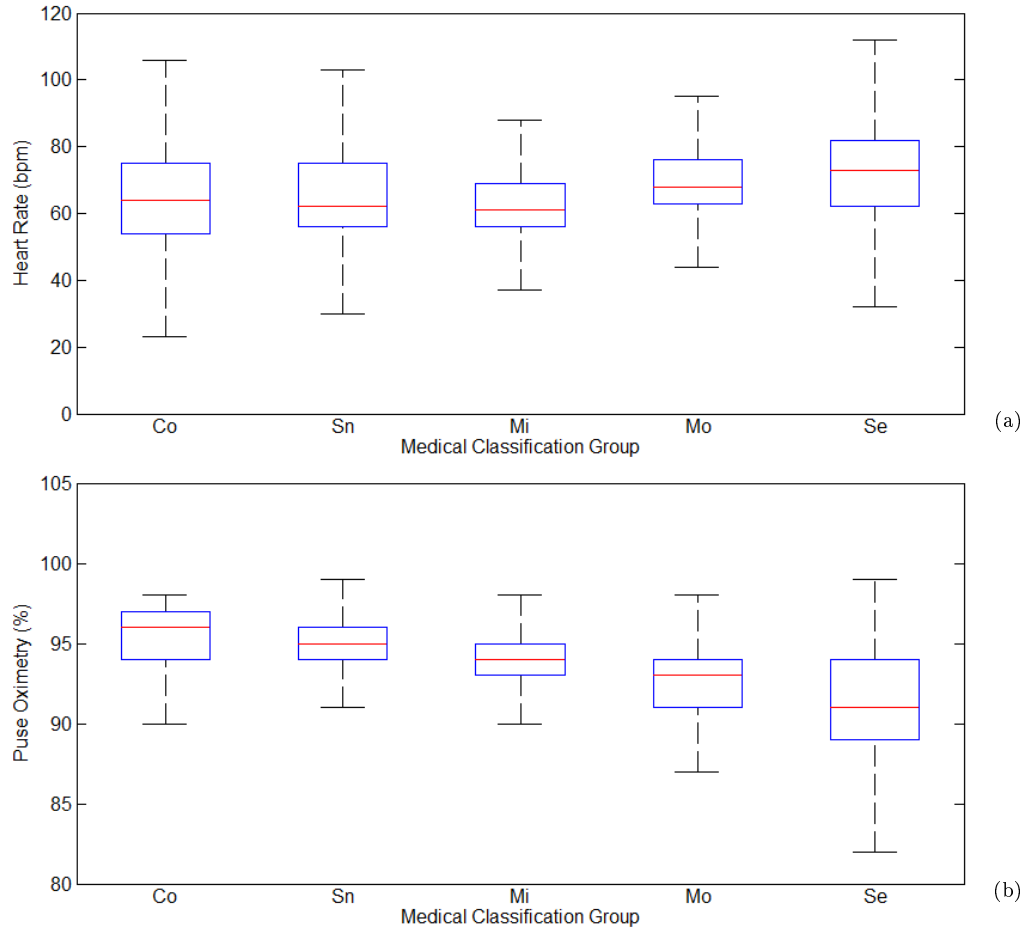

Figure 5.16: The relationship between the patients' medical classification group and two different parameters, heart rate and pulse oximetry, was plotted in a box plot. In graphic (a) is the box plot to relate heart rate and OSAHS severity. The higher the level of OSAHS severity, the higher the heart rate, with Q2 values of 61, 68 and 73 bpm for Mi, Mo and Se, respectively. Co and Sn medical classification groups have heart rates (Q2 value) of 64 and 62 bpm, respectively. In graphic (b) is the box plot to relate pulse oximetry registers and OSAHS severity. Q2 reveals a monotonically behaviour, with an inverse relationship between the O_2 saturation and the OSAHS severity. Q2 saturation levels are 96%, 95%, 94%, 93% and 91% for Co, Sn, Mi, Mo and Se, respectively.

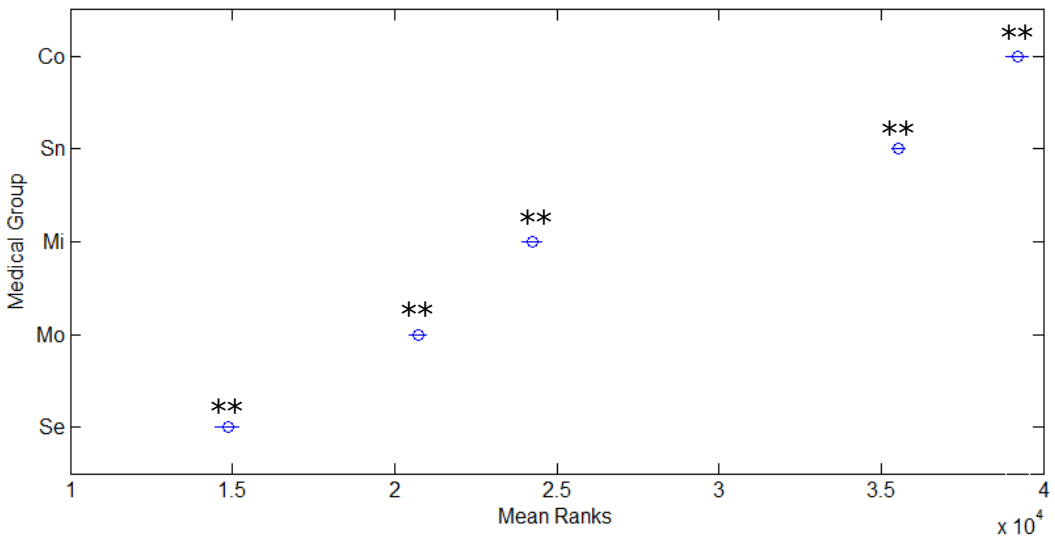

Figure 5.17: Results from the multiple comparison test to the SpO_2 dataset. All medical classification groups have significant differences between them (**p-$value$<0.01), once the intervals are disjunct.

Table 5.6: Distribution of each sleep event over the different sleep stages. The table presents data as the average number of sleep events detected per 1000 sleep stages.

Sleep Event	**Awake**	**N1**	**N2**	**N3**	**REM**
Arousal (Patient awakes between 3 to 10 seconds)	0.5	398.9	193.0	44.4	110.8
Awake (Patient awakes between 11 to 15 seconds)	0.0	75.4	26.0	7.8	25.5
Obstructive hypopnea	1.7	115.0	51.6	19.5	112.2
Periodic leg movement	0.5	41.3	60.6	87.2	5.0
RERA	0.3	55.7	41.1	5.8	20.1
Obstructive apnoea	0.2	58.3	18.4	5.9	42.2
Central apnoea	0.2	3.2	0.5	0.3	2.6
Leg movement	0.9	12.9	8.6	5.8	13.2
SpO_2 desaturation	0.3	9.7	10.1	5.2	7.5
Snore	0.0	1.5	0.8	3.2	0.4
Mixed apnoea	0.0	0.3	0.0	0.0	0.1
REM sleep disorder	0.0	0.1	0.0	0.2	0.3

Table 5.7: Distribution of each sleep event accordingly with the patient's medical classification group. The table presents data as the average number of sleep events detected per 10 patients.

Sleep Event	**Co**	**Sn**	**Mi**	**Mo**	**Se**
Arousal (Patient awakes between 3 to 10 seconds)	803.3	1209.2	900.8	1433.1	1835.0
Awake (Patient awakes between 11 to 15 seconds)	171.1	163.3	183.8	218.5	367.5
Obstructive hypopnea	16.7	100.4	259.2	856.2	1563.8
Periodic leg movement	183.3	498.8	347.7	262.3	417.5
RERA	16.7	136.3	269.2	366.2	335.0
Obstructive apnoea	0.0	27.1	86.2	120.8	1068.8
Central apnoea	5.6	15.0	6.2	5.4	3.8
Leg movement	57.8	57.9	67.7	88.5	56.3
SpO_2 desaturation	5.6	24.6	30.8	20.8	320.0
Snore	0.0	22.9	7.7	0.8	0.0
Mixed apnoea	0.0	0.4	0.0	0.0	2.5
REM sleep disorder	0.0	2.1	0.0	0.0	0.0

5.3 High-Quality Sound Energy and Filtering

The characteristics associated with energy, in signal processing and using Equation 4.3, include the calculation of an array of non-negative values and an increased highlight, from the baseline, of higher values. To finish the energy calculation for a single file, the algorithm only takes less than 120 s to complete the task. The outcome from the energy calculation, for a single patient, is in Figure 5.18. The sound activity was not homogeneous, which means the patient did not snore the entire night.

Figure 5.19 is a single patient 5 min segment from a high-quality sound acquisition file and its energy. Quiet regions have lower energy values, which is visible, especially, in the second half of the figure, while snores are more common and with higher amplitudes in the first half. Energy calculation was performed for regions of 0.1 s, without overlapping, which meant that snore amplitude and duration were both crucial to highlight it from the energy's baseline. Effects of the energy equation are visible, with sounds in the quiet region with less relative amplitude, approaching, visually, from a flat line.

Raw energy arrays have countless peaks of energy, most of them are noise, with Figure 5.20 being an example of how both filters worked together in a 5-minute window. A 1-minute window, with increased detail over each energy peak, is available in Figure 5.21. In general, the filters attenuated the energy array amplitude, smoothing it and decreasing future workload by eliminating some of the existing energy peaks.

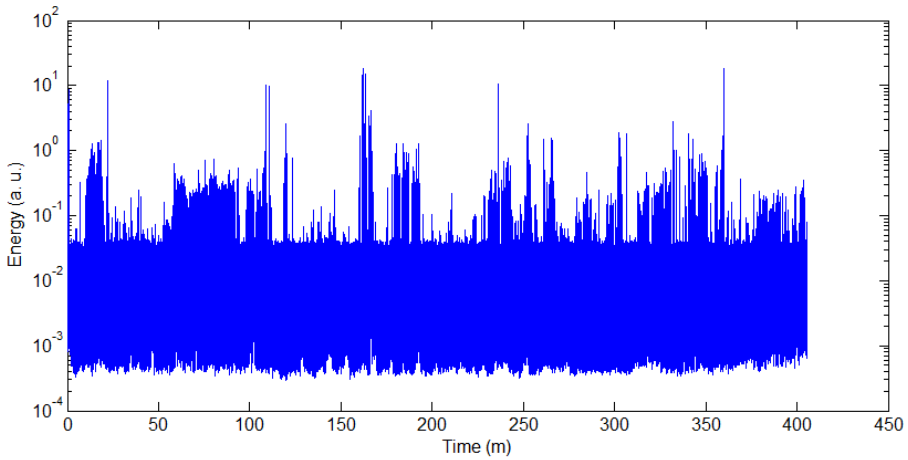

Figure 5.18: Representation of the entire energy array of a single patient, with visible regions of higher sound activity.

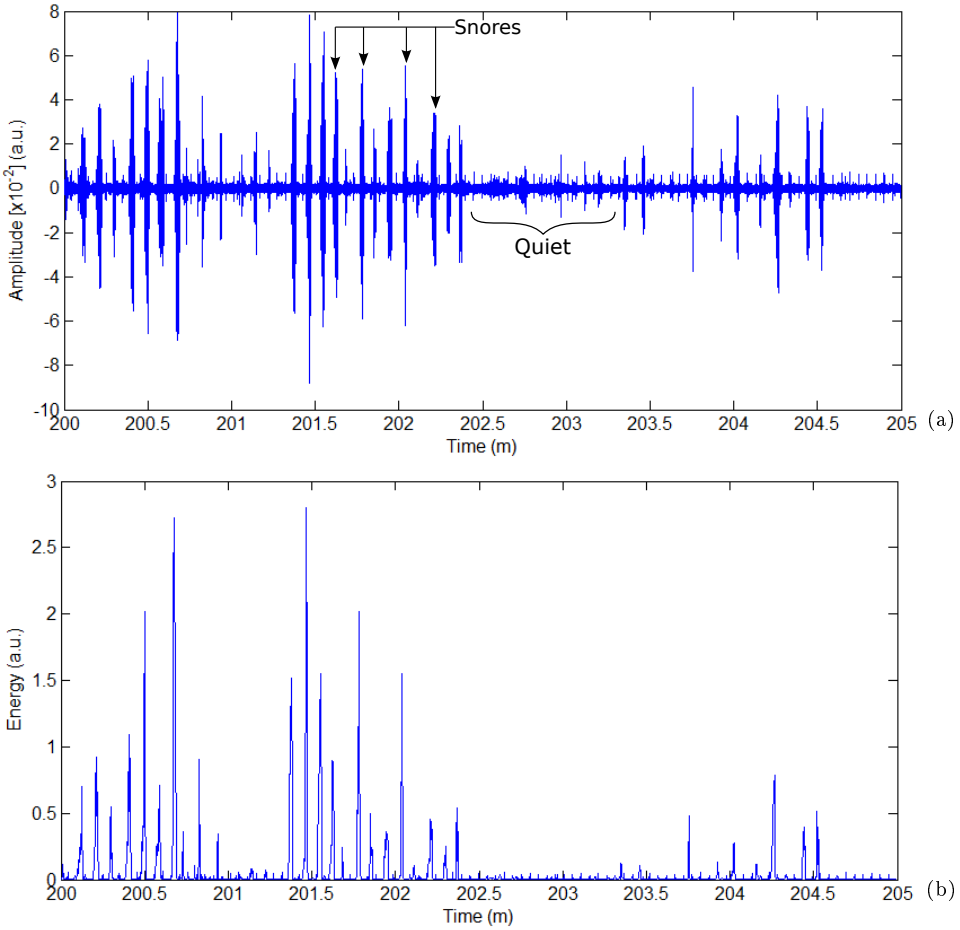

Figure 5.19: A 5 minute segment of a patient's sound record session, starting at minute 200 and ending at minute 205. The upper figure, (a), is the representation of the high-quality acquired sound, in raw, while the lower figure, (b), is the result of the energy calculation for the same time span. Some snores were identified as "Snores" in Figure (a) to give be given as examples, while a area without snores is identified as "Quiet" [332].

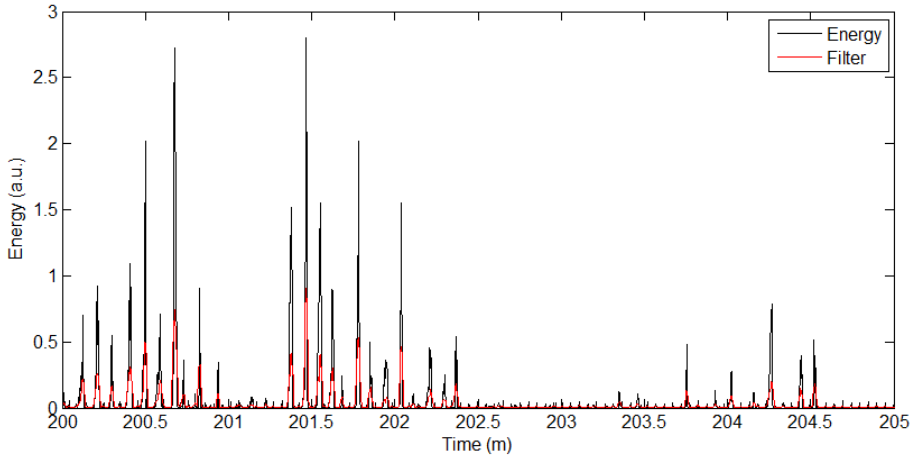

Figure 5.20: Data from a 5 minute segment of a single patient. The raw energy, in black, was filtered by a low-pass and a high-pass filter. The filtering process returned a filtered energy array, in red, with less and smoother peaks.

5.4 Gaussian Fit

The filtered energy time series was windowing in 4 s windows, with 3.5 s overlapping, to be modeled by a Gaussian function. The final result was an array of energy peaks candidates to be identified as the patient's snores. All the plots in Figure 5.22 and in Figure 5.23 came from the same patient. There are a total of 29 plots to exemplify how modeling the energy time series worked. They are chronologically ordered from top to down and from left to the right, with the first 15 plots in the first figure.

Although not quantified, energy modeling can filter and eliminate some local maxima, which could be misunderstood as energy peaks. In Figure 5.22, both energy peaks have, each one, 2 local maxima, but the Gaussian fit "see" just both energy peaks, eliminating 2 potential candidates to energy peaks, and consequentially, to snores. The transition between energy peaks is clear in both figures, Figure 5.22 and Figure 5.23. When no energy peak exists in the selected window, the modeled Gaussian function has its maximum outside that window, which is the exclusion criterion for the presence of an energy peak.

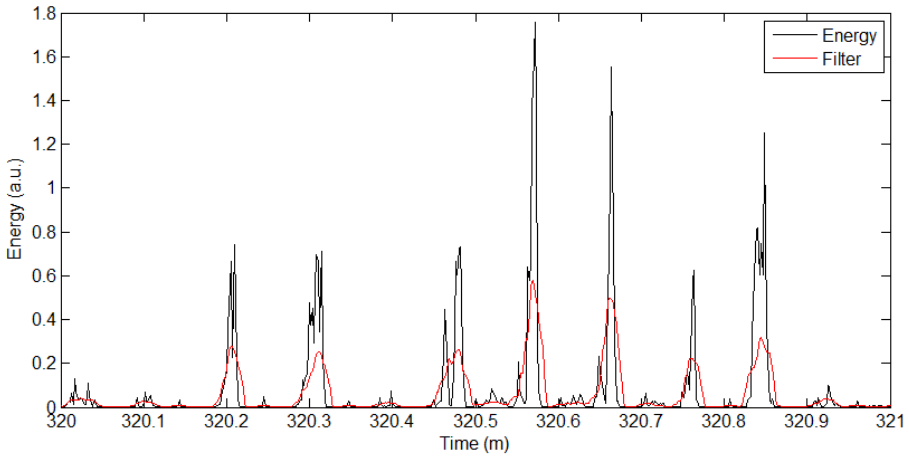

Figure 5.21: Data from a 1 minute segment of a single patient. The results achieved with the filtering process are clear. Filters decreased the number of peaks and energy fluctuations are smoother.

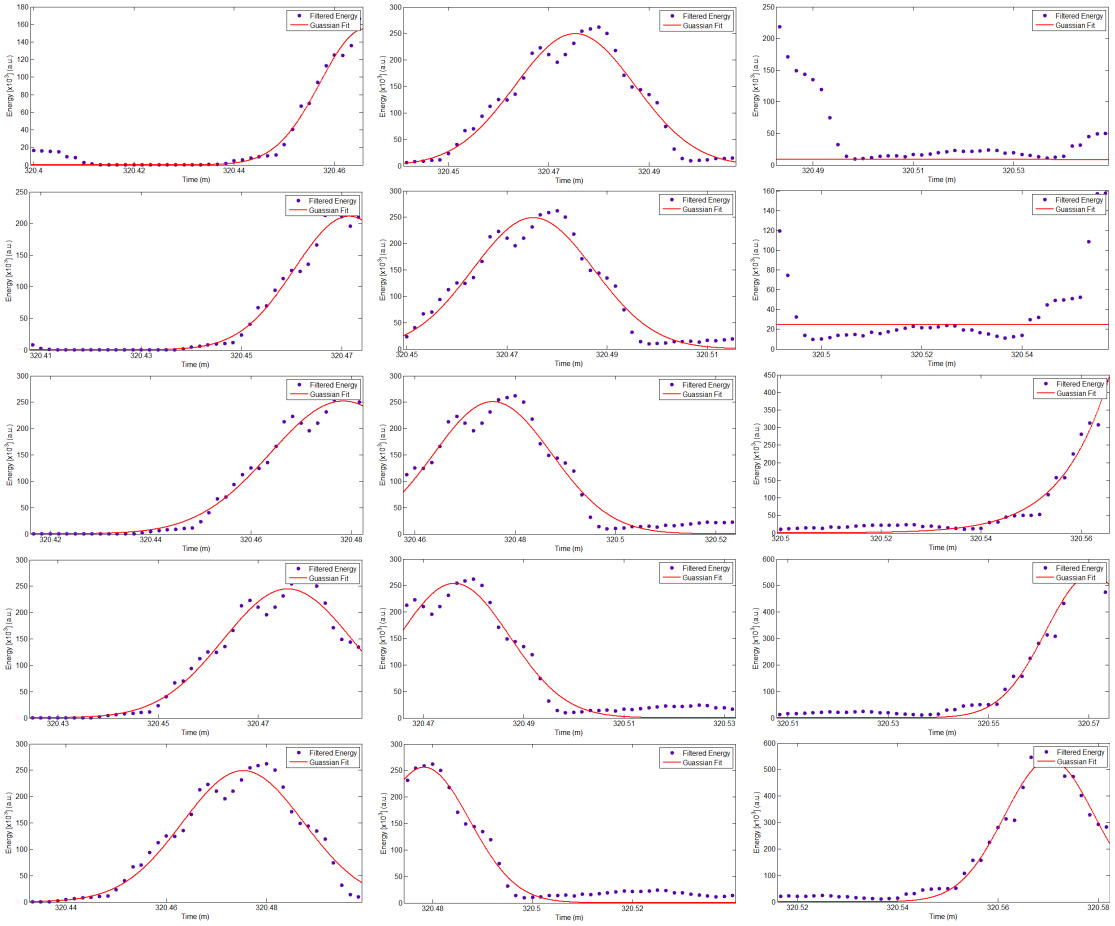

Figure 5.22: The achieved result for the application of a Gaussian function to model the filtered energy time series. This set of 15 images is the first, of 2 (the other is in Figure 5.23), and it gives an example of how modelling works for 2 energy peaks, 1 of them shared with the second figure. Original filtered energy time series was windowing with 4 s window and overlapping of 3.5 s. The algorithm is capable of detecting 2 different energy peaks because between them there is a windows where the maximum of the Gaussian function is outside that windows. The chronological order is top to down and then left to right.

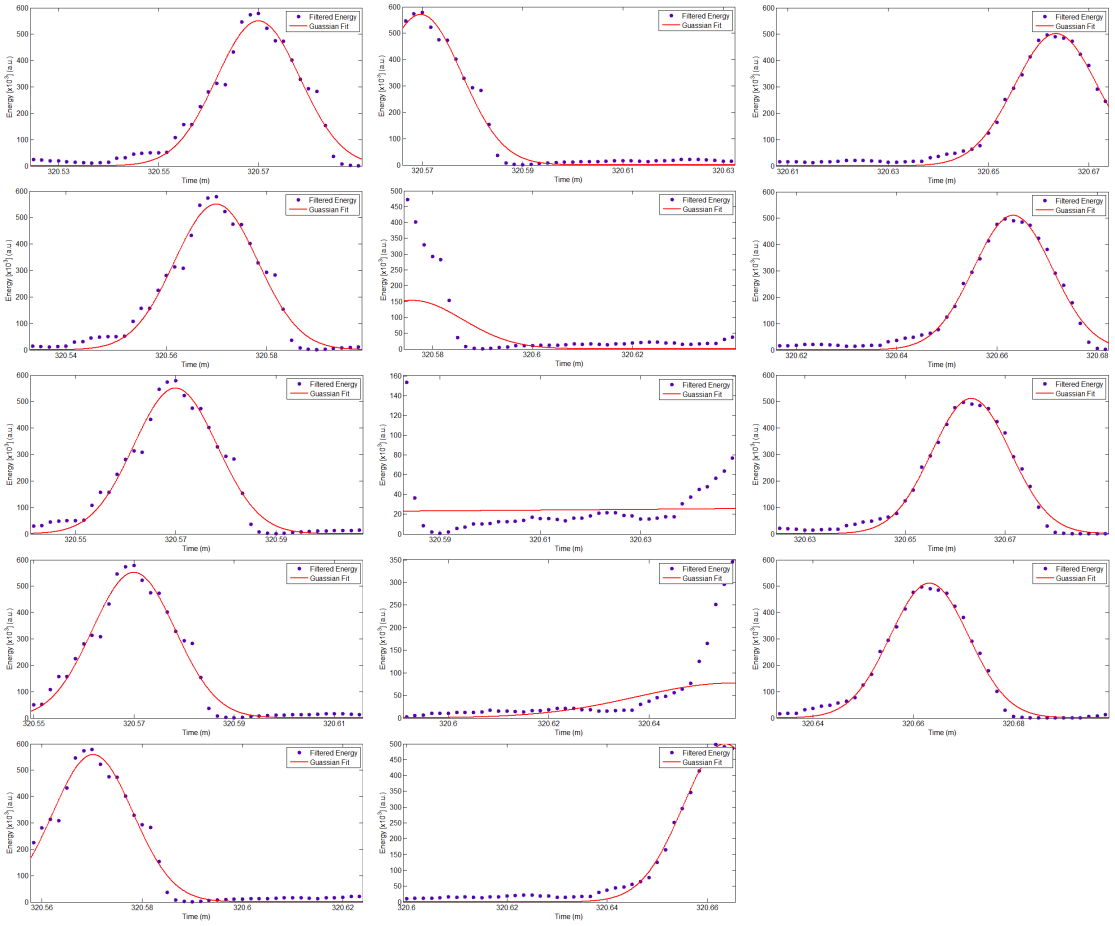

Figure 5.23: The second part, the first part is in Figure 5.22, of modelling the filtered energy. With filtered energy windowing in a 4 s length and overlapping of 3.5 s, the transition from one energy peak to the following one is visible. At that point, the Gaussian function has its maximum outside the window. The chronological order is, also, top to down and then left to right.

5.5 Sound Events Filtering

Detection of energy peaks, by modeling data with a Gaussian function, returns an array of candidates to be identified as snores. The first exclusion criterion was already implemented by the modeling method itself, but more events were filtered by using other criteria. The different exclusion criteria decrease the number of energy peaks, at the end of the modeling process, from 507904 to 51458, the number of snores sounds. This automatic process had a confirmation rate, of energy peaks being snore sounds, of 10.1%. Table 5.8 summarizes the number of energy peaks identified by the modeling process, and which ones were selected as snore sounds, splitting data by patients' medical classification group. The confirmation rate, the percentage of peak energy confirmed as snore sounds, is also available.

The filtering process for detected peaks of energy started with the rejection of peaks of energy due to electronic noise. Figure 5.24 shows the impact of the electronic noise in sound acquisition. There is an example of this type of noise in Figure 5.24 (a), revealing a periodic behaviour associated with the electronic interference of 3.1 s, Figure 5.24 (d). Figure 5.24 (b) has a more detailed profile of a single electronic interference. Data in Figure 5.24 (a) was used to do energy calculation and the result is available in Figure 5.24 (c), with the electronic interference energy emerging from the energy baseline, leading to its detection by the Gaussian fit model.

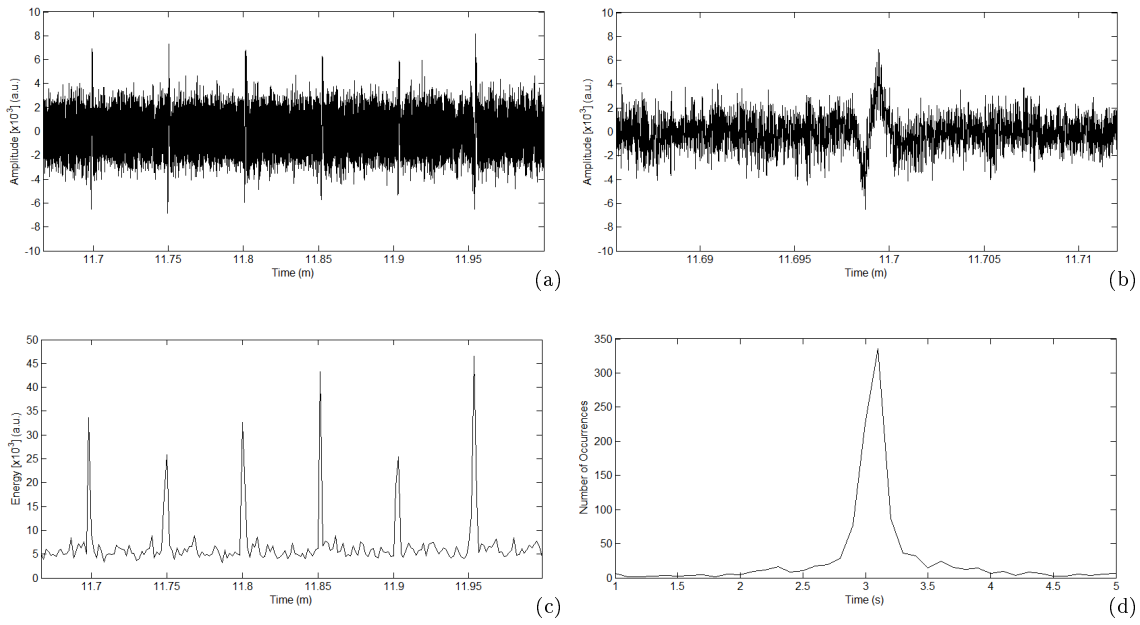

Figure 5.24: Electronic noise in sound acquisition. The noise occurs periodically as visible in the example in (a). A more accurate profile form this type of noise is available in (b). The impact of this electronic interference in the detection of energy peaks is visible in (c), with its energy higher than the surrounding baseline. Distribution of time differences between consecutive peaks of energy was calculated and plotted in (d). Electronic interference periodicity was calculated with a result of 3.1 s.

Table 5.8: This table presents the number of energy peaks detected when modelling the filtered energy data series with a Gaussian function. It also presents the number of snores and the percentage of accepted energy peaks as snores. All data is organized accordingly with the patient's medical classification group.

	Co	**Sn**	**Mi**	**Mo**	**Se**
# Peaks Of Energy	71004	185368	97361	96268	57903
# Snores	1022	12117	10331	14680	13308
Confirmation Rate (%)	1.4	6.5	10.6	15.2	23.0

Table 5.9: Thresholds mean values for each medical classification group. The first line of threshold data is the mean hard threshold to reject electronic noise using the peak of energy. The second line has the mean hard threshold to evaluate peaks of energy below the previous threshold, by analysing the cumulative energy of each peak.

Energy [$\times 10^{-3}$]	**Co**	**Sn**	**Mi**	**Mo**	**Se**
Peak	114	109	114	111	112
Cumulative	298	291	421	292	291

The algorithm to reject noise, with electronic interference origin, used a hard amplitude threshold, and each patient had its threshold, calculated from its sound data. All peaks of energy detected above that threshold were not rejected, but those below were not rejected only if the cumulative energy of the peak was above a second hard threshold. Figure 5.25 is an example for the electronic interference noise rejection. Table 5.9 has the mean values of both thresholds, organized by the medical classification group of each patient. The mean values of both thresholds, amplitude and cumulative, calculated for all the patients are 111 and 318 a. u., respectively. Figure 5.26 shows examples of peaks rejected by the sound event proximity filter.

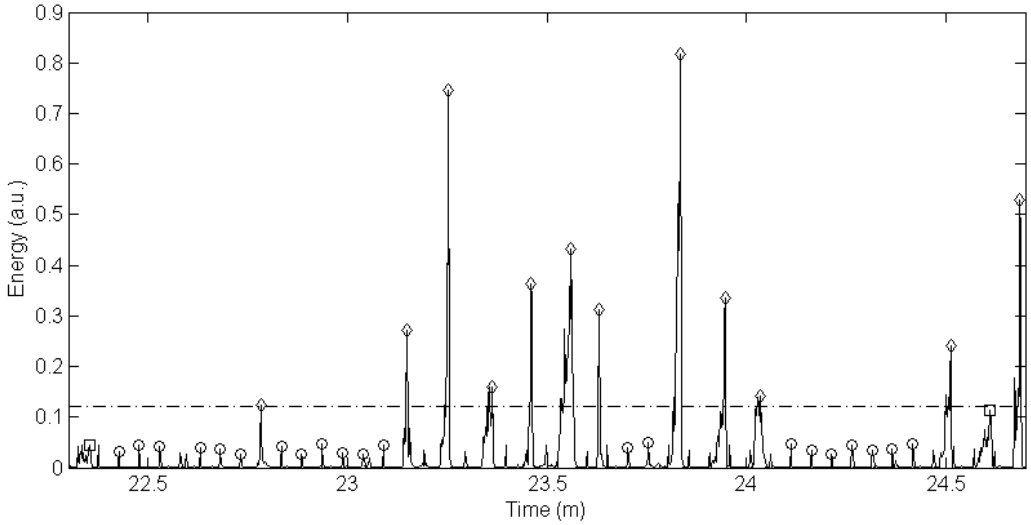

Figure 5.25: The first rejection step after the detection of peaks of energy using the Gaussian fit. All symbols, ◇, □ and ○, represent a candidate to a snore sound. The presence of electronic noise is real and a hard threshold, dash dot horizontal line, defines the limit to eliminate electronic noise. Peaks of energy above the defined threshold, ◇, are not rejected, while the symbol ○ represents those peaks below and rejected. The third symbol, □, represents peaks of energy not rejected, despite below the threshold, due to their cumulative energy.

Table 5.10: Analysis of the snore detection algorithm performance from a sample of 5 min of each patient. The sensitivity, the specificity, the PPV and the NPV were the statistical measurements calculated. The performance was compared using the Bellauer's algorithm.

Algorithm	Sensitivity	Specificity	PPV	NPV
Project	88.1	97.5	97.4	88.5
Bellauer	78.7	94.3	93.6	80.5

Table 5.11: Analysis of the snore detection algorithm performance by medical classification group, and compared with the Bellauer's algorithm. The used statistical tools were the sensitivity, the specificity, the PPV and the NPV.

Medical Group	Algorithm	Sensitivity	Specificity	PPV	NPV
Co	Project	94.5	96.9	82.9	99.1
	Bellauer	87.5	97.4	84.2	98.0
Sn	Project	87.2	95.6	95.1	88.5
	Bellauer	73.9	96.1	94.9	79.1
Mi	Project	74.8	99.3	99.3	74.4
	Bellauer	71.1	99.1	99.1	71.8
Mo	Project	93.9	99.5	99.8	87.8
	Bellauer	78.9	94.4	96.9	66.4
Se	Project	97.9	100.0	100.0	96.7
	Bellauer	98.3	70.9	84.4	96.3

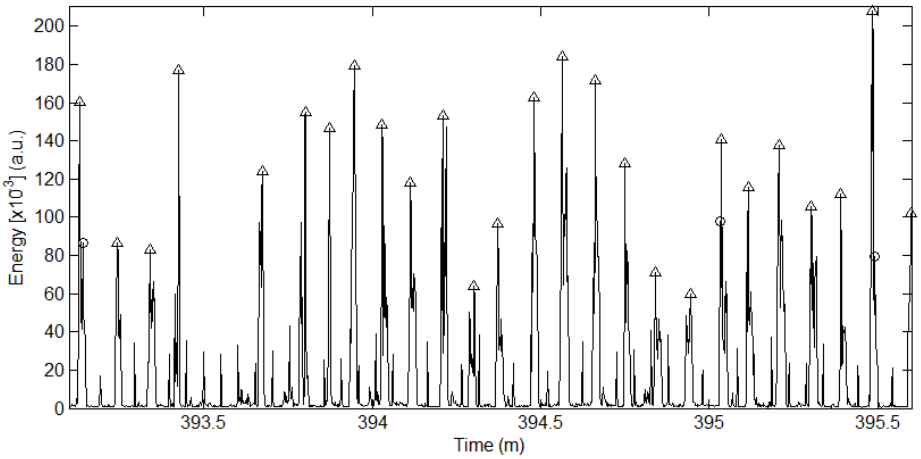

Figure 5.26: Rejection of peaks of energy based in proximity. In this figure, the energy time series is plotted together with the remaining detected peaks of energy. The implementation of the proximity criterion rejected 3 peaks, one at the beginning and one at the end of the figure. Another rejected peak is, also, close to the end of the figure. Symbol △ represents peaks of energy not rejected by the proximity criterion, while the symbol ○ represents those peaks rejected.

The performance of the thesis's algorithm for the snores' detection and noises' rejection was evaluated against the well know Bellauer's algorithm, using the TP, FP, FN, and TN data. Table 5.10 and Table 5.11 summarize the results for both algorithms' performance, using the parameters sensibility, specificity, PPV, and NPV. The first table presents overall results, with the project's algorithm performing better in all parameters under analysis. The second table groups patients by their medical classification group, with the project's algorithm performing better in the majority of the scenarios. The Bellauer's algorithm performed better in 4 scenarios, in the detection of snores in the Se group, in the rejection of noise in Co and Sn groups, and how the algorithm performs when it identifies a snore in the Co group. The difference in those 4 scenarios is small, reaching a maximum of 1.3% in the last one, opposite to the other scenarios, where the maximum difference is 29.1% in the rejection of noise in the Se group.

A hypothesis testing was implemented to analyse the achieved global results for the sensitivity and specificity, using the mid-p-value definition of McNemar's test. A 2x2 matrix was built with the total number of snores detected, by both methods (a), only by the project's method (b), only by the Bellauer's algorithm (c), and not detected by neither one (d). An analogous second matrix was built to analyse specificity (rejection of noise). The mid-p-value definition of the test returned a p-value≈0 for sensibility and a p-value≈0 for the specificity, which means the rejection of the null hypothesis, confidence level (α) of 5%, in both cases.

5.6 High-Quality Sound Distribution

Data of the high-quality sound acquisition device show a deviation from the expected 0 means value μ. A single patient data distribution is represented in Figure 5.27, with a minimal deviation ($\mu = -1$). The complete list has 48 patients with this minimal deviation, 15 and 2 patients, respectively, with a deviation of -2 and -3. There are greater deviations, of -6 and -13, each one with just 1 patient. The deviations are small and no actions were implemented to correct this shift.

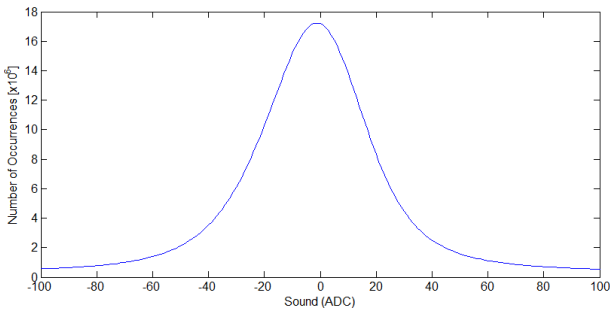

Figure 5.27: Probability density function of a single sound file. All sound file samples were used to calculate the distribution, ranging from -32768 to 32767.

5.7 Data Synchronization

5.7.1 Pause Resume Sequences Detection in PSG Studies

Manual registration of the pause resume sequences in the PSG studies was the responsibility of both sleep technicians and researchers, and Table 5.12 reports all the sequences, handwritten. Accordingly, with the same table, most of the PSG studies have continuous data acquisition, without pauses, and only 15 out of the 67 studies, 22.4%, of them were paused. The maximum number of pauses resume sequences registered for a single PSG was 2, with 6.0% of the PSG studies in this situation.

Lack of confidence in the first method led to the rejection of the manual registration and an automatic algorithm was developed to search for pause resume sequences using data from a single sensor, integrated into the PSG study, the SpO_2 channel. The results for the second algorithm are available in Table 5.13 and in Table 5.14. The first table reports all sequences correctly identified, while the second table reports all sequences misidentified. To perform synchronization, the start of data acquisition in the PSG study, t = 0s, is important, but not taken into account in the current analysis. The analysis of the algorithm's performance points to a total number of 35 PSG studies, 52.3%, with pause resume sequences. Of the 35 studies, 21 studies had a single pause, 10 studies had 2 pauses, 3 studies had 3 pauses and 1 study had 5 pauses, corresponding to 31.3%, 14.9%, 4.5% and 1.5% of the total number of studies, respectively. Figure 5.28 is an example of a sequence properly detected using solely the SpO_2 channel.

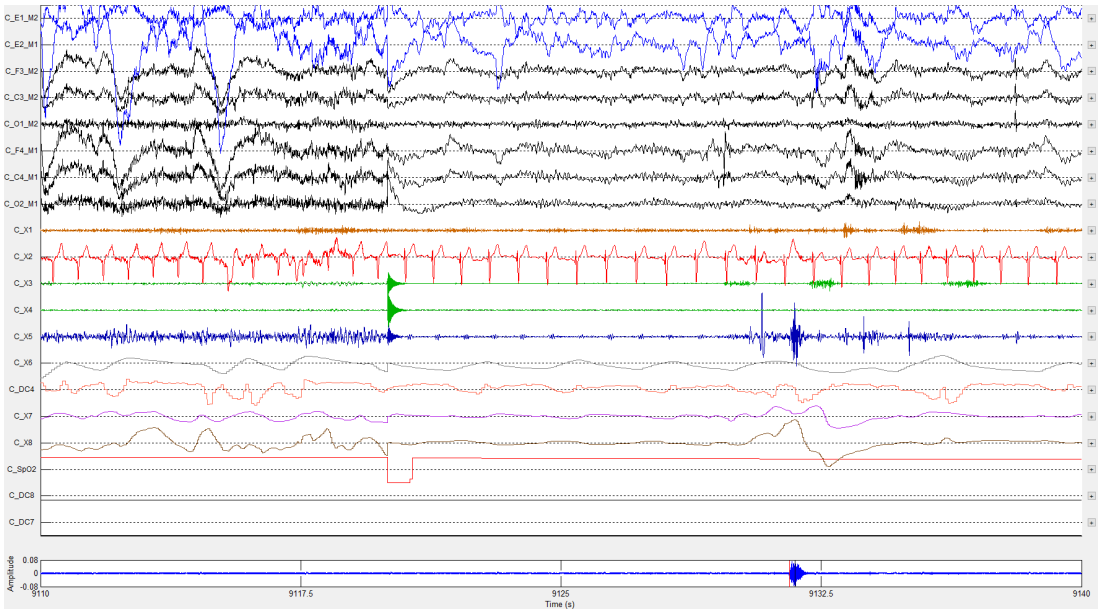

Figure 5.28: A typical TP in the identification of a pause resume sequence. It is located at t=9120 s and it shows the moment at which SpO_2, third channel from down to top, data drops to 0 value. Other channels observation confirms, at the same time instant, the pause resume sequence by observing data discontinuities in several channels.

Although not desired, the algorithm also detected FPs pause resume sequences in 10 studies, 14.9%, and all but 1 with just a single misidentification. Patient ID 90 was a particular case where the algorithm did not work so well, wrongly identifying 5 pause resume sequences. Figure 5.29 is an example associated with a misidentification of a pause resume sequence, and all the cases of FPs have a profile similar to this example.

5.7.2 Coarse Data Synchronization

The synchronization of a PSG cluster, a continuous acquisition process between 2 of the possible events: the beginning or the end of data acquisition, or pause resume sequences, with the high-quality sound signal used the cross-correlation mathematical tool and results are available at Table 5.15. In order to know if all clusters were properly synchronized, each cluster synchronization was evaluated, the necessary corrections to the synchronization were made and the resume is available in Table 5.16. Figure 5.30 shows the relationship between the automatic synchronization and the final synchronization of PSG study and the high-quality sound signal data. The existence of a predominance relationship between both synchronization of the type $y = x$ denotes a correct automatic synchronization, but, nevertheless, some synchronizations perform below the expectation. Most of them belong to the Sn group, a counter-intuitive result, but partially explained by the uneven patient distribution in each medical classification group. Sn group has almost the double of patients of the following groups, Mi and Mo.

The snore detection algorithm searched for snores in the high-quality sound

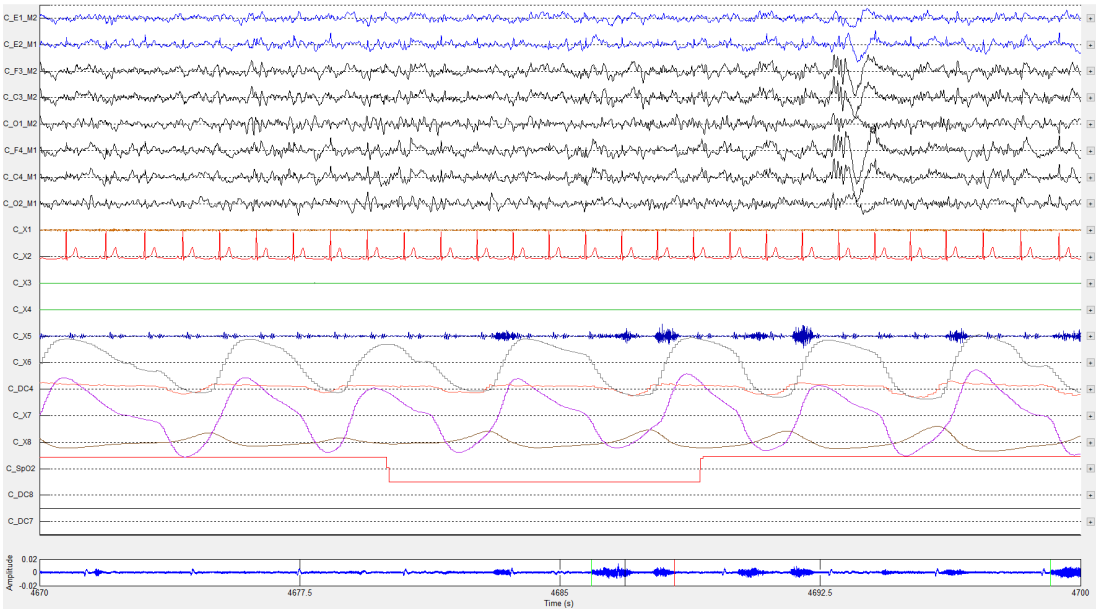

Figure 5.29: A typical FP in the identification of a pause resume sequence. The FP is at time instant 4680 s and it shows the moment at which SpO_2 data drops to 0 value. The observation of the other data at the same time instant do not show any data discontinuity, expected in real pause resume sequences.

Table 5.12: Handwritten annotation, by either a sleep technician or the researcher, of the time at which occurred the PSG studies pause resume sequences. Subjects are referred by their ID.

ID	Pauses	ID	Pauses	ID	Pauses	ID	Pauses
49	-	80	23h56m	103	-	127	-
50	-	81	-	104	01h29m and 02h59m	129	00h43m
51	02h24m	83	01h52m	105	-	130	-
52	05h43m	84	-	106	-	133	-
54	04h20m	86	-	107	-	134	-
57	-	87	03h27m	109	03h28m	136	-
58	-	89	04h25m	110	-	137	-
61	03h04m	90	-	112	-	138	-
63	-	91	-	113	-	139	-
64	-	92	-	114	-	141	-
67	-	94	-	115	-	142	-
68	-	96	-	116	-	143	-
70	-	97	-	118	-	144	-
73	01h01m and 01h48m	99	-	119	-	145	02h35m and 06h12m
77	-	100	-	120	-	146	-
78	01h14m and 03h47m	101	-	125	-	147	05h18m
79	-	102	-	126	-		

signal data, but also it searched for snores in the PSG data. The number of snores, Sn_n, detected belonging to each cluster is available in Table 5.17 and the respective time duration, t_d, of the clusters is available in Table 5.18. We can define the snore density, Sn_d, for each cluster as in Function 5.1, and snore density results are available in Table 5.19, in number of snores per hour.

$$Sn_d = \frac{Sn_n}{(t_d/60)} \tag{5.1}$$

Table 5.13: Results for the performance of the algorithm in the detection of the PSG study pause resume sequences. It made use of a single PSG sensor, the SpO_2, and this table identifies the sequences correctly detected. The table reports the time, number of minutes after starting data acquisition, at which the pauses were detected. Time t = 0 min is, also, a time instant for the beginning of data acquisition, the first, and present in all data files. Its inevitability presence does not require the algorithm to detect it, sparing some computational effort. Subjects are referred by their ID.

ID	**Time (min)**	**ID**	**Time (min)**	**ID**	**Time (min)**	**ID**	**Time (min)**
49	1.5, 27, 115, 152 and 168	80	14	103	63.5	127	-
50	288	81	-	104	134, 219.5 and 449	129	10
51	1.5 and 195.5	83	153	105	-	130	127.5
52	1.5 and 391.5	84	0.5 and 26.5	106	63	133	-
54	315	86	3	107	-	134	-
57	1.5	87	61 and 290	109	209	136	-
58	1	89	284.5	110	-	137	2.5
61	166	90	-	112	-	138	4.5, 94 and 101
63	-	91	-	113	6.5	139	-
64	-	92	-	114	-	141	5
67	-	94	-	115	1.5 and 96	142	-
68	-	96	-	116	2 and 260.5	143	-
70	6 and 7	97	-	118	-	144	-
73	17.5 and 63.5	99	-	119	-	145	153.5, 255 and 359
77	-	100	-	120	406.5	146	301.5
78	107.5 and 254	101	-	125	223	147	3 and 325
79	55	102	-	126	-		

Table 5.14: Results for the performance of the algorithm in the detection of the PSG study pause resume sequences. It made use of a single PSG sensor, the SpO_2, and this table identifies the sequences wrongly detected. The table reports the time, number of minutes after starting data acquisition, at which the pauses were detected. Subjects are referred by their ID.

ID	Time (min)	ID	Time (min)	ID	Time (min)	ID	Time (min)
49	-	80	-	103	240	127	-
50	-	81	-	104	-	129	-
51	-	83	-	105	-	130	-
52	-	84	-	106	69.5	133	-
54	118	86	-	107	-	134	-
57	349	87	-	109	362	136	-
58	-	89	-	110	-	137	39
61	-	90	40, 78, 88, 91 and 234.5	112	-	138	-
63	-	91	21.5	113	-	139	-
64	-	92	-	114	-	141	-
67	-	94	-	115	282	142	-
68	-	96	-	116	-	143	-
70	-	97	-	118	-	144	-
73	-	99	-	119	-	145	-
77	-	100	-	120	-	146	-
78	288	101	-	125	-	147	-
79	-	102	-	126	-		

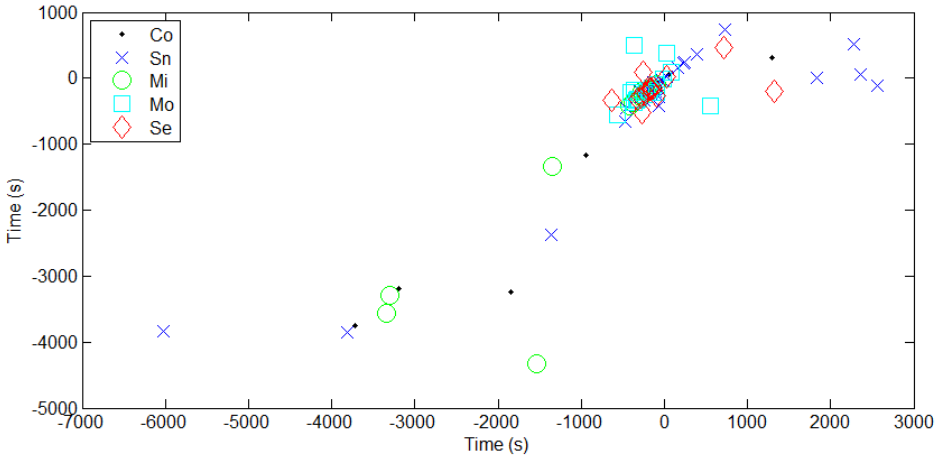

Figure 5.30: Results from the automatic synchronization between PSG and H4n data compared with the final synchronization. In the independent axis, the representation of time for automatic synchronization, while in the dependent axis, the representation of time is for automatic synchronization, but with manual adjustment. The medical classification group with more synchronizations out of the equation $y = x$ was the Sn group.

Table 5.15: Results for the automatic synchronization between PSG and high-quality sound signal data, with cross-correlation applied to all the sound energy data series clusters. Negative values means that high-quality sound signal were delayed related to PSG, discarding PSG data. Positive values means that high-quality sound signal were ahead related to PSG, discarding sound signal data.

ID	Time (s)	ID	Time (s)	ID	Time (s)	ID	Time (s)
49	-107.9, -21.9, 227.7, 393.5 and 2284.6	80	-64.1 and 2555.9	103	-6024.3	127	-56.2
50	-241 and -127	81	-290.8	104	-311.7, -92 and 85.6	129	-86.3 and 1325.1
51	-254 and 1831	83	-94.4 and 31.5	105	-139.8	130	-149.4 and 161.1
52	-213.2 and -138.3	84	-109.6 and -97.7	106	-3806.5	133	-277.8
54	-361.2 and -360.7	86	-232.9	107	-3337	134	-276.9
57	-142	87	-3716.1 and -1846.7	109	-280.3 and -163.5	136	-80.1
58	-89.5	89	-241.5 and 2355.9	110	-156.7	137	-227.3
61	-220.4 and 30.4	90	-1339.7	112	-335	138	-324.8, -248.2 and 709.7
63	-210.7	91	-185.4	113	-411.4	139	-1538.9
64	-219.3	92	-270	114	-70.9	141	-637.1
67	-473.6	94	-229	115	-140 and -130.8	142	-147.6
68	-248.6	96	-80.6	116	-356.5 and -7.3	143	-1356.1
70	-456	97	-944.8	118	-401.8	144	-3197.2
73	-180.3, -158 and 25.9	99	-185.6	119	-317.8	145	-255.8, -49.7, 59.8 and 1294.9
77	-177.1	100	-375.1	120	-152.2 and -149.9	146	-560.2 and -552.3
78	-309.9, 245.2 and 734.3	101	-173.1	125	-279.4 and -237.1	147	-240.7 and -149.3
79	-3298.6	102	-262.3	126	-265.7		

Table 5.16: Results for the automatic synchronization between PSG and high-quality sound signal data, with cross-correlation applied to all the sound energy data series clusters. Negative values means that high-quality sound signal were delayed related to PSG, discarding PSG data. Positive values means that high-quality sound signal were ahead related to PSG, discarding sound signal data. After automatic synchronization, manual synchronization was performed to improve final results. Patient ID 120 has 2 synchronizations but both have the same value. After the last pause resume sequence, the amount of high-quality sound data was low, less than 104 s, and it was decided to keep the same synch value.

ID	Time (s)	ID	Time (s)	ID	Time (s)	ID	Time (s)
49	-107.9, -21.8, 227.7, 357 and 524	80	-411.6 and -121.5	103	-3842	127	-132.6
50	-329.7 and -126.9	81	-222	104	-311.7, -91.9 and 85.7	129	-263.1 and -194.3
51	-254 and 9.5	83	-222.6 and 385.3	105	-139.6	130	-149.3 and 161.1
52	-150.2 and -65.1	84	-193.2 and -89.1	106	-3851.8	133	-122.1
54	-364.8 and 492.7	86	-209.6	107	-3571.4	134	-276.9
57	-142	87	-3754.6 and -3240.5	109	-280.4 and -163.5	136	-113
58	-89.3	89	-228.6 and 62.5	110	-151.4	137	-227.1
61	-220.3 and 30.6	90	-1339.6	112	-334.9	138	-324.7, 83.4 and 469.2
63	-210.8	91	-185.4	113	-411.2	139	-4329.4
64	-192.1	92	-518.3	114	-277.2	141	-341.6
67	-660.6	94	-229.1	115	-195.8 and -144.6	142	-147.8
68	-251.4	96	-143.8	116	-189.6 and -7.2	143	-2375
70	-457.3	97	-1160.8	118	-219.5	144	-3197.4
73	-169, -158 and 25.8	99	-181.7	119	-317.5	145	-255.9, -49.8, 63.7 and 304.3
77	-177	100	-374.7	120	-150.9 and -150.9	146	-560.2 and -418.6
78	-183.9, 245.2 and 734.3	101	-173	125	-279.2 and -237.1	147	-240.8 and -149.3
79	-3298.7	102	-261.9	126	-197.7		

Table 5.17: Number of snores present in each patients' cluster. Subjects are referred by their ID.

ID	Snores	ID	Snores	ID	Snores	ID	Snores
49	5, 314, 62, 3 and 668	80	3 and 1864	103	87	127	18
50	14 and 3	81	14	104	775, 81 and 1252	129	1 and 927
51	6 and 2	83	36 and 680	105	1819	130	11 and 55
52	228 and 0	84	8 and 11	106	34	133	8
54	232 and 10	86	106	107	376	134	1439
57	582	87	97 and 29	109	465 and 354	136	3
58	249	89	136 and 242	110	2	137	3465
61	364 and 302	90	83	112	107	138	196, 2 and 666
63	2365	91	879	113	1625	139	307
64	424	92	1084	114	98	141	777
67	705	94	676	115	1 and 44	142	1450
68	8	96	412	116	847 and 636	143	1075
70	425	97	2	118	137	144	16
73	3, 367 and 2562	99	69	119	2000	145	15, 6, 30 and 28
77	970	100	1838	120	756	146	379 and 28
78	402, 560 and 643	101	64	125	1077 and 783	147	1669 and 147
79	1942	102	146	126	2485		

Table 5.18: The time duration, in minutes, of each one of the patients' cluster. Subjects are referred by their ID.

ID	Time (m)	ID	Time (m)	ID	Time (m)	ID	Time (m)
49	25.2, 88.0, 37.0, 16.0 and 229.0	80	7.1 and 393.0	103	405.7	127	405.7
50	282.5 and 119.8	81	405.7	104	128.8, 85.5 and 184.8	129	5.7 and 389.0
51	191.3 and 210.1	83	149.3 and 246.3	105	405.7	130	125.0 and 275.5
52	389.0 and 15.3	84	23.3 and 380.7	106	405.7	133	405.7
54	308.9 and 82.5	86	405.7	107	393.0	134	405.7
57	405.7	87	227.4 and 169.7	109	204.3 and 199.4	136	405.7
58	405.7	89	280.7 and 120.2	110	405.7	137	405.7
61	162.3 and 230.5	90	405.7	112	405.7	138	88.6, 7.0 and 296.9
63	405.7	91	405.7	113	405.7	139	347.4
64	399.3	92	405.7	114	405.7	141	405.7
67	405.7	94	405.7	115	92.7 and 312.1	142	405.7
68	405.7	96	405.7	116	257.3 and 145.3	143	405.7
70	405.7	97	385.2	118	405.7	144	394.7
73	14.7, 46,0 and 310.0	99	405.7	119	405.7	145	149.2, 101.5, 104.0 and 41.6
77	390.1	100	405.7	120	404.0	146	292.2 and 111.2
78	104.4, 146.5 and 139.5	101	405.7	125	218.4 and 186.7	147	321.0 and 83.2
79	392.0	102	405.7	126	405.7		

Table 5.19: Average number of snores per hour, snore density, present in each one of the patients' cluster. Subjects are referred by their ID.

ID	Snores per hour	ID	Snores per hour	ID	Snores per hour	ID	Snores per hour
49	11.9, 214.1, 100.5, 11.3 and 175.1	80	25.2 and 284.6	103	12.9	127	2.7
50	3.0 and 1.5	81	2.1	104	361, 56.8 and 406.5	129	10.7 and 143.0
51	1.9 and 0.6	83	14.5 and 165.7	105	269	130	5.3 and 12.0
52	35.2 and 0.0	84	20.6 and 1.7	106	5.0	133	1.2
54	45.1 and 7.3	86	15.7	107	57.4	134	212.8
57	86.1	87	25.6 and 10.3	109	136.5 and 106.5	136	0.4
58	36.8	89	29.1 and 120.8	110	0.3	137	512.4
61	134.5 and 78.6	90	12.3	112	15.8	138	132.8, 17.1 and 134.6
63	349.8	91	130.0	113	240.3	139	53.0
64	63.7	92	160.3	114	14.5	141	114.9
67	104.3	94	100.0	115	0.7 and 8.5	142	214.4
68	1.2	96	60.9	116	197.5 and 262.6	143	159.0
70	62.9	97	0.3	118	20.3	144	2.4
73	12.3, 478.7 and 495.9	99	10.2	119	295.8	145	6.0, 3.6, 17.3 and 40.4
77	149.2	100	271.8	120	112.3	146	77.8 and 15.1
78	231, 229.4 and 276.6	101	9.5	125	296 and 251.7	147	312.0 and 106.0
79	297.2	102	21.6	126	367.5		

5.8 Linear Compensation

PSG and high-quality sound acquisition device working mechanism are independent, each one has its own clock. Clock-associated errors change the nominal frequency of the clock, which have implications for the calculation of the data acquisition frequency. For short periods of time, such differences are not visible, but in this project, data acquisition last for hours, which means they are visible, and it leads to the loss of synchronization. Figure 5.31 has examples of how clock errors lead to loss of synchronization. There is an example for a different bed and it reveals relationships of the same type, linear, but with different linear coefficients. The linear relationship between the high-quality sound acquisition and each one of these beds was calculated using data from these 4 patients. Coefficients' results, for the different linear equations, are available in Table 5.20. The correction of the deviation, using the slope coefficient, can be used both in patients with no pause resume sequences during data acquisition, as in the cases of Figure 5.31, as well as in patients with pauses. In such cases, like in Figure 5.32, adjustments in the intercept coefficient must be applied.

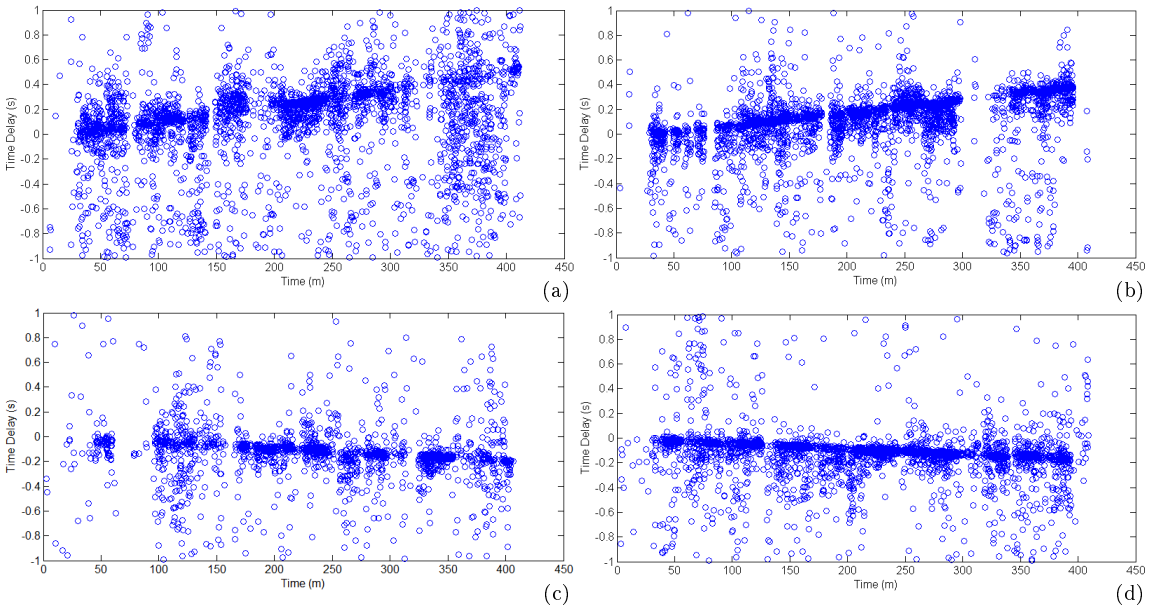

Figure 5.31: Synchronization loss, measured in s as Time Delay, between the high-quality sound acquisition and the PSG study as time goes by from the initial synchronization. Each figure is an example for a different PSG hardware, with (a), (b), (c), and (d) representing synchronization loss in bed 1, 2, 3 and 4, respectively.

Table 5.20: Coefficients to perform fine synchronization using a linear equation. Each bed has its own coefficients, calculated from a different patient, which did not have any pause during data acquisition.

Bed	**ID**	**Slope ($\cdot 10^{-6}$)**	**Intercept ($\cdot 10^{-3}$)**	**r^2 (%)**
1	100	21.6	-33.5	99.5
2	126	17.6	-38.1	99.3
3	142	-7.8	-3.4	94.6
4	63	-7.4	2.7	99.0

Table 5.21: The total number of snores paired for all patients, organized accordingly with their medical classification group. The average number of snores per patient is also available.

Parameter		**Co**	**Sn**	**Mi**	**Mo**	**Se**
Snores	#	1022	12117	10331	14680	13308
	μ	114	505	795	1129	1664

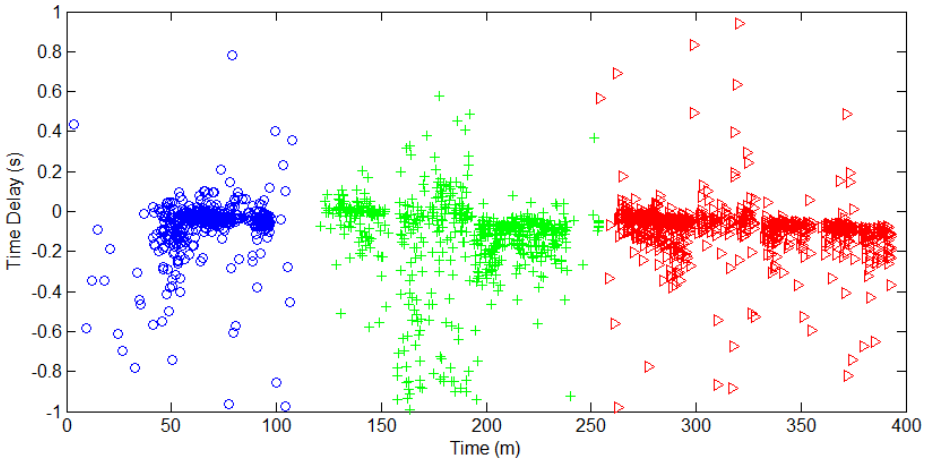

Figure 5.32: Evolution of the time delay between the 2 registers, from the PSG study and from the high-quality sound acquisition, of the same snore throughout the entire data acquisition. Each point represents a snore and a different each symbol represents a different cluster.

5.9 Snore Pairing

The data acquisition process should acquire snores, ideally, in both registers, the PSG and in the high-quality sound device. Later, the algorithms implemented in the processing phase are responsible to detect snores in both registers, and snore pairing had the task to find both registers corresponding to the same snore sound. Two registers, each one from a different acquisition, were considered as being from the same snore if they have a time difference closest to 0 than any other combination. The time span between these 2 registers, to be considered the same snore sound, should not be greater than one second. In the end, a total of 51458 snores were paired (Table 5.17 present snores by each one of the patients' clusters), with their distribution, according to their medical classification group, available in Table 5.21. The average number of snores per patient, for each medical classification group, was also calculated.

5.10 Snore Boundaries

The complete snores' definition includes the calculation of their boundaries. An energy-based algorithm searched for evidence of energy values increasing above the neighbourhood's baseline to calculate the beginning and the end of the snore. Figure 5.33 has multiple examples of the final result of boundaries' calculation. The first figure, Figure 5.33 (a), has several examples of well-behaved snores, i. e., fast changes in energy values at the beginning and the end of the snore. In Figure 5.33 (b) a low-energy snore was successfully detected and its boundaries defined. From Figure 5.33 (c) to Figure 5.33 (h), there are examples of snores in crescendo and snores present in both the inspiratory and the expiratory phase.

Boundaries algorithm calculation was not able to deliver results for all the snores, which compromises their definition, leading to the rejection of these snores. Table 5.22 resumes the final list of snores considered for feature extraction.

Table 5.22: The final list of snores, organized by the patients' medical classification group. Snores paired and excluded from this list had not their boundaries successfully calculated [332].

Parameter		Co	Sn	Mi	Mo	Se
Snores	#	974	12116	10124	14679	13301
	μ	108	505	779	1129	1663

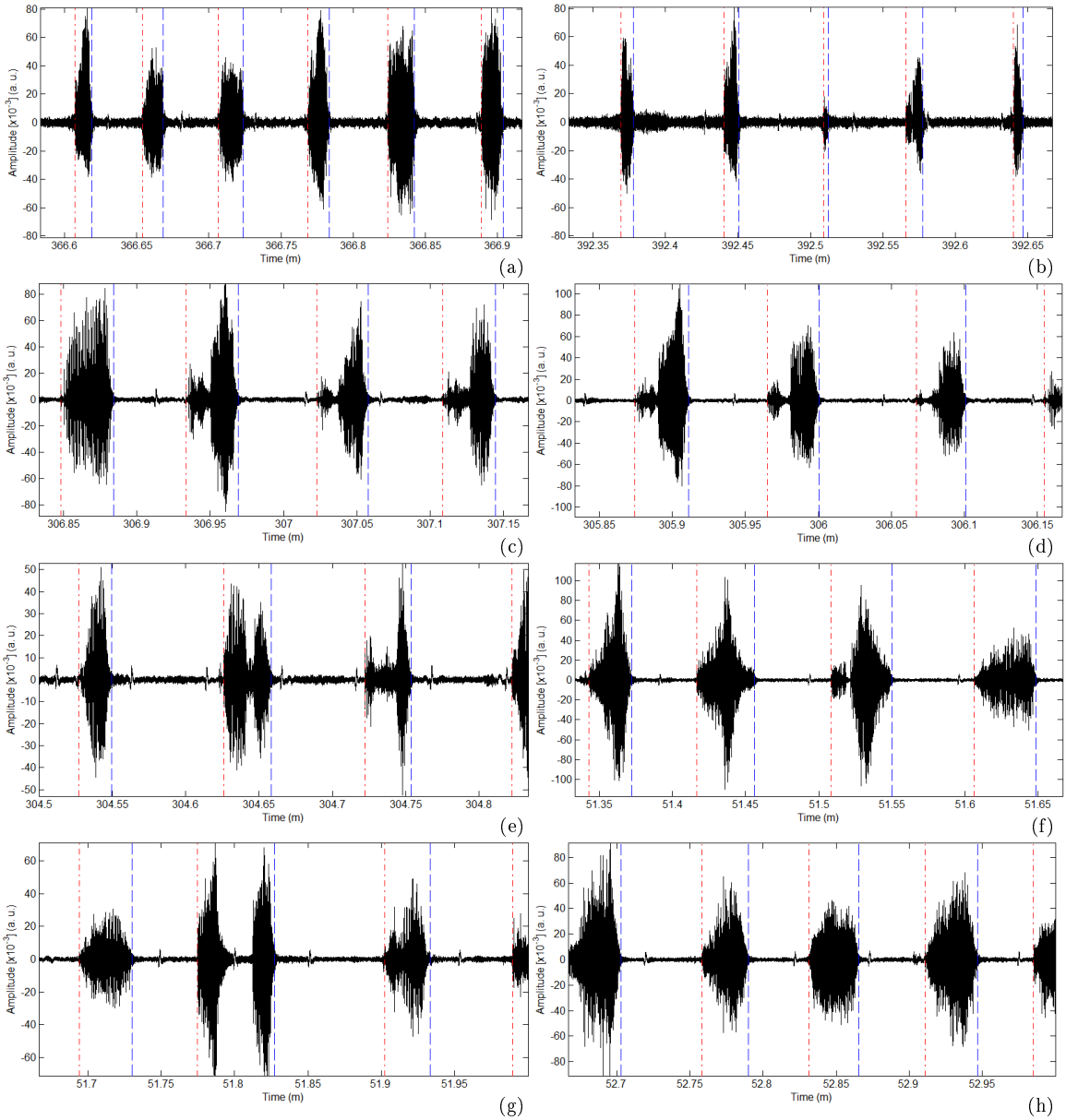

Figure 5.33: Examples of the achieved results for the boundaries calculation of each peak of energy. Multiple examples show evidence for different types of snores in the high-quality sound acquisition data. There are examples for short-duration snores, low-amplitude snores, and snores with components in both inspiratory and expiratory phase. The reasons for such snore variety wasn't the focus of this work, but it can be related with the anatomic origin, the amount of tone lost, or weight. The beginning of a snore was represented by a dash and dot red vertical line, while its end was represented by dash blue line.

5.11 Time-Domain

5.11.1 Snores' Time Duration and Amplitude

Snores' feature extraction started with the calculation of the snores' time duration, amplitude, and Peak-to-Peak (PtP) amplitude. Table 5.23 characterizes those features accordingly with the medical classification group of the patients. The increase in time duration has a direct relationship with the increase in the patient's severity, while the standard deviation is very stable across the different medical classification groups. The other 2 features, amplitude, and PtP amplitude does not have evidence of a linear sleep severity relationship, with only a clear distinguish difference from the Se medical classification group to all other groups.

Time duration, amplitude, and PtP amplitude data distribution among the medical classification groups were analysed using hypothesis testing. Both tests returned p-value=0 to the 3 features. The *post-hoc* test results to the time duration feature, available in Figure 5.34, point to significant differences among all medical classification groups once the intervals are disjunct. Table 5.24 summarizes this process. The *post-hoc* test results for the remaining features show that Co and Mo medical classification groups do not have significant differences in both features, once their intervals are not disjunct.

5.11.2 Energy

Following the definition of a snore, the energy of each snore was calculated for data inside its boundaries, and no relationship was found between energy and medical classification groups. The hypothesis testing previously described returned the same results achieved for both amplitude and PtP amplitude. Table 5.25 resumes data from the energy feature.

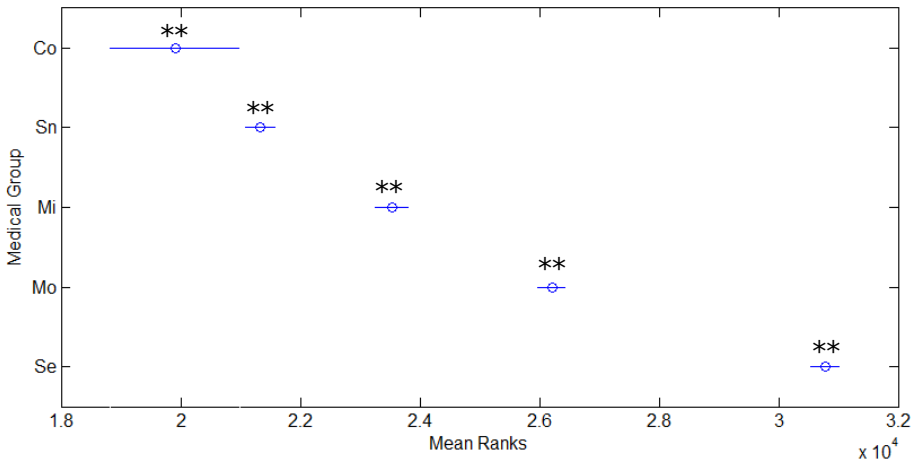

Figure 5.34: Results from the multiple comparison test to the time duration feature. All medical classification groups have significant differences between them (**p-$value$<0.01), once the intervals are disjunct.

Table 5.23: The average, μ, and the standard deviation, σ, of 3 features retrieved from the snores. The snores' time duration [332], amplitude and PtP amplitude are the features displayed in this table. Data are organized accordingly with the medical classification group of the patients.

Parameter		Co	Sn	Mi	Mo	Se
Time	μ	1.106	1.178	1.227	1.368	1.493
Duration (s)	σ	0.497	0.558	0.517	0.608	0.516
Amplitude	μ	0.036	0.029	0.046	0.037	0.082
(a.u.)	σ	0.048	0.030	0.043	0.038	0.063
Amplitude	μ	0.066	0.053	0.083	0.067	0.151
PtP (a.u.)	σ	0.088	0.055	0.079	0.069	0.114

Table 5.24: The application of the Kruskal-Wallis H test (**p-value$<$0.01) and the *post-hoc* test. The mean ranks of each medical classification group and the minimum and the maximum give the intervals for analysis. All the intervals are disjunct and all the medical classification groups are considered significantly different for the time duration feature [332].

Parameter	Co **	Sn **	Mi **	Mo **	Se **
Mean Ranks	19908	21337	23541	26209	30785
Standard Error	474	134	147	122	128
Minimum	18823	21079	23262	25969	30536
Maximum	20993	21596	23820	26449	31034

5.11.3 Kurtosis and Skewness

Tools like kurtosis and skewness measure data distribution to understand the relative heaviness of data in the tail and the distribution symmetry, respectively. The application of such tools, in each snore, allowed to build the snores' profile in the different medical classification groups. Table 5.26 and Table 5.27 present the results for the kurtosis and skewness, respectively.

The kurtosis of normal distribution has a mesokurtic value, 3, while all medical classification groups have kurtosis values higher than that value. They are of the leptokurtic type, which means more data in the tail than in a Gaussian distribution. OSAHS medical classification groups have higher kurtosis values as the severity also increases, while non-OSAHS medical classification groups have lower values, but with the Co group presenting a higher value than the Sn group.

The skewness, S_w, values for all medical classification groups points to fairly symmetrical groups, because their values are $|S_w| < 0.5$. Skewness values in the range $0.5 \leq |S_w| < 1.0$ are considered as moderately skewed, while $|S_w| \geq 1.0$ are considered highly skewed. Sn group is negatively skewed, or left-skewed, while the other medical classification groups are positively skewed, or right-skewed.

5.11.4 Empirical Mode Decomposition

Signal decomposition uses the EMD method to decompose the snoring sound in its first up to 10 elementary components, with the remaining data known as

Table 5.25: The energy feature analysed accordingly with the patients' medical classification group. The parameters average, μ, and the standard deviation, σ, are presented.

Parameter		Co	Sn	Mi	Mo	Se
Energy	μ	4.553	2.686	5.516	3.244	13.209
(a.u.)	σ	35.266	9.112	32.927	15.184	22.387

Table 5.26: The kurtosis features analysed accordingly with the patients' medical classification group. The parameters average, μ, and the standard deviation, σ, are presented.

Parameter		Co	Sn	Mi	Mo	Se
Kurtosis	μ	5.026	4.571	4.978	6.026	8.032
	σ	3.408	4.023	3.199	6.109	6.587

residuals. Figure 5.35 is an example of a snore undergoing signal decomposition using the EMD method, where the 2 figures are, in fact, the same snore sound. In the first one, data are exclusively from the snore itself, with all data inside the snore's boundaries, while in the second figure there are also data 1 s around the snore, revealing a very good signal-to-noise ratio. EMD decomposition was applied in data from Figure 5.35 (a), and the decomposition results are available at Figure 5.36, where the algorithm starts the decomposition by searching for the components with the lower periods, the lowest component is in Figure 5.36 (a), evolving, progressively, to the higher periods, with the higher period in Figure 5.36 (j).

Figure 5.37 reveals how IMFs distribution occurs for the signal amplitude. Data was divided using 2 categories, the patients' medical classification group, identified in different colours, and the IMF component. A boxplot method was implemented to study the relationship of each IMF with the medical classification group. Se highlights from the remaining groups in each IMF, and the comparison of the highest IQR value, from a non-Se boxplot, to the IQR of the Se group returns a maximum width of only 50.9%, in the Mi group at the first IMF. Signal's period was the second parameter retrieved using this method, and Figure 5.38 reports the period of the snore sounds for each medical classification group calculated from each IMF.

A different data arrangement was implemented to study EMD, splitting data according to the respective amplitude range or period band. A total of 10 ranges/bands were created, following a logarithm scale. The limits of each amplitude ranges were $0.000*10^{-3}$ to $1.000*10^{-3}$, $1.000*10^{-3}$ to $1.910*10^{-3}$, $1.910*10^{-3}$ to $3.649*10^{-3}$, $3.649*10^{-3}$ to $6.969*10^{-3}$, $6.969*10^{-3}$ to $13.313*10^{-3}$, $13.313*10^{-3}$ to $25.428*10^{-3}$, $25.428*10^{-3}$ to $48.570*10^{-3}$, $48.570*10^{-3}$ to $92.776*10^{-3}$, $92.776*10^{-3}$ to $177.213*10^{-3}$, and above $177.213*10^{-3}$ a. u. Figure 5.39 shows the results for the range of amplitudes organization. The limits of each period band were 0.000 to 10.000, 10.000 to 13.360, 13.360 to 17.848, 17.848 to 23.845, 23.845 to 31.856, 31.856 to 42.559, 42.559 to 56.858, 56.858 to 75.961, 75.961 to 101.482, and above 101.482 ms. Figure 5.40

Table 5.27: The skewness features analysed accordingly with the patients' medical classification group. The parameters average, μ, and the standard deviation, σ, are presented.

Parameter		Co	Sn	Mi	Mo	Se
Skewness	μ	0.010	-0.011	0.079	0.005	0.002
	σ	0.339	0.394	0.377	0.417	0.450

presents data for the different bands.

5.11.5 Shannon Entropy

Shannon entropy was calculated for 3 different cases, data exclusively from the snore, from the snore and 1 s around the snore's limits, and the snore and 2 s around the snore's limits. Table 5.28 presents the mean and standard deviation Shannon entropy values for each case of each medical classification group. Both statistical parameters, mean and standard deviation, are very similar among the different cases, which led to the selection of the Shannon entropy of data solely from the snore. Shannon entropy is almost proportional to the OSAHS severity, therefore

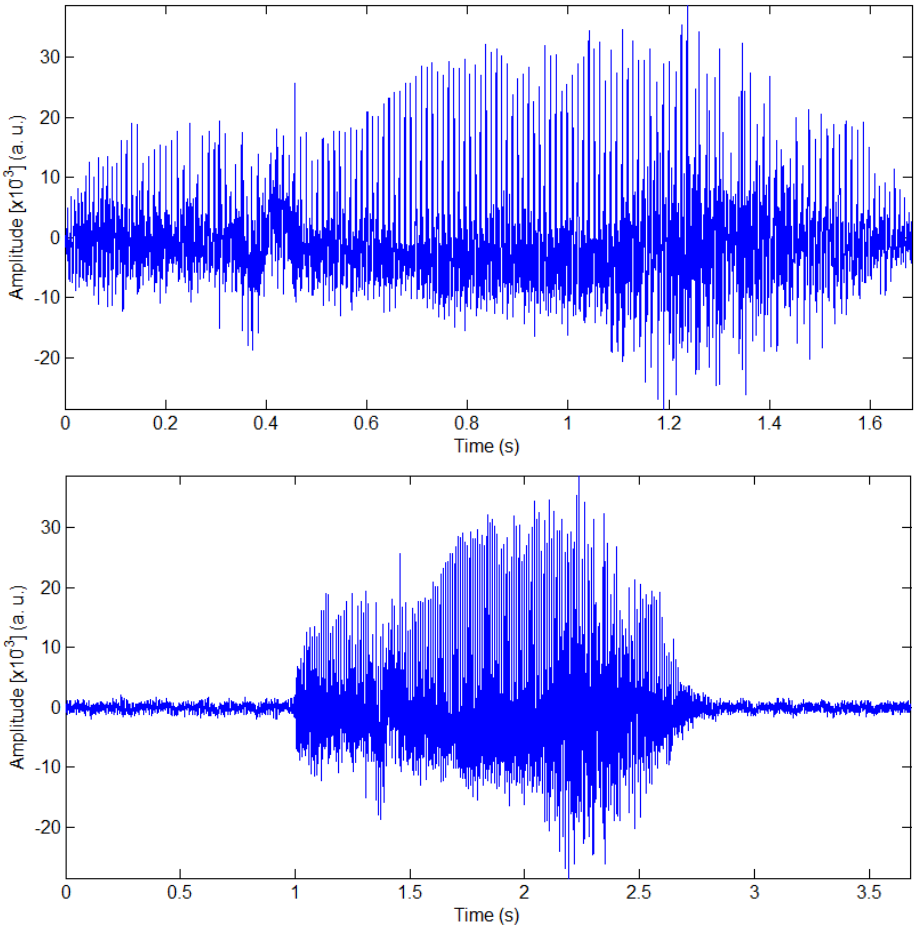

Figure 5.35: The same snore was represented in both figures, (a) and (b). This snore was used as an example for EMD decomposition, and the entire snore, data inside its boundaries, is at (a). In (b), the plot of the entire snore and data 1 s around the snore was performed to show amplitude differences between the neighbourhood and the snore itself.

indicating that this may be a good indicator of the patient's stage in the evolution of the pathology.

The hypothesis testing was implemented to test the Shannon entropy results among the different medical classification groups, with both tests rejecting the null

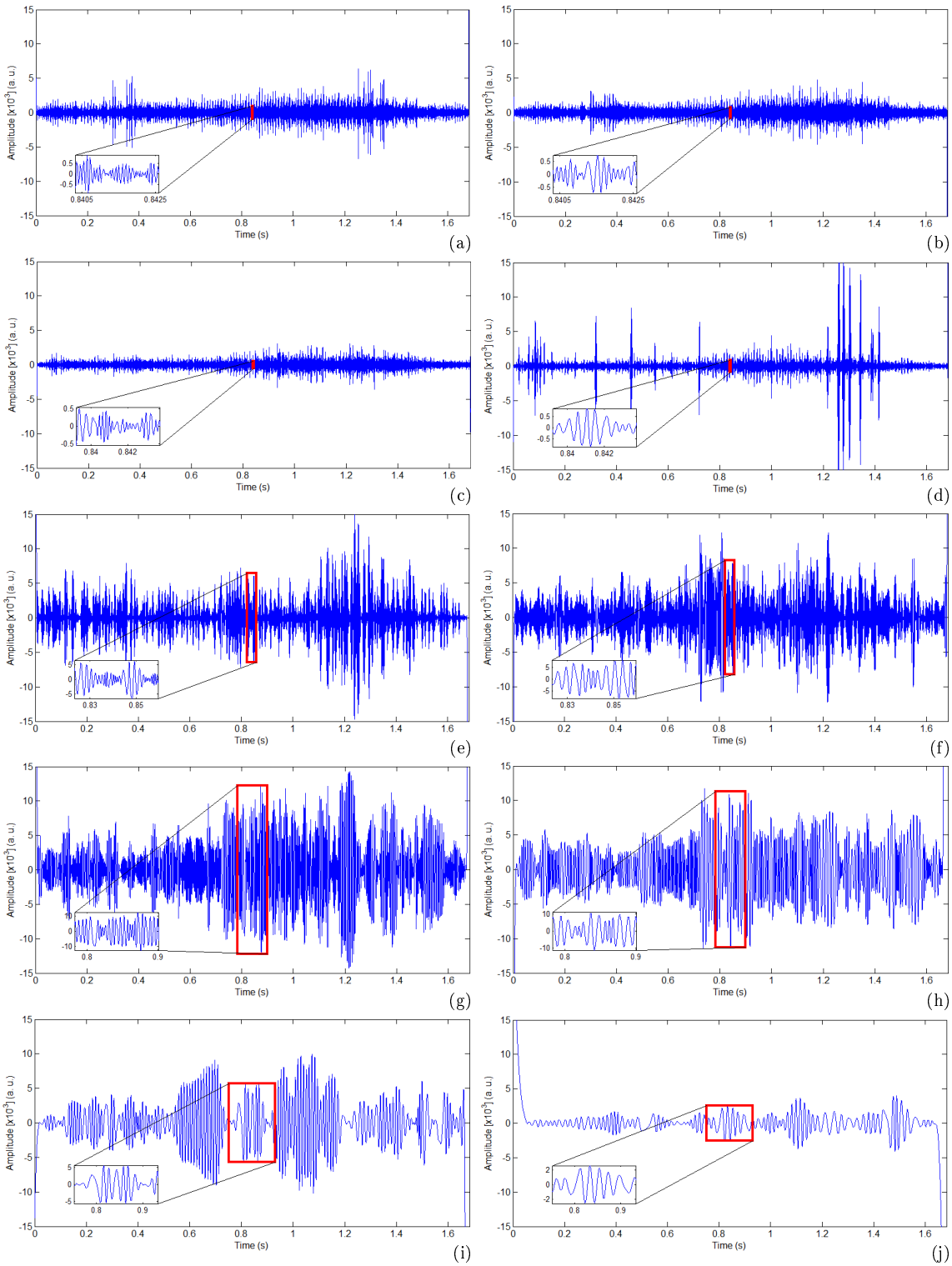

Figure 5.36: The first 10 IMFs from the EMD decomposition of a single snore, snore in Figure 5.35. The decomposition evolves from the lower periods, (a), to the higher periods, (j). Each graphic has the central region zoom in to show the IMF periodicity.

Table 5.28: The Shannon entropy feature was analysed accordingly with the patients' medical classification group, Co, Sn, Mi, Mo, or Se. The average, μ, and the standard deviation, σ, of the Shannon entropy snore events were calculated for 3 cases. The calculus was performed solely to data inside snore's boundaries, 0s, [332] and including data outside snore's boundaries, 1s and 2s.

Parameter			Co	Sn	Mi	Mo	Se
Shannon Entropy	0s	μ	3.489	3.665	3.857	3.732	3.954
		σ	0.286	0.162	0.292	0.151	0.234
	1s	μ	3.531	3.666	3.871	3.734	3.955
		σ	0.123	0.155	0.270	0.135	0.231
	2s	μ	3.531	3.666	3.871	3.736	3.960
		σ	0.123	0.155	0.271	0.135	0.233

hypothesis, p-value of 0. *Post-hoc* test points to significance differences between all medical classification groups, Figure 5.41, once all the intervals are disjunct (Table 5.29).

Entropy distribution of each patient was analysed, and 2 values were retrieved: the percentile 25 (p_{25p}) and the percentile 75 (p_{75p}). The results comprising the data referred to in Figure 5.42 can be represented as the statistical distribution of the percentile difference ($p_{75p} - p_{25p}$) for each patient, grouped accordingly with their medical classification group and where outliers have been discarded. A minimal Mi group deviation avoids a monotonic behaviour between all parameters of this statistical distribution and OSAHS severity. A strictly monotonic behaviour exists when subtracting the percentile 25 to the median ($p_{50c} - p_{25c}$). An increase in the $p_{50c} - p_{25c}$ is followed by an increase in the OSAHS severity, from a healthy subject to a patient diagnosed with Se OSAHS. The obtained results for the 5 medical classification groups were 4.9×10^{-3}, 5.8×10^{-3}, 6.1×10^{-3}, 9.0×10^{-3} and 31.0×10^{-3} bits for Co, Sn, Mi, Mo and Se, respectively. Table 5.30 resumes data from Figure

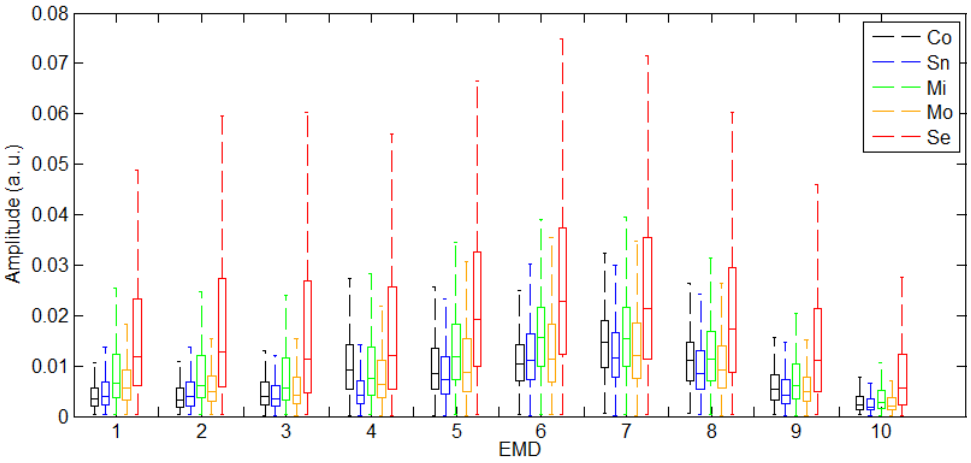

Figure 5.37: The EMD decomposition of snores occurs for a maximum of 10 IMFs. Independent axis was used to represent each one of the 10 IMFs, while the dependent axis has information regarding the IMFs amplitude. The graphic construction was based on boxplot, with data organized accordingly with 2 criteria. The first one was, already, identified, the 10 IMFs, and the second criterium was the patients' medical classification group. For each IMF, there are 5 boxplots, one for each medical classification group, Co, Sn, Mi, Mo and Se. Outliers were removed.

5.42.

Finally, the Mi group deviation was rectified using the weighting factor IQR and percentile 75: $\frac{IQR}{p_{75c}}$. Figure 5.43 reveals that parameters of the entropy's statistical distribution, wp_{25c} and wp_{50c}, have an unambiguous correlation with OSAHS severity. A correlation analysis was performed to evaluate the linear relationship between those parameters. The calculated correlation coefficient was 0.9967 and

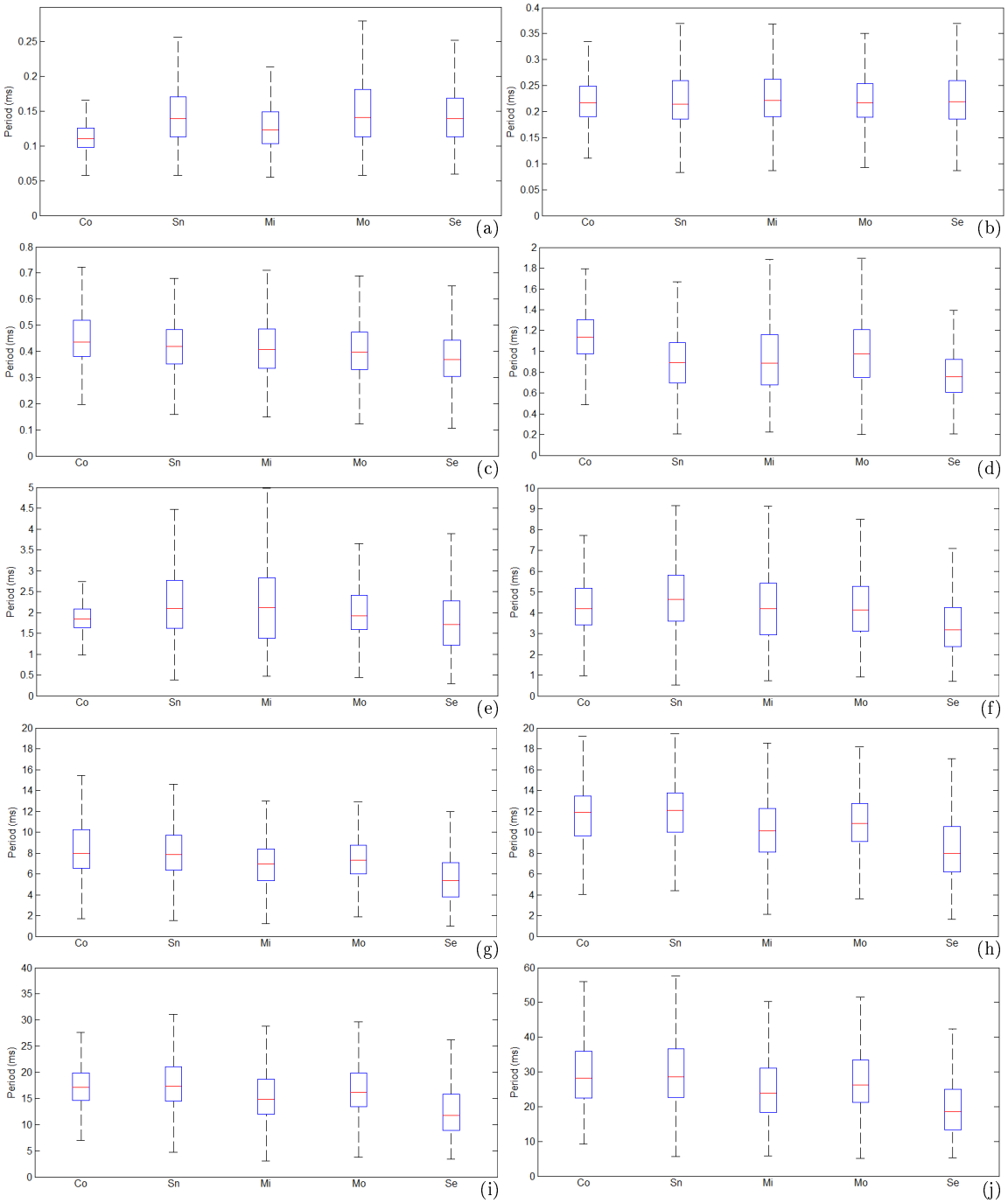

Figure 5.38: Ten graphics representing, each one, a different IMF from the EMD decomposition. EMD was performed for the first 10 IMFs, if they existed, of the snores. Each graphic has 5 boxplots, one for each medical classification group, Co, Sn, Mi, Mo and Se, and all for the same IMF. The first IMF is in graphic (a), the second in graphic (b). The remaining graphics follow the same logic, with the last IMF in graphic (j). Information in each boxplot are for the IMF period, in ms, without outliers.

p-value 0.0002, below the significance level of 0.05, which means the rejection of the null hypothesis (no relationship between the parameters). The correlation coefficient lower and upper limit, for a confidence interval of 95%, are 0.9486 and 0.9998, respectively. The linear regression model uses the least-squares method and it returns the equation $y = 0.5152 \cdot x - 0.0002$ and the coefficient of determination, R^2, to measure the goodness of fit, is 99.3%.

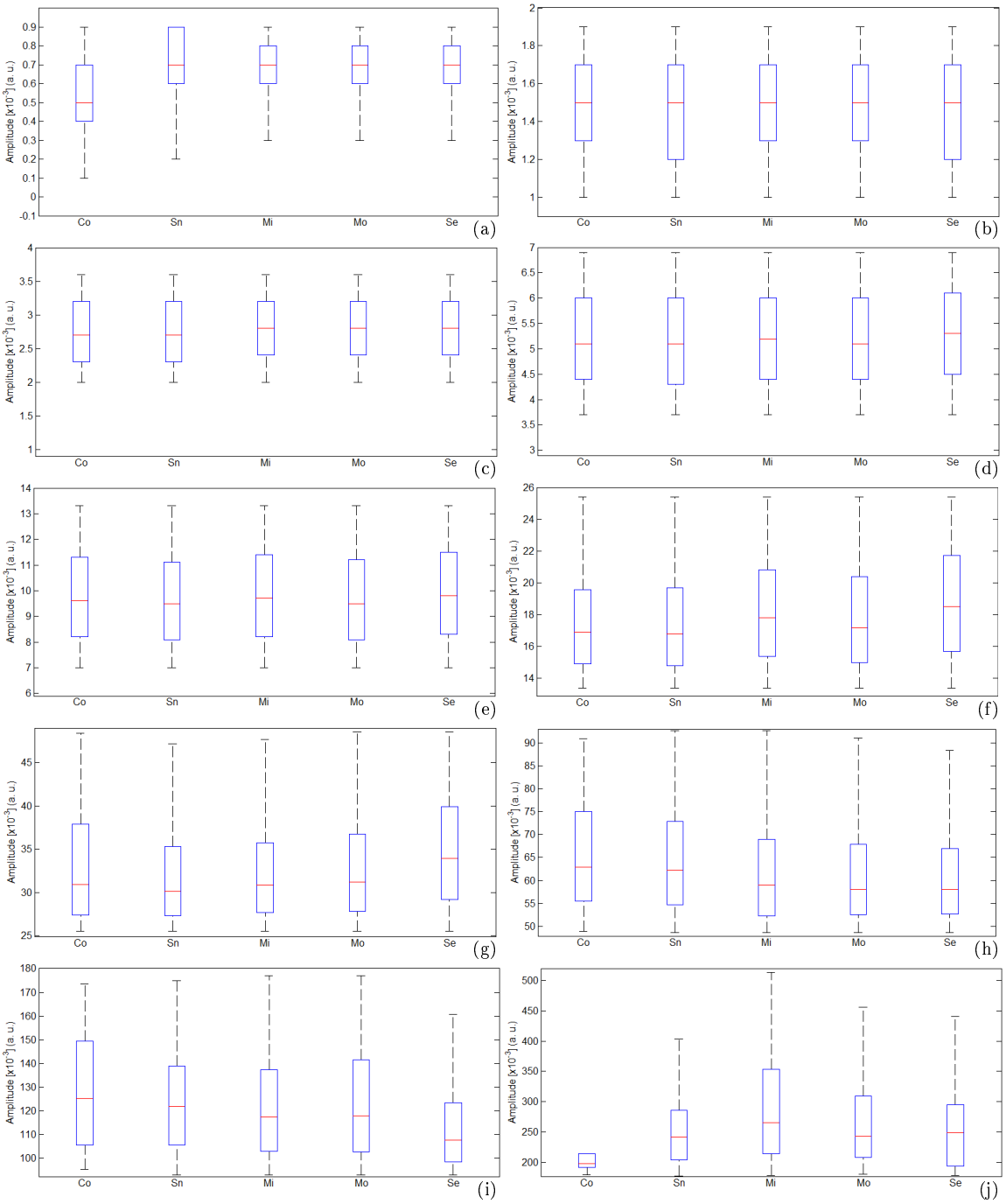

Figure 5.39: Ten graphics representing, each one, a different range of amplitudes from the EMD decomposition. EMD was performed for the first 10 IMFs, if they existed, of the snores. The first amplitude range is in graphic (a), the second amplitude range is in graphic (b), with the last amplitude range in graphic (j). Each graphic has 5 boxplots, one for each medical classification group, Co, Sn, Mi, Mo and Se. Outliers were removed.

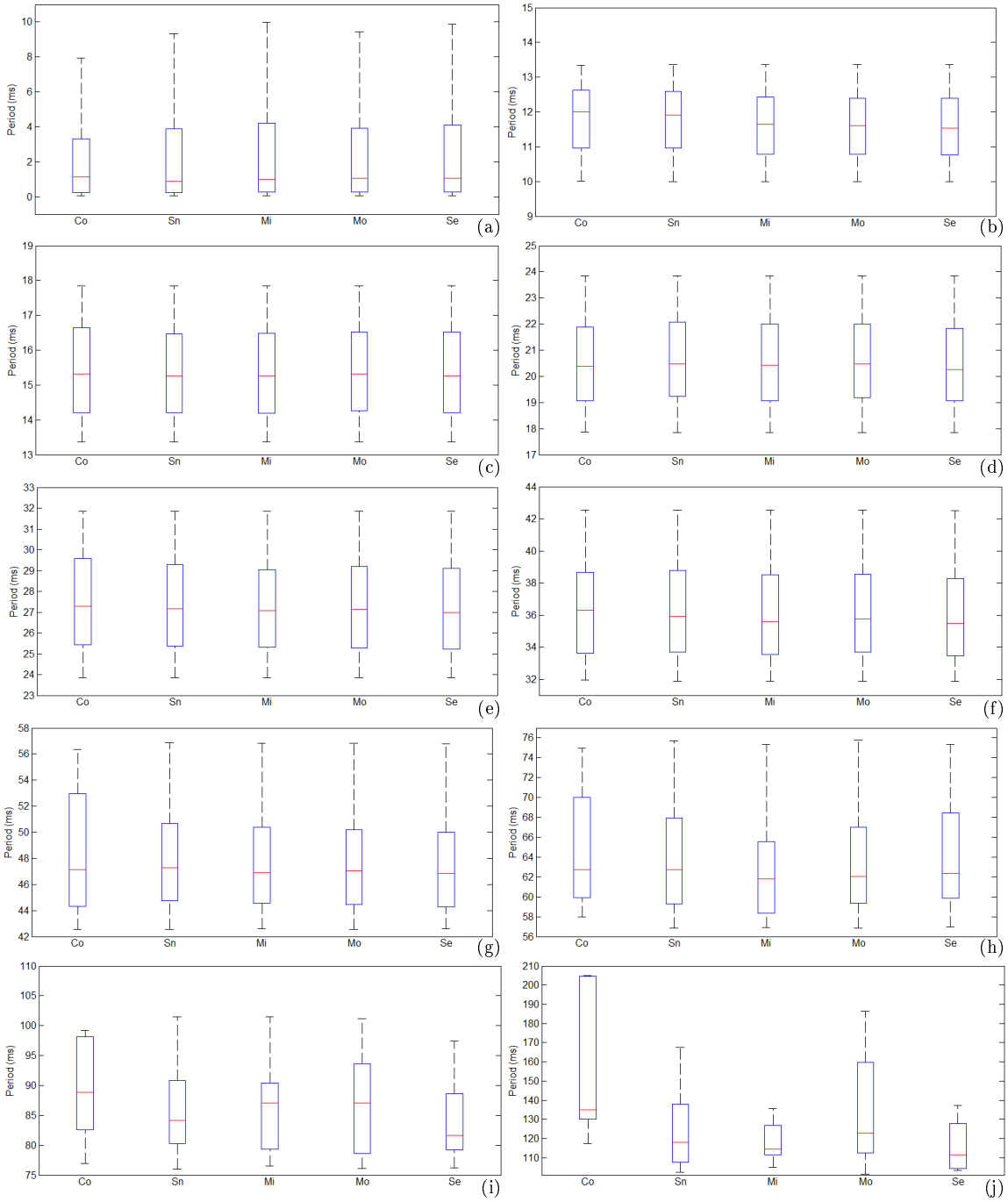

Figure 5.40: Ten graphics representing, each one, a different band from the EMD decomposition. EMD was performed for the first 10 IMFs, if they existed, of the snores. The first band is in graphic (a), the second band is in graphic (b), with the last band in graphic (j). Each graphic has 5 boxplots, one for each medical classification group, Co, Sn, Mi, Mo and Se. Outliers were removed.

Table 5.29: The application of the Kruskal-Wallis H test and the post-hoc test (**p-$value$<0.01). The mean ranks of each medical classification group and the minimum and the maximum give the intervals for analysis. All the intervals are disjunct and all the medical groups are considered significantly different for the Shannon entropy feature [332].

Parameter	**Co ****	**Sn ****	**Mi ****	**Mo ****	**Se ****
Mean Ranks	6399	17513	28879	22788	34971
Standard Error	474	134	147	122	128
Minimum	5313	17255	28600	22547	34722
Maximum	7484	17771	29157	23028	35220

Table 5.30: Statistical distribution of the $p_{75p} - p_{25p}$ for each medical classification group. The parameters' values were taken from the boxplot in Figure 5.42 [332].

Parameter $[\times 10^{-3}]$ (bits)	**Co**	**Sn**	**Mi**	**Mo**	**Se**
Maximum	15.9	39.2	94.0	59.0	122.5
p_{75c}	13.4	19.8	52.0	36.3	85.2
p_{50c}	8.3	12.0	11.2	20.8	62.8
p_{25c}	3.4	6.2	5.1	11.8	31.8
Minimum	1.5	1.5	1.3	4.4	22.5

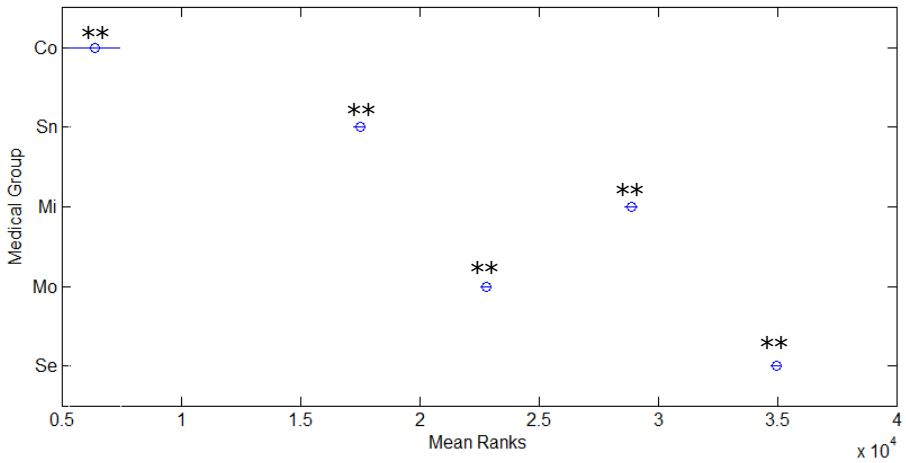

Figure 5.41: Results from the multiple comparison test to the Shannon entropy dataset. All medical classification groups have significant differences between them (**p-$value$<0.01), once the intervals are disjunct.

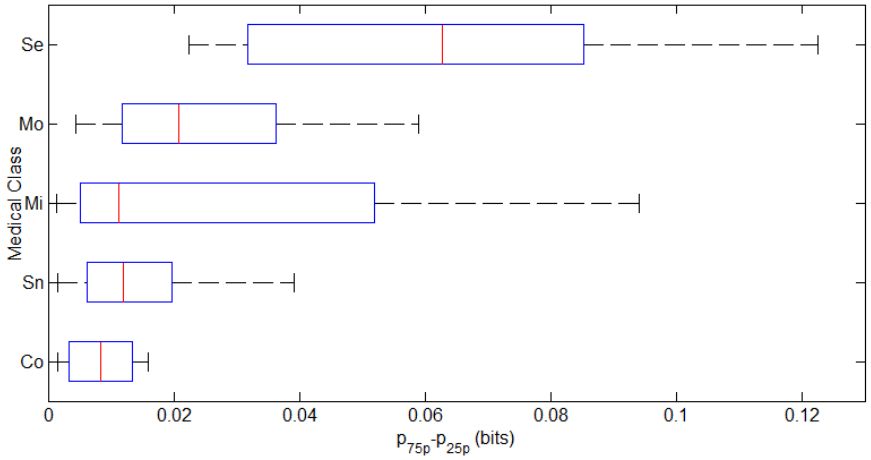

Figure 5.42: Statistical distribution of the percentile difference $p_{75p} - p_{25p}$. Subjects were grouped accordingly with their medical classification group. Outliers were discarded [332].

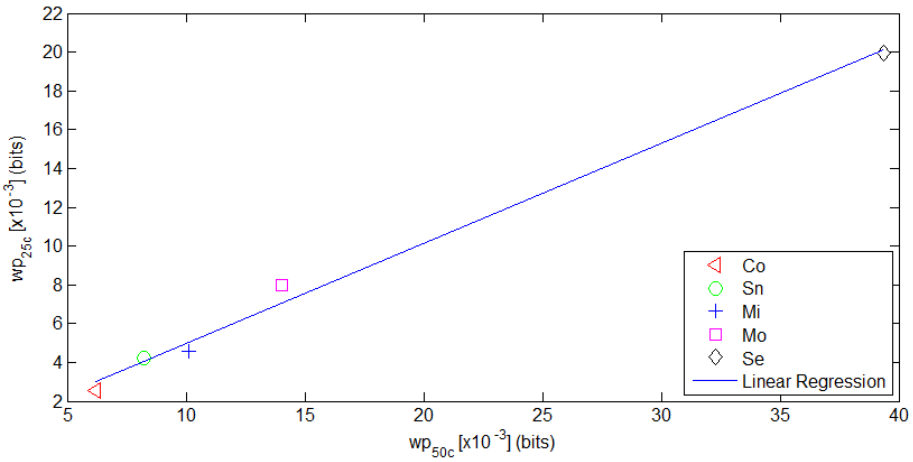

Figure 5.43: The wp_{50c} and the wp_{25c} parameters are directly proportional. The straight line was the result of a linear regression performed with the points in the figure. There is a progressive evolution in the OSAHS severity. For low values, data suggest the subject is healthy, with the condition worsen as the values increase [332].

5.12 Frequency-Domain

PSD estimation, using the Welch method, was the tool implemented to get features from the sound signal in the frequency domain. Figure 5.44 presents data for 4 features, frequency with the highest PSD value, and the frequencies for the 1st, 2nd and 3rd PSD quartiles, each one located in a different plot, (a) to (d), with data displayed using box plots. Box plots organize data by the patients' medical classification group, and all 4 present the same pattern, median follows OSAHS worsening, with the exception of Mi. As an example, the median values for the frequency at the highest PSD value was 83, 92, 127, 100, and 129 Hz values, for Co, Sn, Mi, Mo, and Se, respectively.

Data decomposition was performed to evaluate the contribution of each patient to the overall result of each medical classification group, for the highest PSD frequency feature. Figure 5.45 presents the contribution of each patient to its medical classification group box plot. The median standard deviation of each medical classification group, and for increased worsening conditions, was 52.5, 39.4, 21.5, 18.6, and 29.3 Hz. A patient contributes with a different number of snores and the median standard deviation may not be the best comparison tool, but the analysis shows a higher oscillation in the median in other medical classification groups than in the Mi class. IQR standard deviation corroborates the median standard deviation values, by returning 91.2, 153.6, 37.5, 33.3, and 64.3 Hz. Results for the other 3 features are similar, the Mi group consistently shows as one of the groups with the least dispersion. A single exception occurred to the 3rd quartile feature, where it has the highest IQR standard deviation. The results, in increasing order of medical classification group severity, are 255.4, 296.1, 2256.6, 1333.7, and 1721.2 Hz.

Three additional frequency-domain features were selected to characterize medical classification groups, and their data distribution is in Figure 5.46. The 3 new features are the central frequency, the frequency standard deviation, and the coefficient of symmetry, and their box plots are at Figure 5.46 (a), Figure 5.46 (b), and Figure 5.46 (c), respectively. Central frequency has no relationship with medical classification groups, visible in Figure 5.46 (a), with groups Sn and Mi failing to follow the increase verified in the median of the remaining groups. Frequency standard deviation and coefficient of symmetry have similarities with the first 4 frequency features, Figure 5.44, but with Sn group, instead of Mi group, not following an increase in the median frequency as OSAHS worsens. The median of the frequency standard deviation feature has values of 0.983, 0.898, 1.162, 1.186, and 1.389 kHz, while the median of the coefficient of symmetry has values of 2.069, 1.923, 2.230, 2.320, and 2.512 kHz. Both features has their median values order by OSAHS severity, from a Co subject to a Se patient.

Patient contribution to the respective overall medical classification group was analysed to the coefficient of symmetry and the frequency standard deviation features. Figure 5.47 presents the results for the coefficient of symmetry feature. The

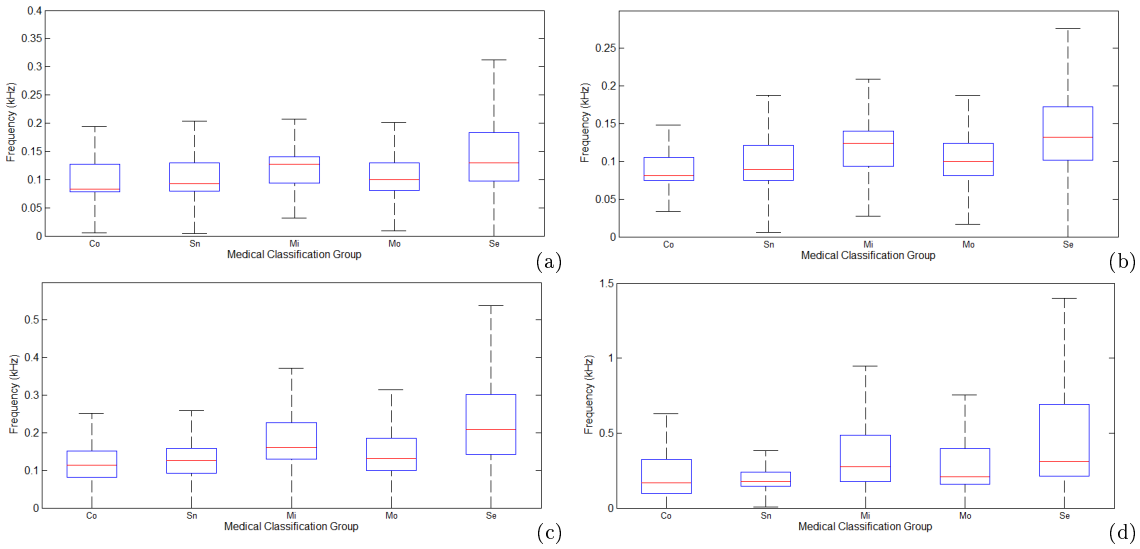

Figure 5.44: Frequency distribution accordingly with the patients' medical classification groups. The Welch non-parametric method was applied in all snores to estimate PSD. Four figures are represented here to identified the frequency, (a), with the highest PSD value, and the frequencies, (b), (c) and (d), for the 1st, 2nd and 3rd quartile of the PSD estimation, respectively. Outliers are not visible.

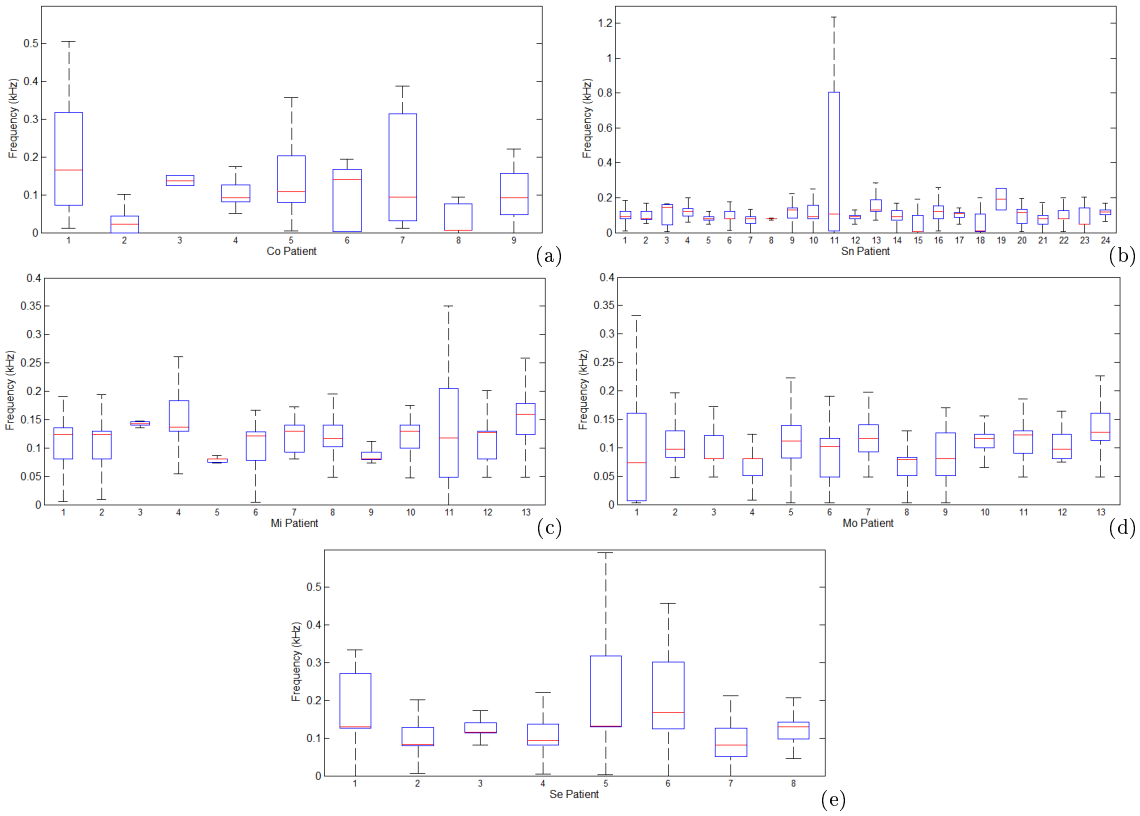

Figure 5.45: How frequency at the maximum PSD distributes for each patient using the Welch method. Patients were grouped by their medical classification group, with plot (a), (b), (c), (d), and (e) representing the Co, Sn, Mi, Mo, and Se medical classification group. Each plot, representing a different medical classification group, has one box plot for each patient. Outliers are not visible.

median standard deviation of each medical classification group was of 653, 659, 1116, 1287, and 974 Hz, ordering OSAHS by its severity, from no disorder (Co) to higher degree of the disorder (Se), while the IQR standard deviation was of 619, 540, 1058, 552, and 620 Hz, considering the same order. Figure 5.48 has data from each patient contribution for the frequency standard deviation feature. The same comparison was made using the median and the IQR, and the results for the median standard deviation were 541, 507, 955, 1357, and 911 Hz, and for the IQR standard deviation was of 561, 510, 1108, 795, and 772 Hz, ordering by increasing severity of OSAHS.

The last three frequency-domain features presented in this thesis, band power ratio, in and out band power ratio, and band spectral flatness, have their results available in Figure 5.49. Results for the band power ratio and the in-out band power ratio features are very similar, with a single visible difference, in the first band. Interesting results were achieved in band 8, where there is a monotonical behaviour, with a direct relationship between the median of these features and the medical classification groups. Median values in the 8^{th} band for the band power ratio feature, Figure 5.49 (a), are of 6.5×10^{-3}, 7.4×10^{-3}, 9.2×10^{-3}, 12.5×10^{-3}, 18.7×10^{-3}, while for the in out band power ratio feature, Figure 5.49 (b), are of 6.5×10^{-3}, 7.5×10^{-3}, 9.2×10^{-3}, 12.7×10^{-3}, 19.0×10^{-3}. If Co medical classification group results are carefully not taken into account, more bands have interesting results, which is the case of band 4 and band 10. The 4^{th} band of the band power ratio feature (in out band power ratio feature) has values of 19.8×10^{-3}, 34.2×10^{-3}, 48.3×10^{-3}, and 57.0×10^{-3} (20.2×10^{-3}, 35.4×10^{-3}, 50.8×10^{-3}, and 60.4×10^{-3}), while the 10^{th} band of the band power ratio feature (in out band power ratio feature) has values of 0.7×10^{-3}, 0.9×10^{-3}, 1.2×10^{-3},

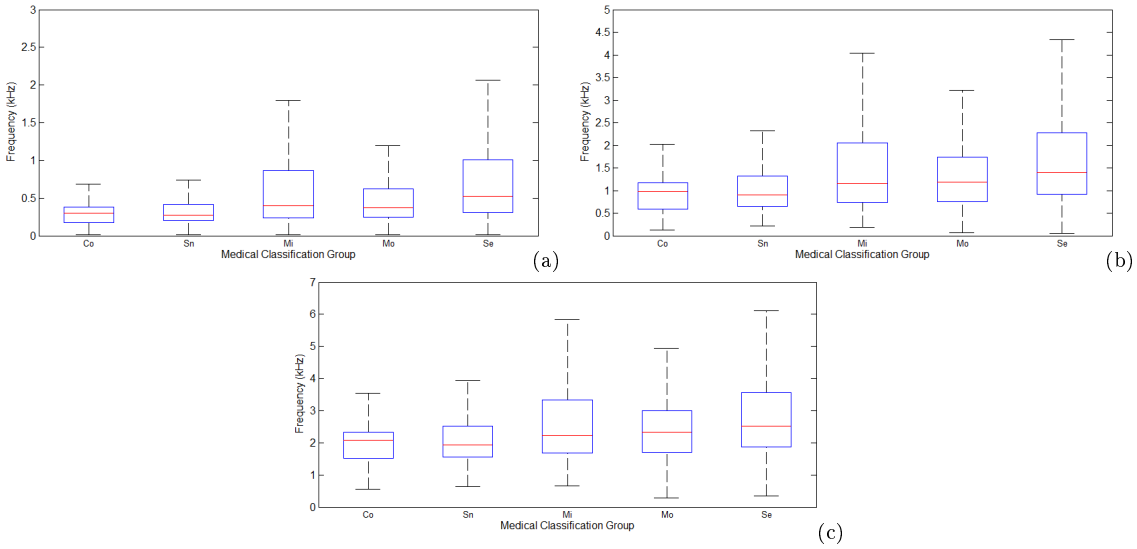

Figure 5.46: PSD estimation using the non-parametric Welch method. Three figures, each one with data from a different frequency feature, present data in a box plot type figure, splitting their content by the different medical classification groups. Figure (a), (b), and (c) are for the central frequency, the frequency standard deviation, and the coefficient of symmetry, respectively. Outliers are not visible.

and 1.6×10^{-3} (0.7×10^{-3}, 0.9×10^{-3}, 1.2×10^{-3}, and 1.6×10^{-3}). Spectral flatness results do not present evidences of an useful tendency in both the median and the IQR, Figure 5.49 (c), to help in OSAHS diagnosis.

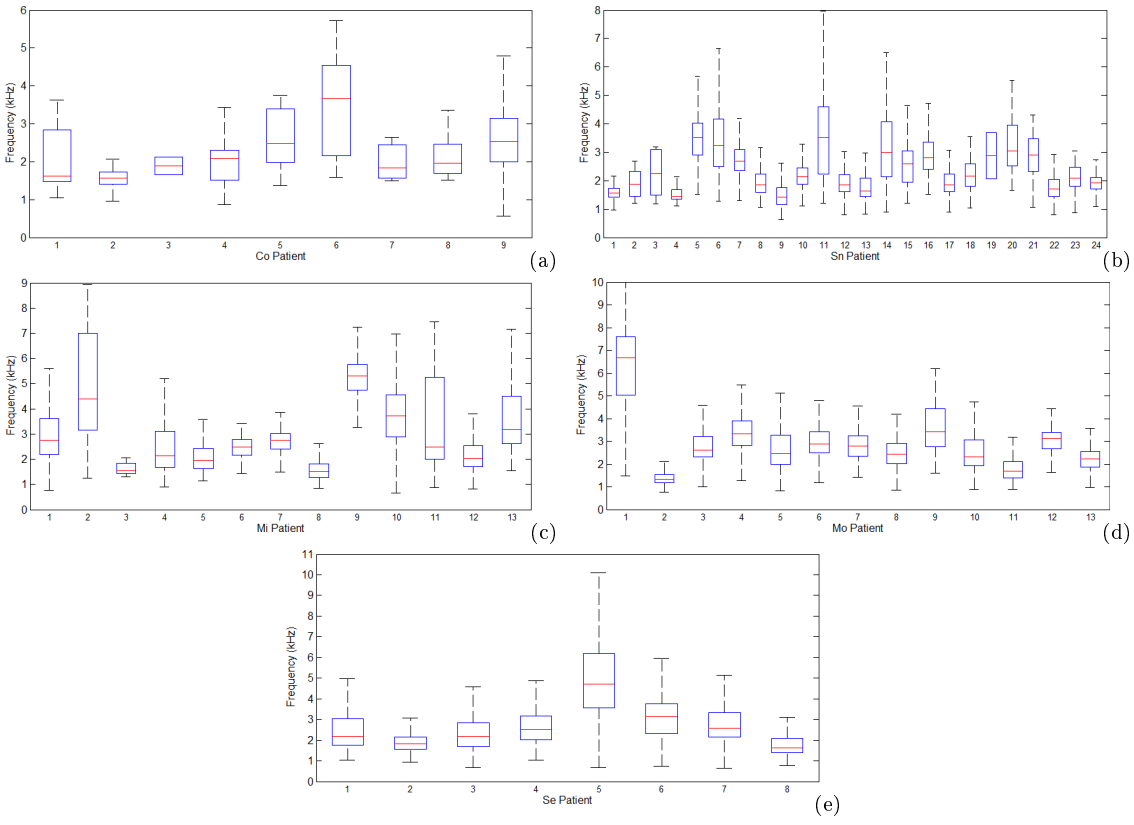

Figure 5.47: How the coefficient of symmetry distributes for each patient at the using the Welch method to calculate PSD. Patients were grouped by their medical classification group, with plot (a), (b), (c), (d), and (e) representing the medical classification group Co, Sn, Mi, Mo, and Se. Each plot, representing a different medical classification group, has one box plot for each patient. Outliers are not visible.

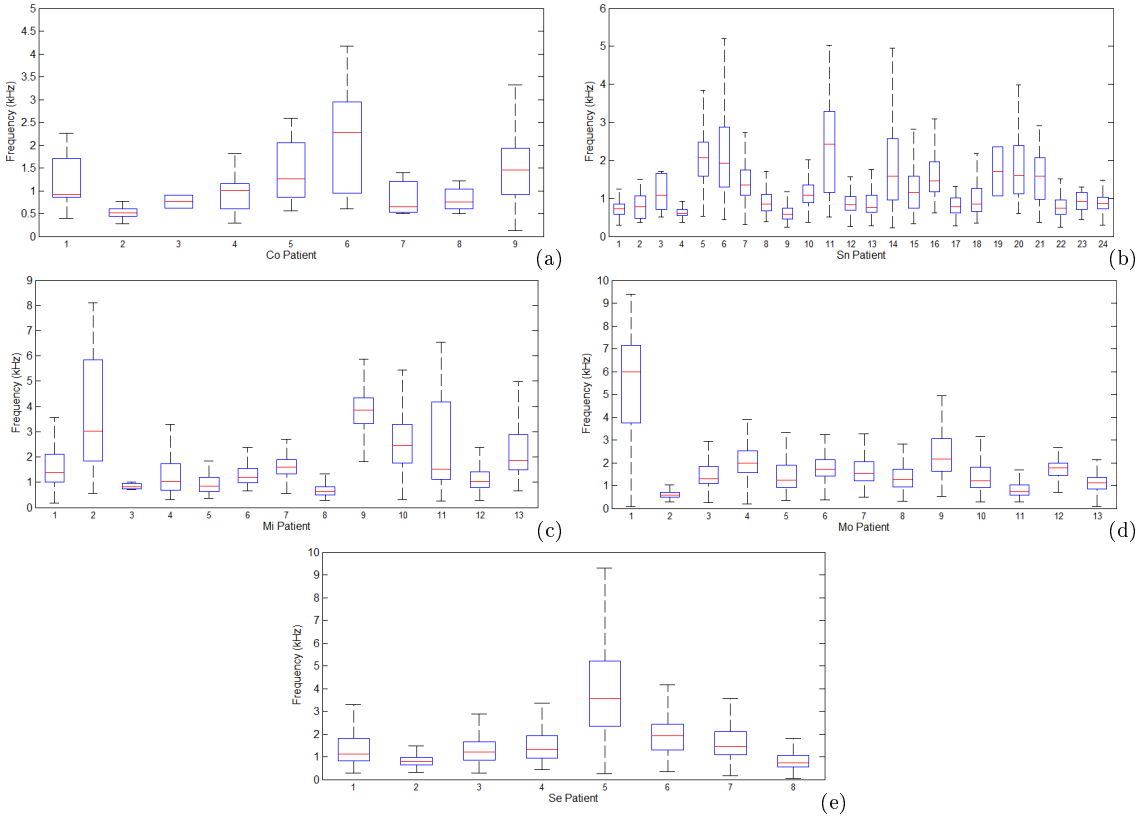

Figure 5.48: How the frequency standard deviation distributes for each patient at the using the Welch method to calculate PSD. Patients were grouped by their medical classification group, with plot (a), (b), (c), (d), and (e) representing the medical classification group Co, Sn, Mi, Mo, and Se. Each plot, representing a different medical classification group, has one box plot for each patient. Outliers are not visible.

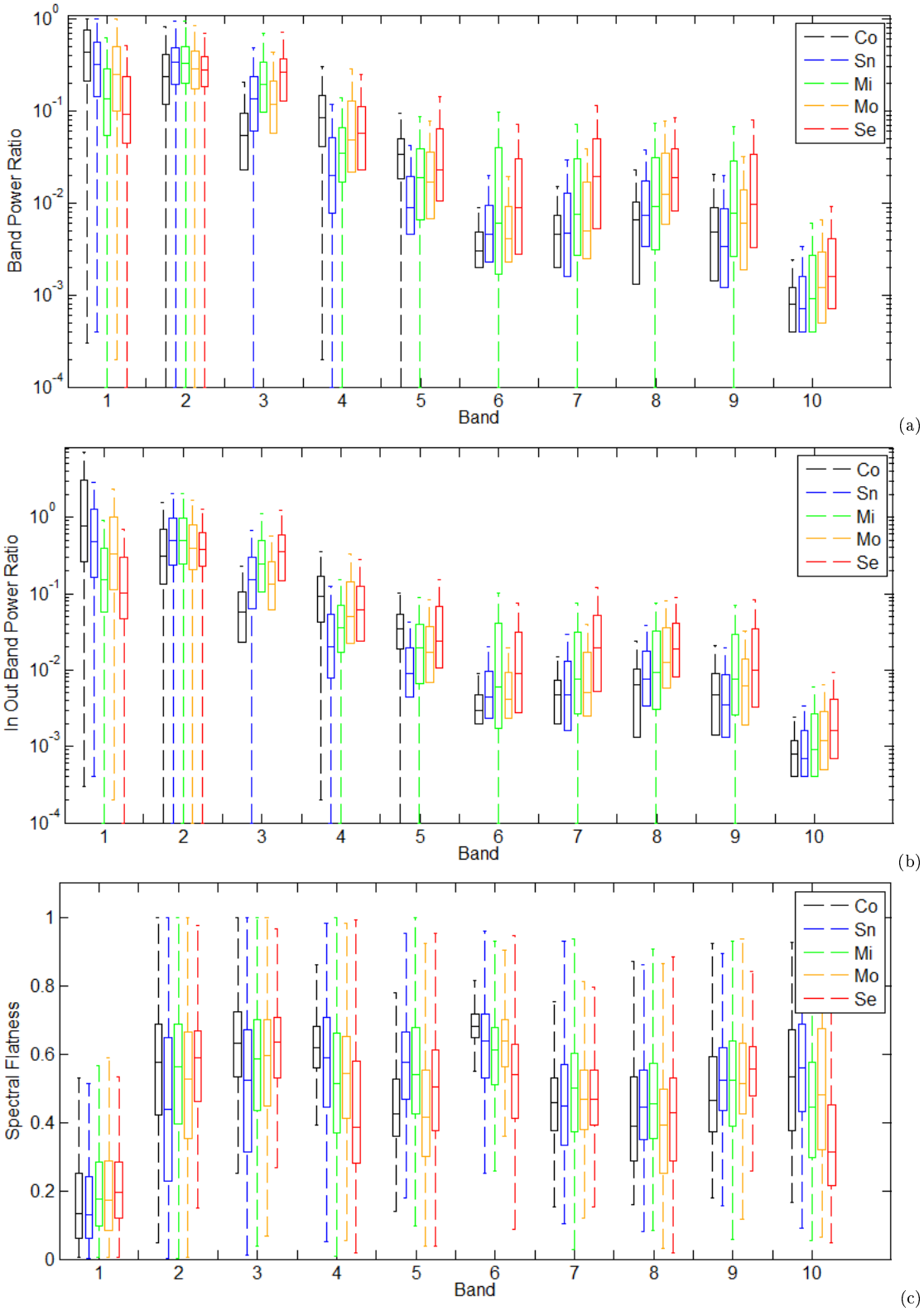

Figure 5.49: The full range of frequencies, from the application of Welch's method in each snore, was divided in 10 bands, using a logarithmic, base 10, scale. The scale goes from 0 Hz to the maximum frequency retrieved, from each snore, in the full range. In this graphic data are, also, organized in the respective medical classification group of each patient, Co, Sn, Mi, Mo and Se. Data in (a) is the ratio between the sum of PSD values inside the band and the total sum of PSD values. The difference from (a) to (b) is that in (b) the ratio is between the sum of PSD values inside the band and the sum of PSD values outside the band. Figure (c) is the spectral flatness for each band. Outliers are not visible.

5.13 Synchrosqueezed Wavelet Transform

SWT method application to a time-domain signal results in a Na by N matrix, with N the number of samples of the time-domain signal and Na the number of scales calculated by Matlab using the formula,

$$Na = 32 \cdot (floor(log_2(numel(X))) - 1) \tag{5.2}$$

where *floor* and *numel* are Matlab functions, respectively, to round a value to the closest lower integer value and to calculate the number of elements of a matrix, in this case a vector, and variable X is the time-domain signal. An example of the transformation of a time-domain signal to the time-frequency plane is in Figure 5.50, with blue colour representing the lowest energy data, while higher energy values were located in the time interval, roughly, between 0.5 s and 1.3 s. This time interval matches the snore location in time and those frequencies characterize this snore.

IFs calculation searched for the frequencies with the maximum energy in each sample of the signal in the independent axis, to calculate the first 10 IFs. So, at each time instant t, the method searched for the 10 highest energies. An example of the IFs calculation is at Figure 5.51, in which a specific frequency range did not hold its position in the same IF. This means, at time instant, t, a frequency range may be in the first IF, the highest energy value, and a few moments later it can be in a different IF. The analysis of the entire picture, Figure 5.51, allowed the identification of the frequency ranges generated while the snore existed.

IFs decomposition identifies the most important frequencies belonging to a specific snore sound, but each frequency has a finite width associated, and Figure 5.52 shows an example of a snore sound histogram decomposition. Snore sound characteristic frequencies were calculated from the respective histogram, with frequencies

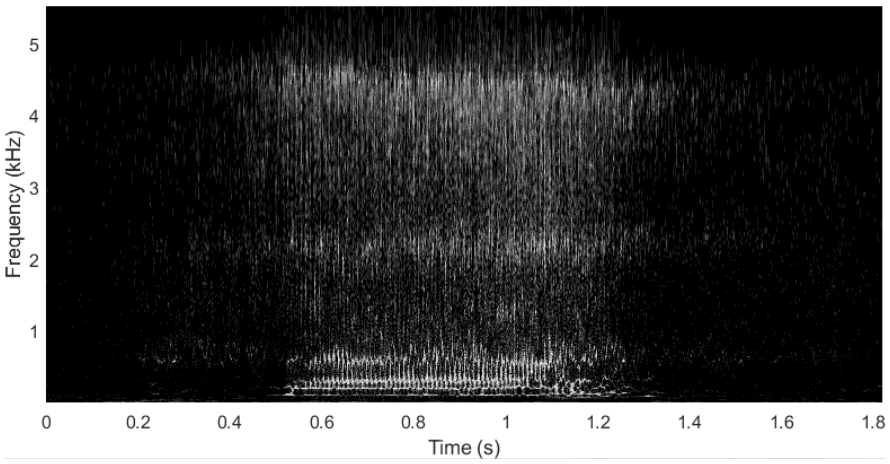

Figure 5.50: The calculation of the time-frequency plane of a snore signal, in the time domain, using SWT. SWT was applied to the snore as well as to the previously 0.5 s and the following 0.5 s of data around the snore. The snore region, between 0.5 s and 1.3 s, had higher energy values.

below 50 Hz discarded. The calculation made use of an upper envelope to remove low amplitude peaks.

SWT method was implemented to decompose 33383 snores, resulting in 319300 frequencies, and the corresponding histogram identifies the most promising frequencies to characterize each medical classification group. Co, Sn, Mi, Mo and Se medical classification groups contributed, respectively, with 19999, 89815, 66363, 85078 and 58045 frequencies. Six histograms in Figure 5.53 present frequency distribution, one for the overall frequency distribution (Figure 5.53 (a)) and the remaining 5 correspond to a different medical classification group (Figure 5.53 (b) to Figure 5.53 (f)). Each histogram has frequencies highlighted from baseline and they are characteristic of its medical classification group. Those highlighted frequencies were selected and marked with red dots, becoming candidates to be defined as a characterization frequency for the group to which belong. The list of those frequencies is in Table 5.31, where the frequency organization relies on the frequency difference between them. A frequency difference less or equal to 20 Hz was considered to be the same frequency

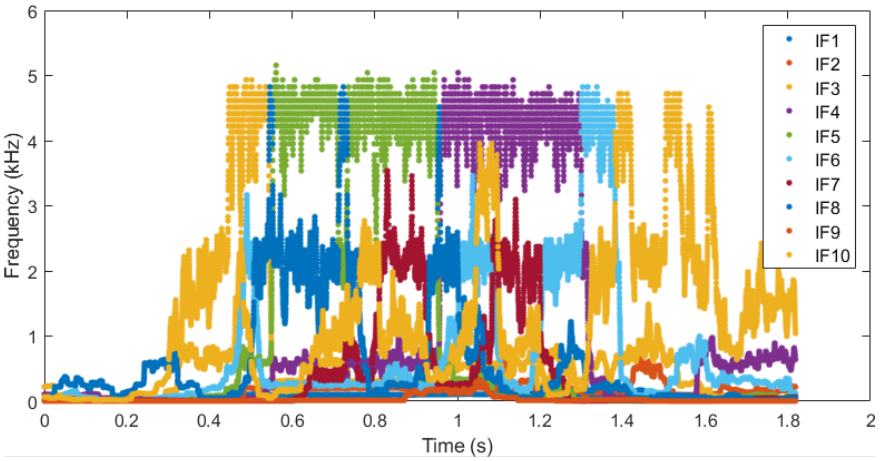

Figure 5.51: The first 10 instantaneous frequencies extracted from the time-frequency plane. These frequencies are the most important, once they have higher energy values, at each instant t.

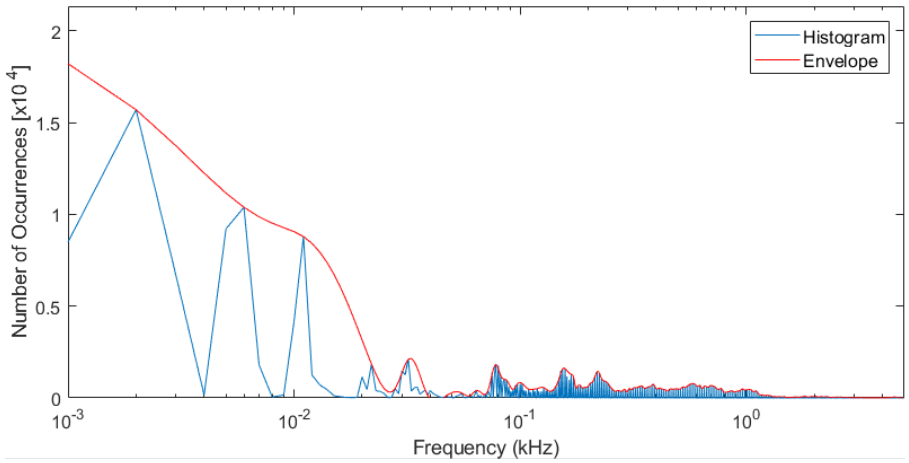

Figure 5.52: A histogram of frequencies of a single snore, blue. Data to build the histogram come from the 10 IFs. The upper envelope, red, filters low amplitude peaks.

among the different medical classification groups, in which frequencies unique to a single medical classification group were the true candidates to be a characterization frequency. The 4377 Hz frequency is an example of a frequency unique to a medical classification group, in this case, the Se group. The number of patients and the weight of their contributions were analysed, for each one of those candidates.

An algorithm searched for all the frequencies, and respective patients, with the exact value of each unique frequency, and Table 5.32 summarizes the performed analysis, and the results show a heterogeneous distribution. There were unique frequencies, strongly, supported by a single patient, as in the case of the 4113 Hz frequency, in Co group. Just 2 patients gave a contribution to this frequency, with the highest contribution being 77.8%. Other unique frequencies were more interesting because more patients gave a contribution and the contribution's weight of a single patient is lower. A good example for this case is the third frequency, 2320 Hz, of the Mo group, in which the highest contributive weight is 28.6% and, almost, all the patients of that group contributed (11 of 13).

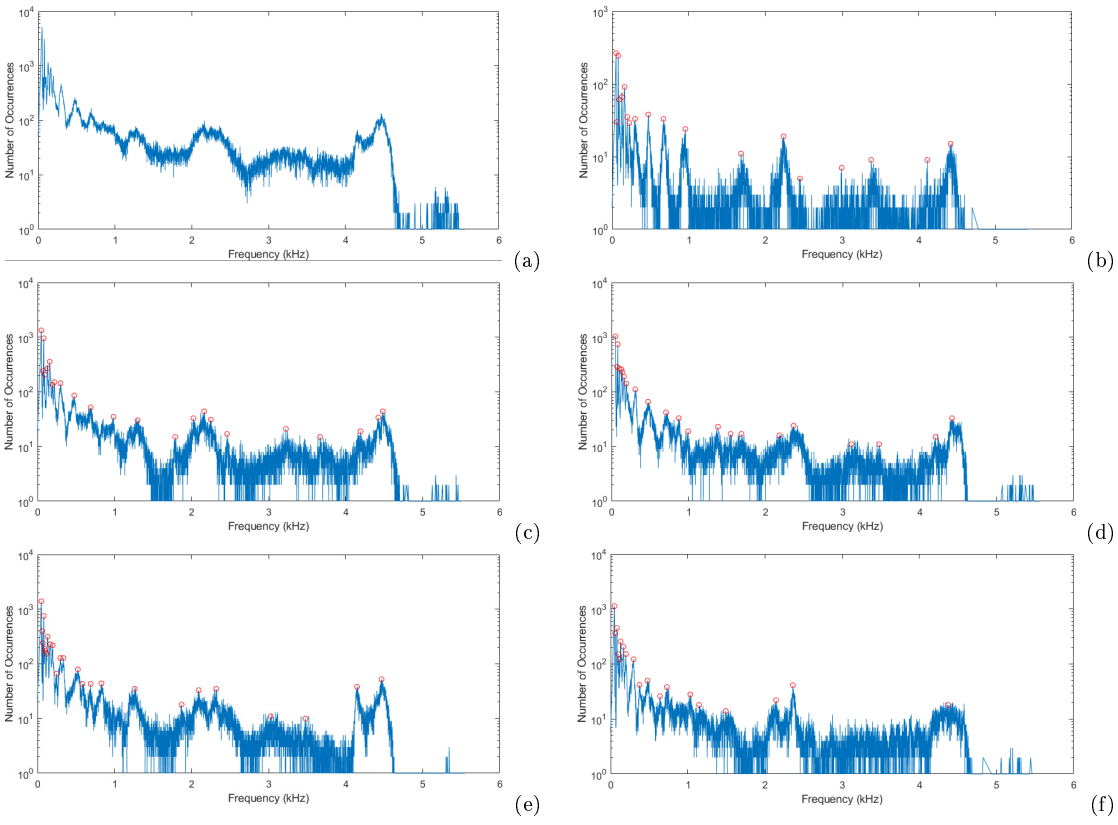

Figure 5.53: Six histograms, in blue, representing different cases of frequency distribution. The frequencies were selected from the first histogram performed for each snore. Histogram (a) contains frequencies from all patients. Histograms (b), (c), (d), (e) and (f) contain, only, frequencies of Co, Sn, Mi, Mo and Se patients, respectively. Red dots are the dominant frequencies in each medical classification group.

Table 5.31: Dominant frequencies of each medical group.

Frequency (Hz)									
Non-OSAHS		*OSAHS*			*Non-OSAHS*		*OSAHS*		
Co	Sn	Mi	Mo	Se	Co	Sn	Mi	Mo	Se
	4482		4466						1146
4416	4425	4419							1033
				4377		987	996		
	4194	4206			956				
			4147				873		
4113								831	
	3669								730
		3475	3478		671	690	708	690	
3380									641
	3224							583	
		3115						524	
			3027		473	478	475		478
2996									373
2452	2461							336	
		2364		2362	300	298	309	296	298
			2320					248	
2237	2250				225	219			
	2164	2180		2145	199	195	194	198	199
			2093		163	158	162	162	167
	2025						140		
			1870		128	129	129	131	129
	1789							118	117
1682		1687					101	102	102
		1545			93	92		94	
				1492	81	81	81	81	82
		1382				70	71	69	
	1300				64			63	60
			1263		52	50	50	50	50

Table 5.32: A statistical summary about the selected frequencies, i. e., highlighted frequencies present in, just, one of the medical groups. The table presents statistical information about the contributions that lead those frequencies to highlight from the baseline. The same row does not represent the same frequency value, and medical classification group frequency sets are unrelated. The first row is reserved for the highest frequency, with their values, in each column, in descending order. The elements in the % columns point the highest contribution, in percentage value, of a single patient for that frequency. The columns N tell the number of patients with that frequency. Only frequencies with the exact value of the selected frequency were considered.

	Non-OSAHS				**OSAHS**					
Frequency	*Co*		*Sn*		*Mi*		*Mo*		*Se*	
Order	%	N	%	N	%	N	%	N	%	N
1^{st}	77.8	2	53.3	5	36.4	6	65.8	6	44.4	4
2^{nd}	66.7	2	42.9	8	29.4	6	27.3	7	42.9	4
3^{rd}	42.9	4	33.3	8	47.8	7	28.6	11	38.9	5
4^{th}	54.2	4	66.7	5	75.8	5	39.4	7	50.0	6
5^{th}			20.0	10	30.7	11	27.8	9	39.5	5
6^{th}							34.3	8	38.5	5
7^{th}							38.6	6	69.0	5
8^{th}							44.2	8		
9^{th}							24.1	10		
10^{th}							32.0	11		
11^{th}							37.9	9		

Chapter 6

Discussion

The Discussion chapter is dedicated to the interpretation of the results, and the discussion of the significance of the findings in the light of what is currently known to science.

6.1 Slow Variation Parameters

Figure 5.2 and Figure 5.3 give a clear picture about the gauge pressure trend. Its low variability is pretty steady during the day and over the weeks of data acquisition, with, according to Figure 5.2, higher variability during the first daylight hours. During the weeks of data acquisition, gauge pressure values distribution also presents an IQR>0, especially in week 16, with different values for each quartile. The decrease of gauge pressure, observed in Figure 5.2, matches patients awakening, from PSG study, and CMS opening to receive patients for daily medical appointments. Doors and windows open and air flows inside the building, leading to fluctuations in pressure.

The silicon gauge pressure MPXV7007 sensor has a working range of ±7 kPa, which is far away from being achieved. After signal filtering and amplification, using hardware, the gauge pressure data range 5 Pa. To improve signal resolution, the selection of a gauge pressure sensor with a lower range is required. NXP has a silicon gauge pressure sensor with a lower range in its portfolio, the MPXV7002, with a working range of ±2 kPa, which may be not enough. Other brands may have better solutions, but they were not investigated. The poor signal resolution has an immediate consequence, the impossibility of using this data to compare with other data, both clinical and non-clinical data. Figure 5.3 has no data for week 26 because during this time interval no acquisition was made in the laboratory.

Indoor temperatures play an important role in health, where too low or too high temperatures are not comfortable and present a hazard to human health. Cold temperatures inflame the respiratory system and may contribute to worsening respiratory diseases, like asthma or Chronic Obstructive Pulmonary Diseases. It also

promotes vasoconstriction, which can promote cardiovascular diseases, among them are strokes and coronary heart disease. World Health Organization recommended a low indoor temperature limit of 18°C, in 2018.

High temperatures also play a role in the quality of life, with the body's response to high temperatures, and its capacity to cool, being a decisive factor to perceive it as comfortable or not. External factors, like relative humidity, influence the capability to decrease body temperature. In respiratory and cardiovascular patients, children and older subjects are more susceptible to higher temperatures. World Health Organization recommendation for a high-temperature limit is not defined, and several studies point to different upper acceptable limits. The World Health Organization guideline presents multiple studies with upper limits ranging from 25°C to 30°C, with the Mediterranean cities presenting an average of 29.4°C [380]. Following those limits, Figure 5.4, in section 5.1, shows that 95.4% of the temperature records are in the range between 18°C and 29°C, the temperature comfort range, and suitable for the realization of PSG studies.

Results for the gauge pressure data fluctuation at the first hours of the day, the consequence of opening doors and windows of the CMS, are confirmed by the temperatures, with a sharper decrease in temperature around 8 a.m. Relative humidity readings also decrease at this time of the day.

Temperature and relative humidity fluctuations in weeks 17 (higher median and IQR) and 25 (higher IQR) are remarkably different from the remaining weeks. Each week under analysis has the device acquiring data for 2 days. To justify these differences, an analysis of the environmental conditions is presented, with the help of historical data. Weather recordings for the time under analysis came from 2 different sources [381,382]. One of the sources, [382], has records from a nearby city in the district of Coimbra, Cernache, located at the latitude of 40.1500° N and the longitude of -8.4670° W, elevation 179 m. It has consistent records of temperature maximum values. The second source returns data for the city of Coimbra, never referring to which weather station is and its location, but, rather, presenting a list of nearby weather stations. Maximum and minimum values are consistently presented in the second source.

The analysis to week 17 reveals a temperature maximum value of 33°C for day 1 and of 28°C for day 2, accordingly with [382], and of 32°C for day 1 and of 27°C for day 2, accordingly with [381]. Temperature minimum values are also available in the second source, with values of 16°C and 14°C for day 1 and day 2, respectively. A decrease in the maximum temperature of 5°C helps explain the high variability in temperature, but without a register with low periods of data acquisition, a relationship can not be completely established. Week 25 has an increase in temperature from day 1 to day 2, with a temperature maximum value of 29°C for day 1 and of

34°C for day 2, accordingly with [382], and of 29°C for day 1 and of 33°C for day 2, accordingly with [381]. The second source reports minimum temperatures of 15°C and 18°C, respectively. Week 25 has a change in temperature of the same magnitude as week 17, accordingly to [382], which can also explain the high variability in temperature. No daily registers were found to analyse relative humidity data with official records.

The XY plot for the relationship between temperature and relative humidity every week shows no interesting relationship between them, but the hour basis XY plot presents a hysteresis curve. After midnight, temperature decreases due to low human activity, patients start the study around midnight, and relative humidity increases, human presence may explain the rise. At the end of the PSG study, and when CMS opens, temperature decreases faster in the following couple of hours, going along with the decrease in the relative humidity. In the middle of the morning, the temperature starts to increase, a probability due to the increase in the environmental/external temperature, and the relative humidity keeps falling, sharply after lunch. Relative humidity reaches stable values around 17h, and until 21h, which matches the time interval pause in the CMS to attend patients. After the pause, 21h, the night shift starts to do PSG studies, and the relative humidity keeps raising. The temperature continues to increase, probably due to the presence of patients, sleep technicians, and undergraduate students.

6.2 PSG Scoring

Manual scoring presents a challenge to the sleep medicine field, without a completely inter-scorer agreement among sleep technicians. Human error is also a concern, with the possibility of missing the score of some epochs. Here, the number of unclassified epochs reaches 0.01%, below 5% are not considered to influence results [383], and they were dropped, instead of imputation.

Sleep architecture changes considerable, considering the medical classification mean, in Se patients. Although there aren't statistically significant differences for each sleep stage, among medical classification groups, there is an evident increase in the N1 sleep stage and an evident decrease in the N3 sleep stage for Se class. Accordingly, with these results, OSAHS starts to have an impact on sleep immediately, with the N3 sleep stage mean value decreasing as the disorder severity worsens. Co and Sn subjects have similar mean N3 sleep stage values, respectively 26.2% and 27.2%, decreasing a little in Mi and Mo patients, to 24.2% and 22.7% respectively. Se patients have half of the N3 sleep stage, when compared to Co subjects, with a mean value of 13.1%. N1 sleep stage is the second sleep stage with changes, in this case, only for the Se group, with a mean value of 33.7%, against the 17.5% for Co subjects. Sleep architecture modifications have an impact on several body functions,

such as the case of memory and immune function impairment.

Snoring and OSAHS severity are sleep position-dependent, with the back sleep position the worst to snore and to promote obstruction of the respiratory upper airway. Overall, the back position is the favourite position to sleep, with 42.9% of the epochs recorded with the body in such position. Sleep position therapy may improve the quality of sleep by reducing both snoring and OSAHS, and it may be the case with Se group. Patients of this group have the smallest percentage of sleep in the back position, but still very high, and sleep position therapy can be more implemented in this group, but also Mi and Mo patients. Starting early with the therapy may postpone the evolution of the symptoms (snoring), and the progression of OSAHS.

Higher IQR (Figure 5.14 (a)) in sleep stage awake, 21 bpm, suggests more irregularity in the heart rate rhythm. IQR may be higher in the awake stage due to the body's response to arousals, and the need to stabilize O_2 levels in the blood by increasing airflow. During the other sleep stages, IQR is very regular, with a value of 16 bpm for all but the N1 sleep stage, with a value of 17 bpm. Their mean values, and standard deviation, supports the heart rate variability during sleep. The mean and standard deviation values, in mean descending order, are 70.3 ± 14.8, 67.8 ± 12.6, 67.1 ± 12.4, 64.9 ± 12.7, 64.1 ± 13.9 bpm, for awake, REM, N1, N2 and N3 stages, respectively. Sleep stage order in mean heart rate follows the expected results, with higher values when awake, followed by REM sleep, where brain activity is higher than in NREM, to consolidate memory and adjust emotional responses. NREM sleep has the lower heart rates, with a decrease in muscle activity, from light to deep sleep, and lower O_2 requirements. Processes like tissue repair and cell regeneration occur at this point.

Pulse oximetry records present a high number of 0 value readings (visible in Figure 5.13 (b)), probably due to the detachment of this device from the finger. The analysis of valid pulse oximetry data shows no statistically significant differences between all sleep stage groups, only N1 and N2 are, and the reason could be related to the need to keep the concentration of O_2 high at any time. The relationship between pulse oximetry and medical classification groups is more interesting, with a clear decrease as OSAHS worsens. OSAHS worsens and obstructive events increase in number and duration, which means a decrease in blood O_2 saturation for longer periods, with important consequences for human health.

6.3 High-Quality Sound Signal

The data distribution deviation from 0 is most likely related to the conditions in which the calibration of the device took place, its microphones, and the conditions for data acquisition. This project targets the high-quality sound signal to find the

most important relationships between medical data and research data, to develop new methods to diagnosis OSAHS, and to hasten its treatment. Its pre-processing is of fundamental importance, with the energy calculation, filtering techniques, and sound events detection. Preliminary results reduce the number of candidates, detected by the Gaussian fit model from 507904 to a final number 51458 of snore sounds, which means a rejection of 89.9%. The electronic interference noise rejection algorithm uses 2 thresholds, and their global means are very similar to the mean values calculated for each medical classification group. This observation is expected since the calculation was performed in the first minutes of data acquisition when the patient is awake, and for that reason not snoring. The cumulative energy is higher in Mi medical classification group due to 2 patients, since both patients had longer conversations with sleep technicians, just after the beginning of sound acquisition.

A comparison between snore detection methods, the project's method, and Bellauer's method shows a high performance of the implemented method for this project, surpassing it in almost all parameters under analysis. With higher specificity and sensitivity values, the method better discards non-snore signals and identifies snore signals, respectively. The mid-p-value definition of McNemar's test confirmed the existence of significant differences between the methods, for both sensitivity and specificity. The test justifies the implementation of the new method to detect snores and to avoid the misidentification of noise as snores, improving the results achieved with Bellauer's method.

6.4 Data Synchronization and Snore Pairing

Single-channel-based automatic algorithm for the detection of pause-resume sequences in the PSG studies performs better than a multi-channel-based automatic algorithm. The single-channel-based automatic algorithm works with SpO_2 data, which has a behaviour similar to an on/off interrupt when the sequence occurs. The PSG software responds to a pause-resume sequence waiting for the completion of data acquisition for the current epoch. SpO_2 data are usually close to the maximum value of 100%, and when the software resumes data acquisition its values drop to 0% for a few ms. SpO_2 binary-like behaviour simplifies algorithm data analysis and improves results of the multi-channel-based automatic algorithm, which searches for data discontinuities, and their detection in several channels.

Synchronization between PSG and high-quality sound signal data splits PSG data in clusters using single-channel-based automatic algorithm results to detect pause-resume sequences. A cluster, from patient ID 120, represents a particular case since one of the pause resume sequences occurred in an advanced stage of PSG data acquisition. The synchronization of the last cluster was not performed because the pause was at a time instant 24390 s, while high-quality sound signal data acquisition

stops after 24493.4 s, already taking into account the synchronizations previously performed. The high-quality sound signal remaining total time was solely 103.4 s and it is very likely that after this time the PSG data acquisition was still halted. Even if the PSG data acquisition resumes before the high-quality sound signal ends, the remaining time was too short to perform a good synchronization. Nevertheless, the patient was awake after the pause resume sequence at a time instant 24390 s, and no research interest exist for the purpose of the thesis. The following results do not take into account this particular pause.

A higher number of snores may help get better synchronization results, and the number of snores per patient is directly proportional to OSAHS severity. Achieved results do not confirm this assumption, with examples of some of the highest snore densities falling to return good synchronization results. Coarse synchronization faces a problem, intrinsic to data acquisition with 2, or more, devices with different acquisition clocks. Devices' clocks have errors associated, which have implications in the modification of their nominal frequency, and a complete synchronization in the entire cluster is very hard. Reduced cluster duration is one more factor to fail a good synchronization, with some clusters last only a few hundred seconds, once there isn't enough time to patients fall asleep and snore. Co subjects snore almost nothing, with implications in the cross-correlation method, and in the desired synchronization.

Snore pairing finds the final pair match of both registers, with the required adjustments from the final synchronization process. The mean number of snores per patient increases, as expected, with the increase of OSAHS severity. However, not all the pairs have their boundaries successfully calculated, resulting in the rejection of those pairs, and in the decrease of snores available to perform feature extraction. An increase in OSAHS severity keeps meaning an increase in the mean number of snores per patient.

6.5 Feature Extraction and Analysis

Time-domain features show a direct link between the number of snores and their duration in time and OSAHS severity. A patient classified having a Se type of OSAHS snores more and they last longer than the other types of OSAHS, and non-OSAHS subjects, classified either as Co or as Sn. Anatomical modifications of the upper respiratory airway may explain this observation, with a decrease in tissue stiffness, and the decrease in neuromotor control also interferes with the correct function of the structure. Regardless of the conditions behind the increase of OSAHS, amplitude and PtP amplitude do not behave with the same relationship. This suggests that these 2 types of amplitudes are independent of OSAHS severity, with a remarkable increase only in the Se group. Energy feature copies both amplitude features when analysed taking into account the patients' medical classification group,

although energy definition does not rely on a single acquisition, as is the case of amplitude. Energy and both amplitude similar behaviour suggest that the evolution of snores throughout the medical classification groups is continuous as long as it lasts, and not just an instantaneous response.

Kurtosis and skewness are statistical tools to evaluate data distribution, and the results obtained for each medical classification group point to heavy tails, or to the existence of a large number of outliers, while the skewness has low mean values, suggesting the existence of symmetrical data distribution among all medical classification groups. However, the standard deviation of the skewness for each medical classification group is high, but still inside the range for symmetrical data distribution.

EMD is a method to get the fundamental components of a signal without leaving the time domain. When studying EMD components, its application in snore sounds reveal a higher amplitude in IMF components 5 to 7. Each IMF presents a boxplot consistently different from all the other boxplots. The Se group has higher parameter values than the other medical classification groups, which is also consistent with the results obtained for both amplitude features. Snore signal periodicity was the second parameter retrieved from the EMD method. Naturally, the components' period increases for higher IMF, but there isn't evidence of a trend between the periodicity and the medical classification group of each IMF. When studying EMD in amplitude ranges or period bands, values increases as the range/band increases, but inside the same range/band, no important differences were visible.

Shannon entropy was calculated for 3 different scenarios, and the achieved results point to no differences, with data organized accordingly with the patients' medical classification group, among them, which led to the selection of data inside snores' boundaries. Entropy distribution led to the selection of 2 particular parameters, p_{75p} and p_{25p}, among each patient with the boxplot of each medical classification group for the $p_{75p} - p_{25p}$ showing a striking efficiency in discriminating the OSAHS severity. All the parameters in this statistical distribution have an almost monotonic behaviour, and are strongly correlated to the OSAHS severity, although with a small deviation in the case of the Mi class. The combination of parameters, from the statistical distribution in Figure 5.42, proves to be even more valuable to assess OSAHS severity. The results for the $p_{50c} - p_{25c}$ calculation present a very interesting relationship with OSAHS severity, with an increase in the $p_{50c} - p_{25c}$ difference meaning worsening OSAHS severity. The introduction of the correction factor $\frac{IQR}{p_{75c}}$ eliminates the Mi class minimal deviation, and creates a strong correlation between OSAHS severity and wp_{25c} and wp_{50c} parameters. The coefficient of determination is close to 1 and positive, meaning a strong positive, direct, relationship between both parameters.

The first 4 frequency features under analysis follow the same pattern of the Shannon entropy feature, with the deviation in the frequencies from the Mi group restraining a strong relationship between these features and the OSAHS severity. A deeper analysis of the contribution of each patient to the medical classification group overall results revels that both Mi median and IQR standard deviation have some of the smaller values, which may rule out the possibility of a single, or a low number of, the patient be responsible for the Mi behaviour, in the evolution of the highest PSD frequency feature. From the following 3 frequency features under analysis, central frequency has no interesting link to OSAHS, but the other 2, coefficient of symmetry and frequency standard deviation, are related to the medical classification group with the Sn group exception. Sn group has a lower standard deviation, in both features, which may point to the absence of a single, or a low number of, patients causing the fluctuation in the trend. From the 3 remaining frequency-domain features, 2 of them (band power ratio and in and out band power ratio) present interesting results, with 3 bands, 4, 8, and 10, presenting a strong relationship with OSAHS severity.

SWT method is relatively recent and widely unexplored in the sleep medicine study. The decomposition of the time-domain signal to the time-frequency plane offers an alternative to the better-known methods. In this work, SWT delivers the decomposition of the snoring sound in its IMF, and the final result delivers frequencies specific to a medical classification group.

6.6 Integrative Discussion

Not all features tend to have a trend as OSAHS worsens, which means they are most likely of no scientific interest, at least, to use as a OSAHS predictor. Sleep stage data distribution among medical classification groups is an example of a feature without interest to study OSAHS, with hypothesis testing results revealing no significant difference among those groups (results point to all the data coming from the same distribution).

Features with significant differences only among some medical classification groups should be analysed more carefully. For example, features like SpO_2 aren't ideal to study sleep stages (only significant differences in N1 and N2 sleep stages), and features like amplitude, PtP amplitude and energy aren't ideal to study medical classification groups (all features have all groups but Co and Mo coming from different distributions). Heart rate showed interesting results and it can be considered a promising feature in sleep assessment (in this case to assess OSAHS severity). The hypothesis testing for this feature points to significant differences only in OSAHS patients (Mi, Mo, and Se medical classification groups). Although not ideal (significant differences aren't for all medical classification groups), it has the best results for the OSAHS patients groups, which are the most important ones.

The most interesting features are the ones presenting significant differences for all groups. Heart rate is an example of significant differences among all sleep stages. Significant differences among all medical classification groups were found for the SpO_2, time duration, and Shannon entropy feature. The time duration feature has a consistent evolution throughout the medical classification groups, with values always increasing. Shannon entropy presented the same pattern after some adjustments to data.

Two methods deliver the most important contributions to science in this thesis, and they were Shannon entropy and SWT. Shannon entropy results are very interesting since no other study shows that entropy is so well related with OSAHS severity in the parameters selected, which results in a candidate to develop a tool to access this syndrome. SWT is a recent method, with a small global implementation in all research fields, which includes OSAHS sleep study field.

Chapter 7

Conclusion

Conclusion chapter presents the most relevant remarks, which features or methods have promising results to continue development in future work. Finally, a research contribution section lists papers published.

7.1 General Overview

OSAHS is a serious worldwide medical condition, with a significant incidence, but a lack of awareness by the general population. The disorder's typical evolution spans several years, and both OSAHS patients and, usually, their families underestimate symptoms and misidentify them as a normal evolution. Media coverage should raise awareness but other medical conditions receive more attention, such as the case of cardiovascular diseases and diabetes, probably due to their impact on morbidity and mortality. Sleep and its associated disorders play a critical role in body and mind functioning, with sleep contributing to the normal function of several organs, tissues, and biochemical processes. Fighting and preventing OSAHS and other SRBD bring extra benefits to heath, once it is proven to exist a link between sleep quality and those diseases.

The data acquisition final list has 67 subjects, organized into 5 medical classification groups, which represents a good number when compared with other researches. Most of them have a similar number of subjects, but there are studies with higher numbers (in order of thousand) but, also, with a lower number (in order of a dozen) of subjects. Observation of OSAHS impact in sleep structure confirms what is already known, especially, with modifications in N1 and N3 sleep stages weight in the overall sleep, which means disturbances in the subjects' physiology. The well-known influence of the sleep position in OSAHS is confirmed by the achieved results, with the back position worsening sleep apnoea, increasing AHI, than other positions. The study confirms the back position as the preferred position, which means the importance of sleep medicine physicians to invest time with the patient, explaining their concerns and encouraging them to implement techniques to avoid the worst posi-

tion to sleep. OSAHS consequences exist and corroborating evidence of its health impairment was found in data for this thesis. Obstructive events lead to a decrease in SpO_2 and the higher the number of events, which means an increase in OSAHS severity, the higher is the overall impact in the final SpO_2 distribution. Heart rate increases when the body responds to an obstructive event, and data distribution follow the increase in OSAHS severity, with higher values as the disorder worsens. SpO_2 and heart rate data also follow the pattern described in the literature.

SVP data were the focus on several sleep studies to address their influence on sleep and its disorders, but here, data were used to access patients' sleep conditions. SVP weren't compared with medical data, but gauge pressure doesn't show promising results, mainly due to the sensor, with a gauge pressure range much higher than the real range required. Data from the remaining 2 SVP, relative humidity and temperature, point to data acquisition inside the recommended relative humidity and temperature limits, bringing comfort to the patient and, consequently, quality to the acquisition itself.

Sleep centres face a reproducibility sleep problem, with the first night effect. Together with the use of sensors attach to the skin, the patient's sleep could be modified and the study may not record a typical night of sleep. Remote sensing presents an advantage over other acquisition devices, data acquisition doesn't require skin contact and, consequently, is less likely to interfere with the patient's sleep. Tracking sounds by using an energy-based algorithm allows the implementation of a fast method to enhance sound events, with the help of filters, a high-pass filter, and a low-pass filter, to smooth the energy array (removing low amplitude peaks and merging close peaks) and to highlight higher sound amplitudes. Gaussian fit isn't a fast method to detect sound events, with overlapping explaining part of the time consumed in the process, but it has the advantage of fitting properly the windowing points, the window size takes into account the average breathing frequency of a human being at rest, and potentially returning a sound event, and discarding close local maxima. The sound events filtering process lowers the confirmation rate of sound events and is identified by the Gaussian fit, specially in healthy and snoring subjects. Sound detection algorithm comparison with a reference algorithm proves the quality of the detection and rejection steps, with better performance in the 4 parameters analysed, sensibility, sensitivity, PPV, and NPV. With very good specificity, the algorithm guarantees that almost all noise is rejected. Sensitivity doesn't achieve the level of specificity, but, it still, is a good value for snore detection and, although it isn't ideal, the final high number of snores has a good snore population to study each medical classification group.

Data synchronization was of critical importance to relate medical data with research data, and the manual register of pause-resume sequences would help complete

the task. The goal wasn't achieved probably due to tiredness, in-laboratory sleep studies are prepared and performed during the night shift, and sleep technicians' main concern, is the correct functioning of PSG data acquisition. The lack of a complete pause-resume sequence list led to the development of a pause-resume sequence automatic detection algorithm, which performed very well to do synchronization in 2 steps. The synchronization leads successfully to 2 problems, a consequence of having 2 clock-independent acquisition devices, the first is the data acquisition initial offset and additional middle offsets. The first automatic synchronization has pragmatic issues which required manual intervention to improve synchronization at the beginning of the cluster. An answer to this intervention may reside in the second problem, approached next. The second problem is related to the intrinsic characteristic associated with the crystal oscillator, frequency errors, responsible to deliver a constant frequency for the device to work properly. The synchronization allows the study of relationships between snores' features and medical data, as in the case of different medical events. Snore density can't explain why some automatic synchronization did not perform so well, but a possible explanation is related to low amplitude snores.

An increase in OSAHS severity means more snoring, but, also, means each snore lasts for more time, which may be related to the loss of muscular tone. These pieces of evidence confirm the results presented in other scientific papers. Other features present interesting relationships with OSAHS severity, which is the case of Kurtosis, Shannon entropy, and band 8 of both band power ratio and in and out band power ratio. Considering 2 major subgroups, OSAHS, grouping Mi, Mo and Se medical classification groups, and non-OSAHS, grouping Co and Sn medical classification groups, features present promising results for the OSAHS subgroup. Coefficient of symmetry, frequency standard deviation, band 4 and 10 of both band power ratio and in and out band power ratio belong to this group of features.

Although not fully exploited, and it should be done in the future, previously named features are serious candidates to develop future solutions to help physicians in the prevention and diagnosis of OSAHS.

7.2 Main Remarks

During the development of the work, several methods were exploited to know which ones could be used in OSAHS prediction. Most of them fail to deliver interesting results, as in the case of features like amplitude, energy, and Skewness of snores. The following remarks summarize the best results achieved for the different methods and features implemented in the work.

- **Remark 1:** Snore's time duration shows partial, but important results. Although statistical results don't reveal a clear separation among all medical

classification groups, the most important groups have it. Data from the OSAHS groups, Mi, Mo, and Se, come from different distributions, and they have a consistent evolution as OSAHS worsens, snore's mean time duration evolves from 1.106, 1.178, 1.227, 1.368, to 1.493 s, for Co, Sn, Mi, Mo, and Se groups, respectively.

- **Remark 2:** Snore's Shannon entropy delivers the most promising results for an immediately practicable application. Shannon entropy's mean values don't follow a consistent evolution in OSAHS. The calculation of the Shannon entropy solely was of 3.489, 3.665, 3.857, 3.732, and 3.954 bits, for data inside snore's boundaries and for Co, Sn, Mi, Mo, Se medical classification groups, respectively. Nevertheless, statistical results points to significant differences among all groups. Further development over Shannon entropy used box plot, and its parameters wp_{25c} and wp_{50c} to analyse data distribution. The implementation of correction factors deliver a consistent evolution of all medical classification groups (figure 5.43). Parameter wp_{25c} values are 2.539, 4.254, 4.599, 7.967, and 19.938 bits, while wp_{50c} has values of 6.198, 8.233, 10.101, 14.043, and 39.374 bits. Both parameters' values are ordered by increase OSAHS severity.

- **Remark 3:** SWT is a recently proposed method to do signal decomposing in the time-frequency plane and is barely used in the sleep medicine field and, in particular, in snoring. The work identified characteristic frequencies specific to each medical classification group, and well represented, in terms of the number of patients. These frequencies, and the method itself, are an important contribution to science. An example of those characteristic is 2996, 1300, 1545, 2320, and 1146 Hz, for the Co, Sn, Mi, Mo, and Se, respectively.

The work provides data and guidelines for the use of snoring signals in the sleep medicine field to evaluate OSAHS. Finally, it answers affirmatively to the questions raised in 1.4, showing the possibility of distinguishing OSAHS using a single PSG channel, in this case, acquired with an independent device with better audio specs. Several different features deliver interesting results to do OSAHS assessment, which confirms snore signal as a reliable source of information.

7.3 Future Work

Sleep importance is well documented and tackling its disorders, specifically OSAHS, should be a top priority in medicine. Improving sleep awareness should focus on 2 areas: preventing new cases and tackling the existing ones. Sleep prioritization should start with the youngest at school and home, with programs to create

healthy sleep patterns and food ingestion, and to educate in physical training. Media coverage of the health-related subject and its diseases should raise awareness of more diseases, besides the most common ones, such as the case of cardiovascular diseases, diabetes, and cancer. The second area of intervention is to track and tackle the disorder by specialists in the sleep medicine field. PSG multi-parametric gold standard study is the best tool available to monitor OSAHS and to help physicians understand the subject's sleep pattern, however, it has a high cost.

Monitoring OSAHS with remote sensing has the advantage of not interfering with a patient's sleep and it does not have the risk of invalid data due to skin detachment. A device should be developed with hardware capability to acquire sound and perform digital signal processing, to do feature extraction and analysis, including in the development of the most promising features discovered in this project. Before implementing this step, a new phase should be implemented to confirm the results of this thesis, using a larger set of patients, and, preferably, including patients from the original set, to evaluate their evolution as the disorders worsen or stay stable, in the same medical classification group.

PSG and its medical reports generate a huge amount of data, with the only part being used for the thesis, and more extensive and exhaustive analysis and correlation with research data may reveal important links. Snores' features should be compared with epoch-based scoring medical data, as in the case of scoring medical events, heart rate, or SpO_2. The comparison should be implemented between snores' features in epochs of consecutive lack of medical events with snores' features in epochs with the presence of medical events. The evaluation of the snores' features should also be performed immediately before and immediately after medical events. The most promising methods and features found in this work should be further exploited to confirm the findings.

New SVP data acquisition should go along with new sound acquisitions, but the first version of the SVP board must be replaced by an improved, second version. The second version must include hardware improvements, including an upgrade to improve gauge pressure signal resolution. SVP data processing only relates the different SVP variables, while future efforts should study relationships between these variables and relevant medical data.

The effort invested in the development of areas such as robotic and artificial intelligence, and present-day real-life examples give an idea of a future where machines replace a human being in routine or complex tasks. Sleep medicine will probably rely one day on these areas, and PSG scoring algorithms will improve their quality to deliver human-like trustworthy reports. Sleep monitoring benefits from the development of hardware to acquire and process data, to incorporate more complex and better algorithms. To achieve this goal, huge databases should exist to develop

artificial intelligence algorithms.

7.4 Research Contribution

In this section, a list of the contributions made during the period of time dedicated to the development of this work is as follows:

1. Marçal, T. A. S., dos Santos, J. M., Rosa, A., and Cardoso, J. M. R., OSAS assessment with entropy analysis of high resolution snoring audio signals, *Biomedical Signal Processing and Control 61* (Aug 2020), 101965. DOI: 10.1016/j.bspc.2020.101965

2. Marçal, T., Antunes, B., Ferreira, R., Correia, C., Pires, D., Matos, A., and Simões, J. N., Wireless Multi-Physiological Signal Monitor for Clinical Discharge and Readmissions Criteria Setting and Ambulatory Usage, *Proceeding of 2015 IEEE 4th Portuguese Meeting on Bioengineering (ENBENG)* (Feb 2015), pp. 1-6. DOI: 10.1109/ENBENG.2015.7088846

3. Marçal, T., Simões, J. B., dos Santos, J. M., Rosa, A. R., and Cardoso, J., Snoring Analysis on Full Night Recordings based in the Energy and Entropy in PSG Basal Studies, *Proceedings of BIOSIGNALS 2013 6th International Conference on Bio-Inspired Systems and Signal Processing* (Feb 2013), pp. 221-227. DOI: 10.5220/0004245202210227

Bibliography

[1] J. M. Shneerson, *Sleep Medicine: A Guide to Sleep and its Disorders*. John Wiley & Sons, second ed., Feb. 2005.

[2] W. C. Dement, "History of sleep medicine," *Neurologic Clinics*, vol. 23, pp. 945–965, Nov 2005.

[3] M. H. Kryger, T. Roth, and W. C. Dement, *Principles and practice of sleep medicine*. Philadelphia, PA: Saunders, fifth ed., 2011.

[4] T. Lee-Chiong, *Sleep medicine : essentials and review*. Oxford New York: Oxford University Press, first ed., 2008.

[5] S. Diekelmann and J. Born, "The memory function of sleep," *Nature Reviews Neuroscience*, vol. 11, pp. 114–126, Jan 2010.

[6] L. Besedovsky, T. Lange, and J. Born, "Sleep and immune function," *Pflügers Archiv - European Journal of Physiology*, vol. 463, pp. 121–137, Nov 2011.

[7] P. E. Peppard, T. Young, J. H. Barnet, M. Palta, E. W. Hagen, and K. M. Hla, "Increased prevalence of sleep-disordered breathing in adults," *American Journal of Epidemiology*, vol. 177, pp. 1006–1014, Apr 2013.

[8] A. V. Benjafield, N. T. Ayas, P. R. Eastwood, R. Heinzer, M. S. M. Ip, M. J. Morrell, C. M. Nunez, S. R. Patel, T. Penzel, J.-L. Pépin, P. E. Peppard, S. Sinha, S. Tufik, K. Valentine, and A. Malhotra, "Estimation of the global prevalence and burden of obstructive sleep apnoea: a literature-based analysis," *The Lancet Respiratory Medicine*, vol. 7, pp. 687–698, Aug 2019.

[9] J. A. Fiz, J. Abad, R. Jané, M. Riera, M. A. Mañanas, P. Caminal, D. Rodenstein, and J. Morera, "Acoustic analysis of snoring sound in patients with simple snoring and obstructive sleep apnoea," *European Respiratory Journal*, vol. 9, pp. 2365–2370, Nov 1996.

[10] A. Levartovsky, E. Dafna, Y. Zigel, and A. Tarasiuk, "Breathing and snoring sound characteristics during sleep in adults," *Journal of Clinical Sleep Medicine*, vol. 12, pp. 375–384, Mar 2016.

[11] World Health Organization, "The top 10 causes of death," Dec. 2020.

[12] World Health Organization, "Cardiovascular diseases," Mar. 2021.

[13] World Health Organization, "Diabetes," Mar. 2021.

[14] W. D. Duckitt, S. K. Tuomi, and T. R. Niesler, "Automatic detection, segmentation and assessment of snoring from ambient acoustic data," *Physiological Measurement*, vol. 27, pp. 1047–1056, Sep 2006.

[15] S.-F. Liang, C.-E. Kuo, Y.-H. Hu, and Y.-S. Cheng, "A rule-based automatic sleep staging method," *Journal of Neuroscience Methods*, vol. 205, pp. 169–176, Mar 2012.

[16] M. K. Moridani, M. Heydar, and S. S. J. Behnam, "A reliable algorithm based on combination of EMG, ECG and EEG signals for sleep apnea detection : (a reliable algorithm for sleep apnea detection)," in *2019 5th Conference on Knowledge Based Engineering and Innovation (KBEI)*, pp. 256–262, IEEE, Feb 2019.

[17] J. M. Kang, S. T. Kim, S. Mariani, S.-E. Cho, J. W. Winkelman, K. H. Park, and S.-G. Kang, "Difference in spectral power density of sleep EEG between patients with simple snoring and those with obstructive sleep apnoea," *Scientific Reports*, vol. 10, pp. 1–8, Apr 2020.

[18] H. Pasterkamp, S. S. Kraman, and G. R. Wodicka, "Respiratory sounds," *American Journal of Respiratory and Critical Care Medicine*, vol. 156, pp. 974–987, Sep 1997.

[19] A. Oliveira and A. Marques, "Respiratory sounds in healthy people: A systematic review," *Respiratory Medicine*, vol. 108, pp. 550–570, Apr 2014.

[20] R. Loudon and R. L. H. M. Jr., "Lung sounds," *American Review of Respiratory Disease*, vol. 130, pp. 663–673, Dec 1984.

[21] M. Sarkar, I. Madabhavi, N. Niranjan, and M. Dogra, "Auscultation of the respiratory system," *Annals of Thoracic Medicine*, vol. 10, p. 158, Jul 2015.

[22] S. Reichert, R. Gass, C. Brandt, and E. Andrès, "Analysis of respiratory sounds: State of the art," *Clinical medicine. Circulatory, respiratory and pulmonary medicine*, vol. 2, pp. 45–58, Jan 2008.

[23] R. X. A. Pramono, S. Bowyer, and E. Rodriguez-Villegas, "Automatic adventitious respiratory sound analysis: A systematic review," *PLOS ONE*, vol. 12, p. e0177926, May 2017.

[24] R. B. Berry, *Fundamentals of Sleep Medicine*. Elsevier, first ed., 2012.

[25] T. J. Barkoukis and A. Y. Avidan, *Review of sleep medicine*. Philadelphia: Butterworth-Heinemann, second ed., 2007.

[26] A. Eban-Rothschild, L. Appelbaum, and L. de Lecea, "Neuronal mechanisms for sleep/wake regulation and modulatory drive," *Neuropsychopharmacology*, vol. 43, pp. 937–952, Dec 2017.

[27] J. Aschoff, "Circadian control of body temperature," *Journal of Thermal Biology*, vol. 8, pp. 143–147, Jan 1983.

[28] K. Kräuchi, "How is the circadian rhythm of core body temperature regulated?," *Clinical Autonomic Research*, vol. 12, pp. 147–149, Jun 2002.

[29] C. O'Reilly, F. Chapotot, F. Pittau, N. Mella, and F. Picard, "Nicotine increases sleep spindle activity," *Journal of Sleep Research*, vol. 28, p. e12800, Dec 2018.

[30] C. Guilleminault, *Handbook of Clinical Neurophysiology: Clinical neurophysiology of sleep disorders*, vol. 6. Edinburgh New York: Elsevier, first ed., 2005.

[31] S. Chokroverty, *Sleep disorders medicine : basic science, technical considerations, and clinical aspects*. Philadelphia: Saunders/Elsevier, third ed., 2009.

[32] E. V. Cauter, "Age-related changes in Slow Wave Sleep and REM sleep and relationship with growth hormone and cortisol levels in healthy men," *JAMA*, vol. 284, pp. 861–868, Aug 2000.

[33] S. Redline, H. L. Kirchner, S. F. Quan, D. J. Gottlieb, V. Kapur, and A. Newman, "The effects of age, sex, ethnicity, and sleep-disordered breathing on sleep architecture," *Archives of Internal Medicine*, vol. 164, pp. 406–418, Feb 2004.

[34] K. R. Peters, L. B. Ray, S. Fogel, V. Smith, and C. T. Smith, "Age differences in the variability and distribution of sleep spindle and rapid eye movement densities," *PLoS ONE*, vol. 9, p. e91047, Mar 2014.

[35] J. F. A. Schwarz, T. Åkerstedt, E. Lindberg, G. Gruber, H. Fischer, and J. Theorell-Haglöw, "Age affects sleep microstructure more than sleep macrostructure," *Journal of Sleep Research*, vol. 26, pp. 277–287, Jan 2017.

[36] D. L. Reed and W. P. Sacco, "Measuring sleep efficiency: What should the denominator be?," *Journal of Clinical Sleep Medicine*, vol. 12, pp. 263–266, Feb 2016.

[37] A. Didikoglu, A. Maharani, G. Tampubolon, M. M. Canal, A. Payton, and N. Pendleton, "Longitudinal sleep efficiency in the elderly and its association with health," *Journal of Sleep Research*, vol. 29, pp. 1–11, Jul 2019.

[38] B. A. Mander, J. R. Winer, and M. P. Walker, "Sleep and human aging," *Neuron*, vol. 94, pp. 19–36, Apr 2017.

[39] L. Kuula, A.-K. Pesonen, K. Heinonen, E. Kajantie, J. G. Eriksson, S. Andersson, A. Lano, J. Lahti, D. Wolke, and K. Räikkönen, "Naturally occurring circadian rhythm and sleep duration are related to executive functions in early adulthood," *Journal of Sleep Research*, vol. 27, pp. 113–119, Jul 2017.

[40] J. F. Duffy, S. W. Cain, A.-M. Chang, A. J. K. Phillips, M. Y. Munch, C. Gronfier, J. K. Wyatt, D.-J. Dijk, K. P. Wright, and C. A. Czeisler, "Sex difference in the near-24-hour intrinsic period of the human circadian timing system," *Proceedings of the National Academy of Sciences*, vol. 108, pp. 15602–15608, May 2011.

[41] M. L. Moline, L. Broch, R. Zak, and V. Gross, "Sleep in women across the life cycle from adulthood through menopause," *Sleep Medicine Reviews*, vol. 7, pp. 155–177, Apr 2003.

[42] B. Rasch and J. Born, "About sleep's role in memory," *Physiological Reviews*, vol. 93, pp. 681–766, Apr 2013.

[43] J. Born, "Slow-wave sleep and the consolidation of long-term memory," *The World Journal of Biological Psychiatry*, vol. 11, pp. 16–21, Jan 2010.

[44] Y. Dudai, A. Karni, and J. Born, "The consolidation and transformation of memory," *Neuron*, vol. 88, pp. 20–32, Oct 2015.

[45] C. Smith, "Sleep states and memory processes in humans: procedural versus declarative memory systems," *Sleep Medicine Reviews*, vol. 5, pp. 491–506, Dec 2001.

[46] S. Ackermann and B. Rasch, "Differential effects of non-REM and REM sleep on memory consolidation?," *Current Neurology and Neuroscience Reports*, vol. 14, pp. 1–10, Jan 2014.

[47] Y. Wei, G. P. Krishnan, M. Komarov, and M. Bazhenov, "Differential roles of sleep spindles and sleep slow oscillations in memory consolidation," *PLOS Computational Biology*, vol. 14, p. e1006322, Jul 2018.

[48] J. Westermann, T. Lange, J. Textor, and J. Born, "System consolidation during sleep - a common principle underlying psychological and immunological memory formation," *Trends in Neurosciences*, vol. 38, pp. 585–597, Oct 2015.

[49] R. M. Benca and J. Quintans, "Sleep and host defenses: A review," *Sleep*, vol. 20, pp. 1027–1037, Nov 1997.

[50] T. Lange, B. Perras, H. L. Fehm, and J. Born, "Sleep enhances the human antibody response to Hepatitis A vaccination," *Psychosomatic Medicine*, vol. 65, pp. 831–835, Sep 2003.

[51] S. Banks and D. F. Dinges, "Behavioral and physiological consequences of sleep restriction," *Journal of Clinical Sleep Medicine*, vol. 03, pp. 519–528, Aug 2007.

[52] M. Tiihonen, M. Partinen, and S. Närvänen, "The severity of obstructive sleep apnoea is associated with insulin resistance," *Journal of Sleep Research*, vol. 2, pp. 56–61, Mar 1993.

[53] K. Spiegel, R. Leproult, and E. V. Cauter, "Impact of sleep debt on metabolic and endocrine function," *The Lancet*, vol. 354, pp. 1435–1439, Oct 1999.

[54] L. F. Drager, S. M. Togeiro, V. Y. Polotsky, and G. Lorenzi-Filho, "Obstructive sleep apnea," *Journal of the American College of Cardiology*, vol. 62, pp. 569–576, Aug 2013.

[55] S. Pamidi, K. Wroblewski, J. Broussard, A. Day, E. C. Hanlon, V. Abraham, and E. Tasali, "Obstructive sleep apnea in young lean men: Impact on insulin sensitivity and secretion," *Diabetes Care*, vol. 35, pp. 2384–2389, Aug 2012.

[56] M. Pauly, A. Assense, A. Rondon, A. Thomas, H. Dubouchaud, D. Freyssenet, H. Benoit, J. Castells, and P. Flore, "High intensity aerobic exercise training improves chronic intermittent hypoxia-induced insulin resistance without basal autophagy modulation," *Scientific Reports*, vol. 7, pp. 1–12, Mar 2017.

[57] D. Morgan and S. C. Tsai, "Sleep and the endocrine system," *Sleep Medicine Clinics*, vol. 11, pp. 115–126, Mar 2016.

[58] T. A. Bedrosian, L. K. Fonken, and R. J. Nelson, "Endocrine effects of circadian disruption," *Annual Review of Physiology*, vol. 78, pp. 109–131, Feb 2016.

[59] R. J. Berger and N. H. Phillips, "Energy conservation and sleep," *Behavioural Brain Research*, vol. 69, pp. 65–73, Jul 1995.

[60] C. M. Jung, E. L. Melanson, E. J. Frydendall, L. Perreault, R. H. Eckel, and K. P. Wright, "Energy expenditure during sleep, sleep deprivation and sleep following sleep deprivation in adult humans," *The Journal of Physiology*, vol. 589, pp. 235–244, Nov 2010.

[61] M. Engle-Friedman, "The effects of sleep loss on capacity and effort," *Sleep Science*, vol. 7, pp. 213–224, Dec 2014.

[62] A. R. Tall and S. Jelic, "How broken sleep promotes cardiovascular disease," *Nature*, vol. 566, pp. 329–330, Feb 2019.

[63] N. T. Ayas, D. P. White, J. E. Manson, M. J. Stampfer, F. E. Speizer, A. Malhotra, and F. B. Hu, "A prospective study of sleep duration and coronary heart disease in women," *Archives of Internal Medicine*, vol. 163, pp. 205–209, Jan 2003.

[64] C. Sabanayagam and A. Shankar, "Sleep duration and cardiovascular disease: Results from the national health interview survey," *Sleep*, vol. 33, pp. 1037–1042, Aug 2010.

[65] S. Aggarwal, R. S. Loomba, R. R. Arora, and J. Molnar, "Associations between sleep duration and prevalence of cardiovascular events," *Clinical Cardiology*, vol. 36, pp. 671–676, Oct 2013.

[66] A. Knutsson, B. Jonsson, T. Akerstedt, and K. Orth-Gomer, "Increased risk of ischaemic heart disease in shift workers," *The Lancet*, vol. 328, pp. 89–92, Jul 1986.

[67] K. Katsumata, T. Okada, M. Miyao, and Y. Katsumata, "High incidence of sleep apnea syndrome in a male diabetic population," *Diabetes Research and Clinical Practice*, vol. 13, pp. 45–51, Jan 1991.

[68] M. Yokoba, H. G. Hawes, T. M. Kieser, M. Katagiri, and P. A. Easton, "Parasternal intercostal and diaphragm function during sleep," *Journal of Applied Physiology*, vol. 121, pp. 59–65, Apr 2016.

[69] S. Fleming, M. Thompson, R. Stevens, C. Heneghan, A. Plüddemann, I. Maconochie, L. Tarassenko, and D. Mant, "Normal ranges of heart rate and respiratory rate in children from birth to 18 years of age: a systematic review of observational studies," *The Lancet*, vol. 377, pp. 1011–1018, Mar 2011.

[70] J. A. Rowley, B. R. Zahn, M. A. Babcock, and M. S. Badr, "The effect of rapid eye movement (REM) sleep on upper airway mechanics in normal human subjects," *The Journal of Physiology*, vol. 510, pp. 963–976, Aug 1998.

[71] E. B. Simon and M. P. Walker, "Sleep loss causes social withdrawal and loneliness," *Nature Communications*, vol. 9, pp. 1–9, Aug 2018.

[72] L. A. Rico-Uribe, F. F. Caballero, N. Martín-María, M. Cabello, J. L. Ayuso-Mateos, and M. Miret, "Association of loneliness with all-cause mortality: A meta-analysis," *PLOS ONE*, vol. 13, p. e0190033, Jan 2018.

[73] E. Mignot, "Why we sleep: The temporal organization of recovery," *PLoS Biology*, vol. 6, p. e106, Apr 2008.

[74] E. C. Harding, N. P. Franks, and W. Wisden, "The temperature dependence of sleep," *Frontiers in Neuroscience*, vol. 13, pp. 1–16, Apr 2019.

[75] V. M. Kumar, "Body temperature and sleep: Are they controlled by the same mechanism?," *Sleep and Biological Rhythms*, vol. 2, pp. 103–124, Jun 2004.

[76] P. Montgomery, "A systematic review of non-pharmacological therapies for sleep problems in later life," *Sleep Medicine Reviews*, vol. 8, pp. 47–62, Feb 2004.

[77] M. Chennaoui, P. J. Arnal, F. Sauvet, and D. Léger, "Sleep and exercise: A reciprocal issue?," *Sleep Medicine Reviews*, vol. 20, pp. 59–72, Apr 2015.

[78] K. A. Kubitz, D. M. Landers, S. J. Petruzzello, and M. Han, "The effects of acute and chronic exercise on sleep," *Sports Medicine*, vol. 21, pp. 277–291, Apr 1996.

[79] J. M. Dzierzewski, M. P. Buman, P. R. Giacobbi, B. L. Roberts, A. T. Aiken-Morgan, M. Marsiske, and C. S. McCrae, "Exercise and sleep in community-dwelling older adults: evidence for a reciprocal relationship," *Journal of Sleep Research*, vol. 23, pp. 61–68, Aug 2013.

[80] V. Garfield, C. H. Llewellyn, and M. Kumari, "The relationship between physical activity, sleep duration and depressive symptoms in older adults: The English Longitudinal Study of Ageing (ELSA)," *Preventive Medicine Reports*, vol. 4, pp. 512–516, Dec 2016.

[81] C. J. Yao and M. Basner, "Healthy behaviors competing for time: associations of sleep and exercise in working Americans," *Sleep Health*, vol. 5, pp. 23–30, Feb 2019.

[82] D. W. Wetter and T. B. Young, "The relation between cigarette smoking and sleep disturbance," *Preventive Medicine*, vol. 23, pp. 328–334, May 1994.

[83] A. Jaehne, T. Unbehaun, B. Feige, U. C. Lutz, A. Batra, and D. Riemann, "How smoking affects sleep: A polysomnographical analysis," *Sleep Medicine*, vol. 13, pp. 1286–1292, Dec 2012.

[84] H. Morioka, M. Jike, H. Kanda, Y. Osaki, S. Nakagome, Y. Otsuka, Y. Kaneita, O. Itani, S. Higuchi, and T. Ohida, "The association between sleep disturbance and second-hand smoke exposure: a large-scale, nationwide, cross-sectional study of adolescents in Japan," *Sleep Medicine*, vol. 50, pp. 29–35, Oct 2018.

[85] I. O. Ebrahim, C. M. Shapiro, A. J. Williams, and P. B. Fenwick, "Alcohol and sleep i: Effects on normal sleep," *Alcoholism: Clinical and Experimental Research*, vol. 37, pp. 539–549, Jan 2013.

[86] M. V. Vitiello, "Sleep, alcohol and alcohol abuse," *Addiction Biology*, vol. 2, pp. 151–158, Apr 1997.

[87] T. Roehrs and T. Roth, "Sleep, sleepiness, sleep disorders and alcohol use and abuse," *Sleep Medicine Reviews*, vol. 5, pp. 287–297, Aug 2001.

[88] B. Feige, H. Gann, R. Brueck, M. Hornyak, S. Litsch, F. Hohagen, and D. Riemann, "Effects of alcohol on polysomnographically recorded sleep in healthy subjects," *Alcoholism: Clinical and Experimental Research*, vol. 30, pp. 1527–1537, Sep 2006.

[89] T. Roehrs and T. Roth, "Caffeine: Sleep and daytime sleepiness," *Sleep Medicine Reviews*, vol. 12, pp. 153–162, Apr 2008.

[90] H.-P. Landolt, J. V. Rétey, K. Tönz, J. M. Gottselig, R. Khatami, I. Buckelmüller, and P. Achermann, "Caffeine attenuates waking and sleep electroencephalographic markers of sleep homeostasis in humans," *Neuropsychopharmacology*, vol. 29, pp. 1933–1939, Jul 2004.

[91] C. Drake, T. Roehrs, J. Shambroom, and T. Roth, "Caffeine effects on sleep taken 0, 3, or 6 hours before going to bed," *Journal of Clinical Sleep Medicine*, vol. 09, pp. 1195–1200, Nov 2013.

[92] H.-P. Landolt, E. Werth, A. A. Borbély, and D.-J. Dijk, "Caffeine intake (200 mg) in the morning affects human sleep and EEG power spectra at night," *Brain Research*, vol. 675, pp. 67–74, Mar 1995.

[93] N. S. Chaudhary, M. A. Grandner, N. J. Jackson, and S. Chakravorty, "Caffeine consumption, insomnia, and sleep duration: Results from a nationally representative sample," *Nutrition*, vol. 32, pp. 1193–1199, Nov 2016.

[94] I. Clark and H. P. Landolt, "Coffee, caffeine, and sleep: A systematic review of epidemiological studies and randomized controlled trials," *Sleep Medicine Reviews*, vol. 31, pp. 70–78, Feb 2017.

[95] I. S. Santos, A. Matijasevich, and M. R. Domingues, "Maternal caffeine consumption and infant nighttime waking: Prospective cohort study," *Pediatrics*, vol. 129, pp. 860–868, Apr 2012.

[96] S. C. Ho and J. W. Y. Chung, "The effects of caffeine abstinence on sleep: A pilot study," *Applied Nursing Research*, vol. 26, pp. 80–84, May 2013.

[97] T. Roehrs and T. Roth, "Drug-related sleep stage changes: Functional significance and clinical relevance," *Sleep Medicine Clinics*, vol. 5, pp. 559–570, Dec 2010.

[98] A. C. Reynolds and R. J. Adams, "Treatment of sleep disturbance in older adults," *Journal of Pharmacy Practice and Research*, vol. 49, pp. 296–304, May 2019.

[99] S. Wilson and D. Nutt, "Insomnia: guide to diagnosis and choice of treatment," *Prescriber*, vol. 19, pp. 14–24, May 2008.

[100] J. Guina and B. Merrill, "Benzodiazepines i: Upping the care on downers: The evidence of risks, benefits and alternatives," *Journal of Clinical Medicine*, vol. 7, p. 17, Jan 2018.

[101] E. D. Chinoy, D. J. Frey, D. N. Kaslovsky, F. G. Meyer, and K. P. Wright, "Age-related changes in slow wave activity rise time and NREM sleep EEG with and without zolpidem in healthy young and older adults," *Sleep Medicine*, vol. 15, pp. 1037–1045, Sep 2014.

[102] B. P. Hasler, L. J. Smith, J. C. Cousins, and R. R. Bootzin, "Circadian rhythms, sleep, and substance abuse," *Sleep Medicine Reviews*, vol. 16, pp. 67–81, Feb 2012.

[103] United Nations, "World Drug Report: Executive Summary - Conclusions and Policy Implications," June 2017.

[104] A. Peacock, J. Leung, S. Larney, S. Colledge, M. Hickman, J. Rehm, G. A. Giovino, R. West, W. Hall, P. Griffiths, R. Ali, L. Gowing, J. Marsden, A. J. Ferrari, J. Grebely, M. Farrell, and L. Degenhardt, "Global statistics on alcohol, tobacco and illicit drug use: 2017 status report," *Addiction*, vol. 113, pp. 1905–1926, Jun 2018.

[105] European Monitoring Centre for Drugs and Drug Addiction, "European Drug Report: Trends and Developments," June 2018.

[106] Centers for Disease Control and Prevention - National Center for Injury Prevention and Control, "Annual surveillance report of drug-related risks and outcomes," 2018.

[107] T. A. Roehrs and T. Roth, "Sleep disturbance in substance use disorders," *Psychiatric Clinics of North America*, vol. 38, pp. 793–803, Dec 2015.

[108] T. Schierenbeck, D. Riemann, M. Berger, and M. Hornyak, "Effect of illicit recreational drugs upon sleep: Cocaine, ecstasy and marijuana," *Sleep Medicine Reviews*, vol. 12, pp. 381–389, Oct 2008.

[109] P. T. Morgan, E. F. Pace-Schott, Z. H. Sahul, V. Coric, R. Stickgold, and R. T. Malison, "Sleep architecture, cocaine and visual learning," *Addiction*, vol. 103, pp. 1344–1352, Aug 2008.

[110] H. P. A. V. Dongen, G. Maislin, J. M. Mullington, and D. F. Dinges, "The cumulative cost of additional wakefulness: Dose-response effects on neurobehavioral functions and sleep physiology from chronic sleep restriction and total sleep deprivation," *Sleep*, vol. 26, pp. 117–126, Mar 2003.

[111] T. M. McMenamin, "A time to work: recent trends in shift work and flexible schedules," *Monthly Labor Review*, vol. 130, pp. 3–15, Dec 2007.

[112] D. Munafo, D. Loewy, K. Reuben, G. Kavy, and B. Hevener, "Sleep deprivation and the workplace: Prevalence, impact, and solutions," *American Journal of Health Promotion*, vol. 32, pp. 1644–1646, Aug 2018.

[113] M. Caporale, R. Palmeri, F. Corallo, N. Muscarà, L. Romeo, A. Bramanti, S. Marino, and V. L. Buono, "Cognitive impairment in obstructive sleep apnea syndrome: a descriptive review," *Sleep and Breathing*, vol. 25, pp. 29–40, May 2020.

[114] E. H. Thorarinsdottir, E. Bjornsdottir, B. Benediktsdottir, C. Janson, T. Gislason, T. Aspelund, S. T. Kuna, A. I. Pack, and E. S. Arnardottir, "Definition of excessive daytime sleepiness in the general population: Feeling sleepy relates better to sleep-related symptoms and quality of life than the Epworth Sleepiness Scale score. results from an epidemiological study," *Journal of Sleep Research*, vol. 28, p. e12852, Apr 2019.

[115] S. Garbarino, P. Durando, O. Guglielmi, G. Dini, F. Bersi, S. Fornarino, A. Toletone, C. Chiorri, and N. Magnavita, "Sleep apnea, sleep debt and daytime sleepiness are independently associated with road accidents. a cross-sectional study on truck drivers," *PLOS ONE*, vol. 11, p. e0166262, Nov 2016.

[116] C. N. Watling, "Young drivers who continue to drive while sleepy: What are the associated sleep- and driving-related factors?," *Journal of Sleep Research*, vol. 29, p. e12900, Jul 2019.

[117] M. Zhang, D. A. Tillman, and S. A. An, "Global prevalence of sleep deprivation in students and heavy media use," *Education and Information Technologies*, vol. 22, pp. 239–254, Sep 2015.

[118] M. Nasim, M. Saade, and F. AlBuhairan, "Sleep deprivation: prevalence and associated factors among adolescents in Saudi Arabia," *Sleep Medicine*, vol. 53, pp. 165–171, Jan 2019.

[119] C. Hublin, J. Kaprio, M. Partinen, and M. Koskenvuo, "Insufficient sleep - a population-based study in adults," *Sleep*, vol. 24, pp. 392–400, Jun 2001.

[120] M. Basner, "Arousal threshold determination in 1862: Kohlschütter's measurements on the firmness of sleep," *Sleep Medicine*, vol. 11, pp. 417–422, Apr 2010.

[121] S. Chokroverty and M. Billiard, *Sleep Medicine: A Comprehensive Guide to Its Development, Clinical Milestones, and Advances in Treatment*. Springer New York, first ed., Aug. 2015.

[122] W. C. Dement, "The study of human sleep: a historical perspective," *Thorax*, vol. 53, pp. S2–S7, Oct 1998.

[123] H. Davis, P. A. Davis, A. L. Loomis, E. N. Harvey, and G. Hobart, "Changes in human brain potentials during the onset of sleep," *Science*, vol. 86, pp. 448–450, Nov 1937.

[124] J. C. Leiter, "Upper airway shape: Is it important in the pathogenesis of obstructive sleep apnea?," *American Journal of Respiratory and Critical Care Medicine*, vol. 153, pp. 894–898, Mar 1996.

[125] M. Marques, P. R. Genta, S. A. Sands, A. Azarbazin, C. de Melo, L. Taranto-Montemurro, D. P. White, and A. Wellman, "Effect of sleeping position on upper airway patency in obstructive sleep apnea is determined by the pharyngeal structure causing collapse," *Sleep*, vol. 40, pp. 1–8, Jan 2017.

[126] J. Verbraecken, "Complex sleep apnoea syndrome," *Breathe*, vol. 9, pp. 372–380, Sep 2013.

[127] Y.-Y. Lin, H.-T. Wu, C.-A. Hsu, P.-C. Huang, Y.-H. Huang, and Y.-L. Lo, "Sleep apnea detection based on thoracic and abdominal movement signals of wearable piezoelectric bands," *IEEE Journal of Biomedical and Health Informatics*, vol. 21, pp. 1533–1545, Nov 2017.

[128] G. Ayoub, T. H. Dang, T. I. Oh, S.-W. Kim, and E. J. Woo, "Feature extraction of upper airway dynamics during sleep apnea using electrical impedance tomography," *Scientific Reports*, vol. 10, pp. 1637–1646, Jan 2020.

[129] B. Calabrese, F. Pucci, M. Sturniolo, P. H. Guzzi, P. Veltri, A. Gambardella, and M. Cannataro, "A system for the analysis of snore signals," *Procedia Computer Science*, vol. 4, pp. 1101–1108, May 2011.

[130] S. Javaheri, "Central sleep apnea," *Clinics in Chest Medicine*, vol. 31, pp. 235–248, Jun 2010.

[131] N. M. Punjabi, "The epidemiology of adult obstructive sleep apnea," *Proceedings of the American Thoracic Society*, vol. 5, pp. 136–143, Feb 2008.

[132] V. Ho, C. M. Crainiceanu, N. M. Punjabi, S. Redline, and D. J. Gottlieb, "Calibration model for apnea-hypopnea indices: Impact of alternative criteria for hypopneas," *Sleep*, vol. 38, pp. 1887–1892, Dec 2015.

[133] D. A. Pevernagie, B. Gnidovec-Strazisar, L. Grote, R. Heinzer, W. T. McNicholas, T. Penzel, W. Randerath, S. Schiza, J. Verbraecken, and E. S. Arnardottir, "On the rise and fall of the apnea-hypopnea index: A historical review and critical appraisal," *Journal of Sleep Research*, vol. 29, pp. 1–20, May 2020.

[134] B. Krakow, J. Krakow, V. A. Ulibarri, and N. D. McIver, "Frequency and accuracy of "RERA" and "RDI" terms in the journal of clinical sleep medicine from 2006 through 2012," *Journal of Clinical Sleep Medicine*, vol. 10, pp. 121–124, Feb 2014.

[135] T. Young, M. Palta, J. Dempsey, J. Skatrud, S. Weber, and S. Badr, "The occurrence of sleep-disordered breathing among middle-aged adults," *New England Journal of Medicine*, vol. 328, pp. 1230–1235, Apr 1993.

[136] K. A. Franklin, C. Sahlin, H. Stenlund, and E. Lindberg, "Sleep apnoea is a common occurrence in females," *European Respiratory Journal*, vol. 41, pp. 610–615, Aug 2012.

[137] E. S. Arnardottir, E. Bjornsdottir, K. A. Olafsdottir, B. Benediktsdottir, and T. Gislason, "Obstructive sleep apnoea in the general population: highly prevalent but minimal symptoms," *European Respiratory Journal*, vol. 47, pp. 194–202, Nov 2015.

[138] J. Kim, K. In, J. Kim, S. You, K. Kang, J. Shim, S. Lee, J. Lee, S. Lee, C. Park, and C. Shin, "Prevalence of sleep-disordered breathing in middle-aged Korean men and women," *American Journal of Respiratory and Critical Care Medicine*, vol. 170, pp. 1108–1113, Nov 2004.

[139] A. M. Alencar, D. G. V. da Silva, C. B. Oliveira, A. P. Vieira, H. T. Moriya, and G. Lorenzi-Filho, "Dynamics of snoring sounds and its connection with obstructive sleep apnea," *Physica A: Statistical Mechanics and its Applications*, vol. 392, pp. 271–277, Jan 2013.

[140] C. V. Senaratna, J. L. Perret, C. J. Lodge, A. J. Lowe, B. E. Campbell, M. C. Matheson, G. S. Hamilton, and S. C. Dharmage, "Prevalence of obstructive sleep apnea in the general population: A systematic review," *Sleep Medicine Reviews*, vol. 34, pp. 70–81, Aug 2017.

[141] J. P. Saboisky, N. L. Chamberlin, and A. Malhotra, "Potential therapeutic targets in obstructive sleep apnoea," *Expert Opinion on Therapeutic Targets*, vol. 13, pp. 795–809, Jun 2009.

[142] R. C. Dedhia, C. A. Rosen, and R. J. Soose, "What is the role of the larynx in adult obstructive sleep apnea?," *The Laryngoscope*, vol. 124, pp. 1029–1034, Dec 2013.

[143] C. A. Kolakowski, D. R. Rollins, T. Jennermann, A. D. Stevens, J. T. Good, J. L. Denson, and R. J. Martin, "Clarifying the link between sleep disordered breathing and tracheal collapse: a retrospective analysis," *Sleep Science and Practice*, vol. 2, pp. 1–7, Oct 2018.

[144] S. M. Umarani and P. Archana, "Computational Analysis of Respiratory Tract with 2D and 3D Models," in *2018 Fourth International Conference on Biosignals, Images and Instrumentation (ICBSII)*, pp. 206–212, IEEE, Mar. 2018.

[145] P. Lévy, M. Kohler, W. T. McNicholas, F. Barbé, R. D. McEvoy, V. K. Somers, L. Lavie, and J.-L. Pépin, "Obstructive sleep apnoea syndrome," *Nature Reviews Disease Primers*, vol. 1, p. e15015, Jun 2015.

[146] A. S. Jordan, D. G. McSharry, and A. Malhotra, "Adult obstructive sleep apnoea," *The Lancet*, vol. 383, pp. 736–747, Feb 2014.

[147] R. B. Fogel, J. Trinder, D. P. White, A. Malhotra, J. Raneri, K. Schory, D. Kleverlaan, and R. J. Pierce, "The effect of sleep onset on upper airway muscle activity in patients with sleep apnoeaversuscontrols," *The Journal of Physiology*, vol. 564, pp. 549–562, Apr 2005.

[148] A. Wellman, A. S. Jordan, A. Malhotra, R. B. Fogel, E. S. Katz, K. Schory, J. K. Edwards, and D. P. White, "Ventilatory control and airway anatomy in obstructive sleep apnea," *American Journal of Respiratory and Critical Care Medicine*, vol. 170, pp. 1225–1232, Dec 2004.

[149] T. Emoto, U. R. Abeyratne, M. Akutagawa, H. Nagashino, and Y. Kinouchi, "Feature extraction for snore sound via neural network processing," in *2007 29th Annual International Conference of the IEEE Engineering in Medicine and Biology Society*, pp. 5477–5480, IEEE, Aug 2007.

[150] D. Pevernagie, R. M. Aarts, and M. D. Meyer, "The acoustics of snoring," *Sleep Medicine Reviews*, vol. 14, pp. 131–144, Apr 2010.

[151] N. Maimon and P. J. Hanly, "Does snoring intensity correlate with the severity of obstructive sleep apnea?," *Journal of Clinical Sleep Medicine*, vol. 06, pp. 475–478, Oct 2010.

[152] W. W. Schmidt-Nowara, "Snoring in a Hispanic-American population," *Archives of Internal Medicine*, vol. 150, pp. 597–601, Mar 1990.

[153] G. T. O'Connor, B. K. Lind, E. T. Lee, F. J. Nieto, S. Redline, J. M. Samet, L. L.Boland, J. A. Walsleben, and G. L. Foste, "Variation in symptoms of sleep-disordered breathing with race and ethnicity: The sleep heart health study," *Sleep*, vol. 26, pp. 74–79, Jan 2003.

[154] A. Azarbarzin and Z. M. K. Moussavi, "Automatic and unsupervised snore sound extraction from respiratory sound signals," *IEEE Transactions on Biomedical Engineering*, vol. 58, pp. 1156–1162, May 2011.

[155] L.-A. Lee, Y.-L. Lo, J.-F. Yu, G.-S. Lee, Y.-L. Ni, N.-H. Chen, T.-J. Fang, C.-G. Huang, W.-N. Cheng, and H.-Y. Li, "Snoring sounds predict obstruction sites and surgical response in patients with obstructive sleep apnea hypopnea syndrome," *Scientific Reports*, vol. 6, pp. 1–11, Jul 2016.

[156] K. Qian, C. Janott, V. Pandit, Z. Zhang, C. Heiser, W. Hohenhorst, M. Herzog, W. Hemmert, and B. Schuller, "Classification of the excitation location of snore sounds in the upper airway by acoustic multifeature analysis," *IEEE Transactions on Biomedical Engineering*, vol. 64, pp. 1731–1741, Aug 2017.

[157] R. Ratnavadivel, D. Stadler, S. Windler, J. Bradley, D. Paul, R. D. McEvoy, and P. G. Catcheside, "Upper airway function and arousability to ventilatory challenge in slow wave versus stage 2 sleep in obstructive sleep apnoea," *Thorax*, vol. 65, pp. 107–112, Oct 2009.

[158] A. Hicks, J. M. Cori, A. S. Jordan, C. L. Nicholas, L. Kubin, J. G. Semmler, A. Malhotra, D. G. P. McSharry, and J. A. Trinder, "Mechanisms of the deep, slow-wave, sleep-related increase of upper airway muscle tone in healthy humans," *Journal of Applied Physiology*, vol. 122, pp. 1304–1312, May 2017.

[159] I. Koutsourelakis, E. Perraki, G. Zakynthinos, A. Minaritzoglou, E. Vagiakis, and S. Zakynthinos, "Clinical and polysomnographic determinants of snoring," *Journal of Sleep Research*, vol. 21, pp. 693–699, May 2012.

[160] S. Akhter and U. R. Abeyratne, "Detection of REM/NREM snores in obstructive sleep apnoea patients using a machine learning technique," *Biomedical Physics & Engineering Express*, vol. 2, pp. 1–18, Oct 2016.

[161] E. Dafna, A. Tarasiuk, and Y. Zigel, "Automatic detection of whole night snoring events using non-contact microphone," *PLoS ONE*, vol. 8, p. e84139, Dec 2013.

[162] A. Zaninelli, R. Fariello, E. Boni, L. Corda, C. Alicandri, and V. Grassi, "Snoring and risk of cardiovascular disease," *International Journal of Cardiology*, vol. 32, pp. 347–351, Sep 1991.

[163] S. A. Lee, T. C. Amis, K. Byth, G. Larcos, K. Kairaitis, T. D. Robinson, and J. R. Wheatley, "Heavy snoring as a cause of carotid artery atherosclerosis," *Sleep*, vol. 31, pp. 1207–1213, Sep 2008.

[164] A. L. Hamdan, R. Al-Barazi, A. Kanaan, W. Al-Tamimi, S. Sinno, and A. Husari, "The effect of snoring on voice: A controlled study of 30 subjects," *Ear, Nose & Throat Journal*, vol. 91, pp. 28–33, Jan 2012.

[165] S. O'Dea, "Number of smartphone users from 2016 to 2021," 2020.

[166] A. Turner, "How many smartphones are in the world?," 2020.

[167] SnoreLab, "Record your snoring," 2020.

[168] S. Ancoli-Israel, R. Cole, C. Alessi, M. Chambers, W. Moorcroft, and C. P. Pollak, "The role of actigraphy in the study of sleep and circadian rhythms," *Sleep*, vol. 26, pp. 342–392, May 2003.

[169] J. L. Martin and A. D. Hakim, "Wrist actigraphy," *Chest*, vol. 139, pp. 1514–1527, Jun 2011.

[170] Sleep as Android, "Sleep as android," Nov. 2020.

[171] SleepCycle, "Wake up easy with sleep cycle," 2020.

[172] Azumio, "Sleep time: Wake up rested with our sleep phase alarm clock and sleep analyzer," 2020.

[173] Fullpower, "The biosensing plataform company," 2020.

[174] SleepSounds, "Sound sleep - relaxing sounds and white noise health and fitness," 2020.

[175] SleepScore, "Do i snore or grind," 2020.

[176] Y. K. Choi, G. Demiris, S.-Y. Lin, S. J. Iribarren, C. A. Landis, H. J. Thompson, S. M. McCurry, M. M. Heitkemper, and T. M. Ward, "Smartphone applications to support sleep self-management: Review and evaluation," *Journal of Clinical Sleep Medicine*, vol. 14, pp. 1783–1790, Oct 2018.

[177] J. Behar, A. Roebuck, J. S. Domingos, E. Gederi, and G. D. Clifford, "A review of current sleep screening applications for smartphones," *Physiological Measurement*, vol. 34, pp. R29–R46, Jun 2013.

[178] Muse, "Eeg-powered meditation and sleep," Nov. 2021.

[179] Fitbit, "How do I track my sleep with my Fitbit device?," Nov. 2021.

[180] Fitbit, "Understand the impact of your sleep.," Nov. 2021.

[181] Garmin, "Garmin sleep score and sleep insights," Nov. 2021.

[182] Garmin, "Garmin support centerwhat is advanced sleep monitoring in garmin connect?," Nov. 2021.

[183] Oura, "Technology in the oura ring," Nov. 2021.

[184] Withings, "Sleep - sleep tracking mat," Nov. 2021.

[185] Thoracic, "Sleep related questionnaires," 2020.

[186] K. J. Klingman, C. R. Jungquist, and M. L. Perlis, "Questionnaires that screen for multiple sleep disorders," *Sleep Medicine Reviews*, vol. 32, pp. 37–44, Apr 2017.

[187] V. Ibáñez, J. Silva, and O. Cauli, "A survey on sleep questionnaires and diaries," *Sleep Medicine*, vol. 42, pp. 90–96, Feb 2018.

[188] A. B. Douglass, R. Bomstein, G. Nino-Murcia, S. Keenan, L. Miles, V. P. Zarcone, C. Guilleminault, and W. C. Dement, "The sleep disorders questionnaire i: Creation and multivariate structure of SDQ," *Sleep*, vol. 17, pp. 160–167, Mar 1994.

[189] N. C. Netzer, R. A. Stoohs, C. M. Netzer, K. Clark, and K. P. Strohl, "Using the Berlin questionnaire to identify patients at risk for the sleep apnea syndrome," *Annals of Internal Medicine*, vol. 131, pp. 485–491, Oct 1999.

[190] F. Chung, B. Yegneswaran, P. Liao, S. A. Chung, S. Vairavanathan, S. Islam, A. Khajehdehi, and C. M. Shapiro, "STOP questionnaire," *Anesthesiology*, vol. 108, pp. 812–821, May 2008.

[191] C. L. Chai-Coetzer, N. A. Antic, L. S. Rowland, P. G. Catcheside, A. Esterman, R. L. Reed, H. Williams, S. Dunn, and R. D. McEvoy, "A simplified model of screening questionnaire and home monitoring for obstructive sleep apnoea in primary care," *Thorax*, vol. 66, pp. 213–219, Jan 2011.

[192] T. E. Weaver, G. Maislin, D. F. Dinges, J. Younger, C. Cantor, S. McCloskey, and A. I. Pack, "Self-efficacy in sleep apnea: Instrument development and patient perceptions of obstructive sleep apnea risk, treatment benefit, and volition to use continuous positive airway pressure," *Sleep*, vol. 26, pp. 727–732, Sep 2003.

[193] W. W. Flemons and M. A. Reimer, "Development of a disease-specific health-related quality of life questionnaire for sleep apnea," *American Journal of Respiratory and Critical Care Medicine*, vol. 158, pp. 494–503, Aug 1998.

[194] T. E. Weaver, A. M. Laizner, L. K. Evans, G. Maislin, D. K. Chugh, K. Lyon, P. L. Smith, A. R. Schwartz, S. Redline, A. I. Pack, and D. E. Dinges, "An instrument to measure functional status outcomes for disorders of excessive sleepiness," *Sleep*, vol. 20, pp. 835–843, Oct 1997.

[195] E. R. Chasens, S. J. Ratcliffe, and T. E. Weaver, "Development of the FOSQ-10: A short version of the functional outcomes of sleep questionnaire," *Sleep*, vol. 32, pp. 915–919, Jul 2009.

[196] D. J. Buysse, C. F. Reynolds, T. H. Monk, S. R. Berman, and D. J. Kupfer, "The Pittsburgh sleep quality index: A new instrument for psychiatric practice and research," *Psychiatry Research*, vol. 28, pp. 193–213, May 1989.

[197] The International Restless Legs Syndrome Study Group, "Validation of the international restless legs syndrome study group rating scale for restless legs syndrome," *Sleep Medicine*, vol. 4, pp. 121–132, Mar 2003.

[198] D. García-Borreguero, R. Kohnen, B. Högl, L. Ferini-Strambi, G. M. Hadjigeorgiou, M. Hornyak, A. W. de Weerd, S. Happe, K. Stiasny-Kolster, V. Gschliesser, R. Egatz, B. Cabrero, B. Frauscher, C. Trenkwalder, W. A. Hening, and R. P. Allen, "Validation of the Augmentation Severity Rating Scale (ASRS): A multicentric, prospective study with levodopa on restless legs syndrome," *Sleep Medicine*, vol. 8, pp. 455–463, Aug 2007.

[199] L. Abetz, R. Arbuckle, R. P. Allen, E. Mavraki, and J. Kirsch, "The reliability, validity and responsiveness of the Restless Legs Syndrome Quality of Life questionnaire (rlsqol) in a trial population," *Health and Quality of Life Outcomes*, vol. 3, p. 79, Dec 2005.

[200] L. Abetz, S. M. Vallow, J. Kirsch, R. P. Allen, T. Washburn, and C. J. Earley, "Validation of the restless legs syndrome quality of life questionnaire," *Value in Health*, vol. 8, pp. 157–167, Mar 2005.

[201] T. Roenneberg, A. Wirz-Justice, and M. Merrow, "Life between clocks: Daily temporal patterns of human chronotypes," *Journal of Biological Rhythms*, vol. 18, pp. 80–90, Feb 2003.

[202] T. H. Monk, D. J. Buysse, K. S. Kennedy, J. M. Potts, J. M. DeGrazia, and J. M. Miewald, "Measuring sleep habits without using a diary: The sleep timing questionnaire," *Sleep*, vol. 26, pp. 208–212, Mar 2003.

[203] C. H. Bastien, A. Vallières, and C. M. Morin, "Validation of the Insomnia Severity Index as an outcome measure for insomnia research," *Sleep Medicine*, vol. 2, pp. 297–307, Jul 2001.

[204] M. W. Johns, "A new method for measuring daytime sleepiness: The Epworth Sleepiness Scale," *Sleep*, vol. 14, pp. 540–545, Nov 1991.

[205] E. Hoddes, V. Zarcone, H. Smythe, R. Phillips, and W. C. Dement, "Quantification of sleepiness: A new approach," *Psychophysiology*, vol. 10, pp. 431–436, Jul 1973.

[206] E. Mignot, R. Hayduk, J. Black, F. C. Grumet, and C. Guilleminault, "HLA DQB1*0602 is associated with cataplexy in 509 narcoleptic patients," *Sleep*, vol. 20, pp. 1012–1020, Nov 1997.

[207] S. Anic-Labat, C. Guilleminault, H. C. Kraemer, J. Meehan, J. Arrigoni, and E. Mignot, "Validation of a cataplexy questionnaire in 983 sleep-disorders patients," *Sleep*, vol. 22, pp. 77–87, Jan 1999.

[208] C. A. Kushida, "A predictive morphometric model for the obstructive sleep apnea syndrome," *Annals of Internal Medicine*, vol. 127, p. 581, Oct 1997.

[209] V. K. Kapur, D. H. Auckley, S. Chowdhuri, D. C. Kuhlmann, R. Mehra, K. Ramar, and C. G. Harrod, "Clinical practice guideline for diagnostic testing for adult obstructive sleep apnea: An american academy of sleep medicine clinical practice guideline," *Journal of Clinical Sleep Medicine*, vol. 13, pp. 479–504, Mar 2017.

[210] M. T. Smith, C. S. McCrae, J. Cheung, J. L. Martin, C. G. Harrod, J. L. Heald, and K. A. Carden, "Use of actigraphy for the evaluation of sleep disorders and circadian rhythm sleep-wake disorders: An American Academy of Sleep Medicine clinical practice guideline," *Journal of Clinical Sleep Medicine*, vol. 14, pp. 1231–1237, Jul 2018.

[211] M. R. Cowie, "Sleep apnea: State of the art," *Trends in Cardiovascular Medicine*, vol. 27, pp. 280–289, May 2017.

[212] M. H. Araghi, Y.-F. Chen, A. Jagielski, S. Choudhury, D. Banerjee, S. Hussain, G. N. Thomas, and S. Taheri, "Effectiveness of lifestyle interventions on obstructive sleep apnea (OSA): Systematic review and meta-analysis," *Sleep*, vol. 36, pp. 1553–1562, Oct 2013.

[213] N. A. Collop, "Advances in treatment of obstructive sleep apnea syndrome," *Current Treatment Options in Neurology*, vol. 11, pp. 340–348, Aug 2009.

[214] J. A. A. D. Dios and S. D. Brass, "New and unconventional treatments for obstructive sleep apnea," *Neurotherapeutics*, vol. 9, pp. 702–709, Sep 2012.

[215] A. B. Newman, G. Foster, R. Givelber, F. J. Nieto, S. Redline, and T. Young, "Progression and regression of sleep-disordered breathing with changes in weight," *Archives of Internal Medicine*, vol. 165, p. 2408, Nov 2005.

[216] Sleep Education, "Sleep apnea - treatment," 2020.

[217] Y. M. Nakao, K. Ueshima, S. Yasuno, and S. Sasayama, "Effects of nocturnal oxygen therapy in patients with chronic heart failure and central sleep apnea: CHF-HOT study," *Heart and Vessels*, vol. 31, pp. 165–172, Oct 2014.

[218] L. Spicuzza, D. Caruso, and G. D. Maria, "Obstructive sleep apnoea syndrome and its management," *Therapeutic Advances in Chronic Disease*, vol. 6, pp. 273–285, Jul 2015.

[219] P. Pavwoski and A. V. Shelgikar, "Treatment options for obstructive sleep apnea," *Neurology: Clinical Practice*, vol. 7, pp. 77–85, Nov 2016.

[220] M. Gelardi, P. Intiglietta, G. Porro, V. N. Quaranta, O. Resta, N. Quaranta, and G. Ciprandi, "Internal nasal dilator in patients with obstructive sleep apnea syndrome and treated with continuous positive airway pressure," *Acta Bio Medica Atenei Parmensis*, vol. 90, pp. 24–27, Jan 2019.

[221] C. Georgalas, "The role of the nose in snoring and obstructive sleep apnoea: an update," *European Archives of Oto-Rhino-Laryngology*, vol. 268, pp. 1365–1373, Feb 2011.

[222] M. Kohler, K. E. Bloch, and J. R. Stradling, "The role of the nose in the pathogenesis of obstructive sleep apnoea and snoring," *European Respiratory Journal*, vol. 30, pp. 1208–1215, Aug 2007.

[223] B. T. Woodson, K. P. Strohl, R. J. Soose, M. B. Gillespie, J. T. Maurer, N. de Vries, T. A. Padhya, M. S. Badr, H. sheng Lin, O. M. Vanderveken, S. Mickelson, and P. J. Strollo, "Upper airway stimulation for obstructive sleep apnea: 5-year outcomes," *Otolaryngology–Head and Neck Surgery*, vol. 159, pp. 194–202, Mar 2018.

[224] C. J. Lettieri, A. H. Eliasson, and D. L. Greenburg, "Persistence of obstructive sleep apnea after surgical weight loss," *Journal of Clinical Sleep Medicine*, vol. 04, pp. 333–338, Aug 2008.

[225] K. Sarkhosh, N. J. Switzer, M. El-Hadi, D. W. Birch, X. Shi, and S. Karmali, "The impact of bariatric surgery on obstructive sleep apnea: A systematic review," *Obesity Surgery*, vol. 23, pp. 414–423, Jan 2013.

[226] W. C. King, A. S. Hinerman, and A. P. Courcoulas, "Weight regain after bariatric surgery: a systematic literature review and comparison across studies using a large reference sample," *Surgery for Obesity and Related Diseases*, vol. 16, pp. 1133–1144, Aug 2020.

[227] Sleep Education, "Surgery - surgical procedures," 2020.

[228] G. Bertino, E. Matti, S. Migliazzi, F. Pagella, C. Tinelli, and M. Benazzo, "Acoustic changes in voice after surgery for snoring: preliminary results," *Acta Otorhinolaryngologica Italica*, vol. 26, pp. 110–114, Mar 2006.

[229] Stanford Health Care, "Positive airway pressure (PAP) therapies," 2020.

[230] M. A. Martinez-Garcia, R. Gomez-Aldaravi, J.-J. Soler-Cataluna, T. G. Martinez, B. Bernacer-Alpera, and P. Roman-Sanchez, "Positive effect of CPAP treatment on the control of difficult-to-treat hypertension," *European Respiratory Journal*, vol. 29, pp. 951–957, May 2007.

[231] N. A. Antic, P. Catcheside, C. Buchan, M. Hensley, M. T. Naughton, S. Rowland, B. Williamson, S. Windler, and R. D. McEvoy, "The effect of CPAP in normalizing daytime sleepiness, quality of life, and neurocognitive function in patients with moderate to severe OSA," *Sleep*, vol. 34, pp. 111–119, Jan 2011.

[232] A. Pataka and R. L. Riha, "Continuous positive airway pressure and cardiovascular events in patients with obstructive sleep apnea," *Current Cardiology Reports*, vol. 15, pp. 1–8, Jul 2013.

[233] J. M. Marin, S. J. Carrizo, E. Vicente, and A. G. N. Agusti, "Long-term cardiovascular outcomes in men with obstructive sleep apnoea-hypopnoea with or without treatment with continuous positive airway pressure: an observational study," *The Lancet*, vol. 365, pp. 1046–1053, Mar 2005.

[234] M. Ángel Martínez-García, J.-J. Soler-Cataluña, L. Ejarque-Martínez, Y. Soriano, P. Román-Sánchez, F. B. Illa, J. M. M. Canal, and J. Durán-Cantolla, "Continuous positive airway pressure treatment reduces mortality in patients with ischemic stroke and obstructive sleep apnea," *American Journal of Respiratory and Critical Care Medicine*, vol. 180, pp. 36–41, Jul 2009.

[235] R. N. Aurora, S. R. Bista, K. R. Casey, S. Chowdhuri, D. A. Kristo, J. M. Mallea, K. Ramar, J. A. Rowley, R. S. Zak, and J. L. Heald, "Updated adaptive servo-ventilation recommendations for the 2012 AASM guideline: "the treatment of central sleep apnea syndromes in adults: Practice parameters with an evidence-based literature review and meta-analyses"," *Journal of Clinical Sleep Medicine*, vol. 12, pp. 757–761, May 2016.

[236] R. S. Rosenberg and S. V. Hout, "The American Academy of Sleep Medicine inter-scorer reliability program: Respiratory events," *Journal of Clinical Sleep Medicine*, vol. 10, pp. 447–454, Apr 2014.

[237] U. J. Magalang, N.-H. Chen, P. A. Cistulli, A. C. Fedson, T. Gíslason, D. Hillman, T. Penzel, R. Tamisier, S. Tufik, G. Phillips, and A. I. Pack, "Agreement in the scoring of respiratory events and sleep among international sleep centers," *Sleep*, vol. 36, pp. 591–596, Apr 2013.

[238] M. Cabrero-Canosa, E. Hernandez-Canosa, and V. Moret-Bonillo, "Intelligent diagnosis of sleep apnea syndrome," *IEEE Engineering in Medicine and Biology Magazine*, vol. 23, pp. 72–81, Mar 2004.

[239] A. S. Karunajeewa, U. R. Abeyratne, and C. Hukins, "Multi-feature snore sound analysis in obstructive sleep apnea–hypopnea syndrome," *Physiological Measurement*, vol. 32, pp. 83–97, Nov 2010.

[240] M. Ronzhina, O. Janoušek, J. Kolářová, M. Nováková, P. Honzík, and I. Provazník, "Sleep scoring using artificial neural networks," *Sleep Medicine Reviews*, vol. 16, pp. 251–263, Jun 2012.

[241] T. Lajnef, S. Chaibi, P. Ruby, P.-E. Aguera, J.-B. Eichenlaub, M. Samet, A. Kachouri, and K. Jerbi, "Learning machines and sleeping brains: Automatic sleep stage classification using decision-tree multi-class support vector machines," *Journal of Neuroscience Methods*, vol. 250, pp. 94–105, Jul 2015.

[242] A. R. Hassan, S. K. Bashar, and M. I. H. Bhuiyan, "On the classification of sleep states by means of statistical and spectral features from single channel electroencephalogram," in *2015 International Conference on Advances in Computing, Communications and Informatics (ICACCI)*, pp. 2238–2243, IEEE, Aug 2015.

[243] A. A. Gharbali, S. Najdi, and J. M. Fonseca, "Investigating the contribution of distance-based features to automatic sleep stage classification," *Computers in Biology and Medicine*, vol. 96, pp. 8–23, May 2018.

[244] S. Raiesdana, "Automated sleep staging of OSAs based on ICA preprocessing and consolidation of temporal correlations," *Australasian Physical & Engineering Sciences in Medicine*, vol. 41, pp. 161–176, Feb 2018.

[245] M. O. Mendez, A. M. Bianchi, M. Matteucci, S. Cerutti, and T. Penzel, "Sleep apnea screening by autoregressive models from a single ECG lead," *IEEE Transactions on Biomedical Engineering*, vol. 56, pp. 2838–2850, Dec 2009.

[246] B. L. Koley and D. Dey, "Selection of features for detection of obstructive sleep apnea events," in *2012 Annual IEEE India Conference (INDICON)*, pp. 991–996, IEEE, Dec 2012.

[247] S. Kainulainen, J. Töyräs, A. Oksenberg, H. Korkalainen, I. O. Afara, A. Leino, L. Kalevo, S. Nikkonen, N. Gadoth, A. Kulkas, S. Myllymaa, and T. Leppänen, "Power spectral densities of nocturnal pulse oximetry signals differ in OSA patients with and without daytime sleepiness," *Sleep Medicine*, vol. 73, pp. 231–237, Sep 2020.

[248] F. Hajipour, M. J. Jozani, A. Elwali, and Z. Moussavi, "Regularized logistic regression for obstructive sleep apnea screening during wakefulness using daytime tracheal breathing sounds and anthropometric information," *Medical & Biological Engineering & Computing*, vol. 57, pp. 2641–2655, Nov 2019.

[249] Z. L. Yu and W. Ser, "Kalman smoother and its application in analysis of snoring sounds for the diagnosis of obstructive sleep apnea," in *World Congress on Medical Physics and Biomedical Engineering 2006* (R. Magjarevic and J. H. Nagel, eds.), vol. 14, pp. 1041–1044, Berlin, Heidelberg: Springer Berlin Heidelberg, 2007.

[250] B. Camcı, C. Ersoy, and H. Kaynak, "Abnormal respiratory event detection in sleep: A prescreening system with smart wearables," *Journal of Biomedical Informatics*, vol. 95, p. 103218, Jul 2019.

[251] S. T. Kuna, R. Benca, C. A. Kushida, J. Walsh, M. Younes, B. Staley, A. Hanlon, A. I. Pack, G. W. Pien, and A. Malhotra, "Agreement in computer-assisted manual scoring of polysomnograms across sleep centers," *Sleep*, vol. 36, pp. 583–589, Apr 2013.

[252] A. Malhotra, M. Younes, S. T. Kuna, R. Benca, C. A. Kushida, J. Walsh, A. Hanlon, B. Staley, A. I. Pack, and G. W. Pien, "Performance of an automated polysomnography scoring system versus computer-assisted manual scoring," *Sleep*, vol. 36, pp. 573–582, Apr 2013.

[253] S.-F. Liang, Y.-H. Shih, P.-Y. Chen, and C.-E. Kuo, "Development of a human-computer collaborative sleep scoring system for polysomnography recordings," *PLOS ONE*, vol. 14, p. e0218948, Jul 2019.

[254] A. S. Karunajeewa, U. R. Abeyratne, and C. Hukins, "Silence-breathing-snore classification from snore-related sounds," *Physiological Measurement*, vol. 29, pp. 227–243, Jan 2008.

[255] C. L. Nino, C. E. Rodriguez-Martinez, M. J. Gutierrez, R. Singareddi, and G. Nino, "Robust spectral analysis of thoraco-abdominal motion and oxymetry in obstructive sleep apnea," in *2013 35th Annual International Conference of the IEEE Engineering in Medicine and Biology Society (EMBC)*, pp. 2906–2910, IEEE, Jul 2013.

[256] S. Puskás, N. Kozák, D. Sulina, L. Csiba, and M. T. Magyar, "Quantitative EEG in obstructive sleep apnea syndrome: a review of the literature," *Reviews in the Neurosciences*, vol. 28, pp. 265–270, Apr 2017.

[257] M. M. Rahman, M. I. H. Bhuiyan, and A. R. Hassan, "Sleep stage classification using single-channel EOG," *Computers in Biology and Medicine*, vol. 102, pp. 211–220, Nov 2018.

[258] M. O. Mendez, J. Corthout, S. V. Huffel, M. Matteucci, T. Penzel, S. Cerutti, and A. M. Bianchi, "Automatic screening of obstructive sleep apnea from the ECG based on empirical mode decomposition and wavelet analysis," *Physiological Measurement*, vol. 31, pp. 273–289, Jan 2010.

[259] C. Nakayama, K. Fujiwara, Y. Sumi, M. Matsuo, M. Kano, and H. Kadotani, "Obstructive sleep apnea screening by heart rate variability-based apnea/normal respiration discriminant model," *Physiological Measurement*, vol. 40, p. 125001, Dec 2019.

[260] D. M. Carlson, E. Onal, D. W. Carley, M. Lopata, and R. C. Basner, "Palatal muscle electromyogram activity in obstructive sleep apnea.," *American Journal of Respiratory and Critical Care Medicine*, vol. 152, pp. 1022–1027, Sep 1995.

[261] Y. Dotan, G. Pillar, N. Tov, R. Oliven, U. Steinfeld, L. Gaitini, M. Odeh, A. R. Schwartz, and A. Oliven, "Dissociation of electromyogram and mechanical response in sleep apnoea during propofol anaesthesia," *European Respiratory Journal*, vol. 41, pp. 74–84, May 2012.

[262] D. Álvarez, R. Hornero, J. V. Marcos, and F. del Campo, "Multivariate analysis of blood oxygen saturation recordings in obstructive sleep apnea diagnosis," *IEEE Transactions on Biomedical Engineering*, vol. 57, pp. 2816–2824, Dec 2010.

[263] A. M. Andrés-Blanco, D. Álvarez, A. Crespo, C. A. Arroyo, A. Cerezo-Hernández, G. C. Gutiérrez-Tobal, R. Hornero, and F. del Campo, "Assessment of automated analysis of portable oximetry as a screening test for moderate-to-severe sleep apnea in patients with chronic obstructive pulmonary disease," *PLOS ONE*, vol. 12, p. e0188094, Nov 2017.

[264] P. I. Terrill, "A review of approaches for analysing obstructive sleep apnoea-related patterns in pulse oximetry data," *Respirology*, vol. 25, pp. 475–485, Jun 2019.

[265] R. G. Norman, M. M. Ahmed, J. A. Walsleben, and D. M. Rapoport, "Detection of respiratory events during NPSG: Nasal cannula/pressure sensor versus thermistor," *Sleep*, vol. 20, pp. 1175–1184, Dec 1997.

[266] M. D. Epstein, S. A. Chicoine, and R. C. Hanumara, "Detection of upper airway resistance syndrome using a nasal cannula/pressure transducer," *Chest*, vol. 117, pp. 1073–1077, Apr 2000.

[267] H.-K. Lee, J. Lee, H. Kim, J.-Y. Ha, and K.-J. Lee, "Snoring detection using a piezo snoring sensor based on hidden Markov models," *Physiological Measurement*, vol. 34, pp. N41–N49, Apr 2013.

[268] Y. Jiang, J. Peng, and X. Zhang, "Automatic snoring sounds detection from sleep sounds based on deep learning," *Physical and Engineering Sciences in Medicine*, vol. 43, pp. 679–689, May 2020.

[269] A. K. Ng, T. S. Koh, E. Baey, T. H. Lee, U. R. Abeyratne, and K. Puvanendran, "Could formant frequencies of snore signals be an alternative means for the diagnosis of obstructive sleep apnea?," *Sleep Medicine*, vol. 9, pp. 894–898, Dec 2008.

[270] S. de Silva, U. R. Abeyratne, and C. Hukins, "Impact of gender on snore-based obstructive sleep apnea screening," *Physiological Measurement*, vol. 33, pp. 587–601, Mar 2012.

[271] L.-F. Chen, C.-T. Su, K.-H. Chen, and P.-C. Wang, "Particle swarm optimization for feature selection with application in obstructive sleep apnea diagnosis," *Neural Computing and Applications*, vol. 21, pp. 2087–2096, May 2011.

[272] K. A. Dudley and S. R. Patel, "Disparities and genetic risk factors in obstructive sleep apnea," *Sleep Medicine*, vol. 18, pp. 96–102, Feb 2016.

[273] P. Y. Ktonas and A. P. Gosalia, "Spectral analysis vs. period-amplitude analysis of narrowband EEG activity: A comparison based on the sleep delta-frequency band," *Sleep*, vol. 4, pp. 193–206, Sep 1981.

[274] T. Penzel, J. W. Kantelhardt, L. Grote, J. Peter, and A. Bunde, "Comparison of detrended fluctuation analysis and spectral analysis for heart rate variability in sleep and sleep apnea," *IEEE Transactions on Biomedical Engineering*, vol. 50, pp. 1143–1151, Oct 2003.

[275] E. L. P. da Silva, R. Pereira, L. N. Reis, V. L. Pereira, L. A. Campos, N. Wessel, and O. C. Baltatu, "Heart rate detrended fluctuation indexes as estimate of obstructive sleep apnea severity," *Medicine*, vol. 94, p. e516, Jan 2015.

[276] S. Motamedi-Fakhr, M. Moshrefi-Torbati, M. Hill, C. M. Hill, and P. R. White, "Signal processing techniques applied to human sleep EEG signals - a review," *Biomedical Signal Processing and Control*, vol. 10, pp. 21–33, Mar 2014.

[277] A. C. Rosa, L. Parrino, and M. G. Terzano, "Automatic detection of cyclic alternating pattern (CAP) sequences in sleep: preliminary results," *Clinical Neurophysiology*, vol. 110, pp. 585–592, Apr 1999.

[278] M. Sekimoto, M. Kato, T. Watanabe, T. Nakajima, T. Hori, N. Kajimura, and K. Takahashi, "Asymmetric interhemispheric sigma waves during all-night sleep in humans," *Sleep and Biological Rhythms*, vol. 3, pp. 130–135, Oct 2005.

[279] A. Piarulli, D. Menicucci, A. Gemignani, U. Olcese, P. d'Ascanio, A. Pingitore, R. Bedini, and A. Landi, "Likeness-based detection of sleep slow oscillations in normal and altered sleep conditions: Application on low-density EEG recordings," *IEEE Transactions on Biomedical Engineering*, vol. 57, pp. 363–372, Feb 2010.

[280] S. Uchida, M. Matsuura, S. Ogata, T. Yamamoto, and N. Aikawa, "Computerization of fujimori's method of waveform recognition A review and methodological considerations for its application to all-night sleep EEG," *Journal of Neuroscience Methods*, vol. 64, pp. 1–12, Jan 1996.

[281] Y. Kawashima, T. Yoshida, M. Hayashi, and N. Aikawa, "An automatic analysis of sleep stage 2 based on the Fujimori method," *Electronics and Communications in Japan*, vol. 101, pp. 34–41, Jul 2018.

[282] J. G. Proakis and D. K. Manolakis, *Digital Signal Processing: Principles, Algorithms and Applications*. Upper Saddle River, N.J: Pearson Prentice Hall, fourth ed., 2006.

[283] M. Kansanen, E. Vanninen, A. Tuunainen, P. Pesonen, V. Tuononen, J. Hartikainen, H. Mussalo, and M. Uusitupa, "The effect of a very low-calorie diet-induced weight loss on the severity of obstructive sleep apnoea and autonomic nervous function in obese patients with obstructive sleep apnoea syndrome," *Clinical Physiology*, vol. 18, pp. 377–385, Jul 1998.

[284] M. Aboy, O. W. Marquez, J. McNames, R. Hornero, T. Trong, and B. Goldstein, "Adaptive modeling and spectral estimation of nonstationary biomedical signals based on kalman filtering," *IEEE Transactions on Biomedical Engineering*, vol. 52, pp. 1485–1489, Aug 2005.

[285] M. H. Asyali, R. B. Berry, M. C. K. Khoo, and A. Altinok, "Determining a continuous marker for sleep depth," *Computers in Biology and Medicine*, vol. 37, pp. 1600–1609, Nov 2007.

[286] S. Wu, D. Liang, Q. Yang, and G. Liu, "Regularity of heart rate fluctuations analysis in obstructive sleep apnea patients using information-based similarity," *Biomedical Signal Processing and Control*, vol. 65, p. 102370, Mar 2021.

[287] D. Álvarez, R. Hornero, J. V. Marcos, and F. del Campo, "Feature selection from nocturnal oximetry using genetic algorithms to assist in obstructive sleep apnoea diagnosis," *Medical Engineering & Physics*, vol. 34, pp. 1049–1057, Oct 2012.

[288] C. D. Richmond, "Cross coherence and joint PDF of the Bartlett and Capon power spectral estimates," in *2007 IEEE International Conference on Acoustics, Speech and Signal Processing - ICASSP '07*, pp. 901–904, IEEE, Apr 2007.

[289] A. K. Sadaghiani and S. Sheikhai, "Hardware implementation of high speed bartlett spectral density estimator based on r4mdc FFT," in *2019 27th Iranian Conference on Electrical Engineering (ICEE)*, pp. 1518–1522, IEEE, Apr 2019.

[290] G. D. Pinna, E. Robbi, M. T. L. Rovere, and R. Maestri, "A hybrid approach for continuous detection of sleep-wakefulness fluctuations: validation in patients with Cheyne-Stokes respiration," *Journal of Sleep Research*, vol. 21, pp. 342–351, Oct 2011.

[291] D. Cvetkovic and I. Cosic, "Sleep onset estimator: Evaluation of parameters," in *2008 30th Annual International Conference of the IEEE Engineering in Medicine and Biology Society*, pp. 3860–3863, IEEE, Aug 2008.

[292] C.-C. Hua and C.-C. Yu, "Smoothed periodogram of oxyhemoglobin saturation by pulse oximetry in sleep apnea syndrome," *Chest*, vol. 131, pp. 750–757, Mar 2007.

[293] J. K. Tugnait, "Wireless user authentication via comparison of power spectral densities," *IEEE Journal on Selected Areas in Communications*, vol. 31, pp. 1791–1802, Sep 2013.

[294] M. Corsi-Cabrera, Z. Muñoz-Torres, Y. del Río-Portilla, and M. A. Guevara, "Power and coherent oscillations distinguish REM sleep, stage 1 and wakefulness," *International Journal of Psychophysiology*, vol. 60, pp. 59–66, Apr 2006.

[295] S. A. Imtiaz, S. Saremi-Yarahmadi, and E. Rodriguez-Villegas, "Automatic detection of sleep spindles using Teager energy and spectral edge frequency," in *2013 IEEE Biomedical Circuits and Systems Conference (BioCAS)*, pp. 262–265, IEEE, Oct 2013.

[296] L. Fraiwan, K. Lweesy, N. Khasawneh, H. Wenz, and H. Dickhaus, "Automated sleep stage identification system based on time-frequency analysis of a single EEG channel and random forest classifier," *Computer Methods and Programs in Biomedicine*, vol. 108, pp. 10–19, Oct 2012.

[297] E. Z-Flores, L. Trujillo, A. Sotelo, P. Legrand, and L. N. Coria, "Regularity and matching pursuit feature extraction for the detection of epileptic seizures," *Journal of Neuroscience Methods*, vol. 266, pp. 107–125, Jun 2016.

[298] C. Richard and R. Lengelle, "Joint time and time-frequency optimal detection of K-Complexes in sleep EEG," *Computers and Biomedical Research*, vol. 31, pp. 209–229, Jun 1998.

[299] I. Chouvarda, N. Maglaveras, A. Boufidou, S. Mohlas, and G. Louridas, "Wigner-Ville analysis and classification of electrocardiograms during thrombolysis," *Medical & Biological Engineering & Computing*, vol. 41, pp. 609–617, Nov 2003.

[300] U. R. Acharya, O. Faust, N. Kannathal, T. Chua, and S. Laxminarayan, "Non-linear analysis of EEG signals at various sleep stages," *Computer Methods and Programs in Biomedicine*, vol. 80, pp. 37–45, Oct 2005.

[301] M. Zucconi, M. Manconi, D. Bizzozero, F. Rundo, C. J. Stam, L. Ferini-Strambi, and R. Ferri, "EEG synchronisation during sleep-related epileptic seizures as a new tool to discriminate confusional arousals from paroxysmal arousals: preliminary findings," *Neurological Sciences*, vol. 26, pp. s199–s204, Dec 2005.

[302] I.-H. Song, D.-S. Lee, and S. I. Kim, "Recurrence quantification analysis of sleep electoencephalogram in sleep apnea syndrome in humans," *Neuroscience Letters*, vol. 366, pp. 148–153, Aug 2004.

[303] M. Chen, D. Sommer, S. Goh, T. Gautama, D. Obradovic, M. Golz, M. Morrell, H. Wang, and D. Mandic, "A novel tool for sequential fusion of nonlinear features: A sleep psychology application," in *2006 IEEE International Conference on Multisensor Fusion and Integration for Intelligent Systems*, pp. 474–478, IEEE, Sep 2006.

[304] J. Fell, J. Röschke, and C. Schäffner, "Surrogate data analysis of sleep electroencephalograms reveals evidence for nonlinearity," *Biological Cybernetics*, vol. 75, pp. 85–92, Jul 1996.

[305] P. Piñero, P. Garcia, L. Arco, A. Álvarez, M. M. García, and R. Bonal, "Sleep stage classification using fuzzy sets and machine learning techniques," *Neurocomputing*, vol. 58-60, pp. 1137–1143, Jun 2004.

[306] E. Niestroj, I. Spieweg, and W. M. Herrmann, "On the dimensionality of sleep-EEG data," *Neuropsychobiology*, vol. 31, pp. 166–172, Mar 1995.

[307] U. R. Abeyratne, S. de Silva, C. Hukins, and B. Duce, "Obstructive sleep apnea screening by integrating snore feature classes," *Physiological Measurement*, vol. 34, pp. 99–121, Jan 2013.

[308] U. Tirnakli and E. P. Borges, "The standard map: From Boltzmann-Gibbs statistics to Tsallis statistics," *Scientific Reports*, vol. 6, pp. 1–8, Mar 2016.

[309] M. Thilagaraj, M. P. Rajasekaran, and N. A. Kumar, "Tsallis entropy: as a new single feature with the least computation time for classification of epileptic seizures," *Cluster Computing*, vol. 22, pp. 15213–15221, Mar 2018.

[310] T. D. Pham, "The Kolmogorov-Sinai entropy in the setting of fuzzy sets for image texture analysis and classification," *Pattern Recognition*, vol. 53, pp. 229–237, May 2016.

[311] A. D. Martino and D. D. Martino, "An introduction to the maximum entropy approach and its application to inference problems in biology," *Heliyon*, vol. 4, p. e00596, Apr 2018.

[312] A. Calcagnì, L. Finos, G. Altoé, and M. Pastore, "A maximum entropy procedure to solve likelihood equations," *Entropy*, vol. 21, p. 596, Jun 2019.

[313] E. M. Ventouras, P. Y. Ktonas, H. Tsekou, T. Paparrigopoulos, I. Kalatzis, and C. R. Soldatos, "Slow and fast EEG sleep spindle component extraction using Independent Component Analysis," in *2008 8th IEEE International Conference on BioInformatics and BioEngineering*, pp. 1–6, IEEE, Oct 2008.

[314] L. Leistritz, P. Putsche, K. Schwab, W. Hesse, T. Süße, J. Haueisen, and H. Witte, "Coupled oscillators for modeling and analysis of EEG/MEG oscillations," *Biomedizinische Technik/Biomedical Engineering*, vol. 52, pp. 83–89, Feb 2007.

[315] S.-M. Cai, Z.-H. Jiang, T. Zhou, P.-L. Zhou, H.-J. Yang, and B.-H. Wang, "Scale invariance of human electroencephalogram signals in sleep," *Physical Review E*, vol. 76, p. 061903, Dec 2007.

[316] J. Miao and L. Niu, "A survey on feature selection," *Procedia Computer Science*, vol. 91, pp. 919–926, Aug 2016.

[317] R. Sheikhpour, M. A. Sarram, S. Gharaghani, and M. A. Z. Chahooki, "A survey on semi-supervised feature selection methods," *Pattern Recognition*, vol. 64, pp. 141–158, Apr 2017.

[318] C. Jalota and R. Agrawal, "Feature selection algorithms and student academic performance: A study," in *Advances in Intelligent Systems and Computing* (D. Gupta, A. Khanna, S. Bhattacharyya, A. E. Hassanien, S. Anand, and A. Jaiswal, eds.), vol. 1165, pp. 317–328, Singapore, Springer: Springer Singapore, 2020.

[319] E. Hancer, B. Xue, and M. Zhang, "A survey on feature selection approaches for clustering," *Artificial Intelligence Review*, vol. 53, pp. 4519–4545, Jan 2020.

[320] G. Chandrashekar and F. Sahin, "A survey on feature selection methods," *Computers & Electrical Engineering*, vol. 40, pp. 16–28, Jan 2014.

[321] H.-L. Nguyen, Y.-K. Woon, and W.-K. Ng, "A survey on data stream clustering and classification," *Knowledge and Information Systems*, vol. 45, pp. 535–569, Dec 2014.

[322] S. Umadevi and K. S. J. Marseline, "A survey on data mining classification algorithms," in *2017 International Conference on Signal Processing and Communication (ICSPC)*, pp. 264–268, IEEE, Jul 2017.

[323] Y. Li, H. Zhang, X. Xue, Y. Jiang, and Q. Shen, "Deep learning for remote sensing image classification: A survey," *Wiley Interdisciplinary Reviews: Data Mining and Knowledge Discovery*, vol. 8, p. e1264, May 2018.

[324] T. U. Rani, C. H. S. Priyanka, and B. S. S. Monica, "A dynamic data classification techniques and tools for big data," *Journal of Physics: Conference Series*, vol. 1228, p. 012043, May 2019.

[325] T. Q. Le, C. Cheng, A. Sangasoongsong, W. Wongdhamma, and S. T. S. Bukkapatnam, "Wireless wearable multisensory suite and real-time prediction of obstructive sleep apnea episodes," *IEEE Journal of Translational Engineering in Health and Medicine*, vol. 1, p. 2700109, Jul 2013.

[326] J. C. Principe, S. K. Gala, and T. G. Chang, "Sleep staging automaton based on the theory of evidence," *IEEE Transactions on Biomedical Engineering*, vol. 36, pp. 503–509, May 1989.

[327] L. Zoubek, S. Charbonnier, S. Lesecq, A. Buguet, and F. Chapotot, "Feature selection for sleep/wake stages classification using data driven methods," *Biomedical Signal Processing and Control*, vol. 2, pp. 171–179, Jul 2007.

[328] P. Fonseca, N. den Teuling, X. Long, and R. M. Aarts, "Cardiorespiratory sleep stage detection using conditional random fields," *IEEE Journal of Biomedical and Health Informatics*, vol. 21, pp. 956–966, Jul 2017.

[329] H.-J. Park, J.-S. Oh, D.-U. Jeong, and K.-S. Park, "Automated sleep stage scoring using hybrid rule- and case-based reasoning," *Computers and Biomedical Research*, vol. 33, pp. 330–349, Oct 2000.

[330] A. K. Ng, T. S. Koh, U. R. Abeyratne, and K. Puvanendran, "Investigation of obstructive sleep apnea using nonlinear mode interactions in nonstationary snore signals," *Annals of Biomedical Engineering*, vol. 37, pp. 1796–1806, Jun 2009.

[331] University of California Los Angeles: Institute for Digital Research and Education - Statistical Consulting, "Choosing the Correct Statistical Test in SAS, Stata, SPSS and R," 2021.

[332] T. A. S. Marçal, J. M. dos Santos, A. Rosa, and J. M. R. Cardoso, "OSAS assessment with entropy analysis of high resolution snoring audio signals," *Biomedical Signal Processing and Control*, vol. 61, p. 101965, Aug 2020.

[333] P. J. Lavrakas, *Encyclopedia of Survey Research Methods*. Sage Publications, Inc., first ed., 2008.

[334] E. P. C. G. Domingos, "Look4MySleep: a screening device for obstructive sleep apnea syndrome," Master's thesis, University of Coimbra, 2009.

[335] Zoom Corporation, "The Zoom H4n: The gold standard in portable recording," Jan. 2020.

[336] A. K. Ng, T. S. Koh, K. Puvanendran, and U. R. Abeyratne, "Snore signal enhancement and activity detection via translation-invariant wavelet transform," *IEEE Transactions on Biomedical Engineering*, vol. 55, pp. 2332–2342, Oct 2008.

[337] K. Inoue, M. Akutagawa, T. Emoto, U. Abeyratne, T. Uemura, H. Nagashino, and Y. Kinouchi, "Order estimation and screening of apneic snore sound using the akaike information criterion," in *World Congress on Medical Physics and Biomedical Engineering 2006* (R. Magjarevic and J. H. Nagel, eds.), vol. 14, pp. 1135–1138, Berlin, Heidelberg: Springer Berlin Heidelberg, 2006.

[338] D. Noonburg, "Download xpdf and xpdfreader," June 2020.

[339] D. Alvarez-Estevez, "Free EDF(+) software and datafiles," 2020.

[340] T. van Beelen, "Edfbrowser," 2013.

[341] B. Zonjy, "Online EDF viewer," 2020.

[342] R. Kostas, "EDF viewer," 2020.

[343] M. H. Kryger, T. Roth, and W. C. Dement, *Principles and Practice of Sleep Medicine*. Elsevier, sixth ed., Feb. 2017.

[344] National Institute of Standards and Technology, "NIST/SEMATECH e-handbook of statistical methods," Oct. 2013.

[345] F. V. Berghen, *CONDOR: a constrained, non-linear, derivative-free parallel optimizer for continuous, high computing load, noisy objective functions*. PhD thesis, Universite Libre de Bruxelles, 2004.

[346] E. Bellauer, "peakdet: Peak detection using matlab," 2013.

[347] J. Mesquita, J. Solà-Soler, J. A. Fiz, J. Morera, and R. Jané, "All night analysis of time interval between snores in subjects with sleep apnea hypopnea syndrome," *Medical & Biological Engineering & Computing*, vol. 50, pp. 373–381, Mar 2012.

[348] S. Sheather, *A Modern Approach to Regression with R*. Springer-Verlag New York Inc., first ed., Dec. 2009.

[349] D. Zwillinger and S. Kokoska, *Standard probability and statistics tables and formulae*. Boca Raton: Chapman & Hall/CRC, first ed., 1999.

[350] R. Shanmugam and R. Chattamvelli, *Statistics for Scientists and Engineers*. Wiley, first ed., Aug. 2015.

[351] J. I. E. Hoffman, *Biostatistics for medical and biomedical practitioners : an interpretative guide for medicine and biology*. Amsterdam: Elsevier, first ed., 2015.

[352] T. T. Soong, *Fundamentals of Probability and Statistics for Engineers*. John Wiley & Sons, first ed., May 2004.

[353] D. P. Bertsekas and J. N. Tsitsiklis, *Introduction to probability*. Belmont, Mass: Athena Scientific, first ed., 2002.

[354] A. M. Fiori and M. Zenga, "Karl Pearson and the origin of kurtosis," *International Statistical Review*, vol. 77, pp. 40–50, Apr 2009.

[355] N. E. Huang, Z. Shen, S. R. Long, M. C. Wu, H. H. Shih, Q. Zheng, N.-C. Yen, C. C. Tung, and H. H. Liu, "The empirical mode decomposition and the Hilbert spectrum for nonlinear and non-stationary time series analysis," *Proceedings of the Royal Society of London. Series A: Mathematical, Physical and Engineering Sciences*, vol. 454, pp. 903–995, Mar 1998.

[356] A. Eftekhar, C. Toumazou, and E. M. Drakakis, "Empirical Mode Decomposition: Real-time implementation and applications," *Journal of Signal Processing Systems*, vol. 73, pp. 43–58, Jan 2013.

[357] X. Dang, R. Wei, and G. Li, "Snoring and breathing detection based on empirical mode decomposition," in *2015 International Conference on Orange Technologies (ICOT)*, pp. 79–82, IEEE, Dec 2015.

[358] H. Liang, S. L. Bressler, R. Desimone, and P. Fries, "Empirical mode decomposition: a method for analyzing neural data," *Neurocomputing*, vol. 65-66, pp. 801–807, Jun 2005.

[359] A. Stallone, A. Cicone, and M. Materassi, "New insights and best practices for the successful use of Empirical Mode Decomposition, Iterative Filtering and derived algorithms," *Scientific Reports*, vol. 10, p. 15161, Sept. 2020.

[360] B. Huang and A. Kunoth, "An optimization based empirical mode decomposition scheme," *Journal of Computational and Applied Mathematics*, vol. 240, pp. 174–183, Mar 2013.

[361] S. sheng Long, T. bao Zhang, and F. Long, "Causes and solutions of overshoot and undershoot and end swing in Hilbert-Huang transform," *Acta Seismologica Sinica*, vol. 18, pp. 602–610, Sep 2005.

[362] R. M. Gray, *Entropy and Information Theory*. Springer-Verlag, first ed., 2013.

[363] J. M. Perez-Macias, J. Viik, A. Varri, S.-L. Himanen, and M. Tenhunen, "Spectral analysis of snoring events from an Emfit mattress," *Physiological Measurement*, vol. 37, pp. 2130–2143, Nov 2016.

[364] V. K. Madisetti and D. B. Williams, *Digital signal processing handbook*. Boca Raton, Fla: CRC Press, first ed., 1999.

[365] B. Najafi and H. Hakim, "A comparative study of non-parametric spectral estimators for application in machine vibration analysis," *Mechanical Systems and Signal Processing*, vol. 6, pp. 551–574, Nov 1992.

[366] I. Daubechies and S. Maes, *WAVELETS in Medicine and Biology*. Routledge, first ed., Nov 1996.

[367] I. Daubechies, Y. G. Wang, and H. tieng Wu, "ConceFT: concentration of frequency and time via a multitapered synchrosqueezed transform," *Philosophical Transactions of the Royal Society A: Mathematical, Physical and Engineering Sciences*, vol. 374, p. 20150193, Apr 2016.

[368] I. Daubechies, J. Lu, and H.-T. Wu, "Synchrosqueezed wavelet transforms: An empirical mode decomposition-like tool," *Applied and Computational Harmonic Analysis*, vol. 30, pp. 243–261, Mar 2011.

[369] M. Mihalec, J. Slavič, and M. Boltežar, "Synchrosqueezed wavelet transform for damping identification," *Mechanical Systems and Signal Processing*, vol. 80, pp. 324–334, Dec 2016.

[370] M. M. Kabir, R. Tafreshi, D. B. Boivin, and N. Haddad, "Enhanced automated sleep spindle detection algorithm based on synchrosqueezing," *Medical & Biological Engineering & Computing*, vol. 53, pp. 635–644, Mar 2015.

[371] Z. Ghanbari and M. H. Moradi, "Synchrosqueezing transform: Application in the analysis of the K-complex pattern," in *2016 23rd Iranian Conference on Biomedical Engineering and 2016 1st International Iranian Conference on Biomedical Engineering (ICBME)*, pp. 221–225, IEEE, Nov 2016.

[372] D. Jarchi, S. Sanei, and A. Prochazka, "Detection of sleep apnea/hypopnea events using synchrosqueezed wavelet transform," in *ICASSP 2019 - 2019 IEEE International Conference on Acoustics, Speech and Signal Processing (ICASSP)*, pp. 1199–1203, IEEE, May 2019.

[373] M. W. Fagerland, S. Lydersen, and P. Laake, "The McNemar test for binary matched-pairs data: mid-p and asymptotic are better than exact conditional," *BMC Medical Research Methodology*, vol. 13, pp. 1–8, Jul 2013.

[374] M. Q. R. P. Smith and G. D. Ruxton, "Effective use of the McNemar test," *Behavioral Ecology and Sociobiology*, vol. 74, pp. 1–9, Oct 2020.

[375] Sleep Foundation, "How to Optimize the Humidity Level for Healthy Sleep," Aug. 2017.

[376] Centers for Disease Control and Prevention, "Target Heart Rate and Estimated Maximum Heart Rate | Physical Activity | CDC," Apr. 2020.

[377] S. DeMeulenaere, "Pulse oximetry: Uses and limitations," *The Journal for Nurse Practitioners*, vol. 3, pp. 312–317, May 2007.

[378] E. D. Chan, M. M. Chan, and M. M. Chan, "Pulse oximetry: Understanding its basic principles facilitates appreciation of its limitations," *Respiratory Medicine*, vol. 107, pp. 789–799, Jun 2013.

[379] V. A. Rossi, J. R. Stradling, and M. Kohler, "Effects of obstructive sleep apnoea on heart rhythm," *European Respiratory Journal*, vol. 41, pp. 1439–1451, Dec 2012.

[380] World Health Organization, "WHO Housing and health guidelines," May 2018.

[381] Visual Crossing, "Historical Weather Dashboard," 2012.

[382] National Centers for Environmental Information - National Oceanic and Atmospheric Administration, "Daily Summaries Station Details," 2012.

[383] J. W. Graham, "Missing data analysis: Making it work in the real world," *Annual Review of Psychology*, vol. 60, pp. 549–576, Jan 2009.

Appendix A

Slow Variation Parameters Schematics

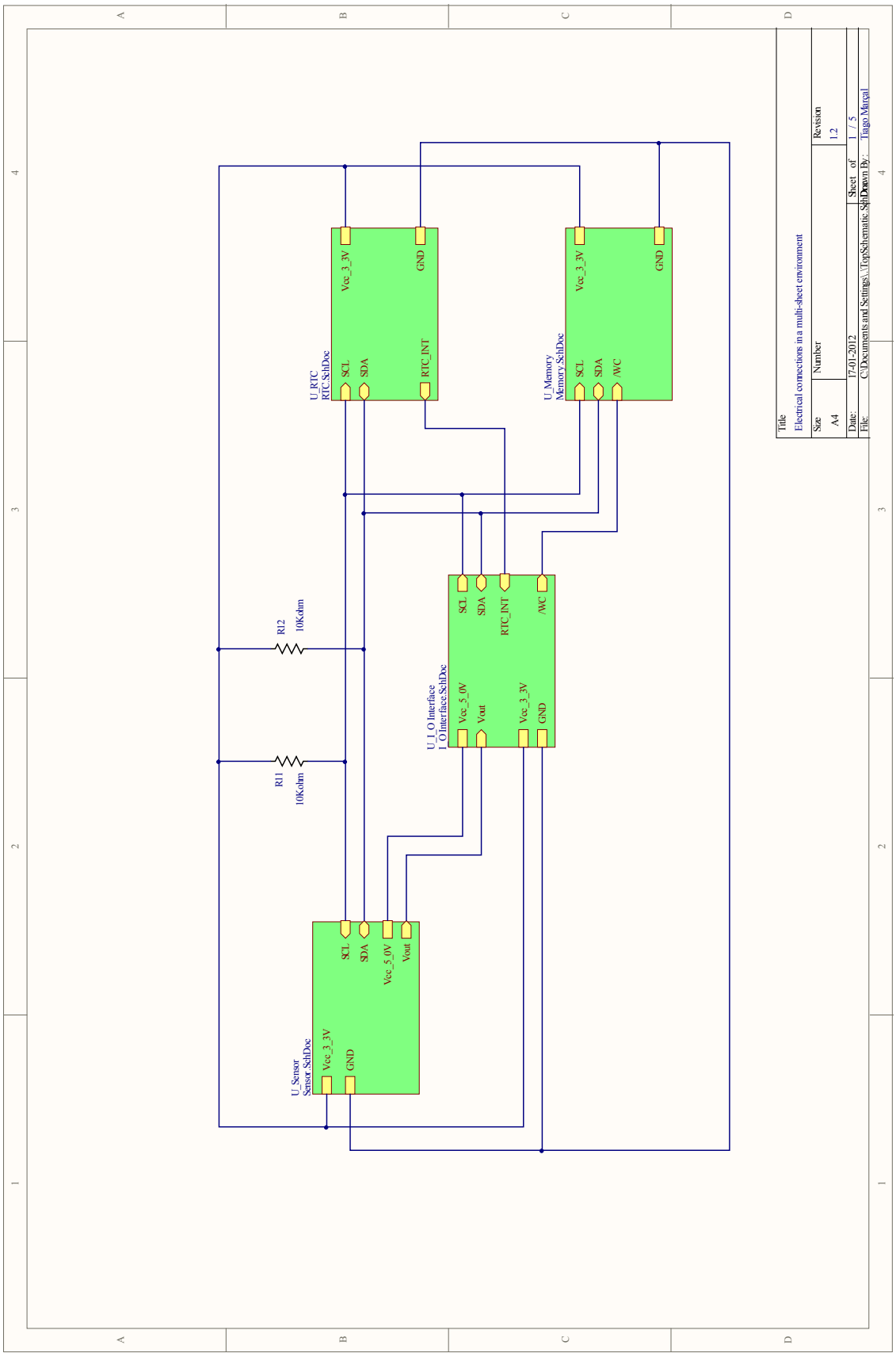
U_RTC
RTC.SchDoc
Vcc_3_3V
GND
SCL
SDA
RTC_INT
U_Memory
Memory.SchDoc
Vcc_3_3V
GND
SCL
SDA
/WC
R12
10Kohm
R11
10Kohm
U_I_O Interface
I_O Interface.SchDoc
SCL
SDA
RTC_INT
/WC
Vcc_5_0V
Vout
Vcc_3_3V
GND
U_Sensor
Sensor.SchDoc
Vcc_3_3V
GND
SCL
SDA
Vcc_5_0V
Vout
Title
Electrical connections in a multi-sheet environment
Size
A4
Number
Revision
1.2
Date:
17-01-2012
Sheet of
1 / 5
File:
C:\Documents and Settings\...\TopSchematic.SchDoc
Drawn By:
Tiago Mateal

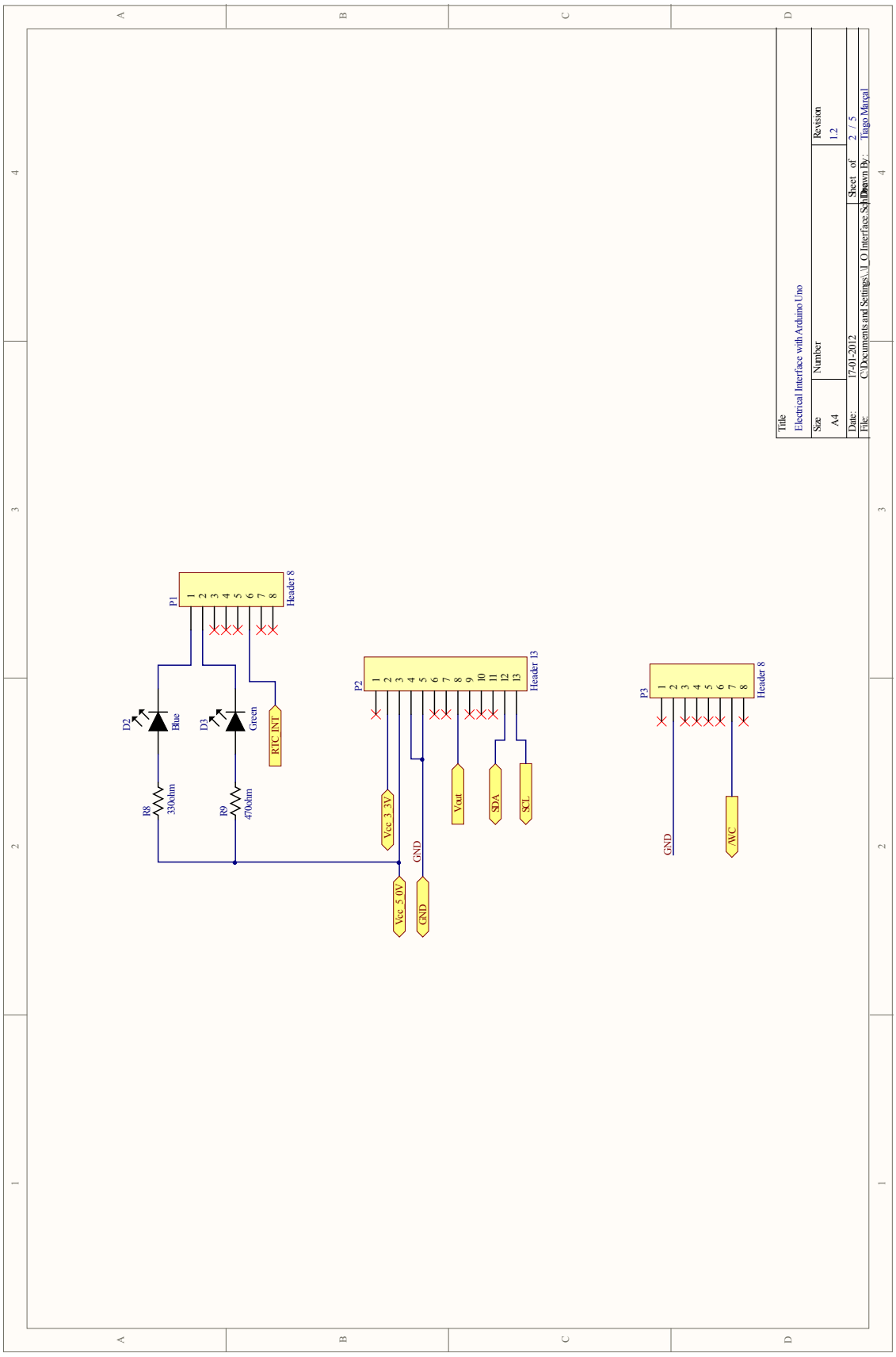
Title
Electrical Interface with Arduino Uno
Size
A4
Number
Revision
1.2
Date:
17-01-2012
Sheet of
2 / 5
File:
C:\Documents and Settings\...\I_O Interface.SchDoc
Drawn By:
Tiago Marcal
P1
Header 8
P2
Header 13
P3
Header 8
D2
Blue
D3
Green
R8
330ohm
R9
470ohm
RTC INT
Vcc 3.3V
GND
Vcc 5.0V
GND
Vout
SDA
SCL
GND
/WC

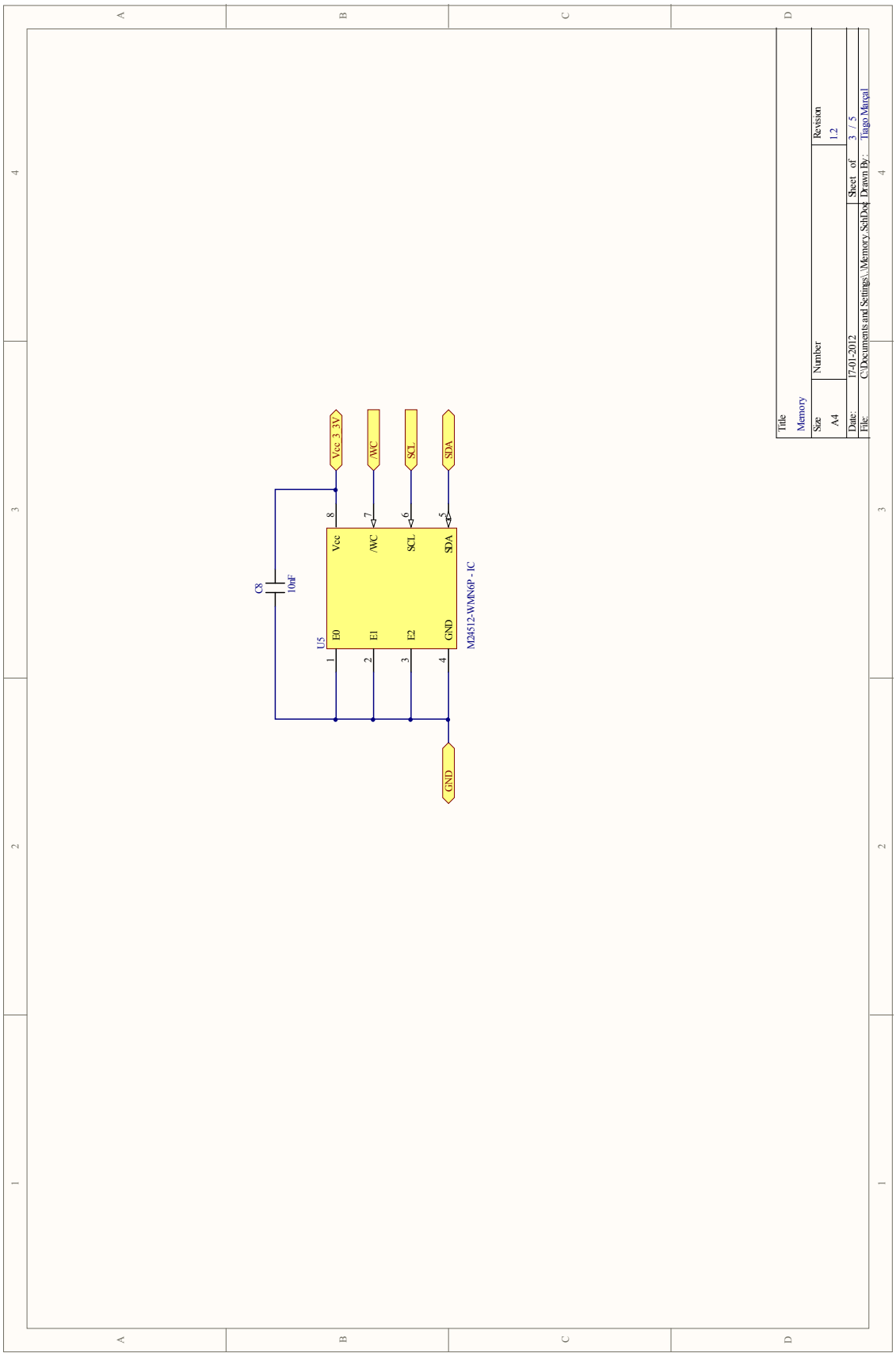
Vcc 3.3V
/WC
SCL
SDA
GND
C8
10nF
U5
M24512-WMN6P - IC
Vcc
/WC
SCL
SDA
E0
E1
E2
GND
Title
Memory
Size
A4
Number
Revision
1.2
Date:
17-01-2012
Sheet of
3 / 5
File:
C:\Documents and Settings\...\Memory.SchDoc
Drawn By:
Tiago Mateal

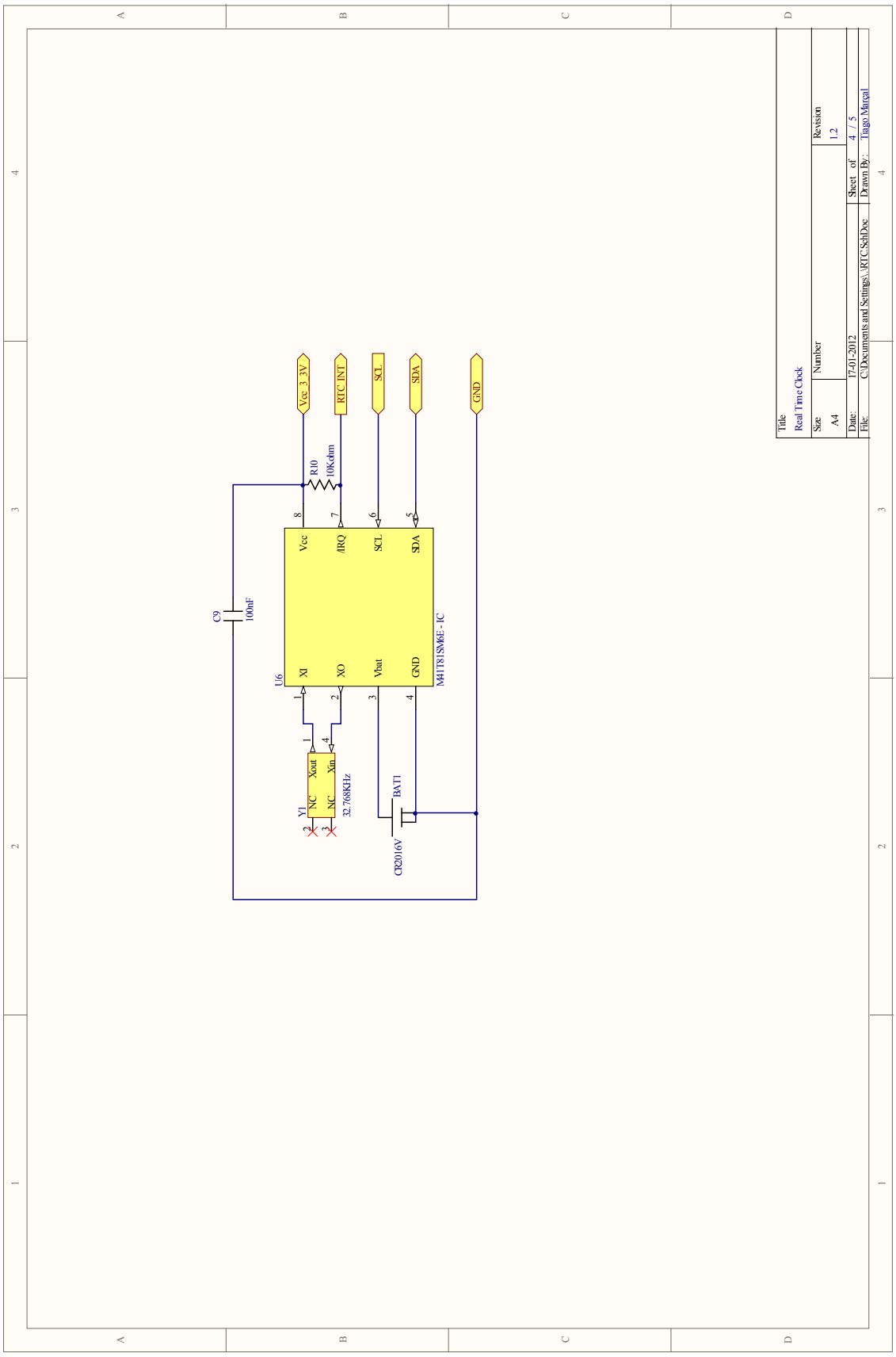
Vcc_3.3V
RTC_INT
SCL
SDA
GND
R10
10Kohm
C9
100nF
U6
M41T81SM6E - IC
Vcc
/IRQ
SCL
SDA
XI
XO
Vbat
GND
Y1
32.768KHz
Xout
Xin
NC
NC
BAT1
CR2016V
Title
Real Time Clock
Size
A4
Number
Revision
1.2
Date:
17-01-2012
Sheet of
4 / 5
File:
C:\Documents and Settings\...\RTC.SchDoc
Drawn By:
Tiago Mateal

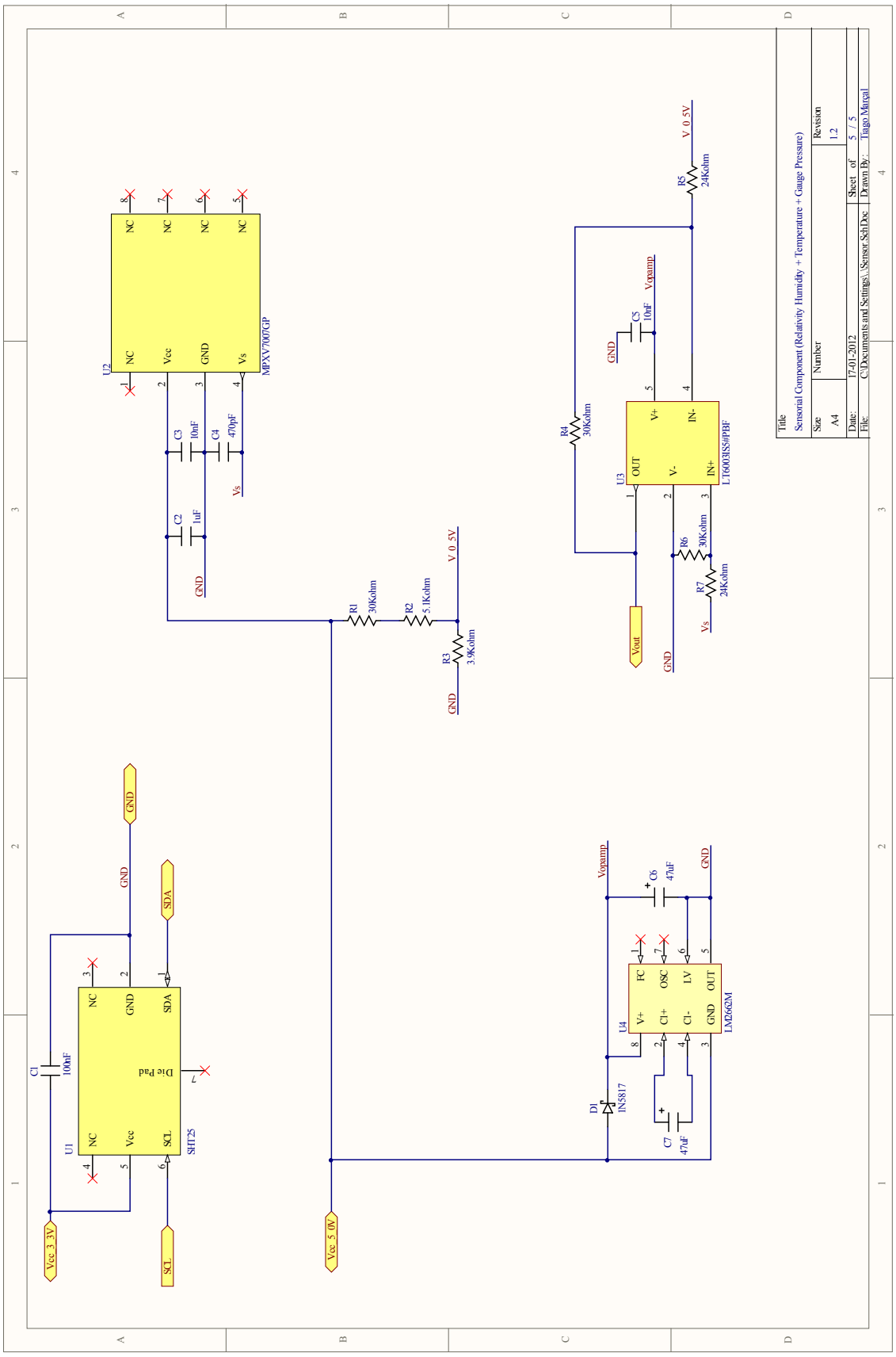
Title
Sensorial Component (Relativity Humidity + Temperature + Gauge Pressure)
Size
A4
Number
Revision
1.2
Date:
17-01-2012
Sheet of
5 / 5
File:
C:\Documents and Settings\...\Sensor.SchDoc
Drawn By:
Tiago Mateal
U2
MPXV7007GP
NC
Vcc
GND
Vs
C3
10nF
C4
470pF
C2
1uF
R1
30Kohm
R2
5.1Kohm
R3
3.9Kohm
V 0 .5V
U3
LT6003IS5#PBF
OUT
V-
IN+
V+
IN-
R4
30Kohm
R5
24Kohm
R6
30Kohm
R7
24Kohm
C5
10nF
Vopamp
Vout
U1
SHT25
SDA
SCL
Die Pad
C1
100nF
Vcc 3 .3V
U4
LM2662M
FC
OSC
LV
OUT
V+
CI+
CI-
GND
C6
47uF
C7
47uF
D1
IN5817
Vcc 5 .0V

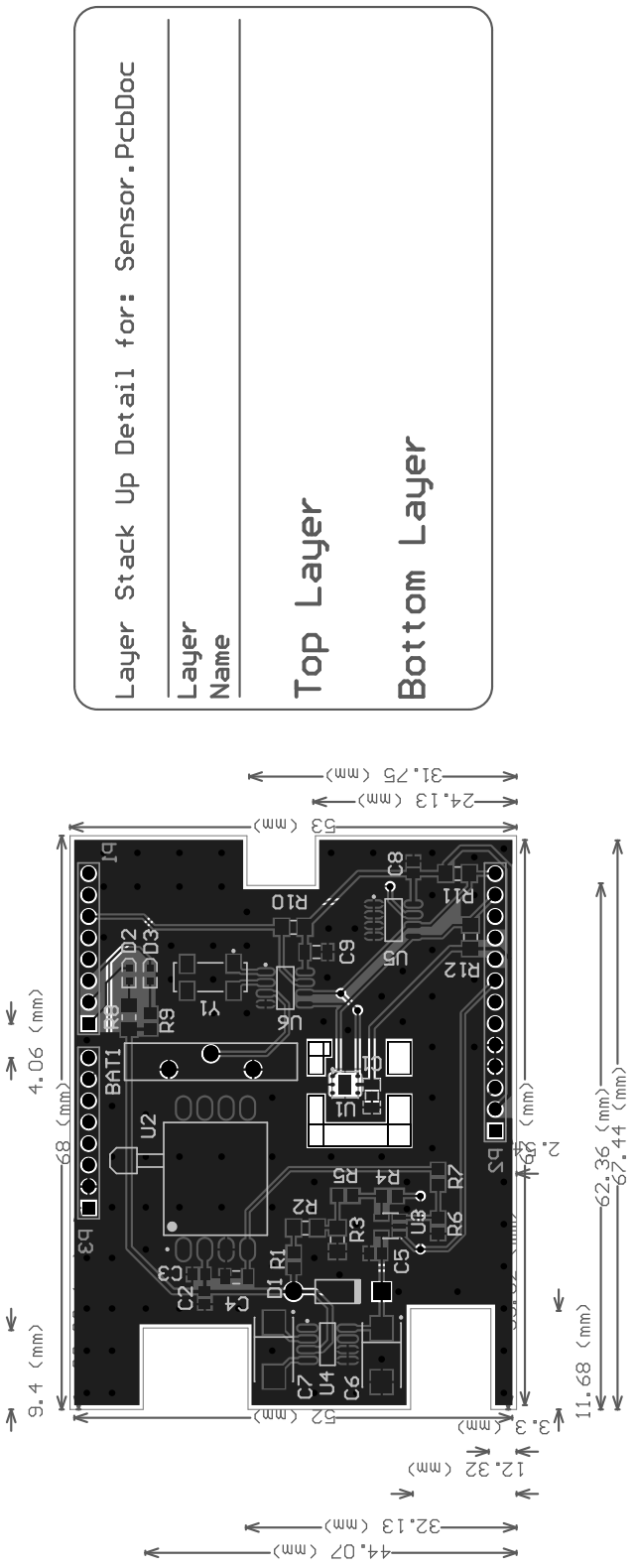
Layer Stack Up Detail for: Sensor.PcbDoc
Layer
Name
Top Layer
Bottom Layer
31.75 (mm)
24.13 (mm)
53 (mm)
4.06 (mm)
68 (mm)
9.4 (mm)
52 (mm)
3.3 (mm)
2.54 (mm)
62.36 (mm)
67.44 (mm)
11.68 (mm)
12.32 (mm)
32.13 (mm)
44.07 (mm)
BAT1
U1
U2
U3
U4
U5
U6
C1
C2
C3
C4
C5
C6
C7
C8
C9
R1
R2
R3
R4
R5
R6
R7
R9
R10
R11
R12
D1
D2
D3
Y1

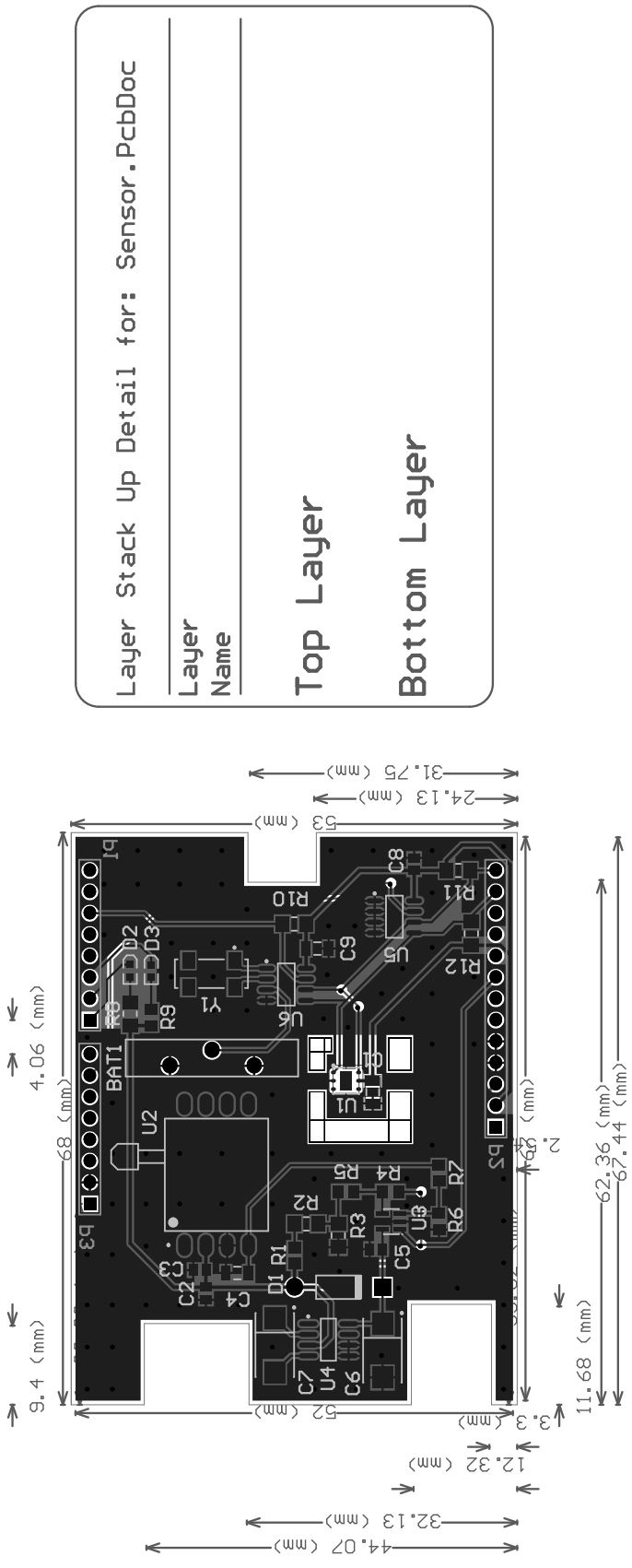
Layer Stack Up Detail for: Sensor.PcbDoc
Layer
Name
Top Layer
Bottom Layer
31.75 (mm)
24.13 (mm)
53 (mm)
4.06 (mm)
68 (mm)
9.4 (mm)
52 (mm)
3.3 (mm)
12.32 (mm)
32.13 (mm)
44.07 (mm)
62.36 (mm)
67.44 (mm)
11.68 (mm)
J1
J2
J3
J4
BAT1
D1
D2
D3
R1
R2
R3
R4
R5
R6
R7
R9
R10
R11
R12
C2
C3
C4
C5
C6
C7
C8
C9
U1
U2
U3
U4
U5
U6
Y1

Appendix B

Questionnaires' Information

Table B.1: Anthropometric data questioned to the patients. Patients are identified by their unique ID. Patient's gender means 1 is male and 0 is female. Sleep related symptoms were also questioned for excessive daytime sleepiness (EDS), insomnia and snore. Patients were tag with 1 for the symptoms they have, while their absence were tag with 0. The onset data referred to the beginning of those symptoms.

ID	**Gender**	**Height**	**Weight**	**Cervical Per.**	**Age**	**EDS**	**Insomnia**	**Snore**	**Onset**
		(cm)	(kg)	(mm)	$(years)$				$(years)$
49	1	167	92	480	65	0	0	1	16
50	1	166	75	400	42	1	0	1	6
51	1	170	58	385	77	0	0	1	20
52	1	167	70	400	44	1	0	1	31
54	0	165	110	380	32	0	1	1	8
57	1	178	85	400	52	1	1	1	8
58	0	156	90	415	55	0	1	1	6
61	1	176	90	410	62	1	1	1	1
63	0	154	88	370	66	1	1	1	8
64	0	153	61	330	46	1	1	1	6
67	1	160	62	445	28	1	0	1	10
68	1	165	80	430	59	0	1	1	15
70	1	167	86	430	44	0	0	1	19
73	1	170	77	400	44	0	0	1	24
77	0	162	79	370	47	1	1	1	3
78	0	154	68	370	53	0	1	1	6
79	0	168	70	370	61	0	1	1	7
80	0	144	57	420	66	0	1	1	3
81	0	169	85	380	55	0	1	1	2
83	0	159	90	430	65	1	1	1	10
84	0	171	71	320	44	1	0	1	2
86	1	165	70	380	32	0	1	0	3
87	1	170	68	390	35	1	1	0	0
89	1	178	75	410	49	1	1	1	8
90	1	190	85	400	42	1	0	1	4
91	1	175	90	430	48	1	0	1	1
92	1	165	80	435	54	0	0	1	5
94	0	156	61	320	39	1	0	1	25

96	1	165	73	395	72	1	0	1	20
97	0	160	58	340	35	1	0	1	25
99	0	160	69	360	41	1	1	1	4
100	1	167	90	425	57	0	1	1	5
101	0	162	55	330	40	1	0	1	7
102	0	160	62	400	69	1	0	1	10
103	0	159	64	310	50	1	1	1	10
104	1	160	88	450	66	0	1	1	40
105	1	159	65	400	67	0	1	1	10
106	1	175	82	425	38	1	1	1	7
107	1	186	90	400	35	0	0	0	36
109	1	169	80	395	50	1	0	1	20
110	0	160	66	340	36	1	0	1	15
112	1	176	88	430	60	0	0	0	3
113	1	155	89	450	54	0	0	1	20
114	0	165	58	340	27	1	1	1	2
115	1	186	83	420	47	1	0	0	2
116	1	178	109	480	45	0	1	1	4
118	1	158	67	410	53	1	0	1	30
119	1	169	85	450	60	1	0	1	10
120	1	178	82	405	51	0	0	1	2
125	1	179	160	465	26	0	0	1	0
126	0	160	72	365	49	1	0	1	5
127	0	156	76	390	45	1	0	1	2
129	1	169	74	405	72	0	0	1	20
130	1	180	77	420	73	1	0	1	2
133	0	159	58	365	50	1	0	1	25
134	1	185	110	440	41	1	0	1	10
136	0	153	65	340	16	1	1	1	16
137	1	164	96	450	45	1	1	1	1
138	1	171	110	550	68	0	0	1	0
139	0	159	57	350	62	1	0	1	10
141	1	175	90	410	57	1	0	1	10
142	1	180	140	475	39	0	0	1	6
143	0	164	115	390	35	1	1	1	25
144	1	180	73	375	33	0	1	0	4
145	1	181	123	490	67	0	1	1	20
146	1	173	77	400	71	0	0	1	20
147	0	156	68	360	59	0	0	1	1

Table B.2: Patient frequency habits to wake at night to go to urinate, nycturia, and to consume alcohol, tobacco and coffee. Alcohol consumption may be either wine or beer, respectively, 1 and 2, with a 0 in Alcohol column meaning absence of alcohol consumption. It was postulated that 1 glass of wine and 1 beer means 250 mL. Data for tobacco are presented as the number of cigarettes smoked per day, with 1 pack of cigarettes containing 20 cigarettes. Volume of coffee intake was not quantified. In columns Nycturia, Alcohol, Tobacco and Coffee, the value 0 means the absence of that particular habit. Otherwise, the habit exists.

ID	**Nycturia**	**Nycturia Freq.** ($\# \cdot night^{-1}$)	**Alcohol**	**Alcohol Freq.** ($L \cdot day^{-1}$)	**Tobacco**	**Tobacco Freq.** ($\# \cdot day^{-1}$)	**Coffee**	**Coffee Freq.** ($\# \cdot day^{-1}$)
49	1	1	0	0	0	0	1	2
50	1	1	0	0	0	0	1	2
51	1	2	1	0.5	0	0	0	0
52	1	1	1	0.143	1	2.9	0	0
54	0	0	0	0	0	0	1	1
57	0	0	1	0.2	0	0	1	1
58	1	2	0	0	0	0	1	4
61	1	2	1	0.625	0	0	1	3
63	1	2	0	0	0	0	0	0
64	1	1	0	0	0	0	1	1.5
67	0	0	0	0	0	0	0	0
68	0	0	0	0	0	0	1	1
70	0	0	0	0	1	12.5	1	4
73	0	0	0	0	0	0	1	3
77	0	0	0	0	0	0	1	1
78	1	3	0	0	0	0	1	1.5
79	1	3	1	0.5	0	0	1	2
80	1	1	0	0	0	0	1	1
81	1	2	1	0.071	0	0	1	2
83	1	3	0	0	0	0	0	0
84	1	1	0	0	0	0	0	0
86	0	0	0	0	1	16.5	0	0
87	1	1	1	0.143	1	7	1	1
89	1	4	1	0.625	0	0	1	1.5
90	0	0	2	0.25	0	0	1	3
91	1	1	0	0	1	1.5	1	3
92	0	0	0	0	0	0	1	2
94	0	0	0	0	0	0	1	1
96	1	1	1	0.75	0	0	0	0
97	0	0	0	0	1	20	0	0
99	1	1	0	0	0	0	1	1.5
100	1	1	1	1	0	0	1	1
101	0	0	0	0	0	0	0	0
102	0	0	0	0	0	0	0	0
103	1	2	0	0	0	0	1	3
104	1	5	1	0.25	0	0	1	1
105	1	3	1	1	0	0	1	2
106	1	1	1	0.625	0	0	1	3.5
107	0	0	0	0	1	11	1	5.5

109	1	1	1	0.5	0	0	1	2.5
110	0	0	0	0	0	0	1	2
112	1	2	1	0.25	0	0	1	2
113	1	1	0	0	1	20	1	4
114	0	0	0	0	0	0	0	0
115	1	2	0	0	0	0	1	2
116	0	0	1	0.7	0	0	1	2
118	0	0	1	0.5	0	0	1	4
119	0	0	1	0.5	0	0	1	3
120	1	1	2	0.5	0	0	1	1
125	0	0	0	0	0	0	0	0
126	1	1	0	0	0	0	0	0
127	0	0	0	0	0	0	0	0
129	0	0	2	1.815	1	20	1	3
130	1	2	1	0.75	0	0	1	1
133	1	1	0	0	0	0	1	2
134	0	0	0	0	1	30	1	4
136	0	0	0	0	0	0	0	0
137	1	1	1	0.5	0	0	1	1.5
138	1	3	1	0.5	0	0	0	0
139	1	1	0	0	0	0	1	1
141	1	1	1	1.125	0	0	1	3
142	1	1	0	0	0	0	1	5.5
143	1	1	0	0	0	0	1	1
144	1	1	0	0	0	0	1	1
145	1	3	0	0	0	0	0	0
146	1	2	0	0	0	0	1	1
147	1	3	0	0	0	0	1	1

Table B.3: A list of diseases questioned to the patients, identified by its unique ID, to know if they have the disease. The patient has the disease if the value is 1. Otherwise, the disease is absence.

ID	Hyper-tension	Cardio-vascular	Pulmonary	Epilepsy	Diabetes	Cholesterol
49	0	1	0	0	0	0
50	0	0	0	0	0	1
51	0	0	0	0	1	0
52	0	1	0	0	0	0
54	0	0	1	0	0	0
57	0	0	0	0	0	0
58	0	1	1	0	0	0
61	1	0	1	0	0	0
63	1	0	1	0	0	1
64	0	0	0	0	0	0
67	0	0	0	0	0	0
68	0	0	0	0	0	0
70	1	0	0	0	0	0
73	0	0	0	0	0	0
77	0	0	0	0	0	0
78	0	0	1	0	0	0
79	0	0	0	0	0	1
80	0	0	0	0	0	1
81	1	0	0	0	0	0
83	1	1	0	0	0	0
84	1	1	0	1	1	0
86	0	0	0	0	0	0
87	0	0	0	0	0	0
89	0	0	0	0	0	1
90	0	0	1	0	0	1
91	0	1	0	0	0	1
92	0	0	0	0	0	0
94	0	0	0	0	0	0
96	0	0	0	0	0	0
97	0	0	0	0	0	0
99	0	0	0	0	0	0
100	0	1	0	0	0	0
101	0	0	0	0	0	0
102	0	0	0	1	0	1
103	0	0	1	0	0	0
104	0	0	1	1	1	0
105	0	0	0	0	0	0
106	0	1	0	0	0	0
107	0	0	0	0	0	0
109	0	1	1	0	0	0
110	1	0	0	0	0	0
112	1	0	0	0	1	0
113	1	1	0	0	0	0

114	0	0	1	0	0	0
115	0	0	0	0	0	1
116	1	0	0	0	0	1
118	1	0	1	0	0	0
119	0	1	0	0	1	0
120	0	0	1	0	0	0
125	0	0	0	0	1	0
126	0	0	0	0	0	0
127	0	1	0	0	0	0
129	0	1	0	0	0	0
130	0	1	0	1	0	0
133	0	0	0	0	0	0
134	0	0	0	0	0	0
136	0	0	0	0	0	0
137	0	0	1	0	0	0
138	0	1	0	0	1	0
139	0	0	0	0	0	1
141	0	1	0	0	0	0
142	0	0	0	0	0	0
143	0	0	0	0	0	0
144	0	0	0	0	0	1
145	1	1	1	0	0	0
146	0	1	0	0	0	0
147	0	1	0	0	0	0

Table B.4: Patients with sleep disorders often have other medical conditions associated. Here, a list of such conditions under treatment is available.

ID	Medicine
49	Blood pressure, blood thinners, vasodilation and asthma.
50	Prostate.
51	Blood thinners and vertigo.
52	Blood pressure, blood thinners, antidepressants and cholesterol.
54	Pulmonary emphysema.
57	
58	Sleeping pills, anxiolytic and hypertension.
61	Bones, lungs and thyroid.
63	Hypertension, stomach, prophylaxis of patients with thromboembolic disorders and neuropathic pain.
64	Depression, thyroid and hormone treatment.
67	
68	Hypertension and depression.
70	Hypertension.
73	
77	Sleeping pills and headache.
78	Depression.
79	Hypobulia, pain killers, arthrosis and depression.
80	Depression, CNS stimulants, respiratory function, cholesterol, thyroid, dizziness and gastric regulation.
81	Hypertension and sleeping pills.
83	Parathyroid, hypertension, iron deficiency, antidepressants, CNS stimulants, anxiolytic, cardiovascular diseases, constipation and gastric protection.
84	Diabetic, hypertension and epilepsy.
86	
87	Anxiolytic.
89	Cholesterol and prostate.
90	To avoid alveoli impair due to a previous pulmonary emphysema.
91	Heart.
92	Cholesterol and hypertension.
94	Birth control pill.
96	
97	Birth control pill.
99	
100	Hypertension and cholesterol.
101	
102	Pain killers, hypertension, epilepsy, cholesterol, Iron deficiency and folic acid, anxiolytic, peptic ulcer, osteoarthritis, Crohn disease, polycythemia reduction, remove swelling in heart failure.

103	Gastric protection drugs, anxiolytic, depression, muscle spasm and anti-inflammatory.
104	Hypertension, sleeping pills, stomach protector.
105	Sleeping pills, hypertension, blood thinners.
106	
107	Anxiolytic.
109	Asthma, gastric protector.
110	Birth control pills.
112	Hypertension, diabetes.
113	Hypertension, alcohol, cholesterol, uric acid.
114	Antiallergics, bronchodilators and anti-inflammatory drugs.
115	
116	Cholesterol and hypertension.
118	
119	Diabetes, cholesterol, hypertension, peptic ulcer, arterial thromboembolism prophylaxis.
120	Bronchodilators and nasal drops.
125	Diabetes.
126	
127	Cholesterol, hypertension and arterial thromboembolism prophylaxis.
129	Cholesterol, hypertension and secondary stroke prophylaxis.
130	Epilepsy, hypertension, cholesterol, depression, blood thinners and benign prostatic hyperplasia.
133	Hypertension, folic acid and rheumatoid arthritis.
134	Hypertension.
136	Birth control pills.
137	Hypertension, depression, Awakening drugs and.
138	Cholesterol, hypertension, diabetes and sleeping pills.
139	Depression and involuntary contraction of muscles.
141	Blood thinners, cholesterol, hypertension and gastric protector.
142	
143	Menstruation and ovulation pills.
144	
145	Hypertension, cholesterol, anxiolytic, asthma, angina, remove swelling in heart failure and prophylaxis of thromboembolic disease.
146	Hypertension, cholesterol, anxiolytic and osteoarthritis.
147	Joint pills and cardiac dysrhythmia.

Appendix C

PSG Scoring Results

Table C.1: Number of events of type RERA, apneas or hypopneas identified in PSG scoring. Obstructive and central sleep may be either apnea or hypopnea, while there is only mixed apneas. These events were also identified as beloging to either a NREM stage or a REM stage.

ID	Respiratory Effort		Apnea and Hypopnea Events									
			Obstructive				*Central*				*Mixed*	
			Apnea		Hypopnea		Apnea		Hypopnea		Apnea	
	NR	R	NR	R	NR	R	NR	R	NR	R	NR	R
49	5	1	4	2	13	1	0	0	0	0	0	0
50	20	1	0	0	0	0	4	3	0	0	0	0
51	27	6	0	0	1	0	0	0	0	0	0	0
52	35	3	0	0	5	6	0	0	0	0	0	0
54	57	18	2	1	8	55	0	0	0	0	0	0
57	9	1	0	0	7	14	0	0	0	0	0	0
58	10	1	18	0	55	1	0	0	0	0	0	0
61	0	0	3	7	0	14	3	0	0	0	0	0
63	17	4	19	26	57	35	0	0	0	0	0	0
64	23	2	8	4	26	5	0	0	0	0	0	0
67	2	2	8	21	1	4	4	1	0	0	0	0
68	28	0	0	1	6	4	0	0	0	0	0	0
70	8	3	0	0	0	0	1	0	0	0	0	1
73	0	0	205	43	243	25	0	2	0	0	0	0
77	21	11	0	0	16	71	0	0	0	0	0	0
78	15	3	3	5	3	12	1	0	0	0	0	0
79	23	1	3	1	41	11	0	0	0	0	0	0
80	22	0	0	0	8	0	0	0	0	0	0	0
81	3	0	0	0	0	0	0	0	0	0	0	0
83	4	2	1	4	68	73	0	0	0	0	0	0
84	7	3	2	2	0	0	0	0	0	0	0	0
86	17	2	1	0	2	2	1	1	0	0	0	0
87	3	0	0	0	0	0	3	0	0	0	0	0
89	23	1	0	0	0	0	0	1	0	0	0	0
90	10	0	5	3	3	2	0	0	0	0	0	0
91	29	3	6	5	48	39	6	0	0	0	0	0

92	80	0	63	1	5	9	0	0	0	0	0	0
94	33	14	0	0	3	7	1	0	0	0	0	0
96	3	0	1	0	8	0	0	0	0	0	0	0
97	5	0	0	0	1	0	0	0	0	0	0	0
99	74	3	0	0	8	2	2	1	0	0	0	0
100	29	6	15	0	13	19	0	0	0	0	0	0
101	0	1	0	0	4	1	0	3	0	0	0	0
102	5	1	0	0	3	5	0	0	0	0	0	0
103	10	0	0	0	1	0	0	0	0	0	0	0
104	38	0	8	1	95	23	0	0	0	0	0	0
105	95	0	34	50	126	0	0	0	0	0	0	0
106	24	1	0	0	2	4	1	0	0	0	0	0
107	49	13	0	0	2	0	0	1	0	0	0	0
109	16	4	4	13	19	9	0	1	0	0	0	0
110	19	1	0	0	4	1	3	0	0	0	0	0
112	79	3	14	0	31	1	0	0	0	0	0	0
113	3	0	7	12	15	30	0	0	0	0	0	0
114	0	3	1	6	6	36	0	3	0	0	0	0
115	3	0	0	0	0	0	0	0	0	0	0	0
116	17	3	0	0	65	63	0	0	0	0	0	0
118	34	2	1	3	69	23	0	0	0	0	0	0
119	77	3	1	0	20	12	0	1	0	0	0	0
120	0	0	0	0	0	3	0	1	0	0	0	0
125	15	0	0	0	45	3	0	0	0	0	0	0
126	14	4	2	1	33	9	0	0	0	0	0	0
127	0	0	0	0	0	4	1	0	0	0	0	0
129	6	0	14	28	57	17	0	0	0	0	0	0
130	0	2	0	0	8	0	6	0	0	0	0	0
133	2	0	0	0	0	1	0	0	0	0	0	0
134	17	0	30	1	278	40	0	0	0	0	0	0
136	0	0	0	0	0	0	0	0	0	0	0	0
137	2	3	165	46	261	26	0	0	0	0	0	0
138	0	0	81	1	21	0	0	0	0	0	0	0
139	15	0	14	0	16	0	1	0	0	0	0	0
141	59	6	87	2	113	21	0	0	0	0	2	0
142	5	2	36	6	108	45	0	0	0	0	0	0
143	0	0	0	0	4	11	0	0	0	0	0	0
144	0	0	0	0	0	2	0	0	0	0	0	0
145	2	0	0	0	2	2	0	0	0	0	0	0
146	27	0	0	0	18	12	0	0	0	0	0	0
147	13	7	7	16	29	18	0	0	0	0	0	0

Table C.2: Results from the PSG scoring with highlights on their final medical evaluation classification performed by M. D. José Moutinho dos Santos. The RDI parameter is the most important one to do the classification. TST parameters indicates the amount of time, effectively, asleep and the remaining parameters, the percentage of sleep spent in each sleep stage.

ID	**Medical Evaluation**	**RDI**	**TST**	**N1**	**N2**	**N3**	**REM**
		$(\frac{\#events}{h})$	*(m)*	*(%)*	*(%)*	*(%)*	*(%)*
49	Sn	5.7	275.5	30.3	38.3	20.9	10.5
50	Sn	4.3	388.5	14.9	41.2	27.8	16.1
51	Sn	7.7	265.5	18.6	57.6	12.6	11.1
52	Sn	7.1	413.0	34.3	38.6	15.0	12.1
54	Mo	22.7	373.0	8.6	46.1	24.1	21.2
57	Sn	4.4	423.5	14.6	41.6	20.9	22.9
58	Mi	15.0	340.0	36.0	25.1	26.3	12.5
61	Sn	5.2	309.0	13.6	39.5	35.9	11.0
63	Mo	24.8	381.5	10.5	44.2	29.9	15.5
64	Mi	11.3	361.5	20.6	48.7	23.2	7.5
67	Sn	7.1	362.5	9.0	53.5	17.8	19.7
68	Mi	9.2	254.0	21.1	35.4	32.3	11.2
70	Sn	2.2	355.0	16.3	44.4	21.1	18.2
73	Se	92.0	338.0	26.0	38.9	21.3	13.8
77	Mo	18.7	382.0	2.9	24.6	37.8	34.7
78	Sn	7.7	326.5	14.2	34.0	40.0	11.8
79	Mi	15.8	303.0	17.0	49.5	18.2	15.3
80	Sn	6.1	294.5	13.2	34.6	52.1	0.0
81	Co	1.5	121.0	53.3	41.3	0.0	5.4
83	Mo	21.7	421.0	6.7	34.7	41.0	17.7
84	Sn	1.9	436.0	8.3	43.8	31.9	16.1
86	Mi	3.6	428.5	14.1	50.4	19.3	16.2
87	Co	1.3	284.0	17.3	42.3	30.5	10.0
89	Sn	4.7	317.0	31.4	39.1	12.0	17.5
90	Mi	9.2	149.5	38.1	42.1	15.4	4.3
91	Mo	22.5	362.0	17.3	47.5	14.8	20.4
92	Se	40.3	235.5	24.4	55.0	9.3	11.3
94	Sn	7.7	451.5	16.4	44.5	19.3	19.8
96	Sn	2.3	314.5	24.3	16.2	46.3	13.2
97	Co	1.0	361.5	13.7	46.1	18.8	21.4
99	Mi	13.2	410.0	8.7	35.0	36.7	19.6
100	Mi	12.9	382.0	10.5	44.9	22.5	22.1
101	Sn	1.3	431.5	12.9	45.4	24.6	17.1
102	Sn	4.0	207.5	8.0	30.4	51.3	10.4
103	Sn	1.6	423.0	22.1	50.6	18.7	8.6
104	Mo	27.9	354.5	27.9	42.3	23.8	5.9
105	Se	62.5	293.0	17.9	37.2	29.5	15.4
106	Sn	5.1	380.0	7.5	46.1	27.5	18.9
107	Mi	13.2	296.5	15.5	31.2	35.2	18.0
109	Mi	10.5	376.5	14.1	47.8	20.1	18.1

110	Sn	4.5	377.5	12.2	49.7	17.5	20.7
112	Mo	22.7	338.0	24.4	33.4	21.4	20.7
113	Mi	13.5	297.5	11.6	66.2	8.1	14.1
114	Sn	7.7	431.0	1.7	45.1	23.1	30.0
115	Sn	0.4	455.0	7.1	44.3	28.0	20.5
116	Mo	26.7	332.0	19.1	41.3	18.7	20.9
118	Mo	21.2	374.0	24.3	51.2	14.7	9.8
119	Mo	18.5	369.5	21.0	43.4	13.0	22.6
120	Co	0.9	274.5	23.7	48.5	14.9	12.9
125	Sn	8.6	440.0	7.4	27.8	44.2	20.6
126	Mi	9.7	389.5	15.5	42.4	25.0	17.1
127	Co	0.8	372.5	10.1	36.0	32.8	21.2
129	Se	38.2	191.5	21.1	45.4	9.7	23.8
130	Sn	2.9	332.5	21.5	51.4	15.0	12.0
133	Co	0.6	313.5	19.5	52.6	15.0	12.9
134	Se	62.7	350.5	29.7	53.4	5.8	11.1
136	Co	0.0	422.0	3.8	33.9	40.0	22.3
137	Se	66.6	453.0	25.9	36.1	17.7	20.3
138	Se	90.9	68.0	78.7	19.1	0.0	2.2
139	Mi	8.6	320.5	4.7	42.1	32.9	20.3
141	Se	43.2	402.5	45.7	21.9	11.4	21.0
142	Mo	30.4	399.0	24.6	51.5	7.9	16.0
143	Sn	2.8	320.0	10.9	44.2	30.3	14.5
144	Co	0.4	314.5	13.0	41.3	33.5	12.1
145	Co	1.1	316.5	3.0	40.8	50.7	5.5
146	Mo	21.5	159.0	7.5	62.3	21.1	9.1
147	Mo	16.6	325.5	20.7	35.5	27.2	16.6

Table C.3: Identification of other sleep events from PSG scoring. The following table presents, for each patient, each event totals.

ID	MChg	AR	Awake	LM	PLM	SN	MA	RBD
49	7	74	18	150	150	0	0	0
50	0	40	1	0	0	0	0	0
51	0	135	10	15	12	0	0	0
52	0	167	15	59	53	14	0	0
54	0	162	16	70	49	0	0	0
57	0	216	29	44	40	0	0	0
58	0	153	21	0	0	0	0	0
61	0	96	2	20	10	0	0	0
63	0	92	17	0	0	0	0	0
64	0	162	14	68	65	0	0	0
67	0	65	4	0	0	0	0	0
68	0	49	16	1	0	0	0	0
70	0	99	15	4	0	0	1	0
73	0	158	35	0	0	0	0	0
77	0	136	19	19	0	0	0	0
78	0	118	13	0	0	0	0	0
79	0	68	25	6	0	0	0	0
80	0	58	21	2	0	0	0	0
81	0	135	22	17	5	0	0	0
83	0	142	13	6	0	0	0	0
84	0	98	29	7	4	1	0	0
86	0	98	20	6	4	0	0	0
87	0	25	11	28	0	0	0	0
89	0	173	35	6	5	0	0	0
90	0	53	19	17	9	0	0	0
91	0	126	14	31	12	0	0	0
92	0	121	77	0	0	0	0	0
94	0	253	14	0	0	0	0	0
96	0	143	14	198	184	39	0	5
97	0	70	20	167	160	0	0	0
99	0	175	16	4	0	0	0	0
100	0	105	7	164	136	0	0	0
101	0	266	33	324	322	0	0	0
102	0	28	4	0	0	1	0	0
103	0	157	29	325	296	0	0	0
104	0	221	32	4	4	0	0	0
105	0	334	13	193	177	0	0	0
106	0	70	8	43	38	0	0	0
107	0	67	24	172	172	0	0	0
109	0	58	29	3	0	0	0	0
110	0	179	35	2	0	0	0	0
112	0	161	21	199	175	0	0	0
113	0	42	2	27	27	10	0	0
114	0	59	12	35	4	0	0	0

115	0	41	4	1	0	0	0	0
116	0	111	18	81	67	0	0	0
118	0	136	31	0	0	0	0	0
119	0	136	22	0	0	0	0	0
120	0	122	31	7	0	0	0	0
125	0	237	23	101	90	0	0	0
126	0	56	29	13	4	0	0	0
127	0	31	3	9	0	0	0	0
129	0	64	16	170	157	0	0	0
130	0	67	17	0	0	0	0	0
133	0	138	19	1	0	0	0	0
134	0	169	24	4	0	0	0	0
136	0	35	13	0	0	0	0	0
137	0	351	48	5	0	0	0	0
138	0	19	18	7	0	0	0	0
139	0	85	17	59	35	0	0	0
141	0	252	63	0	0	0	2	0
142	0	225	61	47	34	1	0	0
143	0	63	7	138	121	0	0	0
144	0	111	25	3	0	0	0	0
145	0	56	11	1	0	0	0	0
146	0	118	11	0	0	0	0	0
147	0	97	9	0	0	0	0	0

Table C.4: The columns to the right of the patient's ID columns have the first epoch from which data recording are considered for the purpose of sleep evaluation. Those epochs are marked with a Lights Out label. The end epoch, for sleep evaluation, were marked with a Lights On label, but that information is not present here. The first epoch of sleep, after Lights Out, is availabe in the First Sleep Epoch column.

ID	Lights Out Epoch	First Sleep Epoch	ID	Lights Out Epoch	First Sleep Epoch
49	7	83	103	130	144
50	13	24	104	12	37
51	13	112	105	6	37
52	6	18	106	128	162
54	13	37	107	121	168
57	8	32	109	12	29
58	4	51	110	6	40
61	14	40	112	13	23
63	9	47	113	17	161
64	8	27	114	11	16
67	24	52	115	8	24
68	10	108	116	8	46
70	17	66	118	9	16
73	2	42	119	12	73
77	11	12	120	6	44
78	8	59	125	12	15
79	111	119	126	8	22
80	15	94	127	6	84
81	9	84	129	10	69
83	9	27	130	8	51
84	9	61	133	5	129
86	8	25	134	11	58
87	126	146	136	5	15
89	9	23	137	9	21
90	47	77	138	13	116
91	9	31	139	146	162
92	19	40	141	16	25
94	10	15	142	7	31
96	6	59	143	80	118
97	40	64	144	109	161
99	8	15	145	10	29
100	14	40	146	20	282
101	7	49	147	9	54
102	10	204			